Characterising emerging viral spillover events in Forested Guinea (Guinée forestière), Republic of Guinea



Grace Ikuko Hood

Nuffield Department of Medicine

Balliol College

University of Oxford

This dissertation is submitted for the degree of

Doctor of Philosophy

Trinity 2025

Declaration of Authorship

This thesis is submitted to the University of Oxford for the degree of Doctor of Philosophy. The dissertation is the result of my own work and has not been submitted for a degree, diploma or any other qualification at the University of Oxford or any other institution. It does not exceed the prescribed word limit for the Nuffield Department of Medicine Degree Committee.

Work from this thesis has resulted in the following peer-reviewed publications (below). Coauthors contributed to the published versions of these manuscripts, however all analyses, code, figures and text in this thesis are my own. Where contributions by others have been incorporated, these have been explicitly stated and attributed in the text. I have obtained permission from collaborators and senior authors to include any work reproduced in my thesis.

1. **Hood G**, Carroll M. Host–pathogen interactions of emerging zoonotic viruses: bats, humans and filoviruses. Current Opinion in Virology. 2024:101436.
2. Roe MD*, **Hood G***, Spencer SL, Yan L, Bore JA, Tipton T, et al. Performance of an envelope glycoprotein-based multiplex immunoassay for Ebola virus antibody detection in a cohort of Ebola virus disease survivors. Journal of Virological Methods. 2024:115057.
   ***Denotes co-equal first authorship.**
3. Akoi Boré J, Timothy JWS, Tipton T, Kekoura I, Hall Y, **Hood G**, et al. Serological evidence of zoonotic filovirus exposure among bushmeat hunters in Guinea. Nature Communications. 2024;15(1):4171.
4. **Hood G**, Akoi Boré J, Tipton T, Onivogui Z, Sovogui K, Zoumanigui K, Tan CW, Hughes G, Broder C, Laing, E, Fornace K, Magassouba N, Carroll M. Filovirus-reactive antibodies in wildlife hunting communities in Forested Guinea may imply ongoing zoonotic spillover events. Revisions ongoing with Nature Communications.

Grace Hood

October 2025

Abstract

Characterising emerging viral spillover events in Forested Guinea (Guinée forestière), Republic of Guinea

Grace Hood

Guinée forestière has been the site of multiple high-consequence viral spillover events, including the index case of the 2013 – 2016 West African Ebola virus disease (EVD) epidemic. Deforestation and wildlife hunting rapidly expand the human-animal interface, increasing opportunities for transmission, underscoring the urgent need for surveillance.

This dissertation investigates the viral spillover of priority pathogens using a One Health model that combines multi-pathogen serological surveillance with satellite, spatial, demographic, questionnaire and interview data. I begin by assessing the performance of serological assays, including an envelope glycoprotein-based multiplexed microsphere-based immunoassay (MMIA) and pseudotyped virus neutralisation assays, for the detection of anti-filovirus antibodies in a cohort of Guinean EVD survivors from the 2013 – 2016 West African EVD epidemic.

I apply these multi-pathogen methods to wildlife hunting communities within Guinée forestière, presenting multiple lines of serological and epidemiological evidence for the ongoing spillover of multiple zoonotic filoviruses. Statistical investigations of questionnaire and satellite-derived land-cover data identified unique virus-specific risk factors, including forest fragmentation and nonhuman primate consumption, demonstrating that wildlife contact and landscape configuration drive pathogen exposure through potentially tractable pathways.

I then conduct serosurveillance, metagenomic sequencing and semi-structured interviews of Australian wildlife rehabilitators with extensive flying fox and microbat contact. Here, I find minimal zoonotic transmission despite significant wildlife exposure, often without personal protective equipment usage. This represents the first serological investigation into the zoonotic potential of recently identified paramyxoviruses (Cedar virus, Yeppoon virus, Grove virus) circulating at high prevalence in flying fox populations of the East coast of Australia.

The work of this thesis demonstrates the value of a One Health, multi-pathogen approach for characterising viral spillover at high-risk interfaces, and in elucidating its ecological, epidemiological and behavioural drivers in pursuit of a more mechanistic understanding of emergence.

Acknowledgements

First and foremost, I would like recognize the trust and invaluable support of the Macenta prefecture village communities, the Coyah and Guéckédou Ebola virus disease survivor associations, and all participants of this research who made this work possible. I further acknowledge the long-term support and commitment from the Guinean Ministry of Health, Agence Nationale de Sécurité Sanitaire, and Guéckédou Health Directorates. It is my hope that this work may serve the communities as intended.

I would like to thank my funders: the National Institute for Health Research Health Protection Research Unit in Emerging and Zoonotic Infections and the Nuffield Department of Medicine Student Prize, in addition to the UK Public Health Rapid Support Team and US Food and Drug Administration. I would also like to acknowledge key collaborators, including most prominently, Dr. Joseph Akoi Bore and colleagues from Centre de Recherche et d'Analyse Médicale. I am grateful for having had the opportunity to build upon your work, and for the generous hospitality that you extended to me whilst I was in Guinea. Je vous remercie beaucoup!

As with all sustained endeavours, this dissertation has taken a village to bring to completion, and I have a long list of personal thanks to extend. My deepest thanks to my supervisor, Professor Miles Carroll, for his steadfast support: our weekly meetings were an education in the art and science of research. I am grateful to Professor Kim Fornace for her ever-insightful guidance and for always providing me with opportunities to return to the field. Special thanks to Dr. Tom Tipton, who I know I can rely on in any situation, in the field or otherwise. I could not have asked for better mentorship on this journey.

I have had the good fortune of collaborating with exceptional scientists, and thank my colleagues for their key technical and moral support: Professors Eric Laing and Chee-Wah Tan, Dr. Edward Wright, Dr. Dung Nguyen, Dr. Jack Crook, Dr. Stephen Laidlaw, Dr. Emily Clayton, Dr. Luke Jones, Dr. Jack Mellors. To Dr. Hannah Klim, Dr. Cillian Gartlan, Dr. Caolann Brady and Tina Kusumaningrum: it was a privilege to undertake the DPhil together, and finish as both colleagues and dear friends.

I am indebted to my friends, who have come along with me on this journey, and the Balliol College MCR community for providing me with a home away from home. Calum Braham, for your enduring support and partnership in life. To my sister, Charlotte Hood, words cannot express the joy of sharing a PhD journey with you, having moved together from the other side of the world to this strange, cold country. Finally, to my parents, Ikuko and Simon Hood, and my grandparents, Jai and Richard Hood, Saiko and Shuichi Ota: I have never known anything but your unwavering love and belief in me. This dissertation is for you.

Table of Contents

Declaration of Authorship i

Abstract ii

Acknowledgements iii

Table of Contents iv

List of figures xii

List of tables xvi

Glossary & abbreviations xviii

Chapter 1 Introduction 1

1.1. Spillover or cross-species transmission (CST) of emerging viruses 1

1.2. Drivers of viral emergence, including land-use change and wildlife exposure 4

1.3. Pathogen prioritisation: high-consequence spillover 5

1.3.1. Filoviruses 5

1.3.1.1. Filovirus overview 5

1.3.1.2. Filovirus structure and function 7

1.3.1.3. Filovirus entry and infectious cycle 9

1.3.1.4. A brief history of human filovirus outbreaks and their origins, including the reactivation of persistent infection 10

1.3.1.5. Ecology of filoviruses: evidence for bats as the key reservoir 12

1.3.2. Paramyxoviruses 16

1.3.2.1. Paramyxovirus overview 16

1.3.2.2. Paramyxovirus structure and function 18

1.3.2.3. Paramyxovirus entry and infectious cycle 21

1.3.2.4. Paramyxovirus ecology 21

1.4. Ecological field studies of viral dynamics in bats 21

1.4.1. Overview of field-based studies 21

1.4.2. Common themes of bat ecological studies and gaps in knowledge 23
1.5. Bats as unique viral reservoirs and cryptic hosts 24
1.6. Surveillance for the detection of spillover 25
1.7. Thesis aims 26
Chapter 2 Methodology 27
2.1. Study populations and ethical approvals 27
2.1.1. Ebola virus survivor, contact and negative cohort 2015 – 2024, Coyah and Guéckédou, Republic of Guinea 27
2.1.2. WLH cohort, 2017 and 2023, Guinée forestière, Republic of Guinea 27
2.1.3. Farmer cohort, 2017 – 2021, Uganda 29
2.1.4. Blood donor cohort, 2020, United Kingdom 29
2.1.5. Wildlife worker cohort, 2023, Australia 29
2.2. Serological assays 29
2.2.1. Reagents 29
2.2.1.1. Monoclonal antibodies and antisera 29
2.2.1.2. Plasmids 31
2.2.1.3. Vesicular Stomatitis Virus (VSV) pseudotyped viruses 31
2.2.1.4. Viral recombinant protein antigens 32
2.2.2. Blood processing (plasma, sera and peripheral blood mononuclear cell isolation) 33
2.2.3. Multiplex microsphere-based immunoassay (MMIA) 33
2.2.3.1. Recombinant envelope glycoprotein ectodomains production, purification and bead-conjugation 33
2.2.3.2. MMIA screening of sera 34
2.2.3.3. Calibration of internal reference to WHO standard for EBOV binding antibody concentration 35
2.2.4. Enzyme-linked immunosorbent assays (ELISAs) 35
2.2.4.1. Ebola Zaire IgG indirect ELISAs 35
2.2.5. Pseudotyped virus production 36
2.2.5.1. Cell culture propagation and maintenance 36
2.2.5.2. Plasmids 36

2.2.5.3. Plasmid transformation, production, DNA extraction and sequencing 37
2.2.5.4. Pseudotyped virus production 38
2.2.5.5. Pseudotyped virus titration 39
2.2.6. Pseudotyped virus neutralisation assays (PVNA) 40
2.2.6.1. Lentiviral vector-based PVNA 40
2.2.6.2. Vesicular stomatitis virus -based PVNA 40
2.2.7. Authentic virus neutralisation assays 41
2.2.7.1. Recombinant Cedar virus (rCedV) neutralisation assay 41
2.2.7.2. Live Ebola virus neutralisation assay 41
2.2.8. IFNγ ELISpot 41
2.3. Metagenomic deep sequencing 42
2.3.1. Sample preparation 42
2.3.1.1. Sample collection 42
2.3.1.2. RNA extraction, DNase treatment, viral particulate purification 42
2.3.1.3. Sequence-Independent Single-Primer Amplification (SISPA) 42
2.3.2. Illumina short-read deep sequencing 43
2.3.3. Oxford Nanopore Technology (ONT) long-read deep sequencing 44
2.3.4. In silico analysis 45
2.3.4.1. Taxonomic classification 45
2.3.4.2. *De novo* genome assembly and alignment 45
2.4. Experimental and computational methods for the characterization of serological data 45
2.4.1. Establishment of serological thresholds through a presumed unexposed cohort 45
2.4.2. Establishment of serological thresholds using finite mixture models 46
2.4.3. Characterisation of immunological phenotypes using unsupervised machine learning methods (*K*-means clustering) 46
2.5. Chapter 3-specific methodologies: Performance of serological assays for filovirus antibody detection 47
2.5.1. Statistical analysis 47
2.6. Chapter 4-specific methodologies: Zoonotic filovirus exposure in WLHs in Forested Guinea (Guinée forestière), Republic of Guinea 2017 – 2023 47

2.6.1. Spatial mapping and investigation of environmental risk factors 47
2.6.2. Univariable and multivariable statistical models 48
2.7. Chapter 5-specific methodologies: Emerging viral infection surveillance in wildlife workers, Eastern Australia 48
2.7.1. Study design and participants 48
2.7.1.1. Patient and public involvement (PPI) activities 48
2.7.1.1.1. Advisory panel recruitment and activities 48
2.7.1.1.2. Public forum 49
2.7.1.2. Participant recruitment 49
2.7.1.3. Semi-structured interview guide design 49
2.7.1.4. Qualitative interviewing of wildlife workers 50
2.7.1.5. Data management and statistical analysis of qualitative data 50
Chapter 3 Performance of serological assays for filovirus antibody detection 51
3.1. Introduction 51
3.1.1. Serological assays for filovirus antibody detection 51
3.1.1.1. Immunofluorescence (IF) 51
3.1.1.2. Enzyme-Linked Immunosorbent Assays (ELISAs) 51
3.1.1.3. MMIAs 52
3.1.1.4. Neutralisation assays and pseudotyped virus neutralisation assays (PVNAs) 53
3.1.2. Challenges of EBOV serology 54
3.1.3. Chapter aims and rationale 54
3.2. Results 55
3.2.1. Performance of an envelope glycoprotein-based multiplex immunoassay for Ebola virus antibody detection in a cohort of Ebola virus disease survivors in Coyah and Guéckédou, Republic of Guinea 55
3.2.1.1. Study participants 55
3.2.1.2. Ebola virus survivor cohort demographics 55
3.2.1.3. Calibration of an internal reference standard to the WHO standard for EBOV 56
3.2.1.4. EBOV-GP reactivity by MMIA in the Guinean Ebola survivor cohort 57
3.2.1.5. MMIA performance for EBOV GP binding antibody detection 58

3.2.2. Agreement between serological assays for filoviruses 60
3.2.2.1. EBOV-Makona ELISA and live EBOV-Mayinga neutralisation assay 60
3.2.2.2. MMIA and EBOV-Makona ELISA 61
3.2.2.3. MMIA and live EBOV-Mayinga neutralisation assay 61
3.2.3. Pan-orthoebolavirus binding antibody cross-reactivity resulting from EBOV infection 63
3.2.4. Anti-filovirus GP binding antibody responses of an rVSVΔG-ZEBOV-GP Ebola virus vaccine recipient 67
3.2.5. Anti-filovirus GP binding antibody responses in Marburg virus survivors from Uganda and the Democratic Republic of Congo 68
3.2.6. Pan-filovirus neutralisation in Ebola virus disease survivors: demonstrated in lentiviral-vector based pseudotyped virus neutralisation assays (PVNAs) 69
3.3. Discussion 70
3.4. Appendix 73
Chapter 4 Zoonotic filovirus exposure in wildlife hunters in Forested Guinea, Republic of Guinea 2017 – 2023 74
4.1. Introduction 74
4.1.1. Viral spillover in Forested Guinea, Republic of Guinea 74
4.1.2. Seroepidemiology of filoviruses in West Africa 75
4.1.2.1. Summary of published orthoebolavirus seroprevalence studies conducted in West Africa, 1978 – 2025 75
4.1.2.2. Asymptomatic Ebola virus infection and interpreting observed orthoebolavirus seroprevalences 80
4.1.3. Chapter rationale and aims 81
4.2. Results 83
4.2.1. Study sites and study populations 83
4.2.2. Wildlife hunting and bat exposure in Forested Guinea 85
4.2.3. Filovirus reactivity in Guinean wildlife hunting communities by MMIA screening 87
4.2.4. Experimental and computational classification of immune responses through use of a seropositivity threshold 88

4.2.5. Classification of immune responses by *K*-means clustering reveals EBOV and non-EBOV filovirus reactivity in WLHs, 2017 and 2023, in comparison to EBOV-reactivity in other populations 92
4.2.6. Filovirus neutralizing activity in Guinean WLHs 103
4.2.7. Durable EBOV antibody responses, 6 years post 2013 – 2016 West African EVD epidemic and antibody decay rates 107
4.2.8. Seroconversion observed in Guinean WLHs between 2017 and 2023 108
4.2.9. Antigen reactivity in Guinean WLHs by village 108
4.2.10. Risk factors for filovirus seropositivity 116
4.2.11. Influence of land cover patterns on exposure to zoonotic filoviruses in Guinean WLHs 122
4.3. Discussion 125
4.4. Appendix 133
4.4.1. Methodology of literature rapid review: Summary of published orthoebolavirus seroprevalence studies conducted in West Africa, 1978 – 2025 133
4.4.2. Anti-filovirus antibody response histograms fitted with a Gaussian mixture model 135
4.4.3. Antibody decay rates for non-EBOV filoviruses in WLHs, Forested Guinea 136
4.4.4. Population-level reactivity to filovirus antigens amongst WLHs and close contacts in Forested Guinea 139
4.4.5. Linear regression analysis of risk factors associated with individual antigens, Guinean WLH cohort 2023 141
Chapter 5 Emerging viral surveillance in wildlife workers, Eastern Australia 143
5.1. Introduction 143
5.1.1. Paramyxovirus spillover and detection in eastern Australia 143
5.1.1.1. Human emergence of three novel zoonotic viruses in Australia 1994-1997 143
5.1.1.1.1. Hendra virus (HeV) in 1994 143
5.1.1.1.2. Australian bat lyssavirus (ABLV) in 1996 144
5.1.1.1.3. Menangle virus (MenV) in 1997 145
5.1.1.2. Virological discovery of novel viruses in Pteropus species in Eastern Australia: Cedar virus (CedV), Yeppoon virus (YepV), Grove virus (GroV) 145
5.1.2. Pteropus species fruit bats or “flying foxes” and human conflict 146

5.1.3. Wildlife and flying fox rehabilitators and rescuers in Australia 148
5.1.4. Chapter aims 149
5.2. Results 150
5.2.1. Patient and public involvement (PPI) activities 150
5.2.2. Study sites 153
5.2.3. Characteristics of study participants 154
5.2.4. Exposure in wildlife workers in Eastern Australia 156
5.2.4.1. Quantification of wildlife exposure 156
5.2.4.2. Flying fox and microbat exposure 156
5.2.4.3. Exposure to flying fox species 157
5.2.5. Safety practices amongst wildlife workers 158
5.2.5.1. Usage of personal protective equipment (PPE) 158
5.2.5.1.1. Drivers of PPE usage 159
5.2.5.1.2. Thematic analysis of PPE usage 161
5.2.5.2. Response to injuries or zoonotic exposures from flying foxes or bats amongst Australian wildlife workers 163
5.2.5.2.1. Types of responses and their frequency 163
5.2.5.2.2. Drivers of responses to injury and exposure 166
5.2.5.2.3. Thematic analysis of response to injuries or zoonotic exposures 167
5.2.6. Perceived risk amongst wildlife workers in Eastern Australia 169
5.2.7. Serological exposure to viral antigens amongst flying fox carers in Australia 171
5.2.7.1. Cedar virus (CedV) neutralisation of high binding samples 175
5.2.8. Metagenomic sequencing of samples from flying foxes and bats in wildlife rehabilitation across East Coast Australia 175
5.3. Discussion 177
5.4. Appendix 183
5.4.1. Injury response patterns in wildlife workers, 2023 183
5.4.2. Metagenomic sequencing of environmental bat samples 184
5.4.2.1. Plant viruses 184
5.4.2.2. Insect viruses 185

5.4.2.3. Vertebrate viruses 185
5.4.2.4. Bacteriophages 186
Chapter 6 Discussion 188
References 192

List of figures

Figure 1 Spillover of high-consequence pathogens 2
Figure 2 Phylogenetic tree of select filoviruses. 6
Figure 3 Ebola virus (EBOV) virion structure and genome organisation 9
Figure 4 *Orthoebolavirus* life cycle 10
Figure 5 Henipavirus virion structure and genome organisation 20
Figure 6 Study sites, Macenta prefecture, Guinée forestière, Republic of Guinea 28
Figure 7 Indirect multiplexed microsphere-based immunoassay (MMIA) 53
Figure 8 Ebola virus disease (EVD) survivor, contact and UK blood donor cohort [223]. 55
Figure 9 Calibration of internal reference standard to the WHO standard for EBOV. 57
Figure 10 EBOV-GP reactivity by EVD history. 58
Figure 11 MMIA performance in EVD survivors and negatives. 59
Figure 12 Correlations between filovirus MMIA, live EBOV-Mayinga neutralization test and whole EBOV ELISA. 62
Figure 13 Anti-filovirus glycoprotein IgG responses of Guinean Ebola virus disease (EVD) survivors. 64
Figure 14 Correlation between Ebola virus (EBOV) glycoprotein (GP) IgG and GP IgG for 8 heterotypic orthoebolaviruses. 66
Figure 15 Anti-filovirus glycoprotein IgG responses of EBOV vaccinee. 67
Figure 16 Anti-filovirus glycoprotein IgG responses of Marburg virus survivors. 68
Figure 17 Phylogenetic tree of filovirus envelope glycoproteins (GP). 69
Figure 18 Cross-neutralising responses from Guinean EVD survivors. 70
Figure 19 MARV pseudotyped virus neutralisation assay optimization 73
Figure 20 EBOV pseudotyped virus neutralisation assay optimization. 73
Figure 21 Wildlife hunted for consumption, by species, Forested Guinea, 2023. 85
Figure 22 Anti-filovirus glycoprotein IgG distributions of among Guinean wildlife hunter 2017 cohort (n=511) and 2023 cohort (n=648), Guinean Coyah controls (n=18) and the United Kingdom blood donor cohort (n=63). 87
Figure 23 Anti-filovirus glycoprotein IgG distributions among Ugandan farmers (n=79) and the United Kingdom blood donor cohort (n=63). 88

Figure 24 Comparison of seropositivity thresholds (experimental and computational) for filovirus antigens on the multiplex microsphere-based (MMIA) assay. 89
Figure 25 Seropositivity classifications of EBOV survivor cohort. 91
Figure 26 *K*-means clustering of anti-filovirus glycoprotein antibody responses of Guinean wildlife hunting communities, 2017 and 2023 (combined) for *k*=15 clusters. 92
Figure 27 Evaluations of different ranges of *k* (number of clusters) 93
Figure 28 Individual MFI responses against (a) TAFV and BDBV (b) TAFV and EBOV 94
Figure 29 Individual MFI responses against (a) BDBV and EBOV (b) BOMV and EBOV 94
Figure 30 Individual MFI responses against BDBV and EBOV from the Guinean wildlife hunting cohort (2017 and 2023) who were categorised into Clusters 4 and 5 from the *K*-means clustering algorithm analysis for *k*=15. 95
Figure 31 *K*-means clustering of anti-filovirus glycoprotein antibody responses of Guinean wildlife hunting communities, 2017 and 2023 (separately) for *k* =11 clusters. 95
Figure 32 Individual anti-filovirus glycoprotein responses in wildlife hunting communities, Forested Guinea. 97
Figure 33 Individual anti-filovirus glycoprotein antibody responses in EBOV-negative, Coyah and Guéckédou, Republic of Guinea (n=15) and UK blood donors (n=63). 99
Figure 34 Average anti-filovirus glycoprotein antibody responses of EVD survivors 100
Figure 35 Individual anti-filovirus glycoprotein antibody responses of EVD survivors 100
Figure 36 Anti-filovirus glycoprotein antibody responses of Ugandan farmers. 101
Figure 37 Individual anti-filovirus glycoprotein antibody responses in Uganda (*k*=6). 102
Figure 38 Individual anti-filovirus glycoprotein antibody responses in Uganda (*k*=3). 102
Figure 39 Neutralising ability of Guinean wildlife hunter sera against Bundibugyo (BDBV) and Ebola (EBOV) viruses by PVNA. 104
Figure 40 Neutralising ability of Guinean wildlife hunter sera against Taï Forest virus (TAFV) and Ebola (EBOV) viruses by pseudotyped virus neutralisation assay. 105
Figure 41 Neutralising ability of Guinean wildlife hunter sera against Lloviu (LLOV) and Ebola-Makona (EBOV) viruses by pseudotyped virus neutralisation assay. 105
Figure 42 Neutralising ability of Guinean wildlife hunter sera against Reston (RESTV) and Ebola-Makona (EBOV) viruses and Bombali (BOMV) and Ebola (EBOV) Makona viruses by pseudotyped virus neutralisation assay. 106
Figure 43 Population-level mean (with 95% confidence interval (shaded)) and individual-level antibody decay models for Ebola virus amongst those identified as seropositive in 2017. 107
Figure 44 Individual anti-filovirus glycoprotein IgG responses of Guinean wildlife hunters in 2017 and 2023 against (a) LLOV (b) RESTV (c) MLAV. 108
Figure 45 Geometric mean anti-filovirus IgG responses amongst Guinean wildlife hunters in 2017, stratified by village. 109

Figure 46 Geometric mean anti-filovirus IgG responses amongst Guinean wildlife hunters in 2023, stratified by village. 110
Figure 47 Individual IgG responses to Ebola virus (EBOV) and TAFV virus amongst Guinean wildlife hunters from Deguedeou in 2017 and 2023. 111
Figure 48 Individual IgG responses to Ebola (EBOV) and Bundibugyo (BDBV) viruses amongst Guinean wildlife hunters from Maraou in 2017 and 2023. 112
Figure 49 Individual IgG responses to Ebola (EBOV) and MLAV viruses amongst Guinean wildlife hunters from Coyamah in 2017 and 2023 112
Figure 50 Village-level IgG responses (mean and median) to filovirus antigens (EBOV, BDBV, BOMV) amongst Guinean wildlife hunters in 2023 113
Figure 51 Village-level IgG responses (mean and median) to filovirus antigens (TAFV, RESTV, SUDV) amongst Guinean wildlife hunters in 2023 114
Figure 52 Village-level IgG responses (mean and median) to filovirus antigens (LLOV, MLAV, RAVV) amongst Guinean wildlife hunters in 2023. 115
Figure 53 Anti-filovirus responses (log-transformed) amongst Guinean wildlife hunters 2023. 116
Figure 54 TAFV seropositivity by wildlife hunting exposure, 2023 among those who report bat consumption (1) and do not (0). 119
Figure 55 RESTV seropositivity by wildlife hunting exposure, 2023 among those who report bat consumption (1) and do not (0). 119
Figure 56 BDBV seropositivity by wildlife hunting exposure, 2023 among those who report nonhuman primate (NHP) consumption (1) and do not (0). 120
Figure 57 Anti-filovirus responses (log-transformed) amongst Ugandan farmers, 2017 to 2021. 121
Figure 58 Landcover map of Forested Guinea, Republic of Guinea 123
Figure 59 Anti-filovirus antibody response histograms fitted with a Gaussian mixture model..... 135
Figure 60 Anti-filovirus glycoprotein IgG distributions (log (MFI) among Guinean wildlife hunters in 2017 compared to 2023. 137
Figure 61 Individual anti-filovirus glycoprotein IgG responses of Guinean wildlife hunters in 2017 and 2023. 138
Figure 62 Anti-filovirus Glycoprotein IgG distributions among Guinean wildlife hunter (WLH) 2017 cohort (a) and 2023 cohort (b) in WLHs compared to non-hunters. 139
Figure 63 Anti-filovirus glycoprotein IgG distributions among Guinean wildlife hunter (WLH) 2023 cohort (n=648) bat hunters compared to non-hunters. 140
Figure 64 Anti-filovirus responses amongst Guinean WLHs 2023. 141
Figure 65 Anti-Ebola virus glycoprotein antibody responses by occupation, Guinean wildlife hunters (WLHs), 2023. 142
Figure 66 Distribution of the four Australian mainland *Pteropus* spp. by Timmiss et al., 2021 [364] 147

Figure 67 Study sites for surveillance of Australian wildlife workers..... 153
Figure 68 Years of experience with Australian wildlife 156
Figure 69 Contact with (a) Flying foxes (b) Microbats in Australian wildlife workers, 2023 157
Figure 70 Exposure to flying fox species in Australian wildlife workers, 2023..... 157
Figure 71 Personal protective equipment (PPE) usage in Australian wildlife workers when handling flying foxes, 2023 159
Figure 72 Personal protective equipment (PPE) usage for handling flying foxes and microbats, by wildlife workers by role, 2023 160
Figure 73 Personal protective equipment (PPE) usage for handling flying foxes and microbats, by wildlife workers, by age..... 160
Figure 74 Personal protective equipment (PPE) usage for handling flying foxes and microbats, by wildlife workers, by frequency of flying fox contact per year..... 161
Figure 75 Frequency analysis of responses to the question: “please describe what you would do following a bite/scratch/exposure to bodily fluids from a flying fox or bat”..... 166
Figure 76 Responses amongst Australian wildlife workers to the statement: I am concerned about contracting an infection from wildlife 169
Figure 77 Personal protective equipment (PPE) usage by response to Q1: I am concerned about contracting an infection from wildlife 170
Figure 78 Responses amongst Australian wildlife workers to the statement: I take sufficient precautions to protect myself. 170
Figure 79 Personal protective equipment (PPE) usage by response to the question: I take sufficient precautions to protect myself. 171
Figure 80 Responses amongst Australian wildlife workers to the statement: I have sufficient training and resources to protect myself. 171
Figure 81 Anti-filovirus glycoprotein IgG distributions among Australian wildlife workers (n=104) and the United Kingdom blood donor cohort (n=63). 172
Figure 82 Anti-paramyxovirus glycoprotein IgG distributions among Australian wildlife workers (n=104) and the United Kingdom blood donor cohort (n=63)..... 173
Figure 83 Anti-filovirus glycoprotein IgG responses of Australian wildlife workers (n=104). 174
Figure 84 Anti-paramyxovirus glycoprotein IgG responses of Australian wildlife workers (n=104). 174
Figure 85 Most common injury response patterns in Australia wildlife workers, 2023..... 183
Figure 86 Thematic emphasis in flying fox injury and exposure responses across participant groups 183

List of tables

Table 1 Summary of select filovirus species, by genera 7
Table 2 Ecological investigation of filoviruses in bats 14
Table 3 Select paramyxoviruses, by genera 16
Table 4 Summary of select paramyxovirus detections (chronological) 18
Table 5 Monoclonal antibodies and antisera 30
Table 6 Viral envelope glycoprotein (GP) plasmids 31
Table 7 Vesicular Stomatitis Virus (VSV) backbone pseudotyped viruses 32
Table 8 Recombinant viral proteins 32
Table 9 Relative quantities of transfection components 39
Table 10 Demographics of EVD survivor, contact and negative cohort, Guéckédou and Coyah, 2015 and 2017 56
Table 11 Performance of a filovirus envelope glycoprotein-based multiplex microsphere-based immunoassay (MMIA) for EBOV detection. 60
Table 12 Summary of published orthoebolavirus seroprevalence studies conducted in West Africa, 1978 – 2025 77
Table 13 Demographic characteristics by cohort 84
Table 14 Wildlife exposure questionnaire responses, Forested Guinea 2023 86
Table 15 Comparison of seropositivity thresholds (experimental and computational) for filovirus antigens on the multiplex microsphere-based (MMIA) assay 90
Table 16 Results from Guinean wildlife hunting cohort (2017 and 2023) *K*-means clustering algorithm analysis for *k*=15. 98
Table 17 Categorization of immune responses from the Guinean wildlife hunting cohort (2017 and 2023) following *K*-means clustering algorithm analysis (*k*=15). 99
Table 18 Univariate linear regression analysis of risk factors for filovirus exposure in Guinean wildlife hunters, 2023 118
Table 19 Outcome variables for logistic regression analysis, derived from *K*-means clustering analysis of Guinean wildlife hunter cohort 2023 (n=607). 122
Table 20 Significant associations between viral antigen exposure risk and environmental factors for wildlife hunters, 2017 and 2023 combined cohort 124

Table 21 Univariable and multivariable logistic regression analysis of BDBV exposure in Guinean wildlife hunters (WLHs), 2023 125
Table 22 Antibody decay rates and half-lives of filovirus responses observed in Guinean wildlife hunters (WLHs), 2017 to 2023 136
Table 23 Patient and public involvement (PPI) activities 151
Table 24 Different roles (volunteer and professional) amongst study participants 154
Table 25 Demographic characteristics of Australian wildlife worker study population (n=108), 2023 155
Table 26 Categories of personal protective equipment (PPE) used by Australian wildlife workers when handling flying foxes 158
Table 27 Thematic analysis of personal protective equipment (PPE) usage amongst Australian wildlife workers, 2023 161
Table 28 Responses to injuries or zoonotic exposures from flying foxes or bats 165
Table 29 Thematic analysis of response to injuries or zoonotic exposures in Australian wildlife workers, 2023 167
Table 30 Vertebrate viruses 176
Table 31 Kraken2 classification of Illumina reads 184
Table 32 Summary of reads classified to vertebrate viruses in Australian bat samples 185
Table 33 Select phages and uses, identified in Australian bat samples 186

Glossary & abbreviations

ABCB1: Adenosine Triphosphate-Binding Cassette subfamily B member 1
ABLV: Australian bat lyssavirus
ACK: Ammonium-Chloride-Potassium lysis buffer
AngV: Angavokely virus
aOR: Adjusted odds ratio
ATP: Adenosine Triphosphate
AUC: Area under the Receiver Operating Curve
BDBV: Bundibuygo virus
BEI: Biodefense and Emerging Infections
BHK: Baby Hamster Kidney cell line
BOMV: Bombali virus
BSA: Bovine Serum Albumin
BSL: Biosafety level
CAR: Central African Republic
CCL8: Chemokine (C-C motif) ligand 8 (also known as monocyte chemotactic protein-2 (MCP-2))
CedV: Cedar virus
CFR: Case Fatality Rate
CHO: Chinese Hamster Ovary cell line
CI: Confidence interval
CRAM: Centre de Recherche et d'Analyse Médicale
CST: Cross-species transmission
Ct: Cycle threshold
DMEM: Dulbecco's modified Eagle's medium
DNA: Deoxyribonucleic acid
DRC: Democratic Republic of Congo
dsRNA: Double-stranded RNA
EBOV: Ebola virus
EDTA: Ethylenediaminetetraacetic acid
ELISA: Enzyme-linked Immunosorbent Assay
ELISpot: Enzyme-Linked ImmunoSpot assay
EM: Expectation-maximization algorithm
EVD: Ebola virus disease
F: Fusion protein (of paramyxoviruses)
FANG: Filovirus Animal Nonclinical Group
FAO: Food and Agriculture Organization of the United Nations
FMM: Finite mixture modelling
FNQ: Far north Queensland, Australia
FD: Fractal dimension - Quantifies the complexity of a shape's boundary. Values closer to 1 indicate simple, smooth shapes; values approaching 2 reflect increasingly complex and irregular boundaries (Range: 1–2)
FUO: Fever of Unknown Origin

GhV: Ghanian bat henipavirus
GISRS: Global Influenza Surveillance and Response System
GLM: Generalized Linear Model
GP: Glycoprotein
GP1: Glycoprotein 1 subunit (receptor binding ectodomain)
GP2: Glycoprotein 2 subunit (transmembrane fusion domain)
GroV: Grove virus
GTR: General Time Reversible model
GVP: Global Virome Project
H1N1: Hemagglutinin type 1, Neuraminidase type 1 influenza A virus
HCW: Healthcare workers
HEK293T: Human Embryonic Kidney 293 cells expressing the SV40 large T antigen
HeLa: HeLa cell line
HeV: Hendra virus
HIV: Human immunodeficiency virus
HSP: Heat shock proteins
IFL: Internal fusion loop
IF: Immunofluorescence
IFAT: Indirect fluorescent antibody tests
IFIT: Interferon Induced proteins with Tetratricopeptide repeats
IFN: Interferon
IgG: Immunoglobulin-G
IgM: Immunoglobulin-M
IL: Interleukin
IR-std: Internal reference standard
ISG: Interferon-stimulated gene
Kb: Kilobase
L: Large protein
LLOV: Lloviu virus
M: Matrix protein (of paramyxoviruses)
MARV: Marburg virus
Mb: Megabase
MeliV: Melian virus
MenV: Manangle virus
MERS: Middle East respiratory syndrome
MFI: Median fluorescence intensity
MFI-bg: Background subtracted MFI
MinION: Oxford Nanopore Technologies (ONT) portable sequencing device
MLAV: Měnglà virus
MLD: Mucin-like domain
MMIA: Multiplexed microsphere-based immunoassay
MNA: Microneutralisation assay
MojV: Mòjiāng virus
MPER: Membrane-proximal external region
mIU/L: Milli-international units per liter
mRNA: Messenger RNA
MUSCLE: Multiple Sequence Comparison by Log-Expectation algorithm
NA: Neuraminidase
NCBI: National Center for Biotechnology Information of the National Library of Medicine (NLM) at the National Institutes of Health (NIH) in the United States

NHP: Nonhuman primate
NIBSC: National Institute for Biological Standards and Control
NIH: National Institutes of Health
NIH NIAID: National Institutes of Health National Institute of Allergy and Infectious Disease
NiV: Nipah virus
NiV-B: Nipah virus-Bangladesh strain
NiV-M: Nipah virus-Malaysia strain
NLRP3: NOD-Like Receptor family, Pyrin domain-containing 3
NP: Nucleoprotein
NPC1: Niemann-pick C1
NSW: New South Wales, Australia
NUS: National University of Singapore
OAS3: 2',5'-oligoadenylate synthetase 3 (an interferon-induced antiviral enzyme)
OD: Optical density
OFFLU: joint network of expertise on animal influenza established by the World Organisation for Animal Health (WOAH) and the United Nations Food and Agriculture Organization (FAO)
ONT: Oxford Nanopore Technology
OR: Odds ratio
ORF: Open Reading Frame
OxTREC: Oxford Tropical Research Ethics Committee
PBMC: Peripheral blood mononuclear cells
PBS: Phosphate buffered saline
PBSA: Phosphate buffered saline without calcium and magnesium
PBST: PBS Tween 20
pCSFLW: Firefly luciferase reporter construct plasmid
PE: Phycoerythrin
PAR: Perimeter-Area Ratio - Measure of the complexity of a forest patch's shape by comparing perimeter to area. Higher values indicate more irregular or fragmented shapes (Range: >0, no fixed upper limit; increases with complexity)
PHEIC: Public health emergency of international concern
PhIP-Seq: Phage ImmunoPrecipitation Sequencing
PPI: Patient and public involvement
PPE: Personal protective equipment
PVNA: Pseudotyped virus neutralisation assay
PYHIN: PYrin and HIN domain-containing proteins
QLD: Queensland, Australia
qRT-PCR: Quantitative Reverse Transcription Polymerase Chain Reaction (also known as real-time PCR)
RAVV: Ravn virus
RBC: Red blood cells
RBS: Receptor Binding Site
RdRP: RNA-directed RNA polymerase
RESTV: Reston virus
RNA: Ribonucleic acid
RNP: Ribonucleoprotein
ROC: Receiver operating characteristic
rVSVΔG-ZEBOV-GP: Recombinant Vesicular Stomatitis Virus with deleted G protein and Zaire ebolavirus glycoprotein (ERVEBO vaccine)

SARS-CoV-2: Severe Acute Respiratory Syndrome Coronavirus 2
SD: Standard deviation
sGP: Soluble GP
SI: Shape Index - Standardizes patch shape relative to a circle (most compact shape). A value of 1 represents a perfect circle; values >1 indicate elongated or irregular shapes (Range: ≥1)
SIR: Susceptible—infected—recovered
SISPA: Sequence-Independent Single-Primer Amplification
SNBTS: Scottish National Blood Transfusion Service
ssGP: Small soluble GP
ssRNA: Single-stranded RNA
STAT-1: Signal Transducer and Activator of Transcription 1
STAT-2: Signal Transducer and Activator of Transcription 2
STING: Stimulator of Interferon Genes
SUDV: Sudan virus
TAFV: Taï Forest virus
UK: United Kingdom
UKBD: United Kingdom blood donors
UPEC: Uropathogenic *Escherichia coli*
UTI: Urinary tract infection
US: United States
US CDC: United States Centers for Disease Control and Prevention
USAID: United States Agency for International Development
USUHS: Uniformed Services University of the Health Sciences
UVRI: Ugandan Virus Research Institute
VHF: Viral Haemorrhagic Fever
VIC: Victoria, Australia
VIZIONS: Vietnam Initiative on Zoonotic Infections
VP24: Viral Protein 24
VP30: Viral Protein 30
VP35: Viral Protein 35 (polymerase cofactor)
VP40: Viral Protein 40 (matrix protein)
vRNA: Viral ribonucleic acid
VSV: Vesicular Stomatitis Virus
WLH: Wildlife hunter
WHO: World Health Organization of the United Nations
WHO-std: World Health Organization of the United Nations standard
WOAH: World Organisation for Animal Health
YepV: Yeppoon virus

Chapter 1

Introduction

1.1. Spillover or cross-species transmission (CST) of emerging viruses

Spillover—the cross-species transmission of a pathogen from a vertebrate animal to a human—is the host-switching mechanism at the origin of every viral pandemic of the past two centuries [1]. Many continue sustained circulation as endemic human pathogens of global importance, including human immunodeficiency viruses types 1 and 2 (HIV-1 and HIV-2, respectively), which originated from multiple cross-species infections from simian immunodeficiency virus (SIV)-infected chimpanzees (*Pan troglodytes*) and gorillas (*Gorilla gorilla*), and sooty mangabeys (*Cercocebus atys*), respectively [2, 3]. The increasing emergence of novel viral diseases presents an ongoing threat to global health and development, with one projection estimating up to a threefold increase in the yearly probability of a major epidemic in the coming decades [4]. Despite an urgent mandate for preparedness, efforts remain hindered by an incomplete understanding of the molecular, evolutionary, and epidemiological processes underlying this complex phenomenon.

Cross-species transmission (CST) may occur from a reservoir host (which develops infection in the absence of pathology) to a recipient human directly or via an intermediate host [5]. An intermediate host represents an essential step for some pathogens, either by providing an epidemiological link (such as facilitating human exposure to a wildlife pathogen via a domestic animal) or virological link (acting as an amplifying host, e.g., horses in Hendra virus, or a mixing vessel facilitating reassortment, e.g., swine in the H1N1 2009 pandemic influenza virus) [6-8].

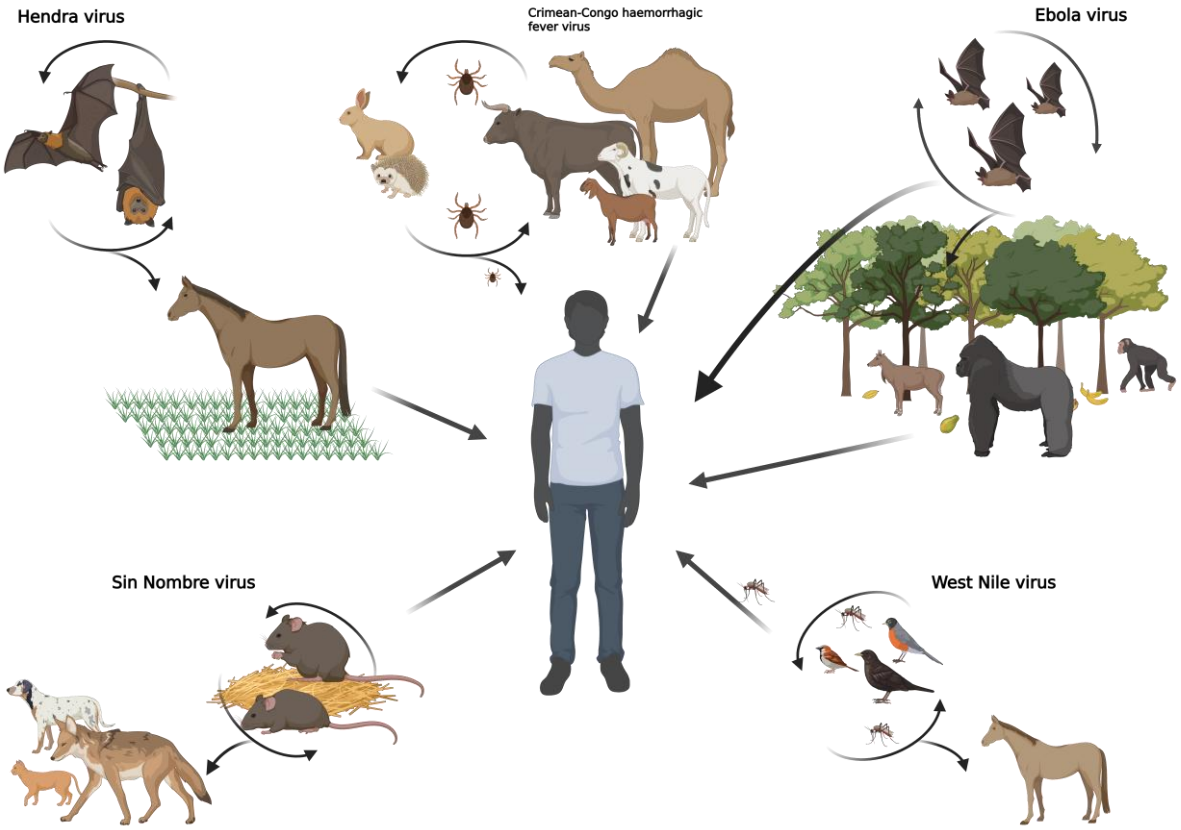


Figure 1 Spillover of high-consequence pathogens (a) Hendra virus is maintained within its natural reservoir by the Pteropodid bat, which sheds virus in excreta, occasionally causing cross-species transmission to grazing horses. Horses serve as amplifying intermediate hosts and humans are infected following exposure to their bodily fluids, tissues and excretions. There is no evidence of direct bat-to-human or ongoing human-to-human transmission. (b) Crimean-Congo haemorrhagic fever is maintained by ticks which serve as both a reservoir and a vector, in sylvatic and domestic cycles involving small mammals, birds and livestock. Humans can be infected via tick bites or via direct contact with infected animal blood or tissue. (c) Ebola virus is thought to persist within a bat natural reservoir, either directly infecting humans during slaughter, or indirectly via the infection of intermediate hosts such as gorillas, chimpanzees and duikers. (d) Sin Nombre virus is maintained by the North American deer mouse, occasionally causing infection in humans or other dead-end hosts such as coyotes, dogs and cats, through the inhalation of aerosolised excreta. (e) West Nile virus is a mosquito-borne virus maintained primarily by the Culex species mosquito in various bird species. Humans and other dead-end hosts such as horses are infected via the bite of infected mosquitoes. Reproduced from Hood et al., Current Opinion in Virology, 2024 [9]

Canonical frameworks within the literature often describe pathogen emergence as a linear, sequential and inherently directional process [10-14]. By contrast, the synthetic model of spillover presented by Plowright et al. seeks to capture the nonlinear and spatiotemporally dynamic nature of these interactive processes spanning from the molecular to the ecological scales [15].

The Plowright model describes three functional phases of CST. The first describes the pathogen pressure, or the total pathogen available to a human host, which is a function of the ecology of the reservoir host, pathogen release and survival [15]. Human behaviour then determines the likelihood,

route and dose of exposure. For example, infected Egyptian rousette fruit bats (*Rousettus aegyptiacus*) shed Marburg virus (species *Orthomarburgvirus marburgens*; genus *Orthomarburgvirus*; family *Filoviridae*) in faeces, which survives up to 5 days in the environment, during which time humans may be exposed to aerosolized excretions during cave disturbing activities, such as mineral or guano mining, or eco-tourism [16-18]. Other filoviruses, such as Ebola virus (species *Orthoebolavirus zairense*; genus *Orthobolavirus*; family *Filoviridae*) are released by excretion or slaughter from the natural reservoir (suspected to be bats), surviving up to 7 days in the environment [19]. The majority of spillover incidents in Gabon and the Democratic Republic of Congo have occurred from human contact with the carcasses of infected intermediate hosts, such as gorillas (*Gorilla gorilla*), chimpanzees (*Pan troglodytes*) and duikers (*Cephalophys* species), which are hypothesized to be infected by the consumption of fruit contaminated by the oral fluid, blood or placenta of infected bats [20-25].

The final phase of the CST model describes the probability of infection given cross-species exposure to the pathogen [15]. Host susceptibility is determined by host-range barriers (i.e., structural barriers, molecular compatibility, innate immunity) and the viruses' ability to overcome them. As a critical early step in the successful infection of a novel host, viruses must be able to bind to cell surface receptors, typically through rapid evolutionary adaptation or the ability to use conserved receptors (for example, the broad species tropism of filoviruses reflects their use of the highly conserved cholesterol transporter Niemann-pick C1 (NPC1)) [26, 27]. Viral adaptation to host receptor variation is complicated by the remarkable number and specificity of viral-host protein interactions, with proteomics studies identifying in excess of 194 protein interactions between Ebola virus and human host cells [28]. Each adaptive change may come at a fitness cost to the pathogen, and thus the accumulation of each of these barriers and their corresponding changes may sum to an insurmountable barrier to novel host infection. Phylogenetic relatedness between reservoir and novel hosts lowers this barrier, as innate similarities in molecular (e.g., cellular receptor) and immunological environments "flatten the fitness valley" traversed during adaptation [11, 29-31]. However, host-switching between close genetic relatives may be thwarted by innate immune resistance or cross-immunity against related pathogens [5].

The alternative pathway for host-switching involves rapid evolution, which requires high genetic variation, such as that found in RNA viruses (particularly with multi-segmented genomes) due to their error-prone rapid replication, short generation times, and large viral populations.

Assuming viruses circumvent or encounter a permissive immune response (including interferon and cytokine antiviral responses), the next key determinant of successful host-switching is completion of replication and dissemination cycles. A hallmark of host-switching success appears to be the ability to replicate in the cytoplasm, thereby bypassing interaction with the host-specific complex cell machinery required to enter the nucleus [32].

Thus, cross-species transmission requires the pathogen to pass through an aligning series of gaps in the barriers which typically constrain the flow of pathogens between species [15]. These enabling conditions are dynamically influenced by virological, physiological, socio-economic, environmental and ecologic factors which serve to modify the risk of spillover across space and time [33].

1.2. Drivers of viral emergence, including land-use change and wildlife exposure

Land-use changes, such as the anthropogenic conversion of natural habitats for agricultural or urban use, drive spillover by fundamentally disturbing host ecology by altering their distribution, behaviour and condition, which may increase both human interaction and pathogen excretion [34-36]. Modelling approaches integrating satellite-based remote sensing data have demonstrated this relationship between deforestation and Ebola virus disease (EVD) outbreaks in Central and West Africa [37, 38]. Further, evidence shows human-disturbed landscapes may select for species traits correlated with host status, driving a net increase in zoonotic host diversity [39]. Other land-use changes including urbanisation and agricultural intensification, alongside climate change, have also been identified as major upstream drivers of spillover [40-43].

More proximal drivers of spillover are often context-dependent. For example, risk factors associated with filovirus spillover events in Africa highlight the relative importance of economic marginalisation, and the hunting and consumption of wildlife (historically referred to as "bushmeat"[1]) [44-53]. Indeed, the increasing frequency of filovirus disease outbreaks in Africa has been partly attributed to wildlife hunting, in addition to deforestation and mining [50]. As highlighted by these examples, filoviruses are critical to study within the context of spillover, not only from a mechanistic perspective as a model for emergence, but because they represent a critical junction of disease and overlapping complex challenges, including climate change, rural poverty, armed conflict, and the legacy of extractive colonialism [54].

[1] While the term "bushmeat" has historically been used in the literature, this terminology has been critiqued as perpetuating colonial narratives that frame traditional wildlife hunting and consumption practices as inherently problematic, abstracted from their cultural context and the structural inequalities that shape food systems (for further reading, see: Muller, S.M., Carnistic Colonialism: *A Rhetorical Dissection of "Bushmeat" in the 2014 Ebola Outbreak*. Frontiers in Communication, 2021, Volume 6). I therefore preferentially use the term "wildlife hunting" to avoid reinforcing stigmatising discourse that views communities' longstanding subsistence practices—specifically the consumption of animals not typically understood as "food animals" through a normative Western lens—as inherently aberrant.

1.3. Pathogen prioritisation: high-consequence spillover

The World Health Organization (WHO) Research and Development Blueprint provides a systematic framework for prioritising pathogens that pose the greatest risk for severe outbreaks with limited countermeasures, focusing on factors like human-to-human transmission potential, disease severity, and the absence of approved therapeutics [55]. Both filoviruses (including Ebola and Marburg viruses) and paramyxoviruses (such as Nipah and Hendra viruses) feature prominently on this list.

1.3.1. Filoviruses

1.3.1.1. Filovirus overview

Filoviruses are a group of enveloped, single-stranded, negative-sense RNA viruses in the *Filoviridae* family known to infect mammals, reptiles and fish [56]. First identified during a 1967 MARV outbreak of European laboratory workers infected by African green monkeys imported from Uganda, they were named for their filamentous appearance from the Latin word “filum” meaning “thread”.

The family *Filoviridae* includes eight genera, *Orthoebolavirus*, *Orthomarburgvirus*, *Cuevavirus*, *Striavirus*, *Thamnovirus*, *Dianlovirus*, *Oblavirus*, and *Tapjovirus*. Of these, only the orthoebolaviruses and orthomarburgviruses have been demonstrated to infect humans, in which they cause clinical disease of varying severity, characterised less by haemorrhage than the designation of “viral haemorrhagic fever” would imply. The predictable clinical course of disease begins with a non-specific febrile prodrome (anorexia, arthralgia, myalgia, headache, malaise) within a mean incubation period of 6.22 ± 1.57 days [57], progressing to severe gastrointestinal illness (vomiting, high-volume diarrhoea) and multiple organ dysfunction (haemorrhagic, renal, respiratory, neurological, cardiac), and finally entering the terminal phase 7-12 days following symptom onset. Fatal outcomes are typically associated with uncontrolled viral load, and a defective and dysregulated immune response (characterised by proinflammatory mediators), whereas survival is associated with early and regulated humoral and cellular immune responses (including robust, EBOV-specific antibodies and T lymphocytes) [58-61].

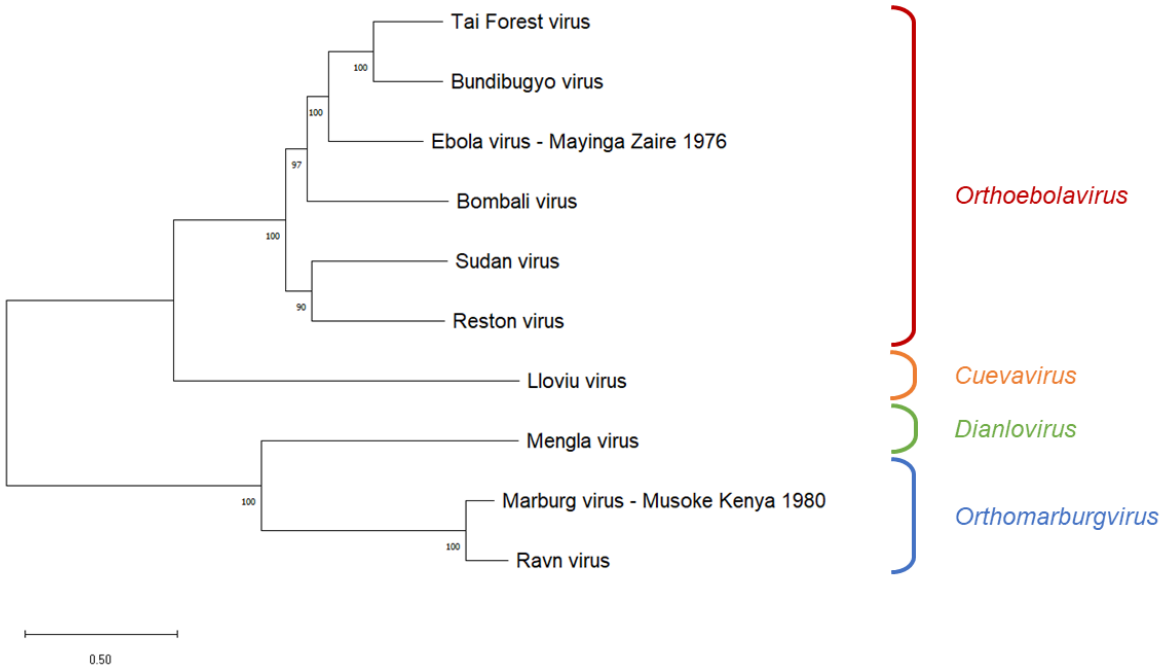


Figure 2 Phylogenetic tree of select filoviruses. The evolutionary history was inferred by using the Maximum Likelihood method and General Time Reversible model [62]. The tree with the highest log likelihood (-125642.17) is shown. The percentage of trees in which the associated taxa clustered together is shown next to the branches. Initial tree(s) for the heuristic search were obtained automatically by applying Neighbor-Join [63] and BioNJ [64] algorithms to a matrix of pairwise distances estimated using the Maximum Composite Likelihood (MCL) approach, and then selecting the topology with superior log likelihood value. A discrete Gamma distribution was used to model evolutionary rate differences among sites (5 categories (+G, parameter = 1.1757)). All positions with less than 95% site coverage were eliminated, i.e., fewer than 5% alignment gaps, missing data, and ambiguous bases were allowed at any position (partial deletion option). There were a total of 14,063 positions in the final dataset. Evolutionary analyses were conducted in MEGA11 [65].

Table 1 Summary of select filovirus species, by genera

Virus name	Abbreviation	Species	Human infectivity
		Cuevavirus	
Lloviu	LLOV	*Cuevavirus lloviuense*	No recorded human infections
		Dianlovirus	
Měnglà	MLAV	*Dianlovirus menglaense*	No recorded human infections
		Orthoebolavirus	
Bombali	BOMV	*Orthoebolavirus bombaliense*	No recorded human infections
Bundibugyo	BDBV	*Orthoebolavirus bundibuyoense*	Human infections associated with Ebola virus disease (EVD)
Reston	RESTV	*Orthoebolavirus restonense*	Human infections - asymptomatic
Sudan	SUDV	*Orthoebolavirus sudanense*	Human infections associated with EVD
Taï Forest	TAFV	*Orthoebolavirus taiense*	Human infections associated with EVD
Zaire	EBOV	*Orthoebolavirus zairense*	Human infections associated with EVD
		Orthomarburgvirus	
Marburg	MARV	*Orthomarburgvirus marburgense*	Human infections associated with Marburg virus disease (MVD)
Ravn*	RAVV	*Orthomarburgvirus marburgense*	Human infections associated with MVD

Grey: no recorded human infections; yellow: asymptomatic human infections, red: human infections causing clinical disease. * Previously Ravn Marburgvirus, however, currently the genus only includes a single species. MARV and RAVV are relatively distinct in genome sequence similarity, but occupy the same ecological niche and cause the same clinical presentation in humans and NHPs. Hence, they are considered by ICTV to be distinct viruses belonging to the same species.

1.3.1.2. Filovirus structure and function

Filovirus genomes share a similar genomic architecture, differing predominantly in the number of open reading frames (ORFs), which express 6-10 proteins, depending on the genus. The *Orthoebolavirus* genome contains 7 canonical ORFs (3′-NP-VP35-VP40-GP-VP30-VP24-L-5′), which direct the synthesis of proteins: nucleoprotein (NP), polymerase cofactor (VP35), matrix protein (VP40), glycoprotein (GP), transcriptional activator (VP30), ribonucleoprotein (RNP)-complex associated

protein (VP24), and a large protein (L) containing an RNA-directed RNA polymerase (RdRP) domain (Figure 3).

As with other *Mononegavirales*, EBOV's non-segmented, negative-sense ssRNA genomes are encapsulated within a helical nucleocapsid, which consists of the NP–viral RNA (vRNA) complex, VP24, VP30, VP35 and viral polymerase. The NP-vRNA complex acts as a scaffold for viral assembly and template for RNA transcription and replication [66]. VP35 initiates ssRNA transcription (as a cofactor of vRNA polymerase), in addition to antagonizing antiviral signalling pathways [67]. VP40 is involved in virus particle formation, coordinating virion assembly and egress [68].

The helical nucleocapsid acquires a host-cell plasma membrane-derived envelope during budding, which is decorated with heavily glycosylated trimeric (trimer of heterodimers) GP spikes on the viral surface, comprised of GP_1 (receptor binding ectodomain) and GP_2 (transmembrane fusion domain) subunits connected by a disulphide bond [69]. Unlike other enveloped viruses, such as paramyxoviruses, EBOV only contains one single surface protein (GP) which single-handedly effects all the processes to initiate infection, including cellular attachment, endosomal entry and membrane fusion. The larger GP_1 subunit comprises the glycan cap (GC), mucin-like domain (MLD) and receptor-binding site (RBS), whereas the GP_2 subunit contains the hydrophobic internal fusion loop (IFL), two heptad repeats (HR1 and HR2), membrane-proximal external region (MPER) and transmembrane anchor [69]. GP_1 is responsible for cell-surface attachment, whereas GP_2 mediates the fusion of viral and host cell membranes [70-72], together (primarily) determining tissue and cell tropism from the viral perspective.

Transcriptional editing of the ebolavirus GP gene involves a slippage region, where stuttering at a poly-uridine repeat results in a GP sequence frameshift, which together with host furin-dependent proteolysis, leads to the expression of smaller, non-structural GP proteins which are secreted from infected cells into extracellular space: soluble GP (sGP) (50-70 kDa, ~70% of mRNA transcripts), small soluble GP (ssGP) (36kDa, ~5% of transcripts) and Δ-peptide (40-residue) [73-75]. While the function of the truncated sGP isoform (364-residue c.f. 676-residue transmembrane-linked $GP_{1,2}$) has been long debated, it is believed to play an important role in host immune evasion, by acting as an antibody decoy (passively absorbing antibodies and interfering with ab-mediated clearance), or through antigenic subversion (actively redirecting the host antibody response towards epitopes not accessible on membrane-bound $GP_{1,2}$, or to induce cross-reactivity with shared epitopes allowing it to compete and bind for anti-$GP_{1,2}$ antibodies) [76].

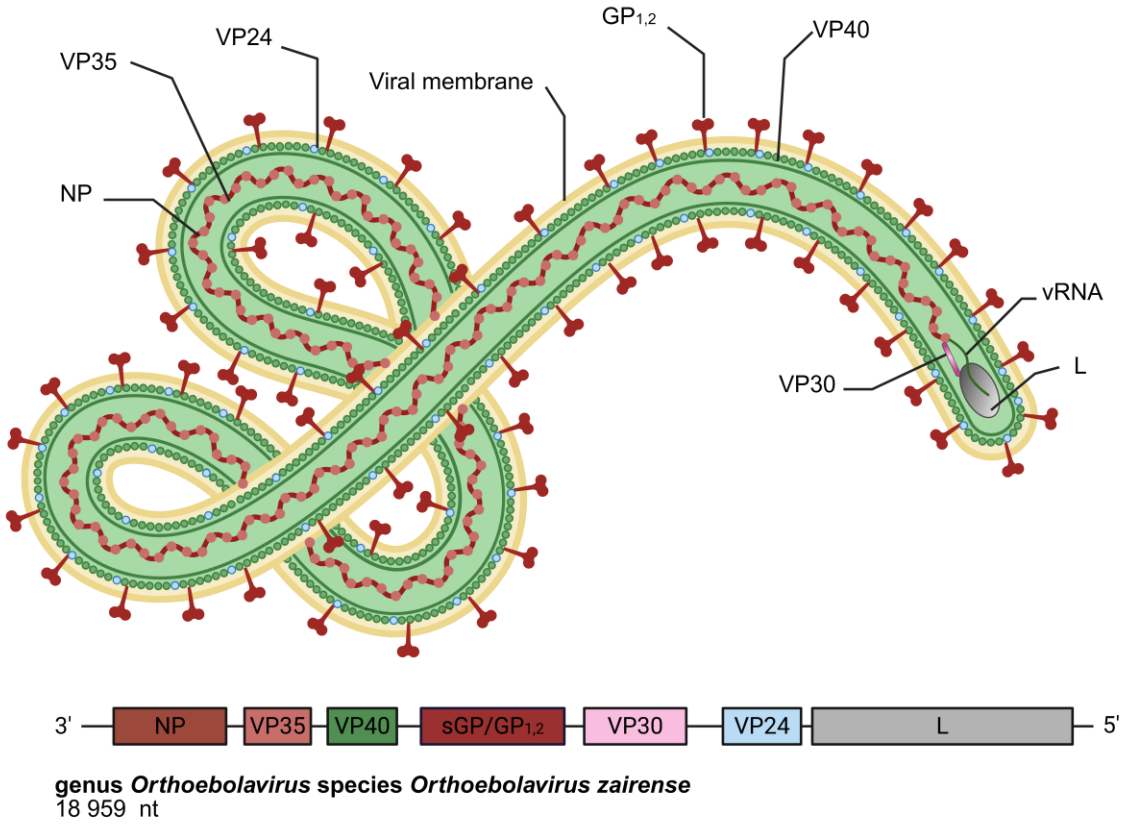


Figure 3 Ebola virus (EBOV) virion structure and genome organisation

(a) Virion structure: The EBOV viral genome (vRNA) is encapsidated by the nucleoprotein (NP) and associated with viral protein 35 (VP35), viral protein 30 (VP30) and the viral polymerase (L) to form the nucleocapsid. VP24 is also associated with the nucleocapsid, while the matrix layer beneath the viral membrane consists of matrix protein (VP40). The viral glycoprotein ($GP_{1,2}$) is anchored as trimers in the viral membrane. (b) Genome organisation: Orthoebolaviruses have a single-stranded RNA genome of negative polarity encoding seven viral genes, with protein-coding regions flanked by untranslated regions. The genome ends (leader (3'-end) and trailer (5'-end)) contain the replication promoters.

1.3.1.3. Filovirus entry and infectious cycle

Early EBOV infection primarily targets mononuclear phagocytes (e.g. macrophages, microglia, Kupffer cells in the liver) and dendritic cells, which migrate to regional lymph nodes, liver and spleen, systemically disseminating the virus [77, 78]. While the definitive host cell surface receptor remains to be identified, EBOV is thought to enter host cells by receptor-mediated micropinocytosis [79]. In the late endosome, GP is sequentially cleaved by cathepsins (removing the glycan cap and mucin-like domain) in order to expose the receptor-binding site of GP_1 [79]. Low endosomal pH (~pH 5.0) induces GP_1 binding to the Niemann–Pick C1 protein intracellular cholesterol transporter 1 (NPC1) receptor, catalysing the GP_2-mediated fusion of viral and endosomal membranes and releasing the RNP complex into the cytosol [26]. Here, the filovirus genome undergoes replication and transcription into mRNAs. Viral proteins are translated by free ribosomes in the cytosol or endoplasmic reticulum (for $GP_{1,2}$).

Progeny RNP complexes (containing NP, L, VP35, and VP40) and viral proteins are transported to the plasma membrane for assembly [80] and budding through the membrane "lipid raft" microdomains [81] (Figure 4).

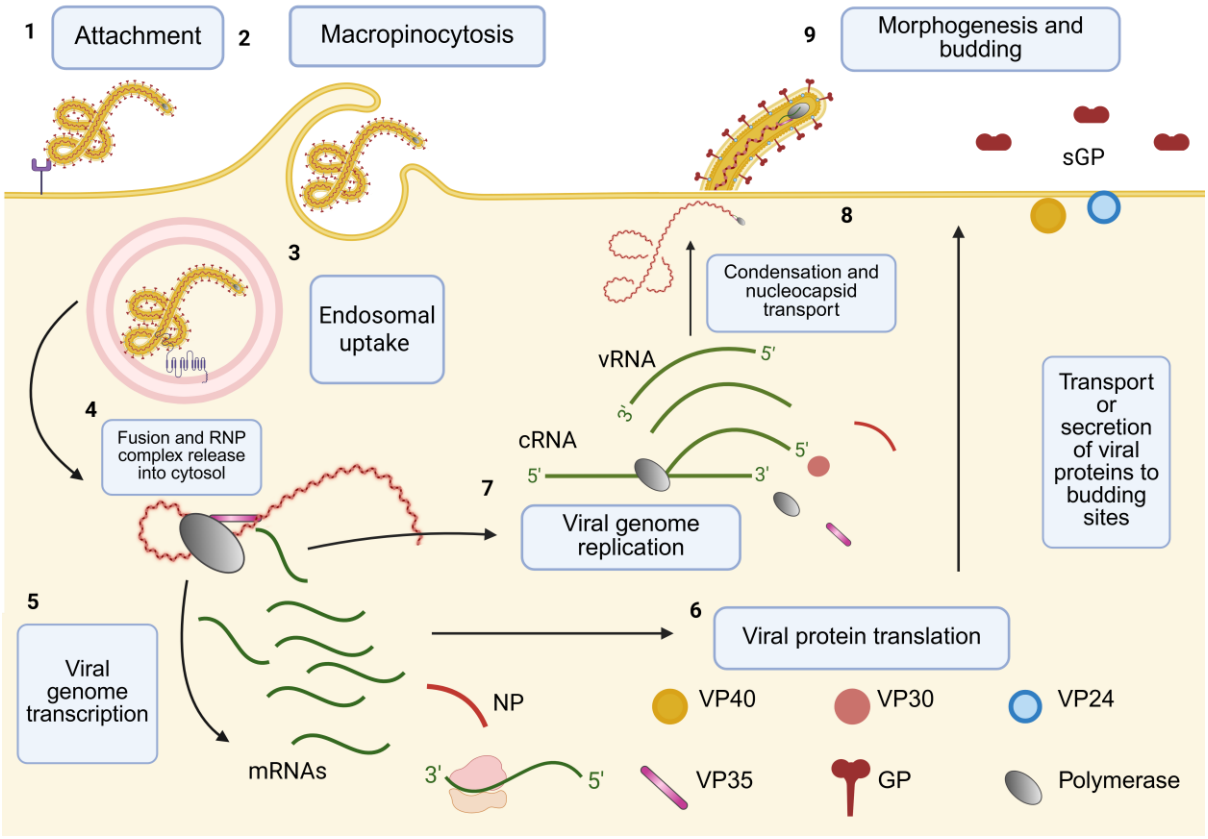


Figure 4 *Orthoebolavirus* life cycle (1) Viruses attach to cell-surface receptors. (2) Viral particles are taken up via micropinocytosis. (3) Late endosomal acidification allows cleavage of $GP_{1,2}$ by host cathepsins leading to (4) Binding to the intracellular NPC1, fusion of viral and endolysosomal membranes and release of the nucleocapsid into the cytosol. (5) Filovirus genes are transcribed into mRNAs. (6) Viral proteins are translated in the cytosol or endoplasmic reticulum (for $GP_{1,2}$). (7) Filovirus genome is replicated. (8) Mature progeny ribonucleoprotein complexes are condensed into nucleocapsids by VP24 and, along with viral proteins (other than GP), are transported to the plasma membrane via actin filaments where (9) Morphogenesis and budding occurs.

1.3.1.4. A brief history of human filovirus outbreaks and their origins, including the reactivation of persistent infection

Of the large-scale zoonotic disease outbreaks, filoviruses have amongst the highest mortality. The largest recorded filovirus outbreak, caused by EBOV, occurred in West Africa in 2013–2016 and resulted in 28,646 cases and 11,323 deaths [51]. This epidemic was unprecedented in both size and location, highlighting gaps in our understanding of the pathogen's biology and epidemiology. A 2024 outbreak of MARV in Rwanda demonstrated yet again the expansion of known endemic zones, and the ongoing threat filoviruses pose to global health and security.

Filovirus outbreaks have been shown by epidemiological and molecular evidence to originate from a single spillover event with sustained human-to-human transmission, or from multiple spillover events with minimal ongoing transmission (short stuttering chains) [82-85]. The size, duration, and case fatality rates (CFRs) of outbreaks have varied substantially, which has been attributed to fundamental differences in virulence between the species, population differences (health status, genetics), and response effectiveness (case recognition, surveillance, healthcare accessibility and quality) [86]. Ongoing human transmission within these outbreaks has historically been driven by under-resourced healthcare systems (due to hospital infection control practices [87], and in early outbreaks, through nosocomial infection following the reuse of contaminated needles [88, 89]), burial practices (washing of corpses before burial and touching at funerals), mobile and interconnected populations, economic and political insecurity and civil conflict [46, 54].

While the zoonotic origins of the majority of filovirus outbreaks are well established [90, 91], the 2018—2020 EVD outbreaks in the Democratic Republic of the Congo (DRC), and 2016 and 2021 outbreaks in Guinea have challenged this paradigm by providing epidemiological and genomic evidence of outbreaks caused by the reactivation of clinically latent persistent infections [92-96].

The persistence of EBOV in immune-privileged anatomical sites such as the testes, eyes, central nervous system and glandular breast tissue has been well described in both animal models [97, 98] and clinically recovered human survivors, including in the presence of circulating anti-EBOV antibodies and the absence of EBOV in peripheral blood and other organs [99-101]. Nonhuman primate (NHP) studies have implicated CD68+ macrophages and monocytes as the cellular reservoir of persistent EBOV infection in the eye, brain ventricles and choroid plexuses, and suggest through archival in situ hybridisation that EBOV may progressively disseminate into sites of persistence through vascular structures [98, 102]. Such persistence may result in recrudescence of severe disease, as documented in a patient who relapsed with meningoencephalitis and high viral load (peak cycle threshold (Ct) value 13.2) 9 months after recovery from the initial episode [103]. Persistence has also resulted in detectable viral shedding in bodily fluids such as semen and breast milk, infrequently causing ongoing silent transmission months after recovery, as seen in various atypical chains of transmission [99, 103-109]. The occurrence and duration of asymptomatic semen persistence among survivors is heterogenous, and many early studies were not designed or powered to produce population-level estimates. A 2015 - 2017 longitudinal cohort study (n=220) of EVD survivors in Sierra Leone found 75% of men were semen positive by qRT-PCR 6 months post-infection and 50% at 204 days [110]. A 2025 meta-analysis of 287 observations from 66 individuals across 3 studies estimated that for 5,000 male EBOV survivors, a median of 7 individuals (95% CI: 0—43) would have detectable EBOV RNA in semen at 5 years post-infection [101]. Risk factors associated with persistence included severe viraemia during acute disease (as measured by cycle threshold (Ct) value) [110], increased age [110-112], and less convincingly, immunosuppression which is hypothesised to delay clearance and allow for resurgence [113].

Interestingly, severe disease and correspondingly high viraemia may not be requisite for the deposition of virus into some immune-privileged sites, with the example of viral persistence in breast milk following an asymptomatic infection, which resulted in the likely vertical transmission to an infant [99].

The molecular mechanisms governing persistence remain unknown, though various theories have been developed. The presence of defective-interfering EBOV genomes has been suggested as one such mechanism, wherein aberrantly synthesised genomes compete with non-defective and cytopathic wild-type genomes, maintaining viral replication below the detectable threshold, allowing for the persistence of a latent and attenuated infection [114]. However, more recent longitudinal deep-sequencing analysis of an acute infection and subsequent recrudescence found relatively low frequency of defective genomes and minimal change in viral sequence at the consensus and minor variant level, lending evidence to alternative theories which suggest the suppression of viral replication as a mechanism for evading host responses [115].

A reduced rate of viral replication may be attributable to either latency or continuous but slow replication. The reduced long-term evolutionary rate of persistent EBOV was consistently reported in Liberia, Sierra Leone and Guinea [106, 116, 117]. For example, multiple 2015 Liberian outbreaks which originated from persistently infected cases were characterised by low genetic divergence and a reduced evolutionary rate (observed five-fold reduction) during persistent infection. Indeed, reduced evolutionary rate was used as a signature to further identify additional EVD cases potentially linked to persistently infected individuals [106, 116].

While the host-pathogen determinants of latency or reduced replication are unknown, a mechanism of selection by the adaptive immune system for replication-deficient variants evading viral recognition within immune privileged sites, has been suggested [118]. The role of further selection pressures, namely antibody-mediated therapeutics (such as convalescent sera or standard-of-care monoclonal antibodies), in the emergence of escape mutants remains unclear [102, 119].

1.3.1.5. Ecology of filoviruses: evidence for bats as the key reservoir

The ecology and natural history of filoviruses in their animal reservoirs has eluded scientific discovery for decades, despite major early field investigations in the DRC [88, 120-122], Sudan [123], Côte d'Ivoire [124], and Central African Republic (CAR) [125] which sampled >7,000 diverse sylvatic and domestic vertebrate and >30,000 arthropod taxa, though individual sample sizes per species were highly variable. Subsequent experimental inoculations of potential hosts found various species to be permissible to filovirus infection, but highlighted Chiropterans' unique ability to asymptomatically develop and survive transient viraemia [126, 127]. In 2005 bats were directly implicated as natural reservoirs of EBOV by the detection of RNA and EBOV-specific antibodies [128], and in 2007 MARV was isolated from an Egyptian rousette fruit bat (*Rousettus aegyptiacus*) [129]. Since then, the rapidly

accumulating body of evidence provided by ongoing ecological, molecular, serological and virological studies have served to establish the Egyptian rousette as the natural reservoir for MARV, and further evidence the role of bats in the maintenance and transmission of other filoviruses [129-135]. Particularly compelling is the repeated isolation of RNA and anti-filovirus antibodies, and rarely, infectious virus, from a growing number of healthy bats of various species (Table 2), and the experimentally demonstrated immunotolerance of filoviral infections among Chiropteran families [136].

Though the sum of evidence implicates bats as the principal reservoir host, the involvement of other understudied species, or the existence of a reservoir complex of multiple species cannot be excluded [137-139]. The role of arthropod vectors is also yet to be determined, with the notable absence of ectoparasites from majority of these investigations, despite their demonstrated competence as vectors [140]. An exception to this is the 2022 *Miniopterus schreibersii* bat and ectoparasite survey which identified Lloviu virus (LLOV) RNA but no evidence of active viral replication in engorged ectoparasites on PCR-positive animals, which highlighted but failed to clarify their role as natural or mechanistic vectors or dead-end spillover hosts [141].

Table 2 Ecological investigation of filoviruses in bats

Virus	Serologic evidence	Molecular evidence (genomic RNA detection)	Virus isolation
MARV	*Hypsignathus monstrosus* [142] *Rhinolophus eloquens*[134] *Rousettus aegyptiacus* [18, 129, 134, 135, 142, 143]	*Miniopterus inflatus* [134] *Rhinolophus eloquens* [134] *Rousettus aegyptiacus*[18, 129, 135, 144]	*R. aegyptiacus* [18, 135]
EBOV	*Epomops franqueti* [25, 142, 145] *Epomophorus gambianus* [145, 146] *Eidolon helvum [146-148]* *H. monstrosus* [25, 142, 145, 146] *Lissonycteris angolensis*[146] *Myonycteris torquata* [25, 142] *Micropteropus pusillus* [142] *Miniopterus schreibersii* [149] *Mops condylurus* [142] *Nanonycteris veldkampii* [145] *Rousettus aegyptiacus* [146]	*Myonycteris torquata* [128] *Epopmops franqueti* [128] *H. monstrosus* [128] *Myotis ricketti* [150]	
SUDV	*E. helvum* [146, 148] *H. monstrosus*[146] *M. pusillus* [146] *R. aegyptiacus*[143, 146]		
RESTV	*Cynopterus sphinx*[151] *E. gambianus* [145] *E. helvum* [148] *Hipposideros* spp.[151] *H. monstrosus* [145] *M. schreibersii*[151] *Pipistrellus pipistrellus*[151] *Myotis* spp.[151] *Myotis ricketti* [150, 151] *Rhinolophus affinis* [151] *R. aegyptiacus* [143] *R. leschenaultia* [151] *Scotophilus kuhli* [151]		
BOMV		*M. condylurus* [152-155] *Chaerephon pumilus* [152-155]	
BDBV	*E. helvum* [148] *R. aegyptiacus* [143]		

TAFV	*E. helvum* [148] *R. aegyptiacus* [143]		
LLOV	*M. schreibersii* [156] *R. aegyptiacus* [143]	*M. schreibersii* [157, 158]	*M. schreibersii* [141]

1.3.2. Paramyxoviruses

1.3.2.1. Paramyxovirus overview

Paramyxoviruses are enveloped, single-stranded, negative-sense RNA viruses in the highly diverse *Paramyxoviridae* family that infect a broad range of vertebrate hosts with varying degrees of specificity, ranging from the highly human-specific measles virus (subfamily *Orthoparamyxovirinae*, genera *Morbillivirus*) to the broadly infecting canine distemper virus (subfamily *Orthoparamyxovirinae*, genera *Morbillivirus*). This large viral family contains four subfamilies, 17 genera, and > 80 viruses, of which only 10 will be described in this thesis (Table 3).

Table 3 Select paramyxoviruses, by genera

Virus name	Abbreviation	Species	Human infectivity
		Henipavirus	
Nipah	NiV	*Nipah henipavirus*	Human infections associated with severe clinical disease
Hendra	HeV	*Hendra henipavirus*	Human infections associated with severe clinical disease
Cedar	CedV	*Cedar henipavirus*	No recorded human infections
Kumasi or Ghanian bat henipavirus	KV or GhV	*Ghanaian bat henipavirus*	No recorded human infections
Mòjiāng	MojV	*Mòjiāng henipavirus*	No recorded human infections
Angavokely	AngV	*Angavokely henipavirus*	No recorded human infections
Melian	MeliV	*Melian henipavirus*	No recorded human infections
		Rubulavirus	
Yeppoon	YepV	*Yeppoon paramyxovirus*	No recorded human infections
Grove	GroV	*Grove paramyxovirus*	No recorded human infections
		Pararubulavirus	
Menangle	MenV	*Menangle pararubulavirus*	Human infections - asymptomatic

Grey: no recorded human infections; yellow: asymptomatic human infections, red: human infections causing clinical disease.

Within this family, henipaviruses and parahenipaviruses, and in particular their prototype Hendra (HeV) and Nipah (NiV) viruses, have been identified as pathogens of public health concern, due to their virulence, epidemic potential, and the absence of licensed vaccines or therapeutic countermeasures.

Both viruses, named for the sites of their initial isolations, circulate asymptomatically in fruit bat reservoirs and occasionally spillover into intermediate hosts (e.g., horses in HeV, domestic pigs in NiV-Malaysia) or humans, causing multi-organ acute systemic vasculitis culminating in neurological and respiratory disease with CFR of 40-70%.

HeV was the first henipavirus to be discovered, and was isolated in 1994 following an outbreak of respiratory disease in 21 horses, and neurologic disease in 2 humans (with a 50% CFR) [159]. Sporadic outbreaks of equine HeV infection have since occurred, with a total of 90 equine cases and 7 human cases, all infected via close contact with bodily fluids of infected horses (57% CFR).

NiV-Malaysia (NiV-M) was initially isolated in 1998 following an outbreak of 282 human cases in peninsular Malaysia (39% CFR) and 11 human cases in Singapore (9% CFR), with pigs acting as an amplifying host (1 million culled) [160]. NiV-M caused a second outbreak in 2014 in the Philippines (17 human cases, 53% CFR) where horses were suspected as an amplifying host, however, it has not been detected in the region since [161]. By contrast, NiV-Bangladesh (NiV-B) continues to cause yearly outbreaks in Bangladesh (341 human cases, 71% CFR) and India (102 human cases, 73% CFR), following direct transmission from the *Pteropus* reservoir, with some human-to-human transmission.

The ongoing discovery of novel henipaviruses, including the non-chiropteran (rodent- and shrew-derived) parahenipaviruses such as Mòjiāng (MojV) virus, along with serological evidence of exposure outside of known outbreak areas (including central Africa) suggests that both the genetic diversity and the global distribution of zoonotic paramyxoviruses may be broader than previously appreciated [162].

Table 4 Summary of select paramyxovirus detections (chronological)

Virus	Year of detection	Detection	Animal reservoir/ intermediate host	Human cases
Hendra (HeV)	1994	Outbreak of fatal respiratory and neurological disease amongst horses and horse trainers in Brisbane, Australia [159]	Fruit bats (*Pteropus* spp.) via horses	Yes
Menangle (MenV)	1997	Outbreak of reproductive disease amongst pigs and respiratory disease in pig farmers in Sydney, Australia [52, 53]	Fruit bats (*Pteropus* spp.) via pigs	Yes
Nipah (NiV)	1998	Outbreak of fatal encephalitis amongst pig farmers in Malaysia [160]	Fruit bats (*Pteropus* spp.) via pigs	Yes
Ghanian bat henipavirus (GhV)	2008	Identified in fruit bat colony in Kumasi, Ghana [54]	Fruit bats (*Eidolon helvum*)	No
Cedar (CedV) Grove (GroV) Yeppoon (YepV)	2012	Identified in fruit bat colony in Queensland, Australia [163]	Fruit bats (*Pteropus* spp.)	No
Mòjiāng (MojV)	2012	Identified following animal reservoir investigation of a cave following 3 cases of fatal pneumonia in miners in Mòjiāng, China [164]	Rat (*Rattus flavipectus*)	Suspected
Melian (MeliV)	2018	Identified in organs collected from rodents and shrews trapped near Guéckédou, Guinea during routine pest control [165]	Large-headed shrew (*Crocidura grandiceps*)	No
Angavokely (AngV)	2022	Identified from urine samples of wild Eidolon bats in Madagascar [166]	Fruit bats (*Pteropus* spp.)	No

1.3.2.2. Paramyxovirus structure and function

The henipavirus genome (organised 3'-N-P-M-F-G-L-5) comprises 6 ORFs encoding the structural proteins: nucleoprotein (N), phosphoprotein (P), matrix protein (M), fusion protein (F), attachment glycoprotein or receptor binding protein (G, H, H/N) and large protein/polymerase (L) (Figure 5). N

encapsidates vRNA, and together with L and P (which form the RNA-dependent polymerase complex), forms the viral replicase responsible for genome amplification. M coordinates virion assembly and budding, while F and G/H/HN glycoproteins mediate host cell entry.

In a defining feature of paramyxoviruses, the P gene undergoes mRNA editing (pre-programmed frameshifts for the use of an alternative start codon) to additionally express truncated versions of the P protein: accessory proteins V, W and C. While our understanding of their function is incomplete, they are implicated as innate immune system antagonists, in part by sequestering STAT1 and STAT2 [167]. Interestingly, CedV is the only known paramyxovirus that lacks both mRNA editing and coding capacity for V and W proteins, rendering it susceptible to interferon-induced effects, providing a potential explanation for its lack of pathogenicity in animal models [168].

Another notable feature of the paramyxovirus genome organisation is that they are governed by the "rule of six" which dictates that genomes must be of polyhexameric length (6n+0 nucleotides in length) for replication. This requirement is thought to reflect the mode of genome encapsidation by the N protein [169].

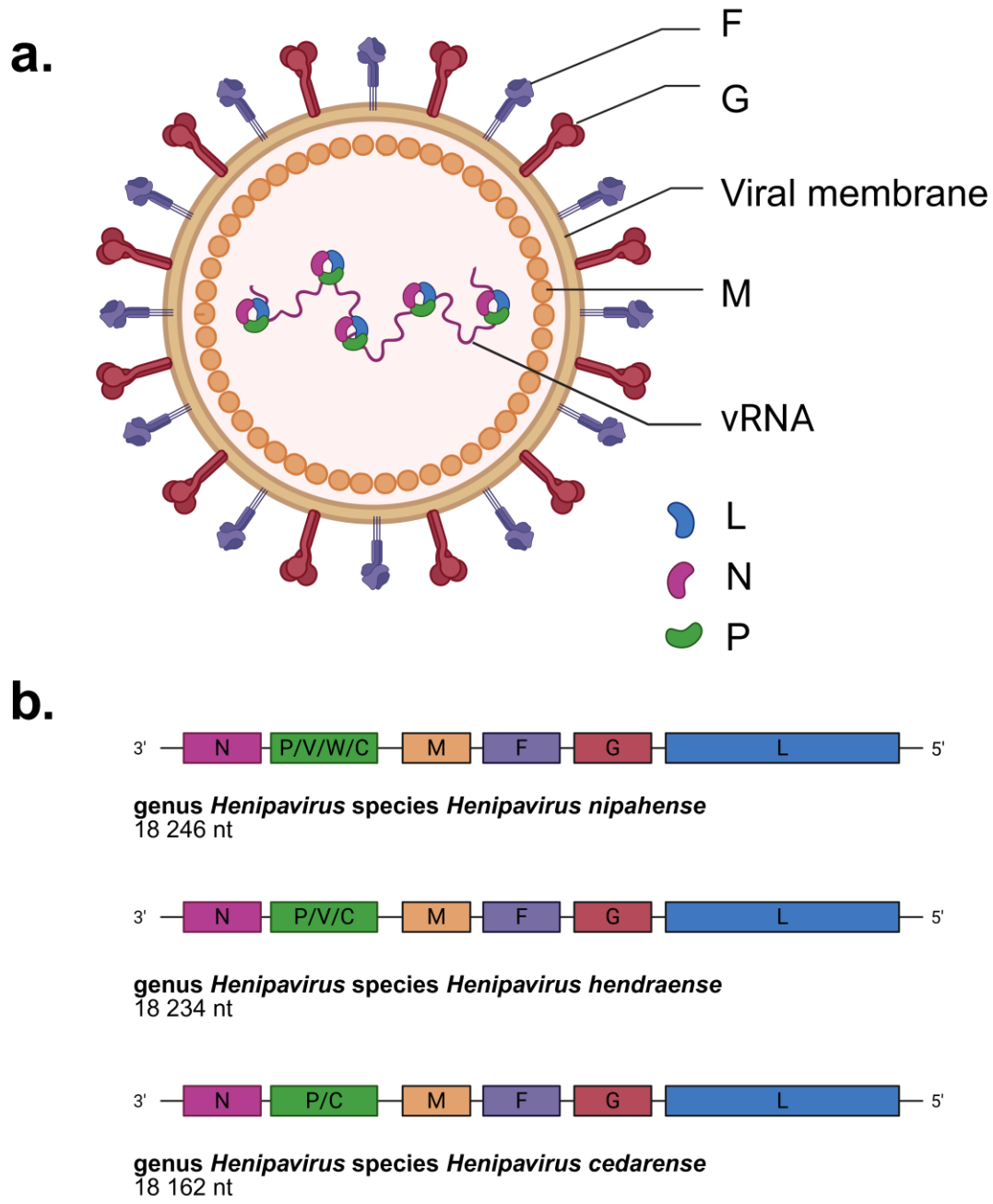


Figure 5 Henipavirus virion structure and genome organisation (a) Virion structure: The henipavirus nucleocapsid-associated proteins consist of viral RNA (vRNA) binding nucleocapsid protein (N), polymerase-associated phosphoprotein (P) and a large protein (L). The membrane-associated proteins include: the unglycosylated inner membrane or matrix protein (M), and two glycosylated membrane proteins, fusion protein (F) and an attachment glycoprotein (G), also known as the receptor binding protein (RBP) or the haemagglutinin-neuraminidase protein. Viral membrane lipids are derived from host cell plasma membrane. (b) Genome organisation (3'- to 5'-) of Nipah virus (NiV), Hendra virus (HeV) and Cedar virus (CedV): Henipaviruses have a single-stranded RNA genome of negative polarity encoding nine to seven viral genes. The unedited P mRNA encodes phosphoprotein (P) protein. Additional non-structural proteins (C, W) are expressed using multiple secondary translational start sites within the P gene. Co-transcriptional editing of the P mRNA leads to expression of the zinc-binding cysteine-rich (V) protein, with the exception of CedV.

1.3.2.3. Paramyxovirus entry and infectious cycle

Henipaviruses are notable for their broad host range due to their ability to utilise the highly-conserved ephrin cell-surface glycoproteins, which are widely distributed in vertebrates, and, in the case of ephrin-B3, highly expressed in arterial endothelial cells [170]. However, profiling of receptor usage amongst henipaviruses is far from complete, and experimental studies of resistant mice with functional viral receptors have highlighted that other host factors may be important [171]. Henipaviruses enter host cells via direct fusion at the plasma membrane, which begins when the receptor-binding protein (G for henipaviruses, H or HN for other paramyxoviruses) binds to cellular receptors [170]. The engagement of RBP with a receptor induces conformational changes in G that trigger F to form a fusion pore with the host cell membrane, releasing viral nucleocapsid into the cytoplasm [172]. Viral RNA is transcribed and replicated by the viral polymerase complex (N, P, L). Newly synthesised viral proteins and RNA are then assembled into new virus particles which bud from the infected host cell plasma membrane. A hallmark of paramyxoviruses is syncytium formation, where cell-cell fusion results in the formation of multinucleated cells, allowing the virus to spread from infected to naïve cells without the assembly and budding of free virions [173].

1.3.2.4. Paramyxovirus ecology

Bats are the suspected ancestral hosts of *Paramyxoviridae*, and Old-World fruit bats (family *Pteropididae*) are recognised reservoir hosts of prototypical zoonotic henipaviruses: HeV and NiV, in addition to GhV, CedV, YepV, GroV, AngV. Shrews and rodents have been identified as important reservoirs for certain paramyxoviruses, such as MojV, particularly in the *Orthoparamyxovirinae* subfamily.

1.4. Ecological field studies of viral dynamics in bats

1.4.1. Overview of field-based studies

Of the published field studies investigating the viral ecology of bats, many utilised a broad range of serological (e.g., Enzyme-Linked Immunosorbent Assays (ELISA), western blot, bead-based assays), molecular (e.g., conventional, real-time, family-wide consensus RT-PCR analysis, metagenomic next-generation sequencing), histopathological (e.g., immunohistochemistry) and virus isolation methods.

The majority of sampling was non-destructive, and consisted of pooled colony-level urine or faecal samples from caves and roosts or individual swabs (oral or rectal), and/or venous blood; while destructive sampling further included muscle, skin, lung, spleen, liver, kidney, bone, bone marrow and ganglia. In general, for paramyxoviruses, urine, tissue, serum, and faecal samples appeared to have higher PCR prevalence than blood, whereas saliva and swab samples had lower prevalence [174]. Of the tissues, spleen had the highest PCR prevalence (excluding pooled tissue) [174].

Sample transport methods included dry with cold chain, viral transport media and RNA stabilisation solution [175], though preservation of genetic material proved challenging [22].

Species identification was performed morphologically or via molecular tests, and the collection of host metadata (e.g., age, sex, reproductive and clinical status) was unfortunately limited overall.

The majority of the filovirus ecology studies were cross-sectional surveys, with only 26% reporting data longitudinally, and others choosing to instead pool data over space and time [176]. Such non-probabilistic and single event sampling designs fail to capture the sporadic nature of viral shedding [177], and pooling the data over time may bias viral detection estimates and epidemiological parameters in ways that cannot be corrected for in a statistical model [176].

Increased bat surveillance has identified several novel filoviruses in bats from Asia [178-180], Bombali virus (BOMV) in Africa [153, 154, 181] and the first endemic filovirus, LLOV, in Europe [141, 157, 158]. However, overall sampling efforts show significant geographic biases, largely representing countries where human outbreaks have occurred [50]. Literature reviews have highlighted geographic surveillance gaps in Latin America, Oceania and Western Asia [176, 182] and also central and southern Africa, including in countries such as Cameroon, despite evidence of henipavirus spillover into human populations [174].

Taxonomic sampling biases are also evident in surveillance, with machine-learning phylofactorization revealing that filoviruses are widely dispersed across the bat phylogeny, and sampling effort, rather than biological factors, was the primary predictor of filovirus detection. Similar species biases affect paramyxovirus surveillance: a single clade of 16 *Pteropus* species (including *P. giganteus, P. lylei, P. poliocephalus, P. alecto*) was significantly oversampled, driven by recent (1994 onwards) interest in the *Pteropus*-Hendra virus system in Australia, and to a lesser extent Nipah virus in South Asia (India and Bangladesh), resulting in disproportionate sampling of *Pteropus* species in these regions in the early 2000s [174]. Viral detection also reflects this bias, with Hendra (52,006 samples), Nipah (46,089 samples) and Cedar (2,139 samples) henipaviruses overrepresented relative to other detected paramyxoviruses [174]. This heterogenous sampling effort highlights the need to expand surveillance both geographically and across the bat and viral phylogenetic trees [183].

Collectively, these studies highlight the manifold challenges of disentangling the complex disease ecology of bat-borne viruses. The highly mobile, nocturnal, and colonial nature of bats present a significant logistical challenge within these remote settings [146]. Methodological inconsistencies further complicate the field: studies employed multiple diagnostic methods, sampling designs and reporting methods, and the absence of standardised assay protocols and reference standards hinders the meaningful comparison of results across studies [25, 120, 121, 142, 145, 147, 148]. Despite continuing methodological advancements such as deep sequencing, which promise a new era of unbiased viral

discovery, the role of viral isolation for functional characterisation remains essential, yet challenging, with only three successful isolations of a filovirus directly from bats thus far.

1.4.2. Common themes of bat ecological studies and gaps in knowledge

These ecological field studies of bats have been invaluable in shedding light on the viral transmission dynamics within the reservoir host. They provide no evidence of vertical transmission of filoviruses, having identified MARV PCR-positive females with PCR-negative placentas and new-borns [135]. Rather, they paint a dynamic picture of horizontal circulation wherein juveniles are exposed to the virus during early independence following the waning of maternal antibody protection [18, 135].

The most revealing ecological studies involve systematic, hypothesis-driven, longitudinal investigations over space and time. For example, many revealed spatiotemporal pulses in viral shedding or seroprevalence, relating to synchronous reproductive patterns, and representing elevated periods of public health risk [18, 135, 143].

In the absence of evidence, spatiotemporal pulses have been hypothesised as being driven by persistently infected bats exposed to common intrinsic or extrinsic stressors (e.g. reproductive status, seasonal nutritional availability) causing reactivation of latent infections and episodic shedding [184]. Alternatively, the transient epidemics hypothesis suggests that colonies go through oscillating cycles of epidemics, driven by waning population immunity and viral reintroduction, causing waves of transmission between susceptible hosts. Birthing periods may increase contact rates, and contribute a seasonal influx of susceptible individuals [185], with pups then contributing to shedding pulses as they develop productive initial infections.

Other critical knowledge gaps regarding the natural history of infection and the disease ecology of the reservoir host remain. While there is evidence to suggest that within-host infection dynamics are best characterised by the "susceptible—infected—recovered" (SIR) cycle [126, 186], the question of persistent infection versus acute re-infection remains. Such questions surrounding the outcomes of filovirus infection, including shedding, persistence and the development of carrier status, may only be definitively answered by individual-level longitudinal animal infection studies [184]. Further questions regarding global viral prevalence, dynamics and spillover over time remain challenged by geographic and taxonomic sampling biases, lack of consolidated data (or databases which exclude negative results), and disaggregated metadata (location, date, seasonality, host metadata, tissue types, sampling and detection methodologies etc.). Finally, novel approaches such as the use of museum specimens for efficient taxonomically broad sampling across space and time, and the development detailed viral-host datasets for the training of predictive machine learning models offer new opportunities for the field.

1.5. Bats as unique viral reservoirs and cryptic hosts

Including both filoviruses and henipaviruses, bats are critical reservoirs for four out of the nine WHO-designated priority viruses of epidemic concern, and are thus the subject of intensive interest.

The pervasive theory that bats have a greater capacity to co-exist with viruses without succumbing to clinical illness has been supported by the frequent isolation of viruses from overtly healthy wild-caught bats [184] and experimental inoculations [187-189]. This paradigm was challenged following mass die-offs of Schreiber's bats (*Miniopterus schreibersii*) in Europe which led to the discovery of LLOV as the proposed causative pathogen [141, 157, 190]. However, more recent serologic evidence of wide-spread anti-LLOV antibodies in the absence of faecal RNA, and lack of correlation between RT-PCR positivity and respiratory pathology in carcasses may suggest a more typical avirulent reservoir host-pathogen relationship, or the occurrence of both fatal and non-fatal outcomes, as seen in bat lyssaviruses [141, 156].

Beyond being refractory to viral disease, most data would also suggest bats host greater viral and zoonotic viral diversity than ecologically similar taxonomic groups such as rodents [188, 191-193], even controlling for reporting effort, though it has been suggested that this may simply reflect species richness [33, 194].

Bats are evolutionarily ancient, and 64 million years of adaptive co-evolution as the only mammals capable of powered flight may have indirectly shaped a uniquely balanced host defence-tolerance system [187, 195]. In order to tolerate the oxidative stresses of flight, bats have adopted multiple strategies to suppress the inflammasome pathway (including reduced DNA sensor activation e.g. dampened STING-dependent interferon activation [196], dampened NLRP3 [197], loss of PYHIN [198]; and downstream IL-1β, and altered interferon-alpha (IFNα), IFNβ and IFNɣ pathway activation [198-202]), thus mitigating the pathological effects of virus-induced inflammation. This tolerance is balanced by a unique and highly efficient antiviral response which includes constitutive expression of interferon and interferon-stimulated genes [203-205], increased expression of heat-shock proteins [206] and the adenosine triphosphate (ATP)--binding cassette (ABC) subfamily B, member 1 efflux transporter (ABCB1) [207], enhanced basal autophagy [208] and other compensatory innate defences [209].

The existence of this inhibitory immune state has been most conclusively demonstrated in the Egyptian rousette fruit bat via in vitro and genomic approaches [210-212]. Most recently, inoculation of 40 fruit bats examined transcriptional immune responses, offering the first functional evidence for tolerance, demonstrating upregulation of canonical antiviral genes, such as ISG15, IFIT1, and OAS3, with a remarkable lack of proinflammatory gene induction (CCL8, FAS, IL6) often seen in filoviral pathogenesis [136].

By contrast, theories which hinged on an active reduction of viral load have largely lost traction, including those advocating for the role of torpor, hibernation [213-215], or the daily temperature spikes associated with the demands of flight, thought to mimic fever [216]. Critics argue that reported bat flight temperatures may be systematically overestimated due to methodological issues, and are not outliers in the context of the mammalian taxon [217]. In vitro replication kinetic studies performed on a range of Old and New World bat cell lines found no decrease in viral titres with increased temperatures [218], further weakening support for this hypothesis.

Other explanations offered refer to Chiropterans' gregarious social structure, metapopulation dynamics, sympatry and high-density colonies, all of which drive intra- and inter-specific contact rates. Life history traits such as highly synchronous birthing cycles and exceptional longevity may further serve to facilitate the observed patterns of viral diversity. Developing specific tools and reagents, including primary and immortalised bat cell lines and live animal breeding colonies will be instrumental in continuing to answer these questions and furthering the critically important field of bat immunology. In recognizing emergent disease, including filovirus disease, as a property of a complex network of host-pathogen interactions, and investigating phenomena such as viral persistence and reactivation, we can continue closing the remaining knowledge gaps shrouding infection, immunity and immune evasion as part of ongoing efforts to minimize the burden of human disease.

1.6. Surveillance for the detection of spillover

Significant scientific effort has been directed towards preparedness for the inevitable emergence of epidemic and pandemic potential pathogens. These initiatives run the gamut from intergovernmental, to academic, and employ a range of approaches, majority of which are event-based, syndromic, passive or focussed on a single pathogen (for example, the WHO Global Influenza Surveillance and Response System (GISRS) established in 1952, and its partnered animal influenza network, the World Organisation for Animal Health (WOAH) and Food and Agriculture Organization (FAO) OFFLU net, established in 2005).

Of the broad-scope, active surveillance projects, the majority focus on direct pathogen discovery; predicated on the idea that our ability to respond rapidly to emergence is primarily hindered by a poor understanding of the diversity and ecology of viral threats. The United States Agency for International Development (USAID) Emerging Pandemic Threats (EPT) PREDICT project, which operated in 35 countries from 2009 - 2020, utilised high-throughput consensus PCR sequencing for viral surveillance in wildlife reservoir hosts in geographic hotspots of disease emergence. The Global Virome Project (GVP), which operated 2018 - 2020, sought to further accelerate the pace of viral discovery; identifying and characterising the majority of currently known viruses in key wildlife groups from highly biodiverse, rapidly developing countries in tropical regions.

One of the major challenges faced during direct pathogen surveillance is the difficulty of catching a pathogen "in the act". Serological surveillance may offer a solution. Particularly given recent advances in high-throughput, highly-multiplexed immunoassay technology, it presents an opportunity to measure past exposure over months to years, providing vast data on vaccine coverage and pathogen exposure, including asymptomatic or mild cases. Indeed, majority of the data in this thesis was generated using MMIAs on the Luminex platform (Luminex Corporation, Austin, TX, USA), which, at the upper limit, allows for the measurement of antibody responses to as many as 100 different antigens with just 1 μL of serum. Applied effectively, longitudinal and multi-pathogen serological surveys present opportunities to identify and respond to global health challenges, from under-vaccination to emerging pathogens.

Despite these opportunities, serological surveillance faces its own set of challenges, ranging from difficulties inherent to the technique, such as antigenic cross-reactivity, to more implementational challenges, such as the lack of international reference standards, performance assessments and comparisons of assays between patient populations. One recent limitation that has arisen with the development of highly-multiplexed serological data is the lack of analytical tools for the interpretation of this data, particularly when evaluating the pathogens together [219]. To date, the bulk of the literature takes the traditional approach of considering each of these pathogens independently, which renders results susceptible to cross-reactive antibodies, and is particularly challenged by contexts where antigenically related pathogens co-circulate.

1.7. Thesis aims

This thesis aims to develop and apply One Health approaches to the surveillance of emerging viruses at high-risk interfaces between humans, animals and the environment.

In Chapter 2, I describe the methodology used throughout the thesis.

In Chapter 3, I aim to assess the performance of an envelope glycoprotein-based MMIA and other serological assays for the detection of *Orthoebolavirus* species in a cohort of EVD survivors from Coyah and Guéckédou, Republic of Guinea.

In Chapter 4, I aim to characterise filovirus spillover in wildlife hunters (WLHs) in Guinée forestière (Forested Guinea) and investigate proximal and upstream drivers using serological, questionnaire and satellite-derived data.

In Chapter 5, I aim to characterise paramyxovirus exposure in human populations with significant exposure to wildlife (in particular flying foxes) on the eastern coast of Australia. I explore perceptions of zoonotic disease risk and safety practices through semi-structured interviews, and investigate zoonotic virus exposure through the metagenomic sequencing of in-contact wildlife.

Chapter 2
Methodology
2.1. Study populations and ethical approvals
2.1.1. Ebola virus survivor, contact and negative cohort 2015 – 2024, Coyah and Guéckédou, Republic of Guinea

The Ebola virus disease (EVD) survivor, contact and negative cohort comes from an observational longitudinal cohort study (2015 – 2023) of Ebola EVD survivors, contacts and negative controls based in Guéckédou (the outbreak epicentre) and Coyah (approximately 450 kilometres away), Republic of Guinea [220]. Survivors were initially recruited from EVD survivor associations, and verified in EVD treatment centre databases, or by the presentation of EVD survivor certificates. Contacts were defined as carers or house-hold contacts of Ebola positive cases. Individuals from the region who reported no history of Ebola virus disease symptoms, had no known exposure to infected cases, and no self-reported attendance at high-risk events (e.g., funerals) were included as negative controls.

Blood (30 – 50 mL) was collected by venepuncture from EVD survivors 3-14 months post infection (p.i.) then resampled annually (where possible) from 2015- 2023. Contacts and negative controls were sampled contemporaneously.

Written, informed consent was obtained from all participants. Ethical approval was granted by the National Ethics Committee for Health Research, Guinea (33/CNERS/15) and from the National Research Ethics Service, United Kingdom.

2.1.2. WLH cohort, 2017 and 2023, Guinée forestière, Republic of Guinea

The WLH study population was recruited in 2017 from Forested Guinea, Republic of Guinea by Joseph Akoi Bore, PhD, Ministère de la Santé et de l'hygiène publique, Rép. Guinée, as part of a serological investigation into the seroprevalence of Ebola and Lassa virus in WLHs and household members [221]. Among other aims, the study sought to demonstrate the circulation of EBOV in groups at high risk of zoonotic exposure, prior to the 2013-2016 West African EVD epidemic.

Villages were selected based on location (within forested regions), and purposively sampled to include those which were affected (n=16 villages) and unaffected (n=28 villages) by the 2013-2016 West African EVD epidemic, as reported in national databases available at the Macenta Prefectural Health

Direction office. These designations were confirmed by key informant interviews with healthcare workers and village leaders. Within villages, families known to practice wildlife hunting were approached, and the senior hunter and their spouse (or next closest relative) were invited to participate.

In 2017, 517 participants from 44 villages within 7 subprefectures of Macenta, the Republic of Guinea were enrolled. Samples were collected weekly between February and December 2017 at local health centres (selected based on available facilities and accessibility) by phlebotomists. Participants < 16 years of age, pregnant, with chronic disease, or visitors to the region were excluded. Interviews were performed in Toma. Demographic data, including age, sex, location (to the village level), occupation, and exposure to wildlife (bushmeat) hunting (yes/no) were collected via self-report.

In 2023, 759 participants were recruited from the same area by Dr. Joseph Akoi Bore, according to the same methods. Where possible, individuals from 2017 were resampled in 2023.

Ethical approval for the study was granted by the National Research Ethics Service, United Kingdom, the national research for health ethics committee of Guinea (permit Nº012/CENRS/2017) and the Oxford Tropical Research Ethics Committee (OxTREC:536-22). Written informed consent was obtained from all participants.

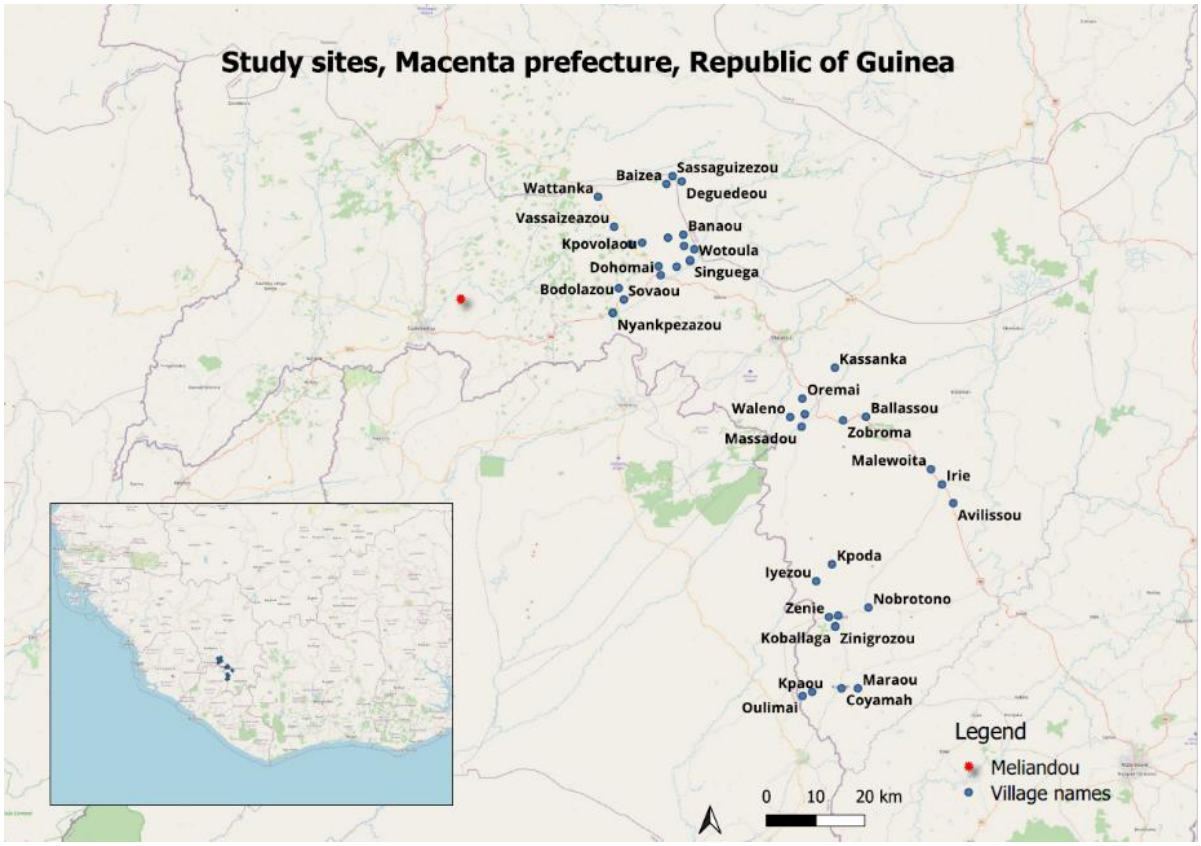


Figure 6 Study sites, Macenta prefecture, Guinée forestière, Republic of Guinea. Figure produced using QGIS version 3.28.2.

2.1.3. Farmer cohort, 2017 – 2021, Uganda

Serum samples were collected from 2017 – 2021 from multiple sites within Uganda as part of the United States Centers for Disease Control (US CDC)-Ugandan Virus Research Institute (UVRI) study. A subgroup (n=79) of farmers from rural Uganda was kindly provided by Professor Emma Thomson, University of Glasgow, for use in this thesis.

Ethical approval for the study was granted by the Uganda Virus Research Institute (UVRI) Research Ethics Committee (GC/127/10/02/19) and the Uganda National Council for Science and Technology (HS767). Written informed consent was obtained from all participants.

2.1.4. Blood donor cohort, 2020, United Kingdom

Serum samples (n=3500) were collected in 2020 from healthy blood donors between the ages of 17 and 80 years by the Scottish National Blood Transfusion Service (SNBTS) as described in Thompson et al., 2020 [222]. A randomly selected subgroup (n=63) of these United Kingdom blood donors (UKBDs) was kindly provided by Dr. Craig Thompson, University of Warwick, and utilized as a control cohort throughout the thesis. Ethical approval was obtained for the SNBTS anonymous archive (IRAS project number 18005). SNBTS blood donors gave fully informed consent to virological testing: donation was made under the SNBTS Blood Establishment Authorisation, and the study was approved by the SNBTS Research and Sample Governance Committee.

2.1.5. Wildlife worker cohort, 2023, Australia

In 2023 I recruited 108 wildlife rescuers, rehabilitators, zoo workers and veterinary professionals from Queensland, New South Wales and Victoria, Australia. Ethical approval for the study was granted by the Oxford Tropical Research Ethics Committee (OxTREC: 545-23), Australian National University (H/2024/0593), and the University of Queensland (2024/HE000385). Written informed consent was obtained from all participants.

2.2. Serological assays

2.2.1. Reagents

2.2.1.1. Monoclonal antibodies and antisera

All monoclonal antibodies or antisera were obtained from academic collaborators, Biodefense and Emerging Infections (BEI) Research Resources Repository, National Institute of Allergy and Infectious Disease (NIAID), National Institutes of Health (NIH), National Institute for Biological Standards and Controls (NIBSC), or purchased through commercial companies as described in the table below.

Table 5 Monoclonal antibodies and antisera

Reagent	Catalogue number; Lot number	Description	Source
Ebola virus WHO standard	15/220	Human plasma from a donor recovered from Ebola virus disease. Country of origin of biological material: United Kingdom	National Institute for Biological Standards and Controls (NIBSC)
Marburg virus convalescent sera	Ug1-Ug8	Human convalescent sera from PCR-confirmed survivors (n=8) from the 1999 MARV outbreak in the Democratic Republic of Congo.	Dr. Christian Kahusu, Dr. Mulangu Sabue
Marburg virus convalescent sera	ITG001-ITG099	Human convalescent sera from PCR-confirmed survivors (n=5) of the 2012 MARV outbreak in Western Uganda.	Collaborative Study for the Establishment of the First WHO International Standard for Marburg virus antibodies
Secondary antibody, anti-human IgG	A0170-1ML; 0000129825	Anti-Human IgG (Fc specific) −Peroxidase antibody produced in goat	Merck Life Science UK Limited; Sigma-Aldrich
Anti-Glycoprotein Marburg virus, Ebola virus MR78	MR78	Rabbit monoclonal antibody. Generated using GP as the antigen from PBMCs of a donor after screening them for MARV antigen-specific antibody-secreting cell lines using ELISAs. Cells from wells with supernatants reacting in a MARV antigen ELISA were fused with HMMA2.5 myeloma cells.	Absolute Antibody
Monoclonal Anti-Sudan Ebolavirus Envelope Glycoprotein, Clone 6D11	NR-12208	Monoclonal Anti-Sudan Ebolavirus Envelope Glycoprotein produced in vitro	Biodefense and Emerging Infections (BEI) Research Resources Repository, National Institutes of Health (NIH)
Monoclonal antibody to Ebola virus envelope glycoprotein, 15H10	NR-12184	Raised against the SUDV GP but recognises all human EBOV GP species, RESTV GP in western blot assays,	BEI Resources, NIAID, NIH

2.2.1.2. Plasmids

Second-generation HIV-1 p8.91 (expressing Gag-Pol, tat and rev) and firefly luciferase (pCSFLW) vectors were kindly provided by Dr. Dalan Bailey, The Pirbright Institute. Viral envelope glycoprotein (GP) plasmids were kindly provided by Dr. Edward Wright, University of Sussex and Professor Nigel Temperton, University of Kent, as described in the table below.

Table 6 Viral envelope glycoprotein (GP) plasmids

Viral glycoprotein	GenBank Accession number	Expression cloning vector	Target cells	Source
		Filoviridae		
BDBV GP	NC_014373	pCAGGS	HEK293T/CHO	Dr. Edward Wright, University of Sussex
BOMV GP	MF319185.1	pCAGGS	HEK293T/CHO	Dr. Edward Wright, University of Sussex
EBOV Kikwit 95	KC242799.1	pCAGGS	HEK293T/CHO	Dr. Edward Wright, University of Sussex
EBOV Makona GP 14	KJ660347.1	pCAGGS	HEK293T/CHO	Dr. Edward Wright, University of Sussex
EBOV Mayinga 76 GP	EU224440	pCAGGS	HEK293T/CHO	Dr. Edward Wright, University of Sussex
MARV Angola 05 GP	DQ447660	pCAGGS	HEK293T/CHO	Dr. Edward Wright, University of Sussex
MARV DRC 99	DQ447650	pCAGGS	HEK293T/CHO	Dr. Edward Wright, University of Sussex
MARV Kenya 80 GP	Z12132	pCAGGS	HEK293T/CHO	Dr. Edward Wright, University of Sussex
RAVN GP	DQ447649.1	pCAGGS	HEK293T/CHO	Dr. Edward Wright, University of Sussex
RESTV GP	AY769362	pCAGGS	HEK293T/CHO	Dr. Edward Wright, University of Sussex
SUDV GP	FJ968794	pCAGGS	HEK293T/CHO	Dr. Edward Wright, University of Sussex
TAFV GP	FJ217162	pCAGGS	HEK293T/CHO	Dr. Edward Wright, University of Sussex
LLOV GP	OQ630505.1	pCAGGS	HEK293T	Dr. Simon Scott University of Kent

2.2.1.3. Vesicular Stomatitis Virus (VSV) pseudotyped viruses

VSV backbone pseudotyped viruses were kindly provided by Dr. Chee Wah Tan.

Table 7 Vesicular Stomatitis Virus (VSV) backbone pseudotyped viruses

Viral glycoprotein (GP)	GenBank accession number	Source
	Filoviridae	
MLAV GP	KX371887	Dr. Chee Wah Tan, National University of Singapore

2.2.1.4. Viral recombinant protein antigens

All recombinant viral protein antigens were obtained from academic collaborators, Biodefense and Emerging Infections (BEI) Research Resources Repository, National Institute of Allergy and Infectious Disease (NIAID), National Institutes of Health (NIH), or purchased through commercial companies as described in the tables below.

Table 8 Recombinant viral proteins

Viral glycoprotein (GP)	GenBank Accession number	Production system	Purification method	Source
		Filoviridae		
Marburg virus (MARV) envelope GP	YP_001531156.1	HEK293 cells	Sheep Fc-tag	Native Antigen Company
Ebola virus (EBOV) Makona strain GP	AHX24649.1	HEK293 cells	C-tag EPEA (glutamic acid-proline-glutamic acid-alanine)	Jenner Institute, University of Oxford
Paramyxoviridae				
Mòjiāng virus GP (MojV G)	YP_009094095.1	Expi293F cells	C-terminal histidine tag	Dr. Dalan Bailey, Nazia Thakur, The Pirbright Institute
Melian virus GP (MeliV G)	UQM99619.1	Expi293F cells	C-terminal histidine tag	Dr. Dalan Bailey, Nazia Thakur, The Pirbright Institute
Nipah virus Bangladesh GP (NiV-B G)	AEZ01397.1	Expi293F cells	C-terminal histidine tag	Dr. Dalan Bailey, Nazia Thakur, The Pirbright Institute

2.2.2. Blood processing (plasma, sera and peripheral blood mononuclear cell isolation)

Ebola Survivors, Conakry and Guéckédou, Republic of Guinea

Blood collection, processing and PBMC isolation was performed by Thom and colleagues from 2015 – 2022, as described in Thom et al., 2021 [220]. In January 2024 I assisted in performing blood collection and processing according to the same protocols. 20 – 50 mL of venous blood was collected into ethylenediaminetetraacetic acid (EDTA) vacutainers. Plasma and PBMC separation were performed by layering whole blood onto LeucoSep-tubes (Greiner Bio-One; UK) over a Ficoll-Paque Plus gradient (GE Healthcare; Amersham, UK) and centrifugation (800 G for 20 minutes). Erythrocyte contamination was removed through preferential lysis with Ammonium-Chloride-Potassium (ACK) lysing buffer (Gibco, New York).

Plasma was aspirated and aliquots stored at -80° Celsius (C). PBMCs were aspirated from the buffy coat layer and used fresh for IFNγ ELISpots. Remaining aliquots were stored in cryomedia (foetal calf serum, 10% DMSO) at -80°C and transported to the United Kingdom for storage in liquid nitrogen.

WLHs, Guinée forestière, Republic of Guinea

Blood collection and processing was performed by Dr. Joseph Akoi Bore and colleagues in 2017 and 2023, as described in Akoi Bore et al., 2024 [53]. 5 mL of venous blood was collected, centrifuged at 2000 G for 10 minutes and serum was aliquoted and stored at −20° C.

Wildlife workers, Australia

Blood collection and processing was performed by myself in April 2023. Venepuncture was performed using a 21 G butterfly catheter from the antecubital fossa. 10 mL of venous blood was collected into a BD serum vacutainer. Sample was allowed to clot at room temperature for 15 – 30 minutes. Sera were separated by centrifugation (2000 G for 10 minutes at 4° C) then collected by sterile Pasteur pipette into 1 mL aliquots for storage at 4° C. Where samples were being processed rurally, sera were separated by aspirating from the clot without centrifugation. Haemolysed, icteric or lipemic samples were noted. Samples were stored at -20° C for 1 month then transported to the United Kingdom for long-term storage at -80° C.

2.2.3. Multiplex microsphere-based immunoassay (MMIA)

2.2.3.1. Recombinant envelope glycoprotein ectodomains production, purification and bead-conjugation

Collaborators at the Uniformed Services University for the Health Sciences (Professor Christopher Broder, Dr. Eric Laing) produced, purified and bead-conjugated the antigens used for the MMIA. Soluble, native-like trimeric filovirus glycoprotein ectodomains and soluble, native-like tetrameric

henipavirus G proteins were expressed in an immortalized mammalian cell-culture system (FreeStyle 293 Expression System) as previously described [223]. Full-length glycoprotein sequences were identified in the NCBI database, transmembrane domains were removed, and remaining ectodomains were human codon optimized and designed with a C-terminal trimeric coiled-coil GCN3 motif (MKQIEDKIEEILSKIYHIENEIARIKKLIGE) followed by a double factor Xa protease cleavage site and Twin-Strep-tag (TST) or S-Tag flanked by 5' BamHI and 3' XbaI restriction enzyme sites. Repeating factor Xa protease cleavage sites (IEGRIEGR) were engineered immediately upstream of the tag to facilitate protein tag removal post-purification.

A mock protein antigen stable cell line was also established (expression vector without the glycoprotein open reading frame transfected into the mammalian cell-culture system) and the same purification protocol was followed. Cell culture supernatant was then used as a measure of non-specific binding.

Trimeric glycoprotein ectodomain purification

Glycoproteins were purified from stable cell line supernatant by affinity chromatography and correct-sized proteins were selected using size-exclusion chromatography. Proteins were concentrated and a buffer exchange step used to ensure no trace materials, including cells, cellular debris and serum remained. Protein tags (TST or S-tag) were removed and Western and Coomassie protein blots were performed to confirm removal. Concentration was determined by NanoDrop. Reactivity was determined by western blot.

Glycoprotein ectodomains were then coupled to carboxylated magnetic microspheres (15 µg of antigen per 1.25 x 10^6 microspheres) according to manufacturer (MagPlex) guidelines.

2.2.3.2. MMIA screening of sera

Human sera were screened for IgG binding against filovirus and paramyxovirus envelope attachment proteins using a MMIA. Sera were diluted 1:400 in PBS without calcium and magnesium and heat inactivated at 60°C for 30 minutes. Following heat inactivation, diluted sera were incubated at room temperature with a master mix of 1:100 diluted antigen-coupled microspheres in a 96-well microtiter plate for 45 minutes with agitation at 900 RPM. Wells were washed with PBS and 0.05% Tween20 (PBST) and subsequently incubated with 100 µL of biotinylated cross-absorbed anti-human IgG (Thermo Fisher Scientific) diluted 1:5,000 in PBST per well for 45 minutes with agitation at 900 RPM. Following secondary incubation, wells were washed with PBST and incubated with 100 µL of streptavidin-phycoerythrin (Bio-Rad) diluted 1:1000 in PBST for 45 minutes with agitation (900 RPM). After tertiary incubation, wells were washed with PBST and resuspended in 100 µL PBST for 10 minutes at 900 RPM. Where plates could not be immediately read, they were stored at 4° C overnight, then agitated at room temperature for 30 minutes at 900 RPM prior to reading.

Antigen specific binding IgG was quantified on a BioPlex 200 HTF multiplexing system as Median Fluorescent Intensity (MFI). Reported MFI values are adjusted to PBS control well averages.

2.2.3.3. Calibration of internal reference to WHO standard for EBOV binding antibody concentration

A WHO international standard for Ebola virus (15/220) was reconstituted, as per instructions for use, to give a working potency of 1.0 IU/mL. An internal reference standard was created from pooled serum from 3 Ebola Virus Disease survivors from the EVD cohort described previously. The WHO international standard (WHO-std) and internal reference standard (IR-std) were diluted two-fold from 1:200 – 1:25,600 and screened by MMIA five times. The MFI of IR-stds were interpolated against the WHO-stds. Interpolated mIU values were multiplied by the dilution factor to calculate mIU/L. The concentration of EBOV binding antibodies in the IR-std was then calculated by averaging the mIU/L (within the linear range) of each reading.

The IR-std was then included in all MMIA plates so samples could be interpolated against the IR-stds to make semi-quantitative assessments of EBOV binding antibodies in mIU/L. Samples above the IR-std's linear range of detection were re-tested at dilutions of 1:400, 1:8,000, 1:32,000, and 1:64,000 dilutions. Samples where the MFI remained above the above the IR-std's upper limit of detection were reported at 16,000 mIU/L. Samples where the MFI was below the IR-std's lower limit of detection were reported at 1 mIU/L.

2.2.4. Enzyme-linked immunosorbent assays (ELISAs)

2.2.4.1. Ebola Zaire IgG indirect ELISAs

EBOV whole-virus, EBOV glycoprotein and live neutralisation data were obtained from a pre-existing database of results available in a link-anonymised format. Whole virus ELISAs and live EBOV neutralisations were performed by Professor Thomas Strecker, Philipps University Marburg, Germany.

EBOV whole virus IgG indirect ELISA

The EBOV whole virus IgG ELISA data was obtained by Thom et al. using the following methods [220]. High-binding microtiter plates were coated with whole Ebola virus inactivated virions and incubated for 16–20 hours. Plates were washed with PBS and 0·1% Tween20 (PBST), blocked (PBS and 5% milk powder), and 1/200 dilutions of plasma sample were added for an hour incubation. Horseradish peroxidase-conjugated polyclonal antibody (P0214, Dako; Santa Clara, CA; dilution 1/1000) and TMB substrate was used to develop the plates, and optical density (OD) was determined at 450nm minus 630 nm. The mean OD from each sample on the mock antigen was subtracted from the OD on the Ebola virus antigen. Arbitrary ELISA units were calculated by linear regression from patient antiserum-derived standard curves.

EBOV glycoprotein (GP) ELISA

The EBOV glycoprotein IgG ELISA data was obtained by Thom et al. using the following methods [220]. High-binding microtiter plates were coated with Ebola glycoprotein (0.5 µg/mL) for 16 – 20 hours. Plasma (1/200 dilution) was analysed for IgG binding with goat anti-human IgG Fcγ antibody conjugated to alkaline phosphatase (1/15,000). OD was measured at 405 nm on a VERSAmax plate reader (Molecular Devices, UK) with SoftMax Pro (v4.7.1). The cut-off was set as the average of the negative control plus five standard deviations.

2.2.5. Pseudotyped virus production

2.2.5.1. Cell culture propagation and maintenance

Human embryonic kidney (HEK) 293T clone-17 cells (HEK 293T/17; American Type Culture Collection (ATCC), CRL-11268) cells were used for production and titration of pseudotyped lentiviral vectors and all neutralization assays. The HEK293T cell line is a derivative of the parental HEK293 cell line, and is preferentially used for retroviral production due to the addition of the simian virus 40 large T antigen (SV40 LTA) encoding sequence, which renders them fast-growing and highly transfectable, particularly with plasmid vectors containing the SV40 promoter [34, 35]. While EBOV GP pseudotyped HIV-1 has a broad tissue tropism, studies have demonstrated titres ($TCID_{50}$/mL) generated by infection of HEK293T/17 cells were 3-fold, 33-fold and 73-fold greater than those generated in Huh-7, HeLa and Vero E6 cells respectively [224].

Cell lines were cultured in Dulbecco's modified Eagle's medium (DMEM) with Glutamax (Gibco, Life Technologies, Paisley, UK), supplemented with 10% (vol/vol) heat-inactivated foetal bovine serum, and 1% (vol/vol) penicillin–streptomycin (PenStrep) (Sigma Aldrich, Dorset, UK P4333), termed herein as complete 10% DMEM. Cells were maintained in tissue culture conditions (37° C and 5% CO_2). Cells were sub-cultured for 3-4 months (passage <40) at a constant ratio and rate (1:5 every 3-4 days) and monitored for changes in cell morphology or growth.

2.2.5.2. Plasmids

Pseudotyped viruses were produced using a second-generation lentiviral (HIV-1) system using backbone plasmid p8.91 [225] (expressing Gag, Pol, Tat and Rev) as a packaging construct and firefly luciferase (pCSFLW) as a reporter construct. The gag provides structural proteins (p18, p24, p15), whereas pol provides replication enzymes required for the cleavage and maturation of proteins (integrase, reverse transcription, p10 protease) [226, 227].

Envelope glycoproteins were provided as kind gifts, cloned within pCAGGS [228] or pCDNA3.1+ expression vectors. All were codon optimized.

2.2.5.3. Plasmid transformation, production, DNA extraction and sequencing

Plasmid transformation

Plasmids were transformed in chemically induced competent *E. coli* cells via the heat-shock method. Filovirus glycoprotein plasmid DNA (20-60 ng) was incubated with 30 uL of high-efficiency competent *E. coli* cells (New England BioLabs, Hertfordshire, UK) on wet ice for 30 minutes, then heat-shocked at 42° C for 30 seconds, before being recovered on wet ice for 5 minutes.

Transformed *E. coli* were incubated in Super Optimal broth with Catabolite repression (SOC) Outgrowth Medium (2% tryptone, 0.5% yeast extract, 10 mM NaCl, 2.5 mM KCl, 10 mM $MgCl_2$, 10 mM $MgSO_4$, 20 mM glucose) for 60 minutes at 37° C in a shaking incubator. Bacterial pellets were produced by centrifugation at 6000 rpm for 2 minutes, resuspended in a 50 μL volume, and plated onto room-temperature Luria Bertani (LB) agar selection plates. Selection plates were inverted and incubated at 37° Celsius and 5% CO_2 for 16 hours for single colony selection.

Selection plates were aseptically prepared in batches using LB agar (Miller) (15 g/l agar, 10 g/l tryptone, 10 g/l NaCl, 5 g/l yeast extract) (Sigma-Aldrich, Gillingham, UK) and 100 μg/ml ampicillin (Sigma-Aldrich), and stored at 4° C.

Bacterial culture

E. coli clones were amplified in liquid starter culture. A single colony was selected from a freshly streaked selective agar plate and used to inoculate 5 mL of LB medium (10 g/l tryptone, 5 g/l yeast extract, 10 g/l NaCl, 2.2 g/l inert binding agents) (Sigma-Aldrich) containing 100 μg/mL ampicillin. Cultures were incubated for approximately 8 hours at 37° C with vigorous shaking (250 rpm).

Cultures were then diluted 1/500 into 100 mL (for high-copy plasmids) of selective LB medium and grown at 37° Celsius for 16 hours with vigorous shaking (250 rpm), with the aim of harvesting at the transition from logarithmic to stationary growth phase (at a cell density of approximately 2-4 x 10^9 cells per mL) for optimal DNA yield and purity. Bacterial cells were harvested by centrifugation at 3000 x g for 30 minutes at 4° C and the supernatant discarded.

DNA extraction

Plasmid DNA was recovered from transformed bacterial cultures using the Qiagen EndoFree Plasmid Maxi-Prep kit as per manufacturer's instructions.

Briefly, bacterial lysates were cleared by centrifugation and loaded onto anion-exchange tips, which selectively bound plasmid DNA under appropriate low-salt and pH conditions. Plasmid DNA was purified by a medium-salt wash (for the removal of protein, metabolites, RNA and other low-molecular-weight impurities). Plasmid DNA was then eluted in a high-salt buffer, concentrated and de-salted by isopropanol precipitation. Plasmid DNA was eluted into endotoxin-free Buffer Tris-EDTA (TE) and stored at -80 °C.

All DNA extracts were quantified using UV spectrophotometry at 260 nm (NanoDrop, Thermo Scientific, Paisley, UK).

DNA sequencing

Entire plasmid constructs were sequenced (long-read) directly by an external sequencing service (Source BioSource, Cambridge, UK). Plasmid maps are provided in the Supplementary. All plasmids were found to have no nucleotide changes from the original sequences provided.

Phylogenetic relationship of filovirus glycoproteins

MEGA version 11 was used to conduct all evolutionary analyses [65]. Sequences were aligned with the Multiple Sequence Comparison by Log-Expectation (MUSCLE) algorithm [229]. A phylogenetic tree of filovirus envelope glycoproteins (GP) (Figure 17) was constructed using the Maximum Likelihood method and General Time Reversible (GTR) model [62]. The tree with the highest log likelihood (-18,356.13) is shown (Figure 17). The percentage of trees in which the associated taxa clustered together is shown next to the branches. Initial tree(s) for the heuristic search were obtained automatically by applying Neighbor-Join [63] and BioNJ algorithms [64] to a matrix of pairwise distances estimated using the Maximum Composite Likelihood (MCL) approach, and then selecting the topology with the highest log likelihood value. A discrete Gamma distribution was used to model evolutionary rate differences among sites (5 categories (+G, parameter = 1.2056)). The tree is drawn to scale, with branch lengths measured in the number of substitutions per site. This analysis involved 12 nucleotide sequences. There were a total of 2,318 positions in the final dataset. The GTR+G model was chosen to best describe the substitution pattern based on the Bayesian Information Criterion (BIC) score.

2.2.5.4. Pseudotyped virus production

Lentiviral-vector (HIV-1) based pseudotypes (virus-like particles with filovirus envelope glycoproteins on a lentiviral vector core) were generated as described previously [36], using a surrogate lentiviral core to display envelope glycoproteins.

Briefly, HEK293/T/17 cells were seeded in DMEM with Glutamax (Gibco, Life Technologies, Paisley, UK), supplemented with 10% (vol/vol) heat-inactivated foetal bovine serum, and 1% (vol/vol)

penicillin–streptomycin (PenStrep) (Sigma Aldrich, Dorset, UK P4333) at a concentration of 5 x 10^5 into culture dishes and incubated at 37° Celsius and 5% CO_2. Once 60-80 % confluency was reached, media were replaced with DMEM/1% FBS/1%P/S. The HIV-1 packaging construct plasmid p8.91 (expressing gag-pol, tat and rev), the firefly luciferase reporter construct pCSFLW and the viral GP expression vector were co-transfected simultaneously at a ratio of 1:1:1.5 µL (for envelope: packaging: reporter respectively) using 0.3 µL of 1 µg/mL FuGENE® HD Transfection Reagent per 100 ng DNA in pre-warmed Opti-Mem® medium. Following 15 minutes of room-temperature incubation, transfection reagents and plasmids were added dropwise to gently agitated fresh media (DMEM Glutamax/1% FBS/1% P/S). Cell culture plates were then incubated at 37° C/5% CO_2, with culture media being replenished at 16-20 hours post-transfection. Pseudotyped virus supernatant were harvested at 45-50 hours and 70-75 hours post-transfection and filtered through a 0.45 µm pore cellulose filter. Titres of pseudotyped virus stock were quantified by luciferase-based transduction of target cells (HEK293T) and TCID50/mL was calculated using the Spearman & Kärber formula [230]. Aliquots were prepared for storage at -80° C (shown to be ideal for long-term storage [231]). Production of each PV was performed as described above, with some alterations in the plasmids and quantities, as shown below.

Table 9 Relative quantities of transfection components

Component	Quantity
p8.91	1 µg
pCSFLW	1.5 µg
Filovirus envelope expression plasmid LLOV GP Other filovirus GP	 700 ng 1 µg
OptiMEM	200 µL
FuGENE HD	10.5 µL

2.2.5.5. Pseudotyped virus titration

Titres of pseudotyped virus stock were quantified by luciferase-based transduction of target cells (HEK293T). A 5-fold dilution series of the pseudotyped virus (starting dilution of 1:5) was titrated in triplicate in DMEM/1% FBS/1%P/S. A final volume of 100 µL per well was added to a white 96-well flat bottom cell culture plate (ThermoFisher, Woolwich, UK) seeded with target cells (HEK293T) at a concentration of 2 x 10^4 cells/well, and incubated at 37° C 5% CO_2. After 48-60 hours, media was removed, and cells were lysed with 50 µL per well of Bright-Glo reagent (prepared at a ratio of 1:1 in

PBS) (Promega, Southampton, UK, E2650). Luciferase expression levels were measured in relative luminescence units per mL (RLU/mL) using a GloMax Navigator plate reader (Promega, Southampton, UK). The assay was performed in white cell culture plates to minimize cross-talk between wells to optimise signal-to-noise ratio. TCID50/mL was calculated using the Spearman & Kärber formula [230], using the open-source calculator provided at: Dr Marco Binder, University of Heidelberg, Germany: https://www.klinikum.uni-heidelberg.de/zentrum-fuer-infektiologie/molecular-virology/welcome/downloads.

2.2.6. Pseudotyped virus neutralisation assays (PVNA)

2.2.6.1. Lentiviral vector-based PVNA

White 96-well microplates were seeded with 2 x 10^4/well HEK293T/17 cells/well prior to the neutralisation assay and incubated at 37° C and 5% CO_2 for a minimum of 2 hours. Three-fold serial dilutions of sera samples at a starting dilution of 1:20 were prepared in triplicate in 1% FBS DMEM solution at a final volume of 90 µL per well and incubated with 150 TCID50/well of pseudotyped virus (as calculated from the titration assay) for 1 hour at 37° C. 100 µL of the sera-pseudotyped virus mixture were added in triplicate to each well and incubated at 37° C and 5% CO_2. Luminescence was measured after 60 hours, using a GloMax® Explorer Multimode Microplate Reader. All plates contained pseudotyped virus-only and cell-only controls.

Statistical analysis

Statistical analysis was performed using GraphPad Prism v.10.1.2 (San Diego, California). Raw data from the pseudotyped neutralisation assay were normalized as a percentage (%) neutralisation relative to mean values for pseudotyped virus-only controls (equivalent to 0% infectivity) and cell-only controls (equivalent to 100% infectivity). The half maximal neutralizing titre (NT50) was interpolated by a 4-parameter nonlinear regression with a Hill-Slope constraint of less than 0.

2.2.6.2. Vesicular stomatitis virus -based PVNA

White 96-well microplates were seeded with 2 x 10^5/well Vero-E6 cells in DMEM 10% FCS/1% P/S and incubated overnight at 37° C and 5% CO_2. Four-fold serial dilutions of sera samples at a starting dilution of 1:10 were prepared in triplicate in 1% FBS DMEM solution at a final volume of 30 µL per well and incubated with 30 uL of pseudotyped virus (diluted at a concentration of 150 TCID50/well, as calculated from the titration assay) for 1 hour at 37° C. 50 µL of the sera-pseudotyped virus mixture were added in triplicate to each well and incubated at 37° C and 5% CO_2. Luminescence was measured after 24 hours.

Statistical analysis was performed as above.

2.2.7. Authentic virus neutralisation assays

2.2.7.1. Recombinant Cedar virus (rCedV) neutralisation assay

A neutralisation assay was performed using rCedV-Luc by Dr. Emily Clayton, University of Oxford. The assay used a recombinant, replication-competent Cedar virus containing a luciferase reporter (rCedV-Luc) provided by Professor Christopher Broder, Uniformed Services University of the Health Sciences [232]. Sera samples were tested in duplicate and serially diluted 1:1 with a starting dilution of 1:20. The rCedV-Luc virus stock was 4.12 x 10^7 PFU/mL with a multiplicity of infection (MOI) at 0.01. An anti-CedV-G monoclonal antibody (m14F3) was used as a positive control with a starting concentration of 1 µL/mL (starting dilution). The positive control for this assay was used at a starting concentration of 1ug/mL for the first dilution point. The positive control was anti-CedV-G monoclonal antibody (m14F3) [233]. All samples were tested in duplicate. I performed all statistical analysis as above.

2.2.7.2. Live Ebola virus neutralisation assay

As described earlier in chapter, all EBOV live neutralisation data were obtained from a pre-existing database of results available in a link-anonymised format. Live EBOV neutralisations were performed by Professor Thomas Strecker, Philipps University Marburg, Germany, as described in the literature [220]. In brief, plasma was heat-treated and serially diluted in supplemented DMEM, then combined with 100 median tissue culture infectious dose (TCID50) units of Ebola virus variant Mayinga in 96-well culture plates. Following incubation for 1 hour at 37° Celsius, a Vero cell suspension in supplemented DMEM was added, then incubated at 37° Celsius, 5% CO_2 for a further 7 days. Cytopathic effect was then evaluated, and neutralisation titres were calculated as the geometric mean titre of four replicates. A titre of 1/8 or higher was considered to be positive.

2.2.8. IFNγ ELISpot

IFNγ ELISpots were performed on freshly isolated peripheral blood mononuclear cells (PBMCs) as described previously [220]. In brief, whole blood was layered on 15 mL of Ficoll-Plaque Plus (Cytiva, 17-1440-03) in sterile LeucoSep-tubes (Sigma, Gillingham, UK) and centrifuged at 800 G for 20 minutes. PBMCs were aspirated from the buffy coat layer by Pasteur pipette. Erythrocyte contamination was removed through preferential lysis with Ammonium-Chloride-Potassium (ACK) lysing buffer (Gibco, New York). PBMCs were then prepared at 2 × 10^6 cells/mL in Leibovitz media with penicillin–streptomycin, foetal calf serum, L-glutamine, HEPES and 2-mercaptoethanol. PBMCs were stimulated

with an EBOV and MARV glycoprotein peptide library at a final concentration of 2.5 µg per peptide per mL, as described previously. Cells were incubated for 24 hours incubation at 37° Celsius.

Spot forming cells were enumerated using a Cellular Technology Limited ELISpot ImmunoSpot® machine upon return to the United Kingdom by Yasmin Jiwa, University of Oxford. IFNγ release was determined as per standard ELISpot protocol (Mabtech; Nacka Strand, Sweden) by subtracting the background from each well and taking the mean of three triplicate wells to determine spot forming units per one million cells. The total IFNγ response to the EBOV glycoprotein peptides were summed to determine the overall T-cell response.

2.3. Metagenomic deep sequencing

2.3.1. Sample preparation

2.3.1.1. Sample collection

Samples (fresh flying fox faeces, urine, spats or partially eaten fruits) were collected from the home environment of wildlife carers (i.e., bottom of cages, aviaries and home floors). Metadata including data of collection, location, sample type and species (where known) were recorded. Samples were collected into sterile tubes containing 2 mL of DNA/RNA Shield (Zymo Research, Cat: R1100-50), stored at room temperature overnight, then at 4° Celsius for up to 3 weeks before further processing.

2.3.1.2. RNA extraction, DNase treatment, viral particulate purification

For metagenomic analysis, samples were individually homogenized in DNA/RNA shield by vortexing, centrifuged, then filtered through a 0.22 µm filter (Millipore) to remove eukaryotic and bacterial cell-size particles. Samples were extracted using QIAamp Viral RNA extraction kit (Qiagen) and columns were shipped at room temperature from Australia to Oxford, United Kingdom. Extracts were eluted from columns into molecular H_2O, and aliquots (10 µl) of 4 individual samples from the same location were pooled. Filtrate was DNAse treated (ezDNase, Thermo Fisher Scientific, Cat: 11766051) to digest non-particle-protected nucleic acids. RNA product in each pool was measured and assessed for contamination with QuBit 4 using the RNA High Sensitivity Kit, and the Nanodrop.

2.3.1.3. Sequence-Independent Single-Primer Amplification (SISPA)

Extracted nucleic acid (RNA) was reverse transcribed and randomly amplified using a Sequence-Independent Single-Primer Amplification (SISPA) method, as described in the literature previously[234]. As part of this protocol, random octamers of RNA were tagged with 20 nt barcode sequence (K-8N) and primers were directly incorporated into the cDNA during RT-PCR. Klenow

enzyme and K-8N primers are added to the cDNA product, and following a Klenow reaction, an aliquot of dsDNA product is added with primer K to high-fidelity PCR mix. The dsDNA is amplified with PCR using a primer consisting of barcode (K), producing a final PCR product.

For first strand synthesis, a volume of 4 µl of purified viral nucleic acids was mixed with 40 uM random primer (GTTTCCCACTGGAGGATANNNNNNNNN 3), denatured at 65° C for 5 minutes, and cooled at room temperature for 5 minutes.

For the reverse transcriptase first strand synthesis, the 5-µl reaction mix containing 2 µl of reverse transcriptase (RT) 5× first strand buffer, 1 µl of H_2O, 1 µl of 10 mM deoxynucleoside triphosphate (dNTP) solution, 0.5 µl of DTT, and 0.5 µl of reverse transcriptase was incubated at 42° C for 10 min.

For the second strand synthesis, 5.65-µl reaction mix containing 3.85 µl of H_2O, 1 µl of sequenase reaction buffer, 0.45 µl of sequenase dilution buffer, 0.3 µl of sequenase enzyme (polymerase 2.0) was incubated at 37° C for 8 min.

For amplification, 45 µl of amplification master mix (containing 19 µl H_2O, 25 µl Q5 master mix, 100 uM of sol B primer (5' GTTTCCCACTGGAGGATA 3')) was added to 5 µl of the reaction product from the second strand synthesis as a template. The PCR conditions were as follows: denaturation at 98° C for 30 seconds, 35 cycles (98° C for 10 s, 50° C for 20 s, 72° C for 2 min), and a final extension at 72° C for 2 minutes.

Nucleic acid clean-up was performed using AMPure XP beads by adding 90 µl of beads per sample, incubating at room temperature for 5 minutes then pelleting on a magnetic rack to remove the supernatant. The pellet was washed with 2 x 200 µl 70% ethanol washes and resuspended into 30 µl molecular H_2O, before pelleting beads again and retaining the elute.

2.3.2. Illumina short-read deep sequencing

Illumina sequencing libraries were prepared using the NEBNext® Ultra™ II FS DNA Library Prep Kit for Illumina® (NEB #E7805S/L), following the manufacturer's protocol. Fragmentation, end repair, and dA-tailing were performed in a single enzymatic step, followed by adapter ligation, bead-based size selection, and PCR enrichment

For the fragmentation and end-preparation reaction, input 26 µl of input DNA in TE buffer, 7 µl Ultra II FS Reaction Buffer, 2 µl Ultra II FS Enzyme mix, were incubated at 37° C for 30 minutes, 65° C for 30 minutes.

For the adaptor ligation reaction, 35 µl of FS reaction mixture, 30 µl NEBNext Ultra II Ligation Master Mix, 1 µl NEBNext Ligation Enhancer, 2.5 µl NEBNext Adaptor for Illumina were incubated at 37° C for 15 minutes.

Clean-up was performed by adding 0.8 x AMPure XP beads for size-selection and incubating at room temperature for 10 minutes then pelleting on a magnetic rack to remove the supernatant. The pellet was washed 2 x 200 µl 80% ethanol washes and resuspended into 15 µl of molecular H_2O.

For the PCR-enrichment of adaptor-ligated DNA, 15 µl of adaptor-ligated DNA fragments, 25 µl of NEBNext Ultra II Q5 Master Mix, 5 µl Index Primer, 5 µl of Universal PCR Primer were combined in sterile strip tube. The PCR conditions were as follows: initial denaturation at 98° C for 30 seconds, 13 cycles (98° C for 10 s, 65° C for 75 s), and a final extension at 65° C for 5 minutes.

Libraries were pooled and sent to a commercial company to be sequenced on an Illumina (Nova-Seq) using paired-end (150 bp) reads.

2.3.3. Oxford Nanopore Technology (ONT) long-read deep sequencing

Library preparation for Nanopore sequencing was performed using ~75 ng per pool and the SQK-LSK114 Ligation Sequencing kit and Native Barcoding Kit EXP-NBD104.

For the end-preparation reaction 1.2 µl of Ultra II End Prep Reaction Buffer (NEB), 0.5 µl of Ultra II End Prep Enzyme Mix (NEB), 8.3 µl of amplicon/SISPA B cDNA (for 187.5 ng of input material per sample) were mixed by pipetting and incubated at 20° C for 5 minutes, and 65° C for 5 minutes.

For the barcoding reaction, 5 µl of Blunt/TA Ligase Master Mix (NEB), 2.75 µl nuclease-free H_2O, 1.25 µl of barcode, 1 µl of end-prepped amplicons were incubated at room temperature for 20 minutes then pooled.

Clean-up was performed by adding 0.4 x AMPure XP beads and incubating at room temperature for 10 minutes then pelleting on a magnetic rack to remove the supernatant. The pellet was washed 2 x 200 µl 80% ethanol washes and resuspended into 35 µl of molecular H_2O.

Adapter ligation was performed by adding 30 µl of the barcoded pool, 5 µl of native adapter, 10 µl of Quick Ligation Reaction Buffer (NEB), 5 µl Quick T4 DNA Ligase, mixing, and incubating for 20 minutes at room temperature.

Bead clean-up was performed again with 2 x 125 µl Sequencing Buffer (ONT) washes, and finally resuspending in 15 uL Elution Buffer (EB).

Nanopore sequencing was performed on an Oxford Nanopore Technology MinION MK1B using a R9 Flowcell. Flow cell was prepared and primed using Flow Cell Tether. Prepared library (containing 37.5 µl Sequencing Buffer, 25.5 µl of Library Beads, 12 µl DNA library) was mixed and 75 µl were added into the SpotON sample port in a dropwise manner for sequencing. Base-calling was performed using MinKNOW (Dorada v0.7) with standard parameters.

2.3.4. In silico analysis

2.3.4.1. Taxonomic classification

Raw sequence reads were pre-processed by trimming low-quality bases and removing primers and adapter sequences from PCR and library preparation steps. Nanopore reads (single-end) were trimmed using Nanofilt to remove 25 bp SISPA primer sequences from the start and end of each read. Illumina reads (paired-end) were trimmed using the Trimmomatic tool in Galaxy, with minimum read quality >30.

Taxonomic classification at the read level was performed using the Kraken2 sequence classification algorithm against the RefQ viral database (release: 04.02.2025) [235]. Kraken2 assigns taxonomic labels by mapping each k-mer in a query read to the lowest common ancestor (LCA) of genomes in the database that contain that k-mer (RefQ viral). The algorithm builds a classification tree where each node is weighted by the number of k-mers in the sequence associated with the node's taxon. All root-to-leaf (RTL) paths are scored by adding all the weights in the path. The RTL path with the highest cumulative weight determines the final taxonomic assignment, with the leaf node of this maximal path being used as the classification for the sequence. Viruses of interest identified by Kraken2 were aligned to their respective reference genomes from NCBI using MUSCLE within MEGA X (v10.2.4) for manual validation and comparison.

2.3.4.2. *De novo* genome assembly and alignment

De novo genome assembly was performed using SPAdes (3.15.1) for both Illumina and Illumina/Nanopore hybrid assemblies [236]. Resulting contigs were screened using BLASTn against the NCBI nucleotide database to identify viral sequences, and E-values from BLASTn searches were used to evaluate the statistical significance of sequence similarity matches [237]. Illumina reads were mapped to assembled contigs of interest using BWA-MEM [238] and Nanopore reads using Minimap2 [239]. Assembly quality was assessed by mapping raw reads to the assembly and generating read depth values using SAMtools (1.10) [240].

2.4. Experimental and computational methods for the characterisation of serological data

2.4.1. Establishment of serological thresholds through a presumed unexposed cohort

Seropositivity cut-off values or thresholds were generated through the use of cohort (UKBDs) with no expected exposure to the pathogens of interest. A pre-specified number of standard deviations (3SD and 5 SD, depending on the stringency) above the mean of the background-subtracted median fluorescence intensity (MFI-bg) was used as a binary seropositivity endpoint.

2.4.2. Establishment of serological thresholds using finite mixture models

Finite mixture modelling (FMM) was utilized to probabilistically model the assumed presence of multiple normally distributed, hidden components or subpopulations (serostatus categories) within the sampled population, as described previously within the literature [241, 242]. By determining an endemic and seronegative population within the sample, the FMM was used to generate a probabilistic cut-off without the use of negative controls.

Analysis was performed in R version 4.2.1 using the `mixtools` package. An initial model was fitted comprising of $k = 2$ Gaussian components, reflecting a two-component mixture of populations with regard to immune status. Maximum-likelihood estimates for the parameters, and membership probabilities for each component distribution were obtained by minimizing the deviance using the iterative expectation-maximization (EM) algorithm due to the incomplete nature of the observed data [41]. In the initial model, component means (itneg, itpos), and proportions of components (Aneg, Apos) and initial guesses remained unspecified, and standard deviations, a, were assumed to be equal. An initial seropositivity cut-off was selected where the probability densities for the two component normal distributions were equal.

2.4.3. Characterisation of immunological phenotypes using unsupervised machine learning methods (*K*-means clustering)

An unsupervised machine learning algorithm, *k*-means clustering, was utilized to partition the serological data into *k* groups [59]. Analysis was performed in R version 4.2.1 (2022-06-23) using `cluster` (version 2.1.4) [243] and `factoextra` (version 1.0.7) [244] packages. The optimal number of clusters (*k*) was determined using the elbow method (plotting the number of clusters against the total within sum of squares in order to examine visually for an "elbow" in the graph using `fviz_nbclust()` function, `factoextra` package); silhouette method using `fviz_nbclust()` function, `factoextra` [245]; and the gap statistic method (comparing the intra-cluster variation for different values of *k* with their expected value for a distribution with no clustering using `clusGap ()` function, `cluster` package [246] and finally, by exploring visually for biological coherence.

2.5. Chapter 3-specific methodologies: Performance of serological assays for filovirus antibody detection

2.5.1. Statistical analysis

All statistical analyses were performed with R version 4.2.1 (2022-06-23) and GraphPad PRISM version 10.6.1 (GraphPad Software Inc., Boston, MA, USA). Differences in filovirus antibody reactivity (measured by MMIA background-subtracted median fluorescence intensity (MFI)) between cohorts were examined using the Kruskal-Wallis test. Post-hoc pairwise comparisons were performed using Mann-Whitney U tests with Bonferroni correction for multiple comparisons. One-tailed tests were used when comparing EVD survivors to EVD contacts and EVD negatives, based on the a priori hypothesis that survivors would exhibit higher antibody responses; two-tailed tests were used for all other comparisons. The Wilson/Brown method for receiver operating characteristic (ROC) curve analysis was used to determine optimal EBOV antibody threshold cut-offs for the MMIA. Spearman's rank correlation coefficients (two-tailed) were calculated to assess associations between assays and viral antigens.

2.6. Chapter 4-specific methodologies: Zoonotic filovirus exposure in WLHs in Forested Guinea (Guinée forestière), Republic of Guinea 2017 – 2023

2.6.1. Spatial mapping and investigation of environmental risk factors

R version 4.2.1 (2022-06-23) was used to examine association between serological exposure and landscape characteristics was examined for each individual viral antigen, as described in previous publications [60]. The land cover classification map was obtained from ESRI land cover classification derived from Sentinel-2 remote-sensing images captured at a 100-meter resolution in 2017 and 2023, classified into mutually-exclusive standardised discrete land cover classifications (trees, water, flooded vegetation, crops, built area, bare ground, snow/ice, clouds and rangeland).

Study sites were geolocated to centroids and environmental data on the composition (proportion of land cover type) and configuration (spatial arrangement) of land cover classes [247, 248]) were calculated within circular buffer radii of 500 m, 1 km, 2 km, 5 km and 10 km from the village centroid to capture how the strength of association varies by spatial scale [249, 250]. Measures of forest fragmentation (perimeter area ratio, shape index (patch perimeter divided by the minimum possible patch perimeter), fractal dimension index (an index of shape complexity)) [251] using R package `landscapemetrics` (version 2.1.4) [251].

A data-driven approach was utilized to identify environmental risk factors, as previously described in the literature [249, 252]. Quantified landscape characteristics were mean-centred and scaled, and

mixed-effects logistic regression models were used to examine each environmental variable at each scale (n=126 models) for each individual antigen. Variables which were insignificant (*p*-value >0.2) or highly correlated (less significant variable when Pearson correlation coefficient >0.75) were removed.

2.6.2. Univariable and multivariable statistical models

All statistical analyses were performed with R version 4.2.1 (2022-06-23). A generalised linear mixed-effects model (GLM) was fitted in R using the `lme4` (version 1.1.37) package [253] for each individual filovirus antigen using *K*-means cluster classifications as binary seropositivity outcomes. Sampling year was included as a random effect within the model and iterative step-wise model selection was utilized to develop the multivariable model of best fit, assessing each demographic and environmental variable for inclusion based on Akaike information criteria (AIC).

Guinean wildlife hunting community, 2023

Associations between individual risk factors from the detailed questionnaire administered to the 2023 wildlife hunting community in 2023 were examined using univariable and multivariable statistical models. A GLM was fitted using the `lme4` package for each individual filovirus antigen to examine the associations between covariates (demographic, behavioural, environmental risk factors) and log-transformed Median Fluorescence Intensity (MFI) as the continuous outcome variable. Mixed effects logistic regression was also used to examine the associations between covariates and the *K*-means clusters (as binary seropositivity outcomes). Location was included as a random effect within the model, and bidirectional step-wise model selection was utilised to develop the multivariable model of best fit, assessing each demographic and environmental variable for inclusion based on Akaike information criteria (AIC).

Guinean wildlife hunting community 2017 and 2023

The same approach was utilised to examine associations between basic demographic variables which were included in both the 2017 and 2023 questionnaire (age, sex, hunter status, exposure to wildlife hunting, village location) and reactivity for each antigen, within the combined 2017 and 2023 Guinean wildlife hunting community population. Following univariable logistic regression analyses, multivariable mixed effects models (with sampling year included as a random effect) were developed as described.

2.7. Chapter 5-specific methodologies: Emerging viral surveillance in wildlife workers, Eastern Australia

2.7.1. Study design and participants

2.7.1.1. Patient and public involvement (PPI) activities

2.7.1.1.1. Advisory panel recruitment and activities

Patient and public involvement (PPI) was integrated throughout the research project. Early in the research prioritisation and design phase of the study, an advisory panel was established comprising experienced wildlife carers who were financially compensated for their contributions throughout the research lifecycle, which included online and in-person consultations, document review and outreach.

Advisory panel members were recruited through targeted outreach to represent diverse geographic regions, species specializations, and organizational affiliations within the Australian wildlife care sector. A total of 21 email addresses for Australian flying fox and wildlife care organisations, as well as wildlife health interest groups and wildlife hospitals were identified via online searches using various combinations of the following keywords: “flying fox”, “bat”, “carer”, “rehabilitator”, “wildlife”, and “Australia”. Additional organisations were identified through outreach to veterinary clinics, wildlife hospitals, and relevant conferences and meetings. All organisations were contacted via a solicitation email with a role description for the paid research project advisory panel position and encouraged to share with suitable candidates. All interested applicants were interviewed and selected to represent diversity in relevant demographic and experiential characteristics (different wildlife caring organisations, geographic areas).

2.7.1.1.2. Public forum

An online public forum was conducted during the recruitment phase, advertised through the advisory panel and direct outreach to wildlife organizations, flyers at veterinary clinics, wildlife hospitals, and training venues frequented by carers. This forum provided an open platform for wildlife carers to voice their priorities, concerns, and expectations regarding the research.

2.7.1.2. Participant recruitment

The previously identified flying fox and wildlife care organisations were contacted with participant recruitment flyers. Participants were encouraged to share recruitment flyers with solo rehabilitators unaffiliated with a care organisation. Panel members identified key gatekeepers within wildlife organizations who could facilitate introductions to potential participants, significantly enhancing the credibility of recruitment efforts.

2.7.1.3. Semi-structured interview guide design

The semi-structured interview guide was developed through an iterative process involving review of relevant literature, consultation with subject matter experts, and pilot testing with three individuals from the target population. Recommendations from the advisory panel were incorporated before wider

distribution to the target audience. The guide consisted of open-ended questions designed to elicit detailed narratives while maintaining flexibility to explore emergent themes.

The interview guide (Appendix) included demographic questions on gender, age, state of residence, years of experience, contact with flying foxes and microbats (number per year), contact with different species of flying foxes. Open-ended questions addressed aspects of caring for flying foxes, including use of personal protective equipment (PPE), and responses to bites/scratches/exposure to bodily fluid from flying foxes. Further questions focused on threat and risk perception using the Likert scale ("Strongly Disagree/Disagree/Neutral/Agree/Strongly Agree"). In the interview, “threat perception” was used to describe the perceived threat of zoonotic infections carried by wildlife, while “risk perception” was used in reference to questions relevant to the behaviour of carers to mitigate the risks associated with bites or scratches or potential exposure to bodily fluids.

2.7.1.4. Qualitative interviewing of wildlife workers

Interviews were conducted in-person between March and April 2024. The semi-structured format allowed the interviewer to follow the general structure of the interview guide while maintaining flexibility to probe responses, clarify meanings, and explore unexpected topics that emerged during conversation. Interviewers employed active listening techniques, including verbal and non-verbal encouragement, reflection, and summarization to facilitate participant disclosure and ensure accurate understanding of responses. Member checking was conducted by providing participants with summaries of key themes from their interviews and inviting feedback on accuracy and completeness of interpretation. Field notes were recorded immediately following each interview to capture contextual observations, non-verbal communication, and initial analytical insights.

2.7.1.5. Data management and statistical analysis of qualitative data

Survey responses were transcribed during the interview into Microsoft Excel (closed-ended) and Word (open-ended). Responses to open-ended questions were manually spell-checked.

Thematic analysis was conducted following Braun and Clarke's six-phase framework, examining open-ended responses regarding injury response protocols and PPE usage among wildlife carers and professionals. Initial codes were generated and refined to classify responses; thematic maps were then created to sort codes into broader themes and sub-themes. Once themes were reviewed and refined, all responses were re-coded. “Any” PPE was defined as all categories of PPE other than “nothing” (i.e., nitrile gloves, heavy gloves, or other PPE). Chi-squared tests were used to assess relationships between categorical variables, including PPE use and reported injury response behaviours; expected cell counts were checked to ensure test assumptions were met. A significance threshold of $\alpha = 0.05$ was applied. All statistical analyses were performed with R version 4.2.1 (2022-06-23).

Chapter 3

Performance of serological assays for filovirus antibody detection

3.1. Introduction

3.1.1. Serological assays for filovirus antibody detection

Over the past decades, a range of serological methods have been developed for antibodies against various EBOV antigens (e.g., GP, NP, and VP40), from traditional neutralisation, immunofluorescence (IF) and ELISAs, to more recent MMIA platforms.

3.1.1.1. Immunofluorescence (IF)

Before the widespread adoption of ELISA, indirect fluorescent antibody tests (IFATs) were commonly used to detect EBOV-specific antibodies. Indeed, an IFAT was utilised to distinguish EBOV from the closely related Marburg virus (MARV) when it was first discovered in 1976, based on the antigen specificity of antibodies in convalescent sera of survivors [254].

IFAT involves the incubation of patient sera with irradiated, EBOV-infected cells fixed on a slide, followed by detection using IF microscopy with fluorescently labelled secondary antibodies [255]. Although IFAT can be highly sensitive during the early convalescence, it suffers from lower specificity and logistical challenges, including the need for high biosafety level (BSL-4) facilities and expensive fluorescence microscopy equipment [256]. In comparison, ELISA not only streamlines the detection process but also presents advantages in specificity and long-term antibody detection, making it more suitable for large-scale epidemiological surveys [256].

3.1.1.2. Enzyme-Linked Immunosorbent Assays (ELISAs)

ELISAs are by far the most commonly used serological assays for EBOV antibody detection due to their high throughput, ease of standardisation, and sensitivity. They are primarily used to detect host antibodies (immunoglobulin M (IgM) and immunoglobulin G (IgG)) produced in response to EBOV infection. IgM antibodies are typically produced 2 – 11 days post symptom onset, peaking within 3

weeks post-infection (p.i.), before declining to undetectable levels 80 days p.i. in nonfatal infections. Consequently, while IgM ELISAs are useful for the diagnosis of recent or acute infection, they have limited utility in long-term seroepidemiological studies [256]. By contrast, IgG antibodies are detectable from 6 days post-symptom onset, and their long-term persistence (documented up to 40 years [257]) makes IgG ELISAs suitable for field investigations, and confirming EBOV exposure, including in asymptomatic or paucisymptomatic individuals [258].

Several ELISA formats have been reported. While early ELISAs utilised antigens derived from infected cell lysates, alternatives using recombinant viral proteins (e.g. recombinant NP, GP, VP40) have been developed, eliminating the need to handle authentic antigen preparations from viral cultures [259]. These recombinant antigen-based ELISAs exhibit high sensitivity and specificity, with NP-based ELISAs achieving sensitivity and specificity values around 85–99% when tested in various patient cohorts [256]. An EBOV envelope attachment GP ELISA, termed the Filovirus Animal Nonclinical Group assay, is also widely utilised in research and clinical settings [260]. Choice of recombinant antigen is key, for example, NP is highly conserved and abundant in infected cells, making it a preferred target for detecting broad exposure, while GP contains variable neutralising epitopes that may distinguish among strain-specific responses. VP40, a matrix protein present in high copy number, is also an attractive antigen due to its immunogenicity and kinetics in infected patients.

3.1.1.3. MMIAs

Technological advances have also led to the development of MMIAs with the capacity to simultaneously screen samples for multiple antigens (e.g., NP, VP40, GP from multiple species) in a single sample volume by employing antigen-coupled microsphere beads with distinct optical encoding [261, 262]. Each microsphere, typically 5–6 μm in diameter, is internally labelled with a unique ratio of fluorescent dyes, creating a spectral “barcode” for identification during flow cytometric reading. Specific antigens are covalently coupled to each bead set, ensuring stable and consistent surface display of antigens for subsequent binding of analytes in the sample. In a typical sandwich immunoassay format, the antigen-coupled beads are incubated with a sample (e.g., serum, plasma, or other biological fluids) allowing the antibodies to bind. After washing, a biotinylated secondary antibody specific for human immunoglobulins (for example, IgG or IgM) is added, followed by a detection antibody conjugated to a reporter fluorophore (commonly phycoerythrin). The beads are then washed to remove unbound reagents, and the sample is aspirated into a flow-based detection system where instrumentation such as the Luminex 100/200, MAGPIX, or FLEXMAP 3D systems employ dual-laser excitation: one laser exciting the internal dyes to determine bead identity, with a second laser exciting the reporter fluorophore bound to the analyte, thereby quantifying its concentration. The emitted fluorescence signals are captured by photomultiplier tubes or avalanche photodiodes, and the resulting data are

processed to generate quantitative measurements for each analyte, typically expressed as MFI (Figure 7).

The multiplexed approach streamlines the diagnostic process (reducing labour, reagent and operational cost while preserving clinical sample), making it ideal for the assessment of complex antigenic landscapes with co-circulating strains, and meeting the need for differential serodiagnosis.

The three-dimensional binding environment provided by beads in suspension is thought to improve the kinetics and efficiency of antigen–antibody interactions compared to immobilized assays on flat surfaces, thus enhancing sensitivity and dynamic range [263]. Studies assessing the performance of MMIAs have been inconclusive, with some comparing their MMIA to commercial EBOV NP and GP ELISAs (Alpha Diagnostic, San Antonio, TX) observing lower sensitivity (92.5%) and high specificity (100%) with the same positivity criteria [261], while others have demonstrated the lower limit of detection (LLOD) and increased sensitivity of the MMIA detection platform over ELISA for EBOV IgM antibody detection [264].

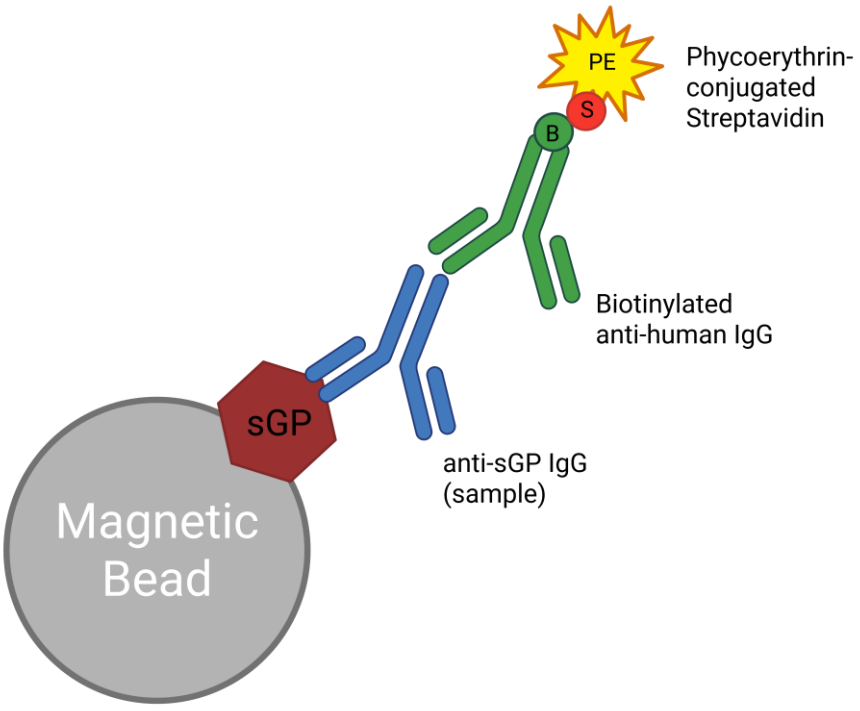


Figure 7 Indirect multiplexed microsphere-based immunoassay (MMIA)

3.1.1.4. Neutralisation assays and pseudotyped virus neutralisation assays (PVNAs)

Neutralization assays are considered the gold standard for confirming the functional activity of antibodies in blocking viral entry, by measuring the ability of convalescent serum to inhibit viral

infection of cultured cells. However, due to the requirement for live virus handling under BSL-4 conditions, neutralization assays are generally confined to research settings and specialized laboratories. To overcome these limitations, pseudovirus-based neutralization assays have been developed; these systems use non-pathogenic viral vectors expressing EBOV GP to assess neutralizing antibody titres, permitting testing under lower biosafety levels while maintaining a strong correlation with authentic VNTs [224, 265]. Here, studies have demonstrated strong correlations between lentivirus-based, EBOV GP-expressing, PVNAs and authentic EBOV-based neutralisation assays [265].

3.1.2. Challenges of EBOV serology

Despite technological advances, establishing safe and cost-effective diagnostics for EBOV remains challenging, particularly in resource-limited settings. EBOV serology is further complicated by antigenic cross-reactivity between *Orthoebolavirus* species, and the existence of a "public" cross-reactive GP epitope that is recognized by polyclonal antibody responses irrespective of the specific virus species [266]. Variability in assay performance and a paucity of established international standards further highlight the need for the rigorous assessment of serological assays to ensure accurate and reliable surveillance data.

3.1.3. Chapter aims and rationale

In this chapter, I aim to describe the use of an envelope GP-based MMIA, consisting of nine filovirus GP antigens, for the detection of anti-EBOV antibodies in a cohort of Guinean EVD survivors and contacts from the 2013 – 2016 West African EVD epidemic. Specifically, I aim to:

(1) Describe the GP-based filovirus MMIA sensitivity and specificity using a cohort of Guinean and United Kingdom-based negatives.
(2) Describe GP-filovirus MMIA agreement with alternative serological assays, including whole-virus ELISA and authentic virus neutralisation assays.
(3) Describe EBOV-GP reactivity and filovirus cross-reactivity (using GP-filovirus MMIA and PVNAs) against related filoviruses in the Guinean EVD survivor cohort. Additionally, I aim to describe filovirus reactivity in Marburg virus disease (MVD) survivors and EBOV vaccinees.

Here, I hypothesise that the GP-filovirus MMIA will demonstrate acceptable sensitivity and specificity compared to alternative assays currently in use, with strong correlation with whole virus ELISA and virus neutralisation tests. I hypothesise significant cross-reactivity will be observed against closely related filoviruses (BDBV, TAFV, SUDV) in the Guinean EVD survivor cohort.

3.2. Results

3.2.1. Performance of an envelope glycoprotein-based multiplex immunoassay for Ebola virus antibody detection in a cohort of Ebola virus disease survivors in Coyah and Guéckédou, Republic of Guinea

3.2.1.1. Study participants

Serum samples from EVD survivors sampled in 2015 (n=109), EVD survivors sampled in 2017 (n=89), EVD contacts sampled in 2015 (n=67), EVD contacts sampled in 2017 (n=88), Guinean negatives sampled in 2015 (n=10), Guinean negatives sampled in 2017 (n=7), and presumed unexposed UK blood donors sampled in 2020 (n=55) were tested for EBOV GP IgG by filovirus MMIA (Figure 8).

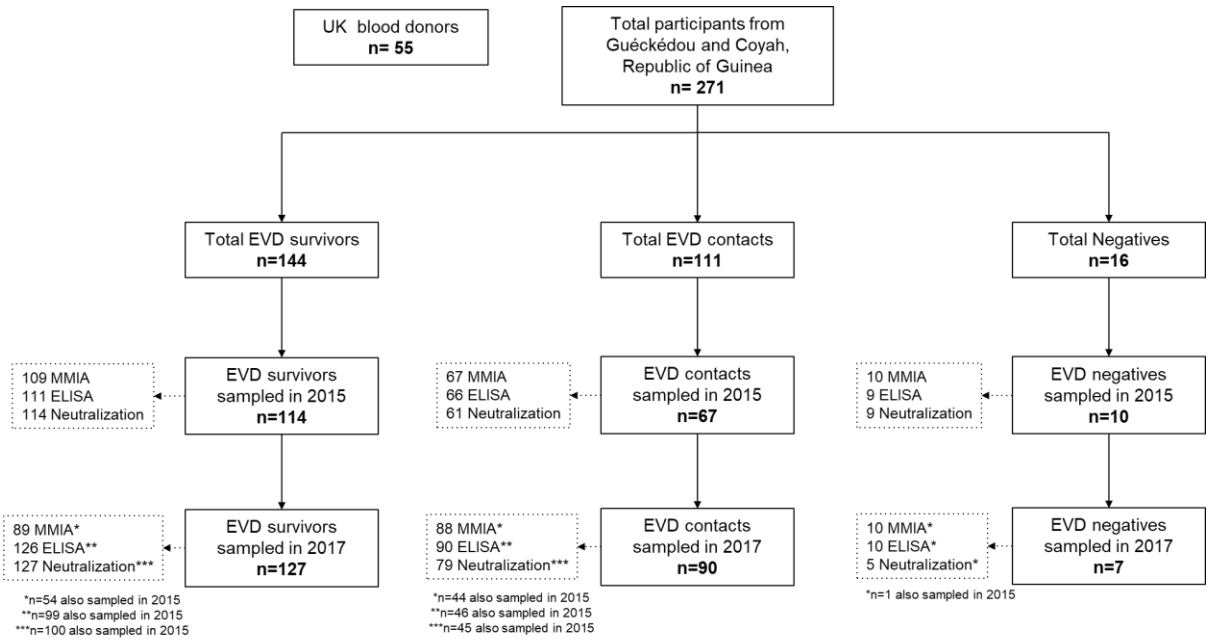


Figure 8 Ebola virus disease (EVD) survivor, contact and UK blood donor cohort [223].

3.2.1.2. Ebola virus survivor cohort demographics

As previously described in Thom et al., a total of 271 participants were recruited in 2015 and 2017 from Guéckédou (n=114, 42.0%) and Coyah (n=157, 58.0%). Of these, 142 (52.4%) were female, 125 (46/1%) were male and 4 (1.5%) were unspecified. The median age was 35 years (range: 17 – 67 years; interquartile range [IQR]: 26.75 – 40.75 years) (Table 10).

Of the study participants, 114 were EVD survivors, 111 were EVD contacts, and 16 were part of a negative cohort with no known exposure or history of EVD. The EVD survivors (n=114) were distributed between Guéckédou (n=64, 44.4 %) and Coyah (n=80, 55.6 %) and reflective of total cohort demographics, with 80 (55.6 %) female, 64 (44.4 %) male and median age of 35 (range 17 – 67; IQR:

25.5 – 45.5). The EVD contacts (n=1110 were from Guéckédou (n=41,36.0 %) and Coyah (n=71, 64.0 %), with 61 (55.0 %) female, 50 (45.0 %) male, and median age of 35 (range: 17 – 65; IQR: 27.25 – 40.0). The negative cohort (n=16) was sampled evenly from Guéckédou (n=8, 50%) and Coyah (n=8, 50%), predominantly male, 11 (69 %) male, one (6.25 %) female, and four (25 %) unspecified, and had a median age of 29 (range 19 – 38; IQR: 23.5 – 35.25).

Table 10 Demographics of EVD survivor, contact and negative cohort, Guéckédou and Coyah, 2015 and 2017

	Guéckédou			Coyah			Total		
	S	**C**	**N**	**S**	**C**	**N**	**S**	**C**	**N**
Total	64	41	9	80	70	7	144	111	16
Sampled in 2015	47	26	5	70	41	5	117	67	10
Sampled in 2017 *also sampled in 2015	54 *37	37 *22	5 *1	73 *63	53 *24	2	127 *100	90 *46	7 *1
Male	27	11	8	37	39	3	64	50	11
Female	37	30	1	43	31	0	80	61	1
Unspecified	0	0	0	0	0	4	0	0	4
Median age [range], years	35 [17-67]	34 [17-52]	28.5 [19-38]	35 [19-40]	65 [50-82]	N/A	35 [17-67]	35 [17-65]	29 [19-38]

S = Survivor, C = Contact, N= Negative.

3.2.1.3. Calibration of an internal reference standard to the WHO standard for EBOV

EBOV GP binding IgG antibodies were quantified from the MMIA using both median fluorescence intensity (MFI) and milli–international units per litre (mIU/L), standardized to the WHO international unit (IU), defined as 1.5 IU/mL of EBOV GP–binding antibodies. An internal reference standard (IR-std) was prepared from pooled serum of 3 EVD survivors and calibrated against the WHO reference standard (WHO-std). Both WHO-std and IR-std were subjected to twofold serial dilutions (1:200 to 1:25600) and 5 independent IR-std dilution curves were interpolated against the WHO-std. The interpolated mIU values were multiplied by the dilution factor to calculate mIU/L. The mIU/L in the linear range of each IR-std was averaged to estimate the EBOV GP IgG concentration (3217.42 mIU/L)

of the IR-std. A dilution series of the IR-std was then included in all subsequent MMIAs in order to make a semi-quantitative assessment (mIU/L EBOV binding antibody concentrations) of all patient serum samples. Samples where the MFI was above the IR-std's upper limit of detection (n=20) were re-tested at 1:400, 1:8,000, 1:32,000, and 1:64,000 dilutions in order to quantify an mIU/L in the linear range of detection. Samples with MFI that remained above the IR-std's upper limit of detection were reported as 16,000 mIU/L. Samples with MFI below the IR-std's lower limit of detection were reported at 1 mIU/L.

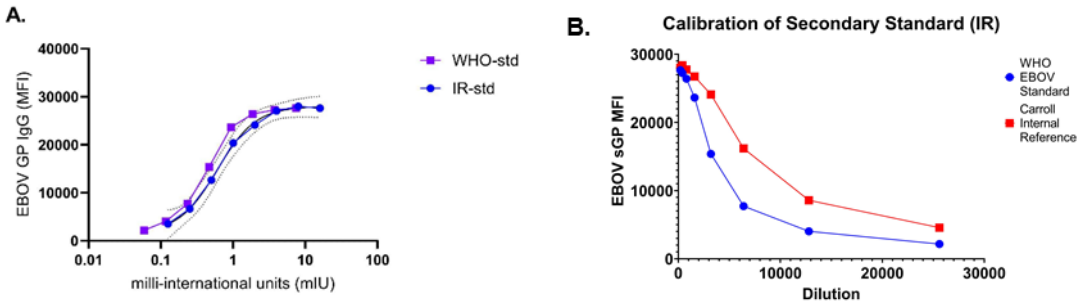


Figure 9 Calibration of internal reference standard to the WHO standard for EBOV. An internal reference (IR-std) composed of pooled serum from 3 EVD survivors was calibrated to the WHO international standard for EBOV (WHO-std). The known concentration of EBOV antibodies in the WHO-std (1500 milli-international units per litre) was used to estimate concentration of EBOV antibodies in the IR standard. Estimated concentration of EBOV antibodies in the IR-std is used to make a semi-quantitative assessment of binding antibodies in subsequent participant serum samples throughout the study. Serum samples from EVD survivors sampled in 2015 (n=109), EVD survivors sampled in 2017 (n=89), EVD contacts sampled in 2015 (67), EVD contacts sampled in 2017 (n=88), EVD negatives sampled in 2015 (n=10), EVD negatives sampled in 2017 (n=7), and naïve UK blood donors (UKBDs) sampled in 2020 (n=55) were tested for EBOV GP IgG by filovirus MMIA. Anti-EBOV binding antibody levels are reported as (A) milli-international units per litre (mIU/L) standardized to the WHO EBOV-std (B) median fluorescence intensity (MFI).

3.2.1.4. EBOV-GP reactivity by MMIA in the Guinean Ebola survivor cohort

Serum samples were tested for anti-EBOV GP IgG by MMIA to compare reactivity between the survivor, contact, Guinean negative and UK blood donor cohorts (Figure 10). Anti-EBOV GP IgG was first measured as MFI and then interpolated against five separately run internal reference standards for mIU/L semi-quantification. The mean anti-EBOV GP IgG levels in the 2015 cohort of EVD survivors was 23,761 MFI, which corresponded to 2,762 mIU/L. The magnitude of anti-EBOV GP IgG was significantly elevated in the 2017 cohort of EVD survivors, with a mean of 7,847 mIU/L (28,108 MFI). By comparison, the 2015 and 2017 EVD contacts had reduced anti-EBOV GP IgG levels, 404.7 mIU/L

(6,711 MFI) in 2015 and 1091 mIU/L (7,508 MFI) in 2017, respectively. Finally, both cohorts of EVD negatives and UK blood donors (UKBDs) had similar distributions of anti-EBOV GP IgG, with mean anti-EBOV GP IgG levels were 59.32 mIU/L (3,798 MFI) in 2015 EVD negatives, 33.64 mIU/L (2,082 MFI) in 2017 EVD negatives, and 46.13 mIU/L (2,938 MFI) in UKBDs.

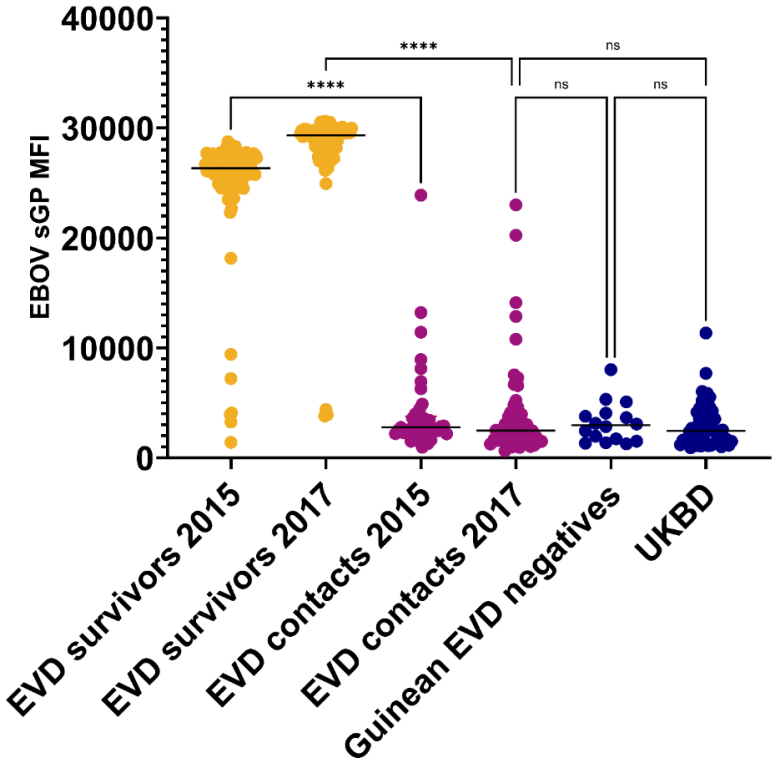


Figure 10 EBOV-GP reactivity by EVD history.

Serum from Ebola virus disease (EVD) survivors sampled in 2015 (n=109), EVD survivors sampled in 2017 (n=89), EVD contacts sampled in 2015 (n=67), EVD contacts sampled in 2017 (n=88), EVD negatives sampled in 2015 (n=10), EVD negatives sampled in 2017 (n=7), and naïve UK blood donors (UKBDs) sampled in 2020 (n=55) were tested for EBOV GP IgG by filovirus MMIA. Anti-EBOV binding antibody levels are reported as median fluorescence intensity (MFI). Horizontal lines indicate median MFI. Differences in filovirus antibody reactivity distributions (measured by MMIA MFI) between cohorts were examined using the Kruskal-Wallis test. Post-hoc pairwise comparisons were performed using Mann-Whitney U tests with Bonferroni correction for multiple comparisons. One-tailed tests were used when comparing EVD survivors to EVD contacts and EVD negatives; two-tailed tests were used for all other comparisons. ns = not significant, $*p \leq 0.05$, $**p \leq 0.01$, $***p \leq 0.001$, and $****p \leq 0.0001$. Yellow denotes EVD survivors, magenta denotes EVD contacts, navy denotes EVD negatives.

3.2.1.5. MMIA performance for EBOV GP binding antibody detection

The confirmed positive sample subset consisted of 198 EVD survivor samples tested by MMIA: 109 from the 2015 cohort and 89 from the 2017 cohort. The negative control sample subset consisted of the 55 UKBD samples and 17 EVD negative samples with absent binding antibody, neutralizing antibody

and T cell responses to EBOV. The 198 positive and 72 negative samples were tested by filovirus MMIA and both MFI and mIU/L data subject to receiver operating characteristic (ROC) curve analysis to establish positivity thresholds and performance of the assay. ROC analysis identified threshold values of 8,721 for MFI and 129.1 mIU/L, achieving 95.96% sensitivity and 98.61% specificity (Figure 11). Of the 198 true EVD survivors, eight participants (4.04%) showed EBOV GP reactivity below the determined threshold, representing false negatives (Type II error). In the control group of 72 participants without EVD exposure, a single individual (1.39%) demonstrated EBOV GP reactivity exceeding the established threshold, constituting a false positive (Type I error) (Table 11).

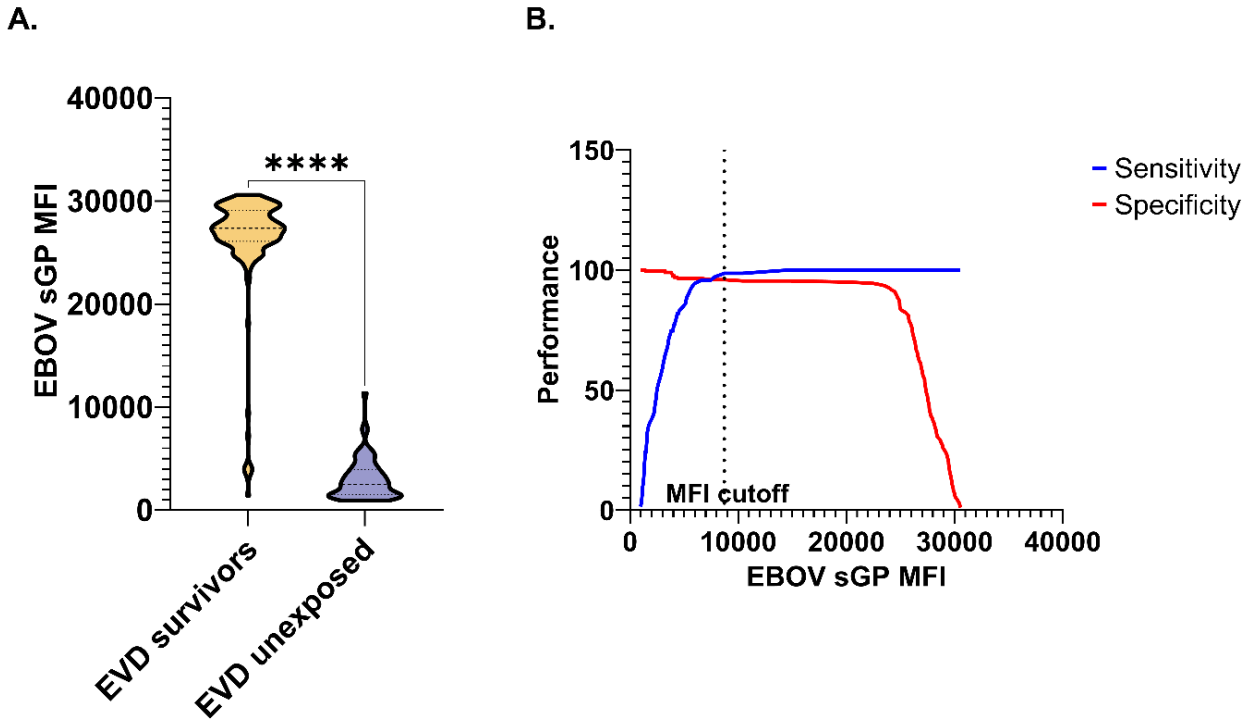


Figure 11 MMIA performance in EVD survivors and negatives.

(A) IgG reactivity in EVD survivors (n=198) and EVD negative individuals (n=72). Reactivity is measured by Ebola virus glycoprotein multiplexed microsphere-based immunoassay (MMIA) median fluorescence intensity (MFI). Median and interquartile ranges are denoted by dashed lines. Statistical significances were assessed by single-tailed Mann-Whitney U test; ns = not significant, $*p \leq 0.05$, $**p \leq 0.01$, $***p \leq 0.001$, and $****p \leq 0.0001$.

(B) The Wilson/Brown method for receiver operating characteristic (ROC) curve analysis was used to determine optimal EBOV antibody threshold cut-offs for the MMIA. Assay sensitivity and specificity of95.96% sensitivity and 96% specificity achieved at an MFI cut-off of 8721 (milli-international units per litre cut-off of 129.1).

Table 11 Performance of a filovirus envelope glycoprotein-based multiplex microsphere-based immunoassay (MMIA) for EBOV detection.

EBOV-GP IgG MMIA	EBOV Survivor status (PCR-confirmed)			
		Positive [a]	**Negative [b]**	**Total**
	Positive	190	1	191
	Negative	8	71	79
	Total	198	72	270

(a) 198 participants with PCR-confirmed EBOV infections and/or EVD survivor certificates from treatment centres are included in the positive group.

(b) 72 participants are included in the negative group, including 17 participants from Guinea with no known history of EVD or EVD exposure and 55 naïve blood donors from the UK. All 198 positives and 72 negatives were tested by filovirus MMIA for EBOV IgG. Sensitivity and specificity are reported based on a cut-off of 8721 median fluorescence intensity (MFI) and 129.1 milli-international units per litre (mIU/L).

3.2.2. Agreement between serological assays for filoviruses

3.2.2.1. EBOV-Makona ELISA and live EBOV-Mayinga neutralisation assay

First, agreement between the whole virion EBOV-Makona ELISA [267] and live EBOV-Mayinga neutralization assay [220] was assessed. Samples were considered seropositive by whole virion EBOV-Makona ELISA for arbitrary ELISA units were greater than three standard deviations above the median value for the negative cohort. The activity of the Ebola virus-specific antibodies present in plasma was determined by neutralisation of Ebola virus variant Mayinga (1976) as previously described. Samples were considered to be neutralising by authentic EBOV-Mayinga neutralisation assay if the titre was 1/8 or greater.

Spearman's correlation analysis revealed a strong positive relationship between ELISA-measured binding antibodies and neutralizing antibody titres in the 2015 Guinean cohort ($r=0.83$, $p<0.0001$), which included 111 individuals with confirmed EVD survival, 60 exposed contacts, and 9 participants with no EVD history. Similarly, robust correlations were observed in the 2017 cohort ($r=0.80$, $p<0.0001$), comprising 126 EVD survivors, 78 individuals with known exposure, and 5 participants without EVD exposure (Figure 12).

3.2.2.2. MMIA and EBOV-Makona ELISA

Agreement between the MMIA and the whole virion EBOV-Makona ELISA [267] was then assessed. Comparison of binding antibody measurements between MMIA and ELISA platforms demonstrated strong agreement in the 2015 cohort ($r=0.78$, $p<0.0001$), which consisted of 104 EVD survivors, 65 individuals with documented exposure, and 9 participants without EVD history (Fig. 2c). The 2017 cohort showed identical correlation strength between the two assay methods ($r=0.78$, $p<0.0001$), encompassing 88 individuals who survived EVD, 87 exposed contacts, and 10 participants with no EVD exposure (Figure 12).

3.2.2.3. MMIA and live EBOV-Mayinga neutralisation assay

Agreement between the MMIA and live EBOV-Mayinga neutralization assay was assessed. Analysis of the 2015 and 2017 cohorts (195 EVD survivors, 137 exposed individuals, and 14 participants without EVD history) revealed strong correlation between MMIA-determined binding antibody concentrations and neutralizing antibody titres ($r=0.76$, $p<0.0001$) (Figure 12).

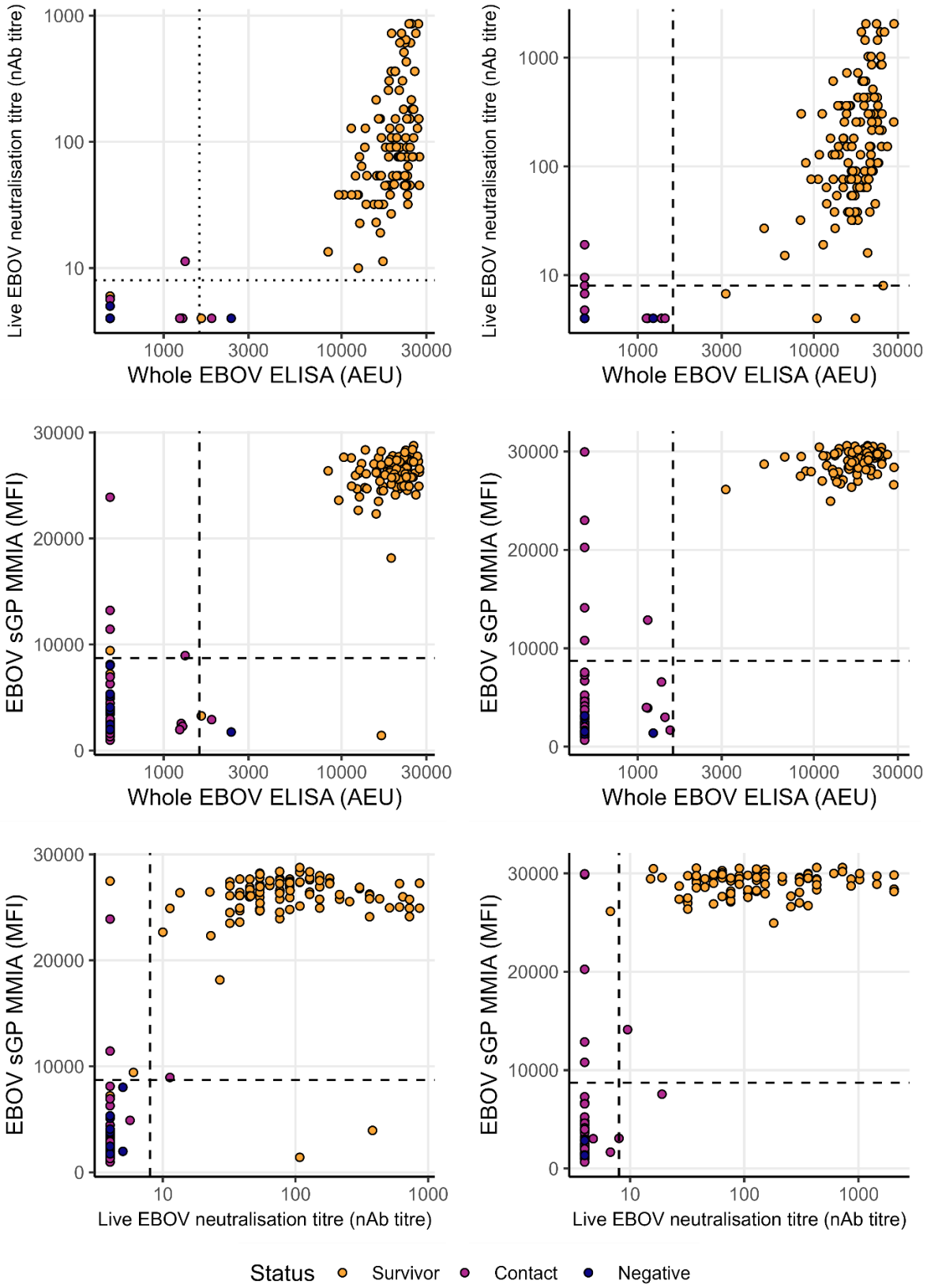


Figure 12 Correlations between filovirus MMIA, live EBOV-Mayinga neutralization test and whole EBOV ELISA. EBOV neutralization titres were measured using a live EBOV-Mayinga neutralization test were compared to binding antibody levels measured using a whole EBOV ELISA from (A) 2015 EVD survivors (n=111), EVD contacts (n=60), and EVD negatives (n=9) and (B) 2017 EVD survivors

(n=126), EVD contacts (n=78), and EVD negatives (n=5) by Spearman's correlation analysis. Binding antibody levels are measured by ELISA as arbitrary ELISA units (AEU) and positivity cut-offs determined by median (Neg) + 3*SD for the 2015 cohort (3046 AEU) and the 2017 cohort (1588 AEU). EBOV binding antibody levels measured using the filovirus MMIA were compared to binding antibody levels measured using the whole EBOV ELISA from (C) 2015 EVD survivors (n=104), EVD contacts (n=65), and EVD negatives (n=9) and (D) 2017 EVD survivors (n=88), EVD contacts (n=87), and EVD negatives (n=10) by Spearman's correlation analysis. (E) EBOV binding IgG levels measured using the filovirus MMIA were compared to neutralizing antibody titres measured using a live EBOV-Mayinga neutralization test from EVD survivors (n=195), EVD contacts (n=137), and EVD negatives (n=14).

3.2.3. Pan-orthoebolavirus binding antibody cross-reactivity resulting from EBOV infection

Cross-reactivity patterns of EBOV-induced binding IgG antibodies against GPs from related filoviruses were examined using the filovirus MMIA platform, and found that cross-reactivity diminished with increasing phylogenetic divergence from EBOV (Figure 13).

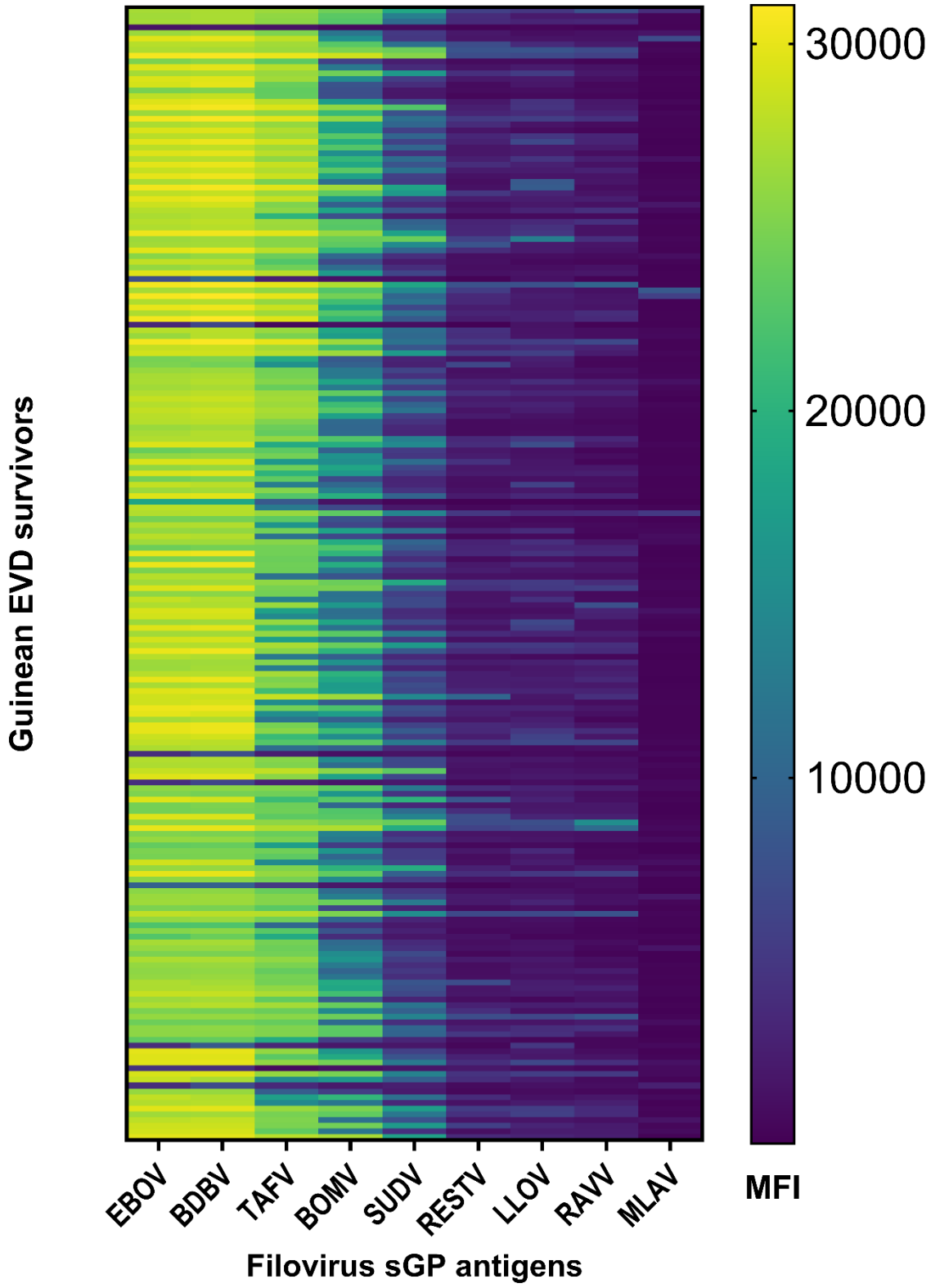


Figure 13 Anti-filovirus glycoprotein IgG responses of Guinean Ebola virus disease (EVD) survivors.

IgG responses were measured by multiplex microsphere-based immunoassay (MMIA) in background subtracted median fluorescence units (MFI-bg) on the Luminex platform.

Using the established EBOV threshold (129.1 mIU/L) across all filovirus antigens, 100% (190/190) of EBOV-GP seropositive survivors were also positive to BDBV-GP. Among the 190 EBOV GP-seropositive survivors, concurrent seropositivity (using the EBOV-GP threshold) was detected for TAFV GP in 188 individuals (98.9%), BOMV GP in 159 (83.7%), SUDV GP in 73 (38.4%), and RESTV GP in 3 (1.6%). EVD contacts with EBOV GP seropositivity (n=34) demonstrated parallel but reduced cross-reactivity: BDBV GP in 31 individuals (91.2%), TAFV GP in 15 (44.1%), BOMV GP in 12 (35.3%), SUDV GP in 6 (17.6%), and RESTV GP in 1 (2.9%).

Spearman's correlation analysis examined relationships between EBOV-specific IgG and antibody responses to eight additional filovirus glycoproteins among all EBOV-seropositive participants (n=227). Consistent with co-positivity findings, BDBV GP IgG demonstrated the strongest association with EBOV GP IgG ($r=0.99$, $p<0.0001$) (Figure 14). Intermediate correlation coefficients were identified for TAFV GP IgG ($r=0.54$, $p<0.0001$), BOMV GP IgG ($r=0.34$, $p<0.0001$) relative to EBOV GP IgG levels. Phylogenetically distant filoviruses showed weaker associations with EBOV GP IgG: SUDV GP IgG ($r=0.13$, $p<0.0001$), RESTV GP ($r=0.10$, $p<0.0001$), LLOV GP ($r=0.07$, $p=0.0002$) and RAVV GP ($r=0.06$, $p<0.0003$) (Figure 14).

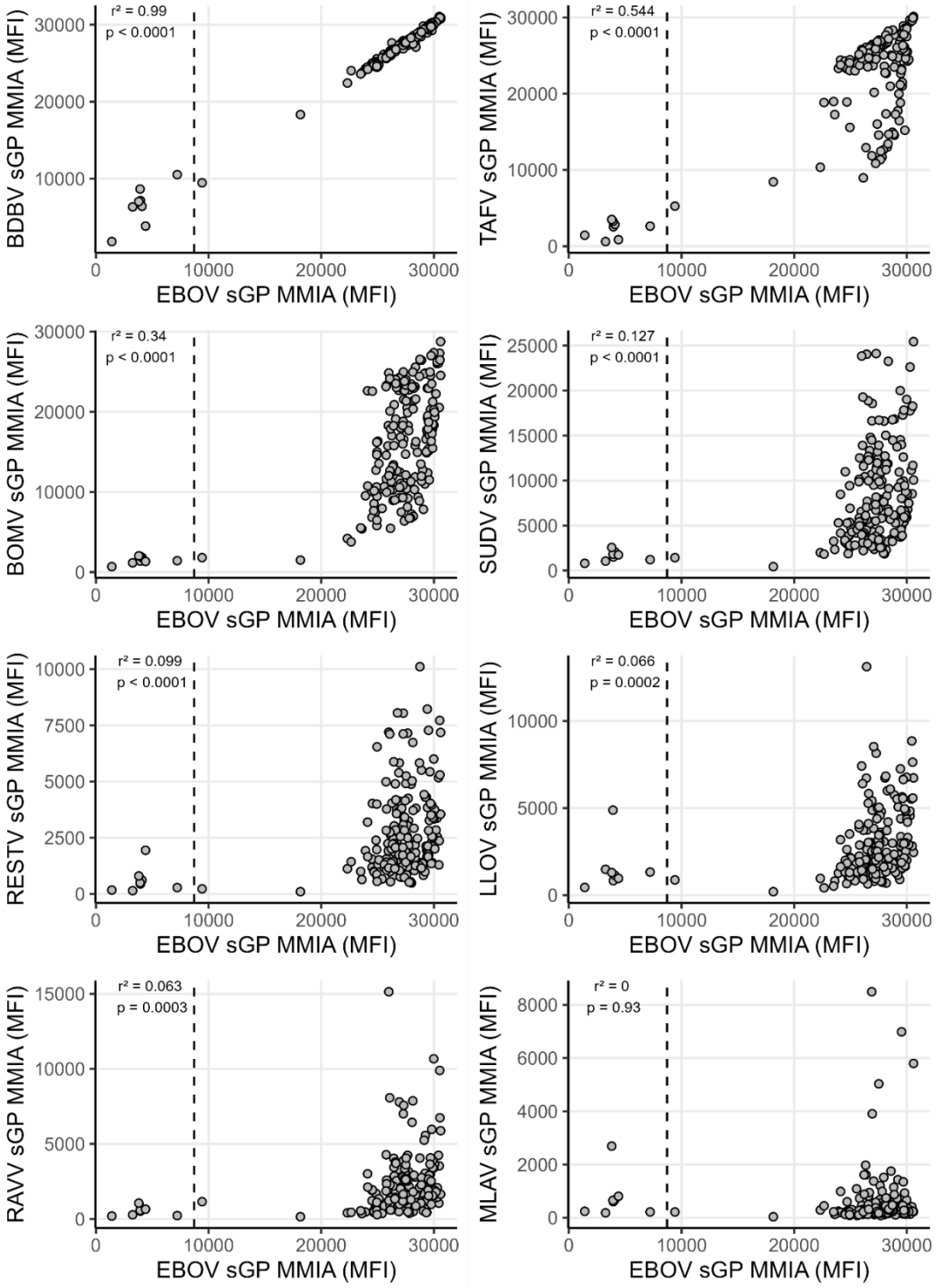


Figure 14 Correlation between Ebola virus (EBOV) glycoprotein (GP) IgG and GP IgG for 8 heterotypic orthoebolaviruses.

EBOV binding IgG data from EBOV-positive individuals (n=227) were compared to (A) BDBV IgG, (B) TAFV IgG, (C) BOMV IgG, (D) SUDV IgG (E) RESTV IgG (F) LLOV IgG (H) RAVV IgG and (I) MLAV IgG by Spearman's correlation analysis. Significant correlations ($p<0.001$) were found between EBOV IgG and orthoebolaviruses except MLAV. A strong correlation was observed between EBOV and BDBV, moderate correlations observed between EBOV and TAFV and EBOV and BOMV, and weak correlations observed between EBOV and SUDV and EBOV and RESTV.

3.2.4. Anti-filovirus GP binding antibody responses of an rVSVΔG-ZEBOV-GP Ebola virus vaccine recipient

The replication-competent, recombinant vesicular stomatitis virus (rVSV)-vectored Ebola vaccine, rVSVΔG-ZEBOV-GP (ERVEBO) is approved for the prevention of EVD by the European Medicines Authority (EMA) and United States Food and Drug Administration [268]. The anti-filovirus GP IgG response was examined by MMIA in an ERVEBO recipient (n=1) of the at 14, 30 days and 18 months after the final primary series boost, and showed anti-EBOV GP binding but minimal cross-reactivity against related filovirus GPs at D14 and D30, but not M18 (Figure 15).

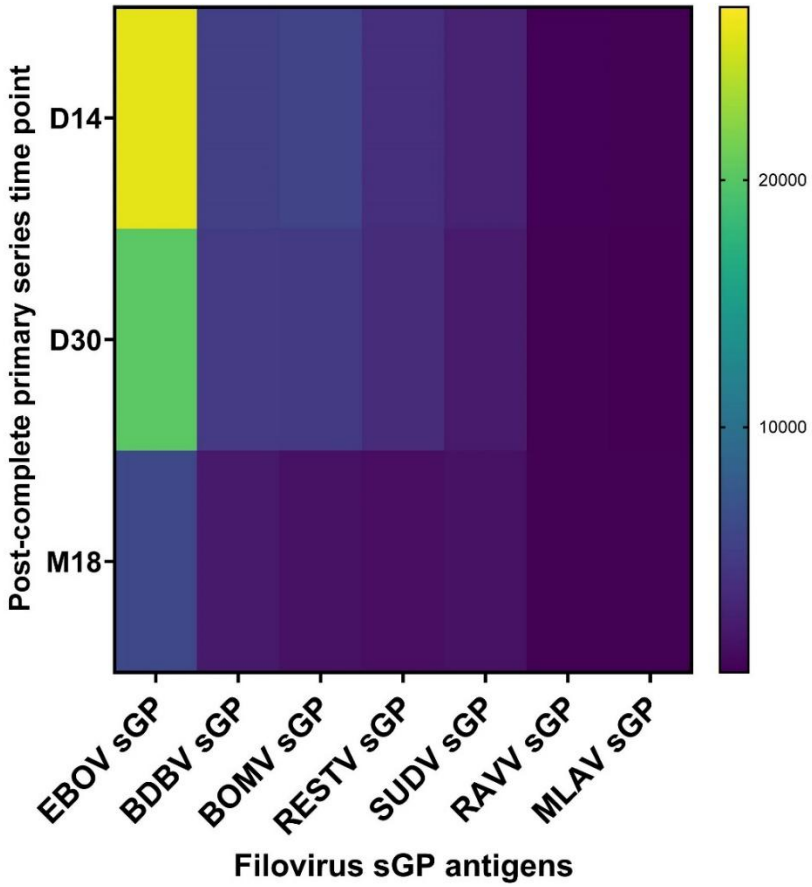


Figure 15 Anti-filovirus glycoprotein IgG responses of EBOV vaccinee.

IgG response of a recipient of a replication-competent, recombinant vesicular stomatitis virus (rVSV)-vectored Ebola vaccine, rVSVΔG-ZEBOV-GP (ERVEBO) (n=1) at 14, 30 days and 18 months after the final primary series boost.IgG responses were measured by multiplex microsphere-based immunoassay (MMIA) in background subtracted median fluorescence units (MFI-bg).

3.2.5. Anti-filovirus GP binding antibody responses in Marburg virus survivors from Uganda and the Democratic Republic of Congo

In order to examine antibody cross-reactivity induced by MARV infection, sera samples from MVD survivors from the 2012 MARV outbreak in Western Uganda (n=8, 11 years post-infection) and the 1999 outbreak in the DRC (n=5, 16 years post-infection) were also examined using the MMIA platform (Figure 16). For 3/13 MARV survivors, antibody responses above the serological threshold against EBOV and BDBV. Interestingly, minimal antibody cross-reactivity was demonstrated against the more highly homologous RAVV glycoprotein.

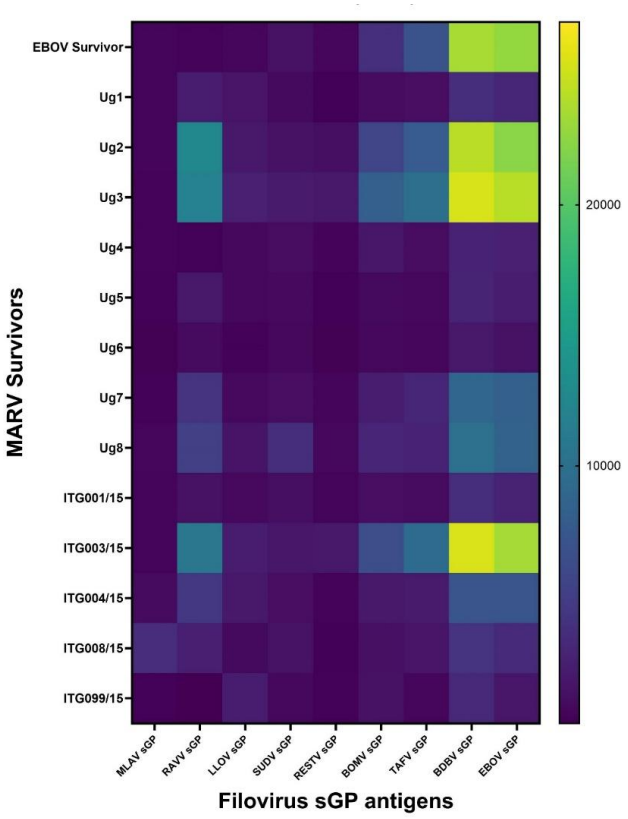


Figure 16 Anti-filovirus glycoprotein IgG responses of Marburg virus survivors.

Anti-filovirus responses in MARV survivors from the 2012 MARV outbreak in Western Uganda (Ug1 – Ug8, n=8, 11 years post-infection) and the 1999 outbreak in the Democratic Republic of Congo (ITG001 – ITG099, n=5, 16 years post-infection).IgG responses were measured by multiplex microsphere-based immunoassay (MMIA) in background subtracted median fluorescence units (MFI-bg) on the Luminex platform.

3.2.6. Pan-filovirus neutralisation in Ebola virus disease survivors: demonstrated in lentiviral-vector based pseudotyped virus neutralisation assays (PVNAs)

Pseudotyped viruses expressing filovirus GP (EBOV Kikwit, EBOV Makona, BOMV, BDBV, TAFV, RESTV, SUDV and LLOV) (Figure 17) were produced using a second-generation lentiviral (HIV-1) system using backbone plasmid p8.91 (expressing Gag, Pol, Tat and Rev) as a packaging construct and firefly luciferase (pCSFLW) as a reporter construct. PVNAs were optimised using PCR-confirmed convalescent sera from MARV survivors (n=5) and SUDV survivors (n=9) (as part of the Collaborative Study for the Establishment of the First WHO International Standard for Marburg virus antibodies and SUDV virus antibodies) (Figure 19) and Guinean EVD survivors (n=11) (Figure 20).

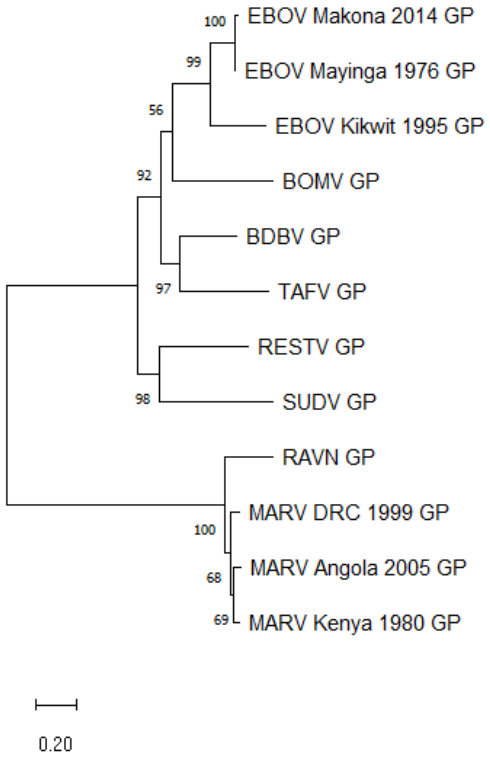


Figure 17 Phylogenetic tree of filovirus envelope glycoproteins (GP).

Tree estimated by Maximum Likelihood method and General Time Reversible model (see methods).

Cross-reactivity patterns of EBOV-induced neutralising IgG antibodies against GPs from related filoviruses were examined using parallel pseudotyped virus neutralisations in a pool of EVD survivors (n=3) and a non-endemic UKBD. EVD survivor sera showed some neutralising activity against all filovirus GP, with the strongest activity against EBOV Kikwit GP, followed by SUDV GP, then BDBV GP (Figure 18).

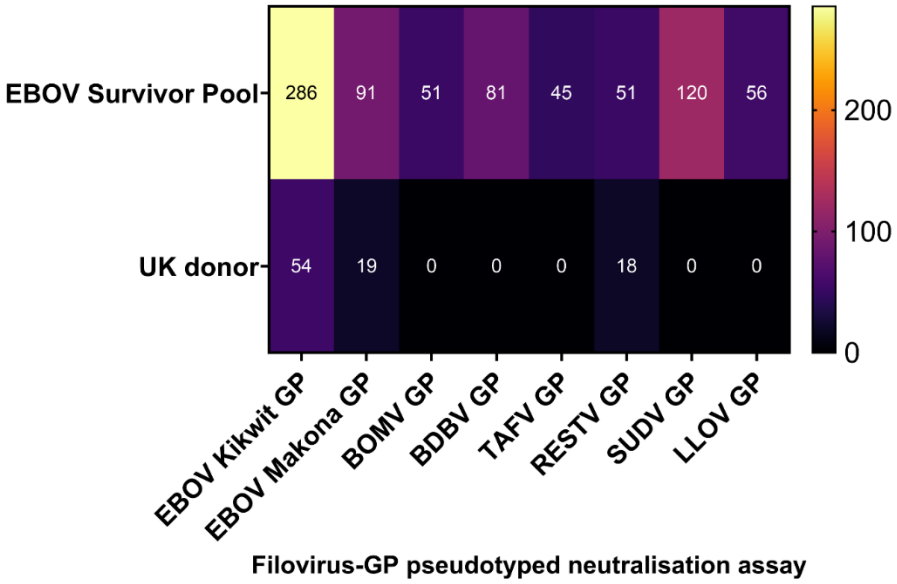


Figure 18 Cross-neutralising responses from Guinean EVD survivors.

Filovirus glycoprotein expressing pseudotyped lentivirus neutralisation titres of Guinean Ebola virus disease (EVD) survivors (n=3).

3.3. Discussion

In this chapter I describe the performance of a filovirus envelope-GP MMIA in a large cohort of PCR-confirmed Guinean EVD survivors, contacts, and EVD negative study participants. The MMIA utilised native-like GP trimer ectodomain targets, which were produced in mammalian cell-lines in order to conserve appropriate post-translational modifications and glycoepitopes. When used for the detection of anti-EBOV IgG, sensitivity was found to be 95.96% and specificity was found to be 98.61%. A high level of agreement was found between the MMIA and previously conducted whole virus EBOV ELISA and live EBOV neutralization assays for this cohort, further supporting its robustness as a surveillance tool.

Early serological methods, such as IF assays, and subsequent techniques like ELISA have each demonstrated limitations related to reproducibility, assay calibration, and inter-laboratory comparability. Differences in antigen preparation, sample dilution methods, cut-off determination using ROC analysis, and potential reagent degradation under field conditions contribute to the variability observed between assays. In this chapter, the use of the WHO EBOV serology standard enabled measurement of a standardized mIU/L concentration of EBOV antibodies, allowing for future standardization of EBOV binding antibody concentrations across assays, and better comparison of serological data across studies and geographic regions.

Live virus neutralization assays are considered to be the gold standard for orthoebolavirus-specific antibody detection [269], however, high biocontainment requirements significantly limit their use. Additionally, EBOV convalescent sera and EBOV-specific monoclonal antibodies have been shown to cross-neutralize all other heterotypic orthoebolaviruses, including more distantly related RESTV and SUDV [270, 271], highlighting the need to assess the ability of neutralisation assays to differentiate between related filovirus species. In this chapter, I demonstrated strong agreement between the GP-filovirus MMIA and authentic EBOV neutralisation assays, highlighting how measurement of antibody binding against EBOV GP (an antigenic target of both neutralizing and non-neutralizing effector antibodies) could serve as an appropriate proxy for neutralization tests [272, 273]. Further, I optimised a pseudotyped virus neutralisation assay in PCR-confirmed Marburg, Sudan and Ebola virus survivors, demonstrating its utility as a BSL-2 surrogate for authentic virus. A significant limitation of this analysis was the lack of sera volume, which prevented a comparison of pseudotyped and live neutralisation data, though previous studies have demonstrated strong correlations [224, 265]. The PVNA was then used to assess cross-neutralisation induced by EBOV-infection against related filoviruses, and demonstrate its ability to differentiate viruses within the genus.

Serological cross-reactivity between filovirus species presents a significant challenge to surveillance, particularly in non-outbreak settings with co-circulation of viral species. Convalescent sera from EBOV, BDBV and RESTV survivors is highly cross-reactive with heterotypic virus antigens; furthermore, RESTV antisera has been shown to preferentially interact with EBOV antigens suggesting virus species-specific immunodominance [274]. This cross-reactivity may be driven by antibodies directed against the GP2 subunit of the GP, which contains the highly conserved N-terminal internal fusion loop (IFL), and heptad repeats HR1 and HR2.

Amongst the EVD survivor cohort, cross-reactivity (and presumed antigenic relatedness) decreased with phylogenetic distance. Of the EBOV seropositive individuals, 100% were co-positive for BDBV, with a strong correlation observed between EBOV binding IgG and BDBV binding IgG. BDBV and TAFV, followed by SUDV and RESTV, showed intermediate correlations, with more distantly related filoviruses (LLOV, RAVV, MLAV) showing minimal co-positivity. Similarly, the EBOV IFL has 86% sequence similarity to the BDBV IFL, 85% similarity to the TAFV IFL, and 73% similarity to the BOMV IFL. The EBOV HR1/2 has 100% sequence similarity to the BDBV HR1/2, 98% identity to TAFV HR1/2, and 95% to BOMV HR1/2. Cross-reactivity was less frequent in the EVD-contact population, with only 44.1% co-positivity observed in the EBOV-positive contacts. This may reflect that cross-reactivity only occurs at the upper limits of antibody concentration, as paucisymptomatic infections may induce a less robust antibody response compared to overtly symptomatic infections [275]. Of the MARV seropositive individuals (n=3/13), 100% were co-positive for BDBV and EBOV.

Interestingly, antibodies induced by EBOV vaccination (n=1) showed no cross-reactivity to filovirus species. This finding supports the hypothesis of a cross-reactivity dominated by GP_2 directed antibodies, given previous findings where natural infection, but not ChAd3-MVA EBOV prime-boost vaccination, induced increased IFL and HR2 antibodies [276].

These findings may have implications for the interpretation of seroepidemiological data from non-outbreak settings, as well as cross-protection following vaccination effectiveness or infection by other orthoebolaviruses. Further, future serological tools may investigate the use of GP_1 antigens for greater specificity, by limiting the influence of fusion domains and glycoepitopes or glycosylations in the glycan gap and mucin-like domain.

While many other filovirus assays are based on nucleoprotein (NP), and matrix protein (VP40) antigens, the highly conserved nature of these proteins (sequence similar of 63 – 79% for NP, 73 – 89% for VP40) renders them inherently less suitable than GP (51 – 73% sequence similarity) for differentiating between species. Further, as internal structural proteins, NP and VP40-based assays cannot be verified against viral neutralization assays. However, given the highly multiplexed capabilities of the MMIA, future refinement of the assay may benefit from the inclusion of these additional antigens.

3.4. Appendix

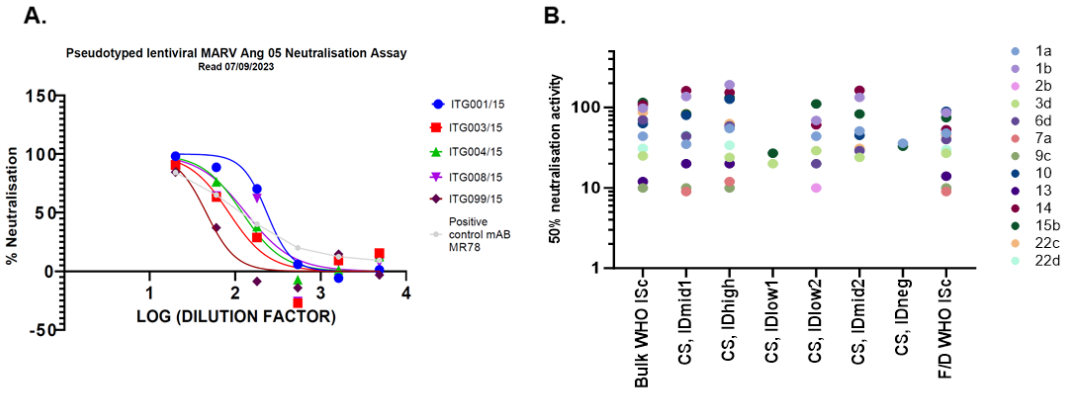


Figure 19 MARV pseudotyped virus neutralisation assay optimization. (A) The Marburg virus pseudotyped virus neutralisation assay (PVNA) was optimized in Marburg convalescent sera provided by Dr. Christian Kahusu and Dr. Mulangu Sabue from survivors (n=8) of the 2012 MARV outbreak in Western Uganda. (B) Data from the assay formed part of the Collaborative Study for the Establishment of the First WHO International Standard for Marburg virus antibodies and compared to PVNAs from other laboratories. Data from my MARV PVNA is denoted 3d in this figure, which was sourced from the report.

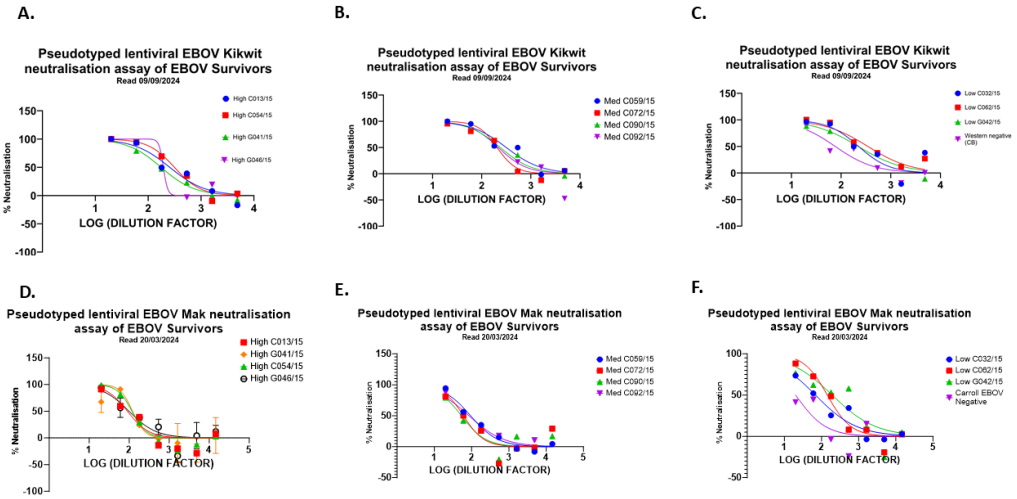


Figure 20 EBOV pseudotyped virus neutralisation assay optimization. Ebola virus glycoprotein expressing pseudotyped lentivirus was used to perform pseudotyped virus neutralisation assays (PVNA) PCR-confirmed Guinean Ebola survivors in (A) High responding EVD survivors (n=4) in Ebola-Kikwit PVNA (B) Medium responding EVD survivors (n=4) in Ebola-Kikwit PVNA (C) Low responding EVD survivors (n=4) in Ebola-Kikwit PVNA (D) High responding EVD survivors (n=4) in Ebola-Kikwit PVNA (E) Medium responding EVD survivors (n=4) in Ebola-Kikwit PVNA (F) Low responding EVD survivors (n=4) in Ebola-Kikwit PVNA.

Chapter 4

Zoonotic filovirus exposure in wildlife hunters in Forested Guinea, Republic of Guinea 2017 – 2023

4.1. Introduction

4.1.1. Viral spillover in Forested Guinea, Republic of Guinea

Forested Guinea (Guinée forestière), Republic of Guinea has been the site of multiple high-consequence viral spillover events, including the index case of the 2013-16 West African EVD epidemic, which was designated by the WHO as a public health emergency of international concern (PHEIC) [277]. The first case of MARV in West Africa was also detected in Forested Guinea in 2021, demonstrating yet again the ongoing threat that zoonotic filovirus spillover poses to the health and economic security of the region [278].

Forested Guinea is a historically forested and mountainous region sharing porous borders with Sierra Leone, Liberia and Cote d'Ivoire. It has the highest incidence of poverty in the country, with 66.9% of the population living below the poverty line; majority engaged in subsistence farming in rural areas. Access to healthcare is limited, with World Bank estimates of 0.2 medical doctors per 10,000 people falling far below the global average of 17.2 per 10,000 and Sustainable Development Goal targets. Overlapping challenges of climate change, political instability and multiple refugee crises from neighbouring civil wars further confound infectious disease surveillance and control.

Here, manifold opportunities for viral emergence present at Forested Guinea's extensive human-wildlife interface, which is further expanded by ongoing deforestation. Land-use changes, such as the anthropogenic conversion of natural habitats for agricultural or urban use, drive spillover by fundamentally disturbing reservoir species' ecology, altering their distribution, behaviour and physiology, simultaneously increasing both human interaction and pathogen shedding [34, 35, 279]. Further, evidence shows human-disturbed landscapes systematically select for species traits correlated with host status, driving a net increase in zoonotic host diversity [39]. Analyses of landcover surrounding EBOV spillover events in Central and West Africa have suggested associations with deforestation, highlighting the need for further investigation [37, 280].

More proximal drivers of spillover, such as wildlife hunting, have also been implicated. Historical outbreak investigations have identified epidemiological links between individual cases and exposure to susceptible host species [9, 48, 52, 90, 91, 277, 278, 281], while large-scale seroprevalence studies have uncovered significant population-level associations between viral exposure and wildlife hunting [162]. In the case of filoviruses, bats are often spotlighted as the known reservoirs of MARV and Ravn virus [135, 282], and suspected reservoirs of other filoviruses based on a growing body of molecular, serological and ecological evidence [128, 139]. This evidence includes the detection of EBOV RNA and antibodies in multiple insectivorous and fruit bat species in the DRC and Gabon [128, 283]; the recovery of the complete BOMV genome from insectivorous bats in Sierra Leone [154] and RNA in Guinea [181], Kenya [284], Mozambique [285] and the presence of anti-SUDV and anti-RESTV virus antibodies from multiple bat species across Asia and Africa [143, 146, 148]. Similarly, LLOV has been detected in Schreiber's bats in Spain and isolated in Hungary and Italy [141, 156, 286] and the complete genome for MLAV has been recovered from Rousettus bats in China [179]. Other animal species, including non-human primates [20, 21, 287, 288] and duikers (*Cephalophus* spp.) [24] are known to be susceptible, and may serve as intermediate hosts, as in the case of the only documented human case of TAFV), who was infected in Cote d'Ivoire while performed a necropsy on a wild chimpanzee [289, 290].

The severe pathogenicity of many of these filoviruses has been established (with EBOV, MARV, SUDV, and BDBV viruses causing human outbreaks with CFRs ranging from 25% to 90%) while others cause milder (TAFV) or even asymptomatic disease (RESTV) [291]. For others, including BOMV, LLOV and MLAV, as well novel undiscovered filoviruses, the human infective and pathogenic potential remains unknown, highlighting the urgent need for ongoing surveillance. Seroepidemiological methods provide great utility in the study and surveillance of infrequent spillover events at the human-animal interface, particularly for pathogens of variable clinical presentation and reliably sustained, measurable IgG responses, as is documented for EBOV [220, 257, 277, 292-294].

4.1.2. Seroepidemiology of filoviruses in West Africa

4.1.2.1. Summary of published orthoebolavirus seroprevalence studies conducted in West Africa, 1978 – 2025

Accurately quantifying filovirus exposure in humans in West Africa is essential for our understanding of their natural history, transmission, and clarifying the widely disputed role of subclinical infection. However, despite more than 76 investigations into the seroprevalence of orthoebolaviruses since the first outbreak in Yambuku, Zaire (modern-day DRC), a wide range of estimates have been reported, even among similar populations.

In a 2024 systematic review of 76 studies, Semancik reported *Orthoebolavirus* seroprevalences across the African continent ranging from 0.0 – 20.9% for EBOV, 0.0 – 19.9% for SUDV and 0.2% for BDBV in the general population [295]. I performed a rapid literature review of *Orthoebolavirus* seroprevalence surveys conducted in West Africa up until August 10th 2025 that have been published in peer-reviewed scientific journals in English or French (methodology in Supplementary). I identified 26 studies assessing *Orthoebolavirus* seroprevalence in West Africa: 21 in countries affected by the 2013-2016 EVD epidemic (during or shortly after the outbreak) (Table 12). The majority of these (15/26) assessed seroprevalence in high-risk populations: individuals with fevers of unknown origin (FUO), asymptomatic contacts of known EVD cases, or healthcare workers (HCW). Studies which assessed seroprevalence in the general population (11/26) observed EBOV seroprevalence ranges from 1.3 – 19.4% (Table 12). Interestingly, the highest seroprevalence estimates came from Forested Guinea, where 19.4% (52/268) were seropositive at least one EBOV antigen; 1.1% (3/268) were NP reactive and 9.33% (25/268) were reactive to GP-m. Several studies (highlighted in Table 12) also provided evidence of the circulation of EBOV in the area prior to the 2013-2016 epidemic: for example, 8.5% of febrile individuals 2011-2012 (n=129) in Guinea [296].

These discrepancies may reflect heterogeneity in study populations (general population vs. contacts vs. symptomatic individuals), settings (outbreak vs. non-outbreak), sample sizes (often small), exposure and control group selection, as well as differences in antibody detection assays and their associated intra-assay parameters and cut-offs. All pre-1998 studies utilised IF, which was subsequently replaced by ELISAs, and from 2012, less commonly, MMIAs. Assay antigens varied, as did the level of detail in the methodological descriptions (species, strain, whole virus vs. recombinant proteins – and associated expression systems, purification methods and verification). For example, many early ELISA antigens were produced by lysing EBOV-infected Vero E6 cells and collecting supernatant (IgM) or by detergent basic buffer extraction of infected cells for lysate antigen preparations (IgG), methods known to induce cross-reactivity between strains, particularly in IgG antibodies [274]. Many studies took place in field settings with insecure cold-chains for serum samples and laboratory reagents. All studies focused on immunological reactivity, and virus neutralization was largely unexamined, with the exception of Steffen et al., 2019 [297].

Overall, these studies demonstrate that while EVD outbreaks are sporadic, EBOV antibodies are prevalent amongst human populations, even in non-outbreak settings. Whether this is due to cross-reactivity resulting from infection by less pathogenic filoviruses, or asymptomatic or paucisymptomatic EBOV infection remains to be established.

Table 12 Summary of published orthoebolavirus seroprevalence studies conducted in West Africa, 1978 – 2025

Population sampled	Country	Year	Seroprevalence	Assay	Citation
Very low risk (general population in non-outbreak setting)					
General population	Liberia	1978 – 1979	6% (26/433)	IF	Knobloch et al., 1982, Ann de l'Institut Pasteur [298]
General population (including epilepsy patients)	Liberia	1986	13.4% (30/225)	EBOV -May IF	Van der Waals, 1986, Trop and Geo Med [299]
General population	Nigeria	1988	EBOV: 1.3% (22/1677); SUDV: 1.8% (30/1677)	IF	Tomori et al., 1988, Am Jour of Trop Med and Hyg [300]
General population prior to outbreak	Guinea	2012	≥1 EBOV antigen: 10.4% (154/1483); GP-Mayinga: 5.5% (81/1483); NP: 0.6% (9/1483); VP40: 4.2% (62/1483). Forested Guinea — ≥1 antigen: 19.4% (52/268); NP: 1.1% (3/268); GP-m: 9.33% (25/268)	NP, GP, VP40 EBOV IgG MMIA	Keita et al., 2018, Am J Trop Med Hyg [301] *
General population in EVD unaffected area	Mali	2015	3.7% GP-positive and 4.0% NP-positive and 1.5% both 6.1% (37/600); GP: 3.7% (22/600); NP: 4.0% (24/600); GP and NP: 1.5% (9/600)	GP, NP IgG ELISA	Bane et al., 2021, EID [302]
General population in EVD unaffected area	Guinea	2022	GP-Kiss: 6.6% (58/878); GP-May: 7.2% (63/878); VP40: 3.6% (32/878); NP: 0.8% (7/878)	NP, GP-Kiss, GP-May, VP40 EBOV; GP, VP40 SUDV; GP,	Hounmenou et al, 2024, Int Journ of ID[303]

				VP40 BDBV, GP RESTV, GP BOMV IgG MMIA	
General population (rural population and case-control study examining nonhuman primate bites)	Cameroon	2024	Rural population: ≥2 EBOV antigen: 10.2% (81/795); ≥2 SUDV antigen: 9.6% (76/795); BDBV antigen: 3.5% (28/795) NHP bites: ≥2 EBOV antigen: 15.6% (97/622); ≥2 SUDV antigen: 14.1% (88/622); BDBV antigen: 6.1% (38/622)	GP, NP, VP40 EBOV; SUDV, BDBV, BOMV, RESTV IgG MMIA	Ramassamy et al. 2024, Journ of ID [294].
Low risk (general population in outbreak setting)					
General population in EVD affected community	Sierra Leone	2015 – 2016	7.5% (12/187)	GP and NP IgG ELISA	Richardson, 2016, PLoS Neglected Tropical Diseases [304]
General population in EVD affected community	Guinea	2017	3.6%, 95% CI: 1.55–6.92 (8/224)	GP IgG ELISA (oral fluid)	Timothy et al., 2019, Lancet ID [277]
General population in EVD affected community	Guinea	2017	4.0% (20/498)	GP, NP, VP40 IgG ELISA	Akoi Boré et al., 2024, Nat Commun [53]
General population in EVD affected community	Sierra Leone	2016 – 2018	8% (107/1282)	GP IgG ELISA (FANG)	Manno et al., 2022, EID [305]
High risk (contacts of confirmed cases, febrile patients (Fevers of Unknown Origin), healthcare workers)					
Febrile patients, General population	Cameroon, Congo, DRC,	1997–2012	2-3.5%	PV MNA then confirmed by NP IgG ELISA	Steffen et al., 2019, EID [297]

	Ghana, Uganda				
Febrile patients	Sierra Leone	2006 – 2008	8.6% (19/220)	EBOV cell lysate IgM/IgG ELISA	Schoepp et al., 2014, EID [306]
Acutely ill patients	Mali	2009 – 2013	0% (0/376)	EBOV cell lysate IgM/IgG ELISA	Safronetz et al., 2016, EID [307]
Febrile patients	Guinea	2011 – 2012	8.5% (11/129)	NP IgG MMIA	Surtees et al., 2020, PLoS Neglected Tropical Diseases [296]
Febrile patients	Sierra Leone	2011 – 2014	22% (53/242)	GP, VP40 IgG/IgM ELISA	Boisen et al., 2015, Viral Immunology [308] *
Febrile patients	Guinea	2016 – 2017	0%	NP IgM ELISA	Dedkov et al, 2021, Int J of Env Res and Public Health [309]
Asymptomatic or paucisymptomatic contacts of EVD survivors	Sierra Leone	2014 – 2015	Paucisymptomatic: 12.0%, 95% CI: 6.1–20.4% (11/92); Asymptomatic: 2.6%, 95% CI: 1.2–4.7% (10/388)	GP IgG ELISA (oral fluid)	Glynn et al., 2017, Lancet ID[310]
Asymptomatic or paucisymptomatic contacts of EVD survivors	Sierra Leone	2015 – 2016	Paucisymptomatic: 25%, 95% CI: 14–40%; Asymptomatic: 4%, 95% CI: 1–14%	GP IgG ELISA	Kelly, 2018, Journal of ID[311]
International HCW returning from West Africa	West Africa	2015 – 2016	0.0% (0/268)	GP IgG ELISA (oral fluid)	Houlihan et al., 2017, PLoS Medicine [312]
Asymptomatic or paucisymptomatic contacts of EVD survivors	Liberia	2015 – 2017	8.25% (222/2688)	GP IgG ELISA (FANG)	Kelly et al., 2022, Lancet ID [313]

Asymptomatic or paucisymptomatic contacts of EVD survivors	Liberia	2015 – 2017	11.6% (222/1909)	GP IgG ELISA (FANG)	Gayedyu-Dennis, 2023, J Infect Dis [275]
Asymptomatic or paucisymptomatic contacts of EVD survivors	Guinea	2015 – 2017	17% (11/66)	Whole EBOV IgG ELISA	Thom et al., 2020, Lancet ID [220]
Asymptomatic contacts of EVD survivors	Guinea	2016 – 2017	Paucisymptomatic: 8.33%, 95% CI: 5.01–12.80% (18/216); Asymptomatic: 3.32%, 95% CI: 1.23–5.01% (39/1174)	GP, NP, VP40 IgG MMIA	Diallo et al., 2019, Lanced ID [314]
Asymptomatic or paucisymptomatic contacts of EVD survivors	Liberia	2016 – 2017	Paucisymptomatic: 5.2% (22/421); Asymptomatic: 4.3% (18/421)	GP IgG ELISA (FANG)	Kelly et al., 2022, Open Forum Infectious Diseases [315]
Asymptomatic contacts of EVD survivors	Sierra Leone	2017	12.7% (34/267)	GP IgG ELISA	Halfmann et al., 2019, PLoS Neglected Tropical Diseases [316]

IF = Indirect immunofluorescence, ELISA = Enzyme-linked immunosorbent assay, IgG = Immunoglobulin G, IgM = Immunoglobulin M, GP = Glycoprotein, NP = Nucleoprotein, VP40 = 40-kDa viral protein , EBOV = Ebola virus, May = Mayinga, Kiss = Kissidougou, SUDV = Sudan virus, BDBV = Bundibugyo virus, RESTV = Reston virus, BOMV = Bombali virus, MMIA = Multiplex microsphere-based immunoassay, PV = Pseudovirus, MNA = Microneutralization assay, FANG = Filovirus Animal Nonclinical Group, HCW = Healthcare worker, EVD = Ebola virus disease.

*Evidence of EBOV circulating in West Africa prior to outbreak

4.1.2.2. Asymptomatic Ebola virus infection and interpreting observed orthoebolavirus seroprevalences

Asymptomatic ebolavirus infections have the potential to greatly influence transmission dynamics, however, there is little consensus on their frequency. Recognition of these subclinical infections is important for understanding the full spectrum of disease, refining epidemiological models, and designing appropriate public health strategies. Given the challenges of surveillance in remote locations, many outbreak investigations rely on retrospective detection, and thus overlook mild clinical presentations of EVD. Typically, these studies take cross-sectional seroprevalence of asymptomatic contacts of EVD cases, and report anywhere from 1.0% (2/210) in Uganda [317], 2.5% (10/404) in

Yambuku, DRC [88]; 2.6% (10/388) in Sierra Leone [310], 4.0% (4/101) in Kikwit, DRC [318]; 6.0% (115/1909) in Liberia [275]; 6.5% (12/185) in Kono, Sierra Leone [304]; 21.4% (12/56) in Gabon [319]; 45.9% (11/24) in Gabon [320]; up to 71% in Gabon [321]. A meta-analysis drawn from studies estimated a secondary attack rate of 27% (95% CI, 14.5–39.6) [322], however, as of yet, their relative contribution to the high seroprevalences observed throughout the African continent is unclear.

Until the 2013-2016 West African EVD epidemic, EVD had only been recognized within Central Africa, within a restricted geographic range defined by the Gabonese coast, Congo River basin and the Great Lakes. However, studies have provided evidence since 1976 of a much wider serological footprint across sub-Saharan Africa (Table 12). Several explanations have been posited for this, including an unrecognized contribution of asymptomatic EBOV infections, or the silent circulation of clinically milder species of filoviruses over a broader geographic range. Here, highly multiplexed serosurveillance for filovirus species may serve to shed some light on the question: qui-vive (who goes there)? [323]

4.1.3. Chapter rationale and aims

Previous serosurveillance of WLHs in Forested Guinea in 2017 identified distinct immune signatures to multiple EBOV antigens (GP, NP, VP40) by ELISA or western blot, which were non-neutralising and thus not plausibly explained by prior EBOV-Makona exposure, suggesting exposure to other antigenically related non-EBOV filoviruses [53]. In this chapter, I examine this cohort of WLHs in Forested Guinea, which was resampled and expanded 6 years later, in order to deeply characterize these serological signatures with a MMIA consisting of 9 filovirus GP antigens and a panel of pseudotyped virus neutralisation assays for Ebola (EBOV), Bundibugyo (BDBV), Taï Forest (TAFV), Bombali (BOMV), Reston (RESTV), Sudan (SUDV), Lloviu (LLOV), Měnglà (MLAV), and Ravn (RAVV) viruses. My aims were to integrate serological, demographic, behavioural and satellite-derived environmental and spatial data, in order to characterise the extent of zoonotic filovirus circulation among WLHs in Forested Guinea and to assess risk factors associated with any putative zoonotic transmission, including environmental land-use changes.

Specifically, I aim to:

1. Estimate the seroprevalence of IgG antibodies against multiple *Orthoebolavirus* species (EBOV, BDBV, TAFV, BOMV, RESTV, SUDV, LLOV, MLAV) in a 2017 and 2023 cohort of WLHs in Guinée forestière using a filovirus-GP antigen-based MMIA, and compare to geographically distinct cohorts in the UK, Uganda and urban Guinea (Coyah and Guéckédou).

   Here, I hypothesise that the seroprevalence of EBOV-GP antibodies will fall within a similar range to those reported using similar methods (ranging from 3.6% [277] to 7.2% [303]) and all

filovirus reactivity will be significantly higher amongst the wildlife hunting cohort than cohorts in the UK, Uganda or urban Guinea.

2. Compare experimental (deriving seropositivity thresholds from non-endemic cohorts) and computational (finite mixture modelling, *K*-means clustering) methods for the interpretation of multiplexed serological data.

   Here, I hypothesise that binary seropositivity thresholds, derived experimentally or computationally, will result in significant misclassification of cross-reactive responses as "true positives", leading to an overestimation of co-positivity.

3. Distinguish species-specific from cross-reactive anti-filovirus antibody responses in Guinean WLHs using parallel pseudotyped virus neutralisation assays (PVNAs).

   Here, I hypothesise that parallel virus neutralisation assays will allow me to differentiate individuals who were infected with EBOV (inducing cross-reactive responses against related species) from individuals infected by other *Orthoebolavirus* species. EBOV cases will neutralise EBOV more strongly in a parallel PVNA, whereas other cases will neutralise the relevant *Orthoebolavirus* species (e.g., BDBV, TAFV, SUDV) more strongly.

4. Estimate the persistence of EBOV antibodies amongst Guinean individuals who are EBOV-positive in 2017 and resampled in 2023.

   Here, I hypothesise that individuals who were EBOV GP-positive in 2017 will demonstrate a durable and slowly decaying antibody response when resampled in 2023.

5. Identify demographic and behavioural risk factors for filovirus reactivity.

   Here, I hypothesise that male sex, wildlife hunting, and the hunting and consumption of bats and nonhuman primates (for EBOV, TAFV, BDBV) will be significantly associated with increased seroreactivity for filovirus species.

6. Examine the spatial distribution of filovirus reactivity at the village level in Guinée forestière.

   Here, I hypothesise that filovirus reactivity will demonstrate statistically significant positive spatial autocorrelation, consistent with geographic clustering, highlighting potential outbreaks or areas of increased risk (possibly explained by proximity to bat caves, or deforestation).

7. Investigate associations between filovirus seroreactivity and landscape patterns, including land cover and forest fragmentation (measured by perimeter area ratio, shape-index and fractal dimension) at varying spatial scales.

Here, I hypothesise that increased forest fragmentation will be positively associated with seroreactivity for all filoviruses, whereas proximity to built-up areas will be associated with EBOV (due to human-to-human transmission).

4.2. Results

4.2.1. Study sites and study populations

Forested Guinea WLHs and close contacts, 2017 and 2023

A total of 511 participants were recruited from 40 villages in 2017, and 648 participants were recruited from 44 villages in 2023. Of the 2017 cohort, 52.45% (268/511) were resampled as part of the longitudinal follow-up 6 years later. WLHs (all male) constituted 54% of study population, with the remaining 46% (predominantly female) reporting close household contact with a WLH. Farming was the dominant occupation in 2017 (93%, 476/511) and 2023 (68%, 556/648), however some HCW were also enrolled (3% and 12% in 2017 and 2023 respectively) (Table 13).

Ugandan farmers, 2017 – 2021

A total of 79 participants from Uganda were recruited between 2017 – 2021 (samples kindly provided by Professor Emma Thomson, University of Glasgow) and were utilised as a geographically distinct comparison cohort. All participants were farmers (79/79) and all participants reported no wildlife hunting activities (79/79).

United Kingdom blood donors, 2020

Serum samples (n=63) collected in 2020 from healthy blood donors, aged 17-80 years from the UK were utilized as a presumed negative, non-endemic comparative cohort [3].

Coyah and Guéckédou Ebola virus survivors and negatives, 2015 and 2017

Serum samples (n=3) were collected between 2015 and 2017 from PCR-confirmed EVD survivors 3 – 14 months post-infection and pooled for use as a positive control for EBOV in all assays. Serum samples (n=15) were also collected from urban settings (Coyah and Guéckédou, Guinea) in 2015 - 2017 from individuals with no known epidemiological contact with EVD, no known case history, who were negative by EBOV-GP ELISA [220].

Table 13 Demographic characteristics by cohort

Characteristic	Guinea 2017 cohort n/N (%)	Guinea 2023 cohort n/N (%)	Uganda cohort n/N (%)
Total no. of participants	511	648	79
Sex			
Male	228 (56)	407 (63)	35 (44)
Female	223 (44)	241 (37)	44 (56)
Age, group by years			
18- 30	144 (28)	143 (22)	28 (35)
30- 40	120 (23)	154 (24)	18 (23)
40- 50	133 (26)	156 (24)	21 (27)
50- 60	75 (15)	107 (17)	7 (9)
>65	39 (8)	88 (14)	5 (6)
Age, years			
Median [IQR]	39 [28-48]	40 [30 – 51]	35 [24 – 47]
Mean [Range]	39 [18-90]	42 [18 – 110]	36 [18 – 80]
Wildlife hunting			
Hunter	278 (55)	341 (53)	0 (0)
Non-hunter	232 (45)	306 (47)	79 (100)
Primary occupation			
Farmer	476 (93)	556 (68)	79 (100)
Healthcare worker	17 (3)	76 (12)	0 (0)
Tradesperson	1 (0)	8 (1)	0 (0)
Other	16 (3)	4 (1)	0 (0)
Student	1 (0)	4 (1)	0 (0)

4.2.2. Wildlife hunting and bat exposure in Forested Guinea

In 2023, a 123-item questionnaire on wildlife hunting and other activities was administered to all participants in Toma and French. Consumption of wildlife or "bushmeat" was ubiquitous, with 90% of respondents (581/648) buying bushmeat, and 94% (583/619) helping handle, wash or prepare bushmeat carcasses prior to cooking. Bushmeat was consumed a median of 7 [IQR: 4 – 15] days per month, and amongst WLHs, hunting was practiced a median of 6 [IQR: 3 – 10] days per month. Wildlife hunting generally was not considered to be seasonal by the majority of respondents (93%, 576/619), with the notable exception of bat hunting. Bat exposure and hunting was reported to be highly seasonal, with 87% (292/334) of respondents seeing them or hunting them (92%, 122/133) at the start of the dry season. Agouti was the most commonly reported food source, followed by rodent, antelope and boar, then by monkey, pangolin and bat (Figure 21). Bat hunting was found to be a relatively less frequent and specialised practice with only 31.94% (207/648) individuals either hunting bats or living with a bat hunter. Bats are typically hunted in the forest, in trees, or in the village, and rarely in caves.

Bat contact was more frequent, and was typically reported as 2-3 days per week (46%, 296/648), taking place around the village (45%, 259/574) or in the house (28%,158/574) or the forest (14%, 80/574) between 12 am – 6 am and in the afternoon. Forest activities included hunting or collecting wood, plants or food. Caves usage was rare (25%, 139/546) and for short visits only, with an average time of 13 minutes [min – max; 0 – 60] minutes spent per visit. Caves were typically used by both hunters and non-hunters. Guano harvesting was rarely reported (0.3%, 2/648).

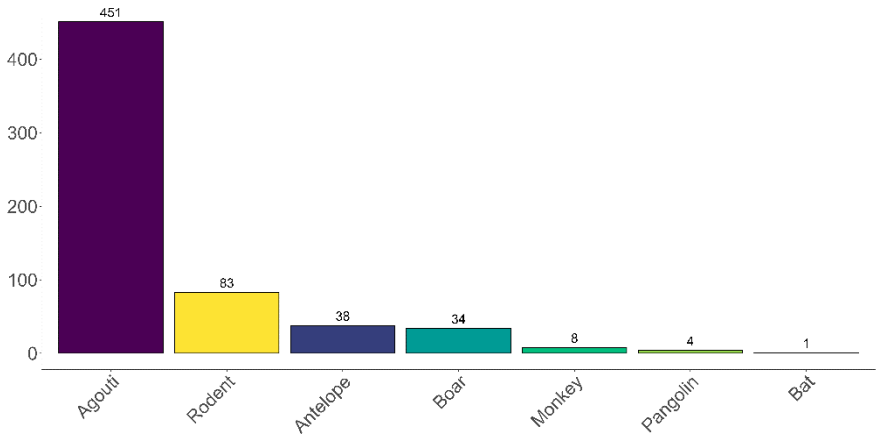


Figure 21 Wildlife hunted for consumption, by species, Forested Guinea, 2023.Questionnaire respondents were able to list any number of species in response to the item "What are the common types of bushmeat that you hunt or buy?".

Table 14 Wildlife exposure questionnaire responses, Forested Guinea 2023

Question	n	N	%
Do you ever hunt or trap bats?			
Yes	156	641	24
No	485	641	76
Do other members of your household hunt or trap bats?			
Yes	51	491	10
No	440	491	90
Do you handle bats during preparation or cooking for food?			
Yes	274	535	51
No	261	648	40
Do you buy bats from other people or markets?			
Yes	130	646	20
No	516	648	80
Which season do you hunt more frequently?			
Start of dry season	122	133	92
Middle of dry season	4	133	3
End of dry season	5	133	4
Start of rainy season	2	133	2
Middle of rainy season	0	133	0
End of rainy season	0	133	0
What do you do with the hunted bats?			
For food only	145	155	94
For food and to sell	8	155	5
Other	1	155	1
To sell only	1	155	1
Do you ever go into bat caves?			
Yes	139	546	25
No	407	546	75
Do you do any other kind of activities with the bats when inside the cave?			
No	85	86	99
Yes	1	86	1
On a normal visit, how long (minutes) do you spend inside the cave?			
Median [IQR]	2 [0 - 20]		
Mean [Min - Max]	13 [0 - 60]		
Do you harvest bat guano?			
Yes	2	648	0
No	646	648	100

4.2.3. Filovirus reactivity in Guinean wildlife hunting communities by MMIA screening

Population-level differences in the distributions of IgG antibodies against multiple zoonotic filoviruses can be seen between the Forested Guinea WLH cohorts (2017 and 2023), and the EBOV-negative control cohorts from Coyah and Guéckédou (n=18) and UK (n=63). Initial seropositivity cut-offs were based on the presumed unexposed non-endemic cohort (UKBD) by calculating five standard deviations above the background subtracted (MFI-bg) mean. As seen in Figure 22, a high proportion of the wildlife hunter population fell above the seropositivity threshold for not only EBOV and closely related filoviruses, such as BDBV and TAFV, but also more distant filoviruses including BOMV, LLOV, RESTV and MLAV. Increased antigen reactivity could also be seen amongst the Forested Guinea population, as compared to Coyah and Guéckédou, highlighting the discrepant immune landscapes between regional villages and urban cities even within the Republic of Guinea.

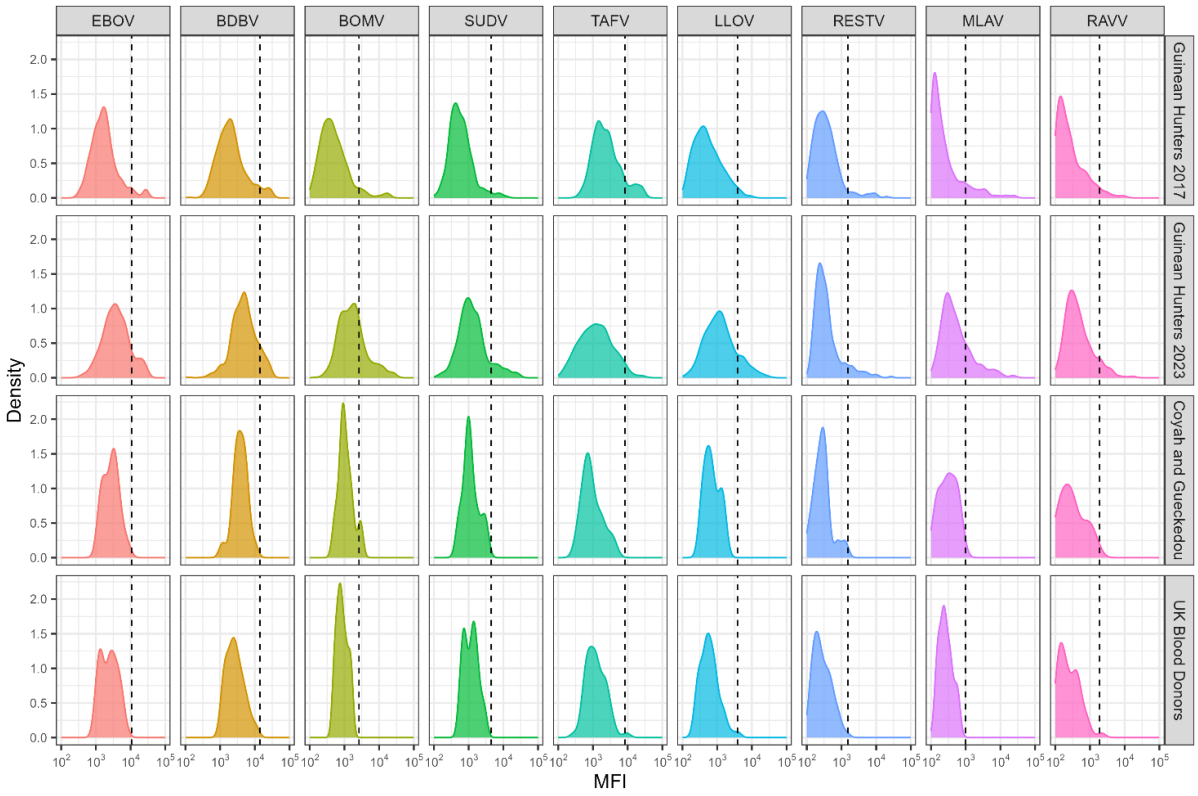


Figure 22 Anti-filovirus glycoprotein IgG distributions of among Guinean wildlife hunter 2017 cohort (n=511) and 2023 cohort (n=648), Guinean Coyah controls (n=18) and the United Kingdom blood donor cohort (n=63). IgG responses were measured by multiplex microsphere-based immunoassay (MMIA) in background subtracted median fluorescence units (MFI-bg) on the Luminex platform. Dashed vertical lines mark seropositivity cut-offs based on the presumed unexposed non-endemic cohort (UK blood donor) by calculating five standard deviations above the background subtracted (MFI-bg) mean.

Filovirus reactivity in Ugandan farmer cohort

Population-level reactivity against multiple filovirus antigens could also be seen in the Ugandan farmer cohort (n=79), as compared to UK blood donors (n=63) (Figure 23).

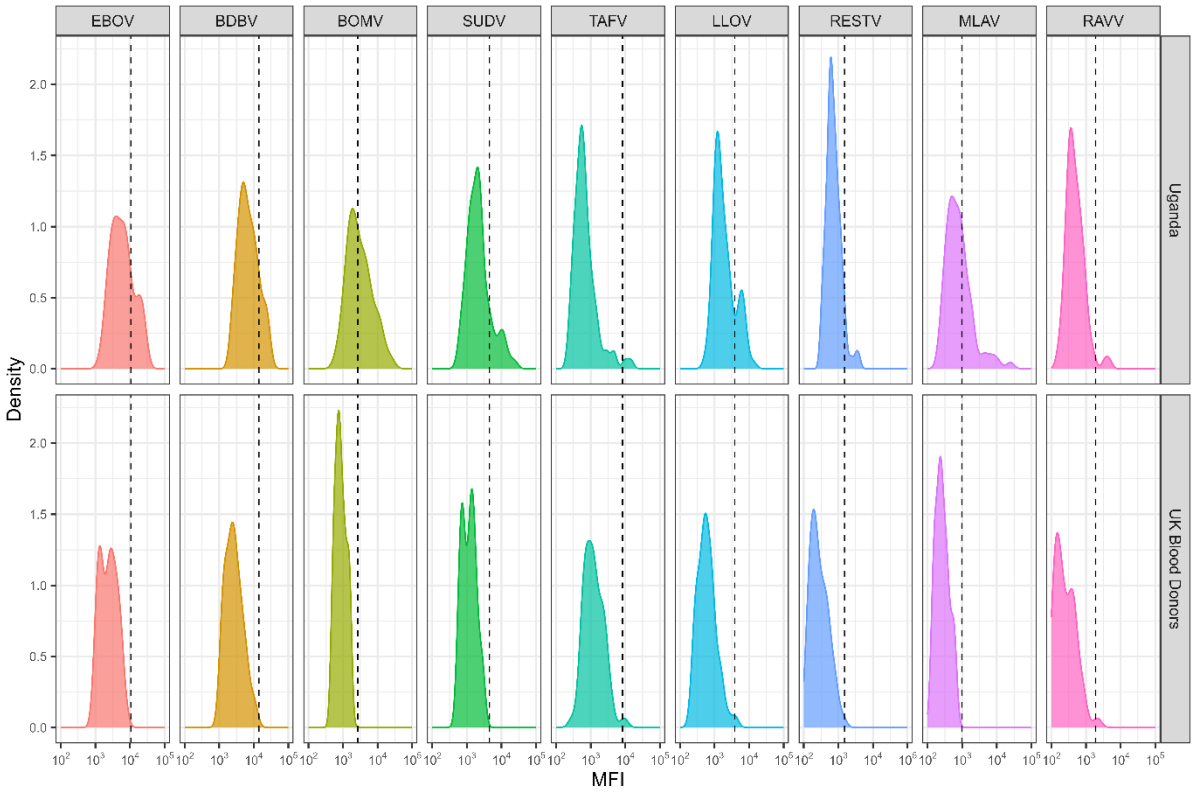


Figure 23 Anti-filovirus glycoprotein IgG distributions among Ugandan farmers (n=79) and the United Kingdom blood donor cohort (n=63). IgG responses were measured by multiplex microsphere-based immunoassay (MMIA) in background subtracted median fluorescence units (MFI-bg) on the Luminex platform. Dashed vertical lines mark seropositivity cut-offs based on the presumed unexposed non-endemic cohort (UK blood donor) by calculating five standard deviations above the background subtracted (MFI-bg) mean.

4.2.4. Experimental and computational classification of immune responses through use of a seropositivity threshold

Serological data are typically interpreted by classifying individuals as seronegative or seropositive based on a defined threshold (with values above the defined cut-off considered to be seropositive) thus allowing the calculation of epidemiological metrics such as seroprevalence. In the absence of assay-specific international standards or harmonised methods, we generated binary seropositivity endpoints for assay-specific continuous MFI readout both empirically (based on a presumed seronegative cohort) and computationally (via finite mixture modelling). Cut-off values were initially experimentally derived from a presumed unexposed population with no expected exposure to the filovirus antigens of interest

(UKBD cohort). Standard and stringent thresholds were calculated based on 3 and 5 standard deviations above the means of the background subtracted MFI (MFI-bg) (Table 15).

Given the differing immunological backgrounds between the UKBD cohort and the Guinean WLH cohort, seropositivity cut-off values were also computationally derived using a probabilistic finite mixture model based on the WLH cohort. This model assumes the presence of two normally distributed subpopulations (seropositive and seronegative) within the target population, and therefore represents a distribution of MFI values more closely resembling the antibody landscape of the population. The iterative expectation-maximization (EM) algorithm was used to find the maximum likelihood estimates for the parameters, and the membership probabilities for each component. A seropositivity cut-off was set at the MFI value at which the probability densities for the two distributions were equal (Appendix Figure 59).

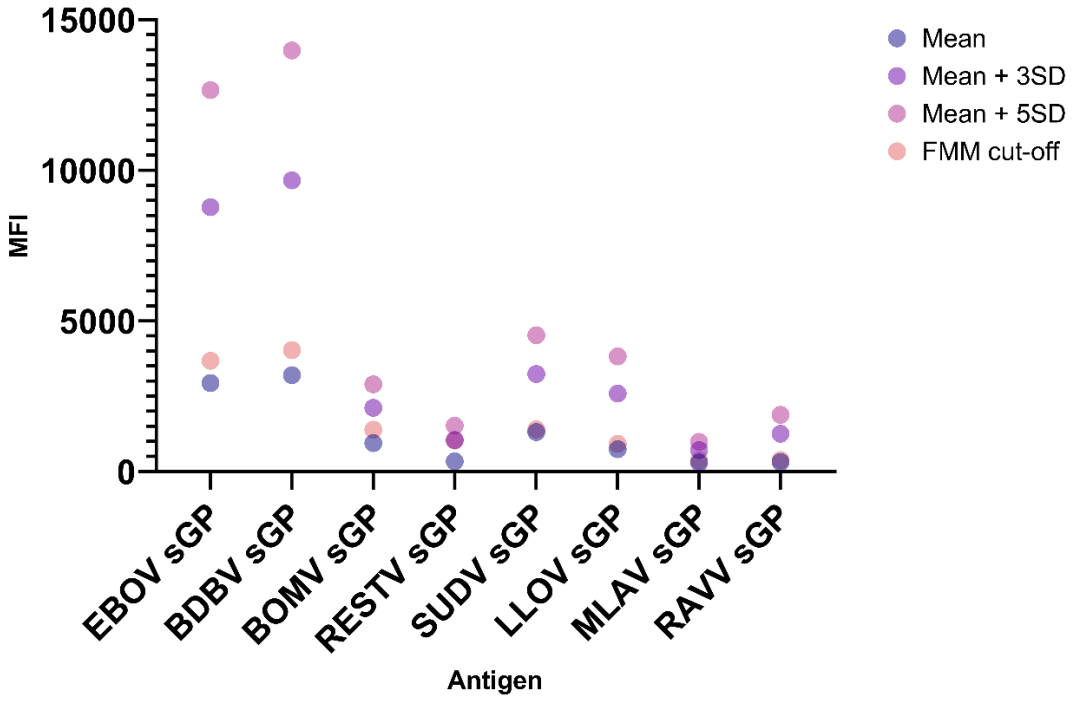


Figure 24 Comparison of seropositivity thresholds (experimental and computational) for filovirus antigens on the multiplex microsphere-based (MMIA) assay. Mean and standard deviation are calculated from the antibody responses of the presumed seronegative cohort (UK blood donors) as measured by multiplex microsphere-based immunoassay (MMIA) in median fluorescence intensity (MFI) units on the Luminex platform. Finite mixture model (FMM) thresholds are computationally derived from the Guinean wildlife hunter cohort 2017.

Table 15 Comparison of seropositivity thresholds (experimental and computational) for filovirus antigens on the multiplex microsphere-based (MMIA) assay

	EBOV sGP	BDBV sGP	BOMV sGP	RESTV sGP	SUDV sGP	LLOV sGP	MLAV sGP	RAVV sGP
Mean*	2938	3197	944	341	1307	744	295	316
Mean + 3SD	8772	9666	2116	1049	3235	2589	709	1254
Mean + 5SD	12662	13978	2897	1522	4521	3819	985	1879
FMM cut-off	3678	4031	1385	1027	1399	917	361	384

* Mean of presumed seronegative cohort (UK blood donors) where IgG responses were measured by multiplex microsphere-based immunoassay (MMIA) in median fluorescence intensity (MFI) units on the Luminex platform. Finite mixture model (FMM) thresholds are computationally derived from the Guinean wildlife hunter cohort 2017.

Misclassification of EBOV survivor cohort using seropositivity thresholds

Threshold-based definitions of seropositivity are inherently susceptible to misclassification, particularly in the context of antigenic cross-reactivity. Given the heterotypic cross-reactivity demonstrated in earlier chapters among PCR-confirmed EBOV survivors, the experimentally and computationally derived serological cut-offs to applied to a cohort of EBOV survivors 3 – 14 months p.i. (n=373) to assess their performance. As hypothesised, EBOV survivors were frequently misclassified as being seropositive for other orthoebolaviruses, including BDBV (63.8% of EBOV survivors by mean + 3 SD), BOMV (65.1% of EBOV survivors by mean + 3SD) and RESTV (50.4% of EBOV survivors by mean + 3SD). Misclassification was even demonstrated amongst more phylogenetically distant filoviruses such as LLOV (25.7% of EBOV survivors by mean + 3SD) or MLAV (14.5% of EBOV survivors by mean + 3SD) (Figure 25).

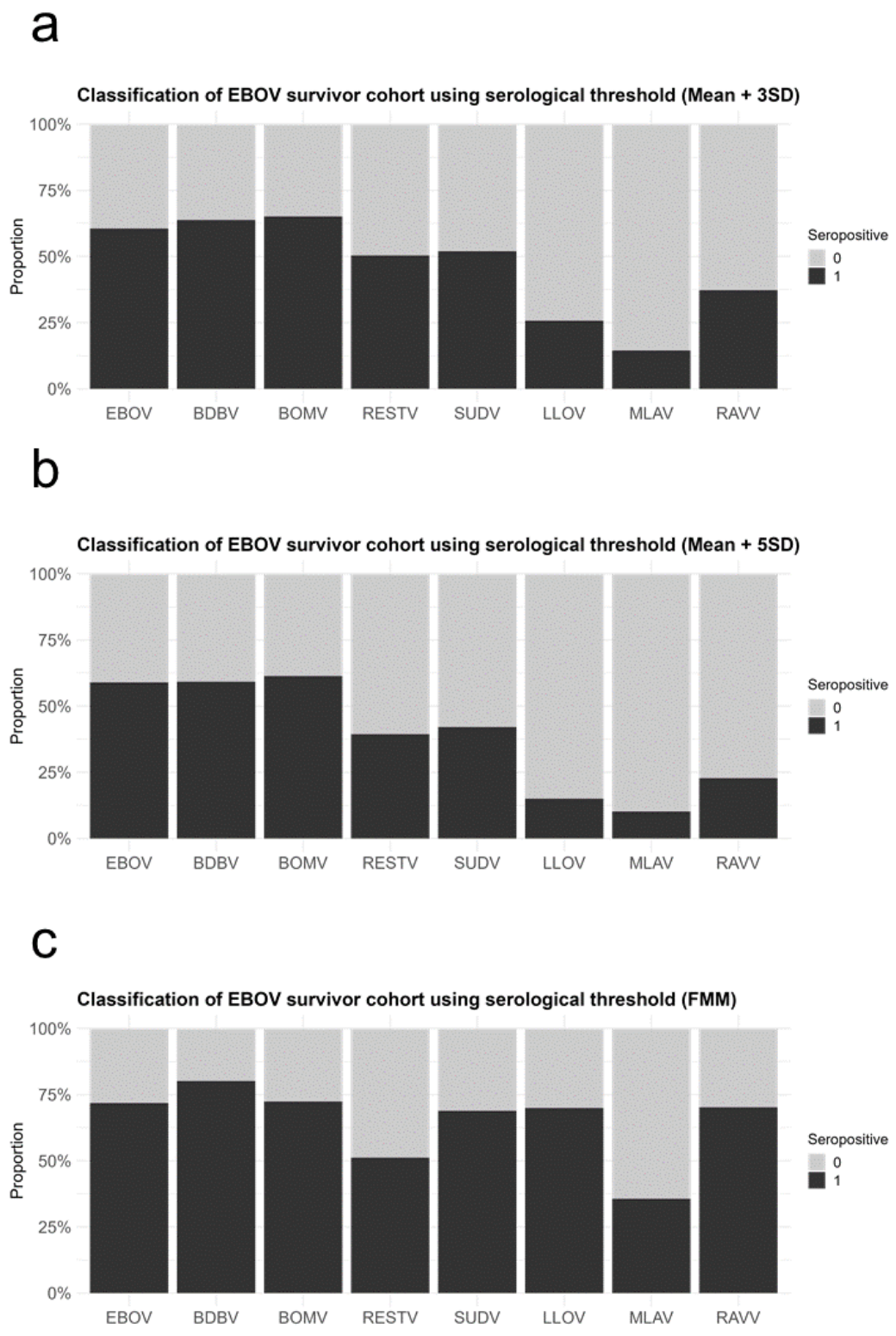


Figure 25 Seropositivity classifications of EBOV survivor cohort. Seropositivity classifications for filoviruses in the EBOV survivor cohort (n = 373) using thresholds based on (a) presumed unexposed UK blood donor cohort mean + 3 standard deviations (b) presumed unexposed UK blood donor cohort mean + 5 standard deviations (c) finite mixture models.

4.2.5. Classification of immune responses by *K*-means clustering reveals EBOV and non-EBOV filovirus reactivity in WLHs, 2017 and 2023, in comparison to EBOV-reactivity in other populations

Given the heterotypic cross-reactivity seen between antigenically related viruses, an unsupervised machine learning algorithm (*K*-means clustering) was used to classify the IgG binding antibody responses of individuals against multiple filoviruses into "clusters", or unique exposure profiles. This pathogen-agnostic approach to determining seropositivity allowed for the identification of novel viruses, and avoided the use of a serological threshold for each virus, thus minimizing the misclassification of cross-reactive individuals as true positives. The *K*-means clustering algorithm revealed a stable underlying data structure in the wildlife hunting cohort, grouping individuals from 2017 and 2023 with similar serological responses together into *k*=15 clusters (Figure 26).

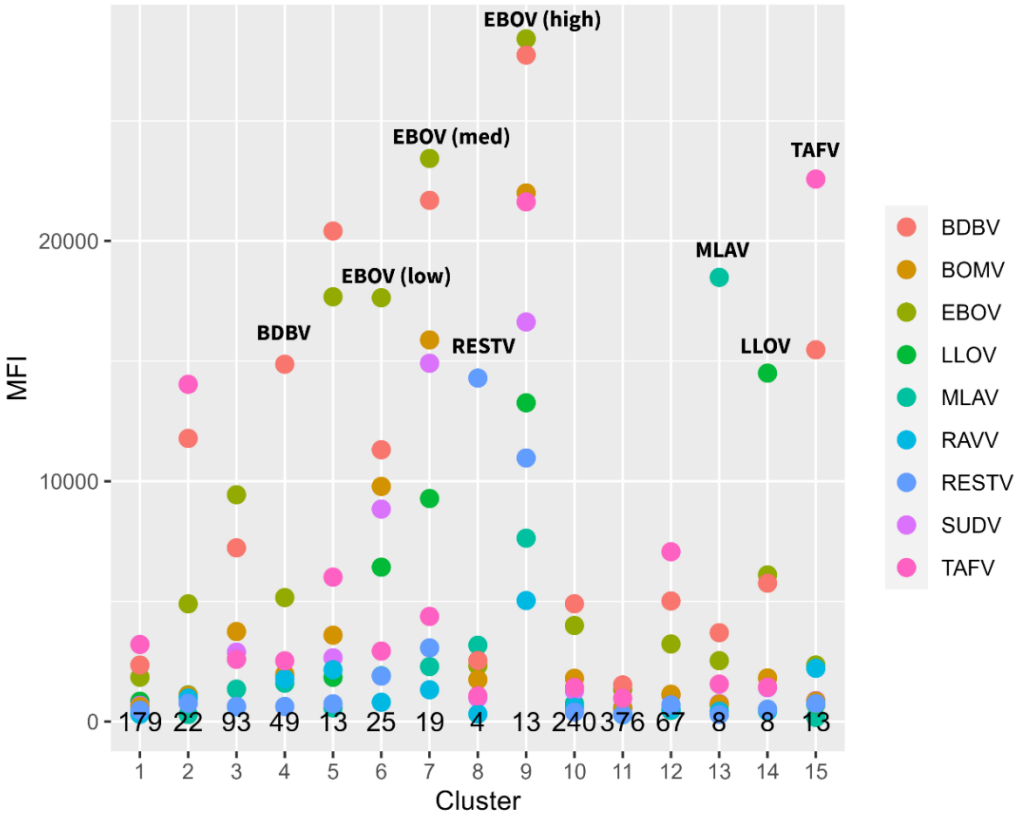


Figure 26 *K*-means clustering of anti-filovirus glycoprotein antibody responses of Guinean wildlife hunting communities, 2017 and 2023 (combined) for *k*=15 clusters. The *K*-means clustering algorithm partitioned anti-filovirus antibody responses into *k*=15 clusters with qualitatively different serological responses. The mean reactivity for each filovirus antigen by cluster, and the number of samples in each cluster is shown. IgG responses were measured by multiplex microsphere-based immunoassay (MMIA) in median fluorescence intensity (MFI) units on the Luminex platform.

Clustering results were evaluated for biological relevance and stability, in addition to cluster validity, using composite metrics of compactness and separation including silhouette width [245] and the gap statistic [246] (Figure 27).

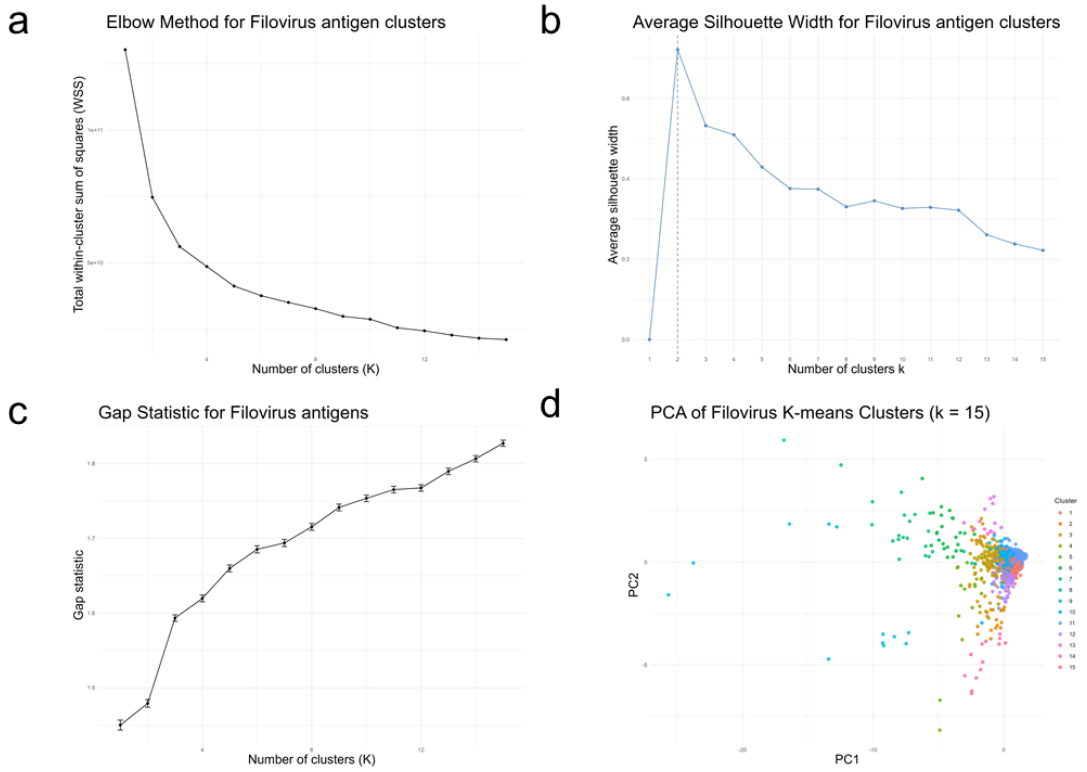


Figure 27 Evaluations of different ranges of *k* (number of clusters) (a) Within-cluster sum of squares (WCSS) (b) Silhouette width (c) Gap statistic (comparison of WCSS to a null distribution) and (d) Principal Component Analysis of *K*-means clustering results for *k*=15.

Several sets of clusters showed similar ordinal profiles, therefore I present plots of the individual responses of WLHs who were categorised into these clusters to demonstrate the appropriateness of designating them as separate clusters. Clusters 2, 12 and 15 showed the same ordinal profile (average MFI for TAFV > BDBV > EBOV) (Figure 28). Clusters 3, 6, 7, and 9 showed the same ordinal profile (average MFI for EBOV > BDBV > BOMV) (Figure 29). Cluster 4 and 5 showed the same ordinal profile (average MFI for BDBV > EBOV) (Figure 30).

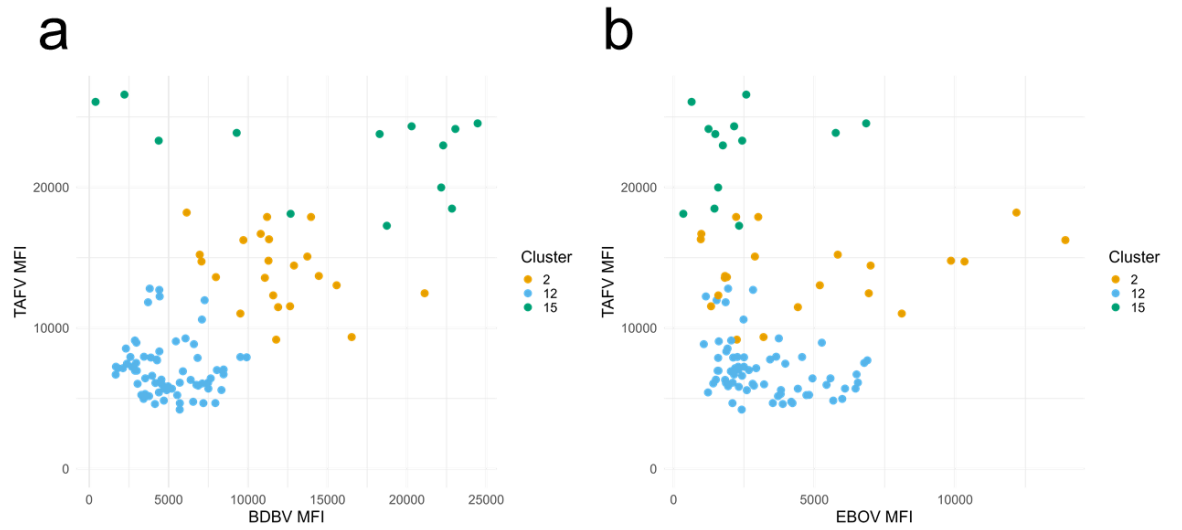


Figure 28 Individual MFI responses against (a) TAFV and BDBV (b) TAFV and EBOV for all hunters from the Guinean wildlife hunting cohort (2017 and 2023) who were categorised into Clusters 2, 12 and 15 from the K-means clustering algorithm analysis for k=15.

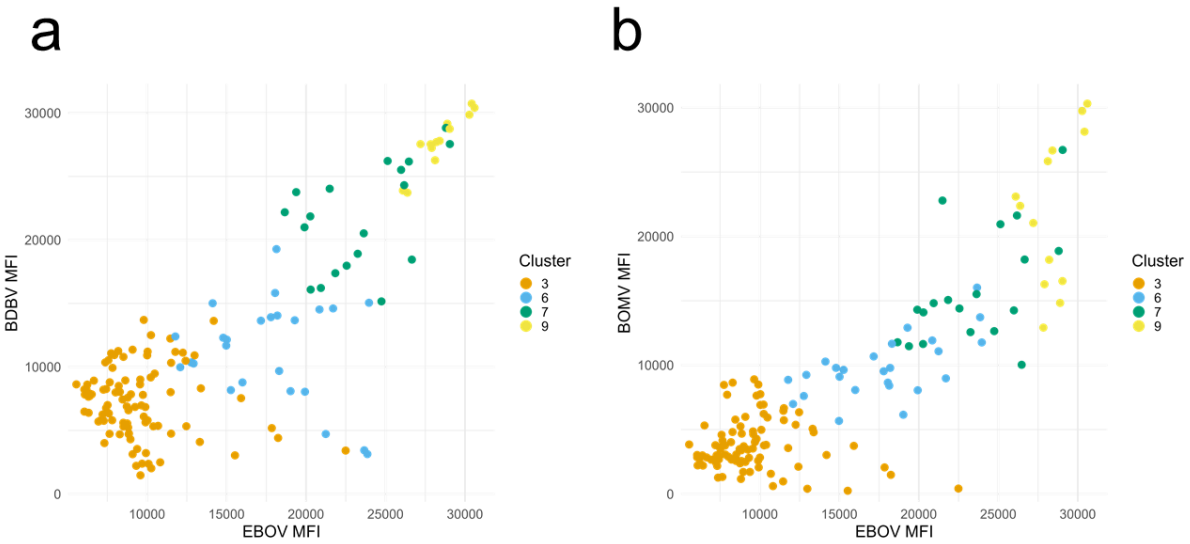


Figure 29 Individual MFI responses against (a) BDBV and EBOV (b) BOMV and EBOV for all hunters from the Guinean wildlife hunting cohort (2017 and 2023) who were categorised into Clusters 3, 6, 7 and 9 from the K-means clustering algorithm analysis for k=15.

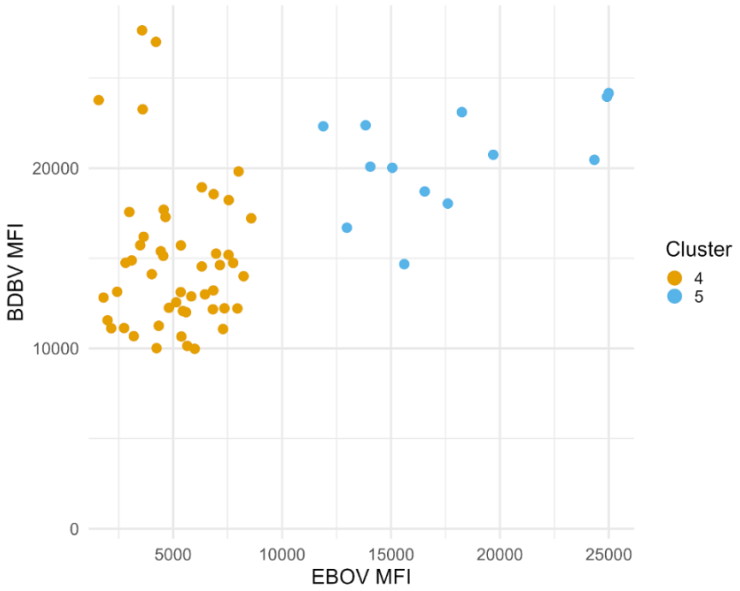


Figure 30 Individual MFI responses against BDBV and EBOV from the Guinean wildlife hunting cohort (2017 and 2023) who were categorised into Clusters 4 and 5 from the *K*-means clustering algorithm analysis for *k*=15.

Similar clusters were identified when 2017 and 2023 cohorts were clustered separately, with the identification of an additional BOMV cluster (n=1) in 2017 (Figure 31).

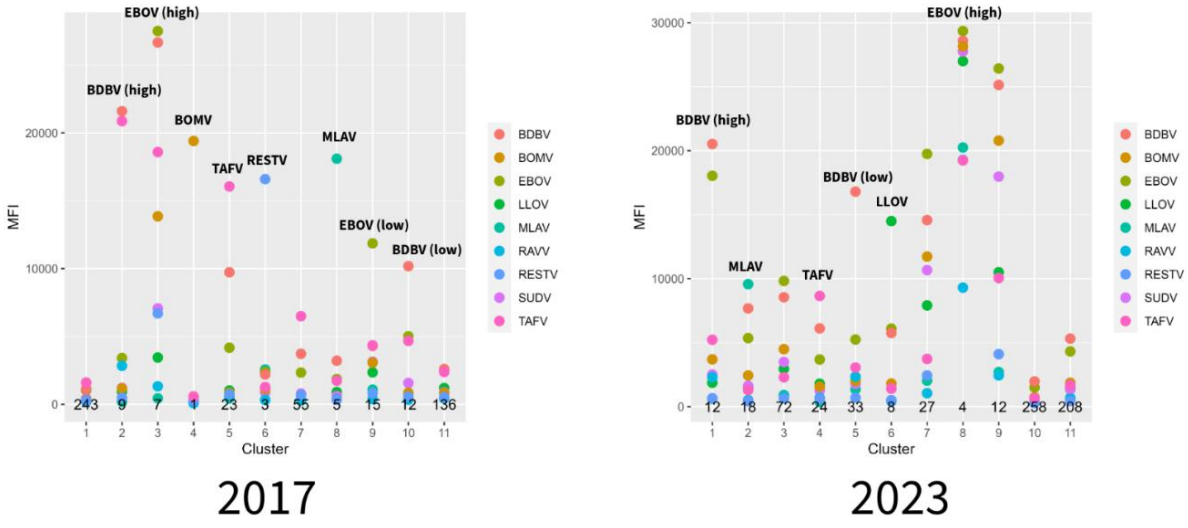


Figure 31 *K*-means clustering of anti-filovirus glycoprotein antibody responses of Guinean wildlife hunting communities, 2017 and 2023 (separately) for *k* =11 clusters. The mean reactivity for each filovirus antigen by cluster, and the number of samples in each cluster is shown. IgG responses were measured by multiplex microsphere-based immunoassay (MMIA) in background subtracted median fluorescence units (MFI-bg) on the Luminex platform.

In the combined (2017 and 2023) analysis of all Guinean WLHs (Figure 26), 3 clusters with a total of 57 individuals (57/1159, 4.9%, Clusters 6, 7, 9) showed high anti-EBOV binding, and heterotypic cross-reactivity against related filoviruses which decreased with phylogenetic distance and were considered to be likely "EBOV exposed" (Figure 26) based on their similarity to binding patterns observed in PCR-confirmed EBOV survivors 12- and 24- months post infection (Figure 34). Interestingly, clusters were also identified with species-specific antibody binding against singular filoviruses, often in the absence of anti-EBOV antibodies. This included clusters of individuals with antibody binding against BDBV (n=49, 4.2%, Cluster 4), TAFV (n=13, 1.1%, Cluster 15), RESTV (n=4, 0.3%, Cluster 8), MLAV (n=8, 0.7%, Cluster 13), LLOV (n=8, 0.7%, Cluster 14) (Table 16). The multiple species-specific, non-EBOV clusters (Figure 32) are in clear contrast to the UKBDs (Figure 33), EBOV-negative cohort from Coyah and Guéckédou (Figure 33), EBOV survivor cohort (Figure 34), and Ugandan farmers (Figure 36), highlighting the diverse range of unique viral exposures in the wildlife hunting community in Forested Guinea.

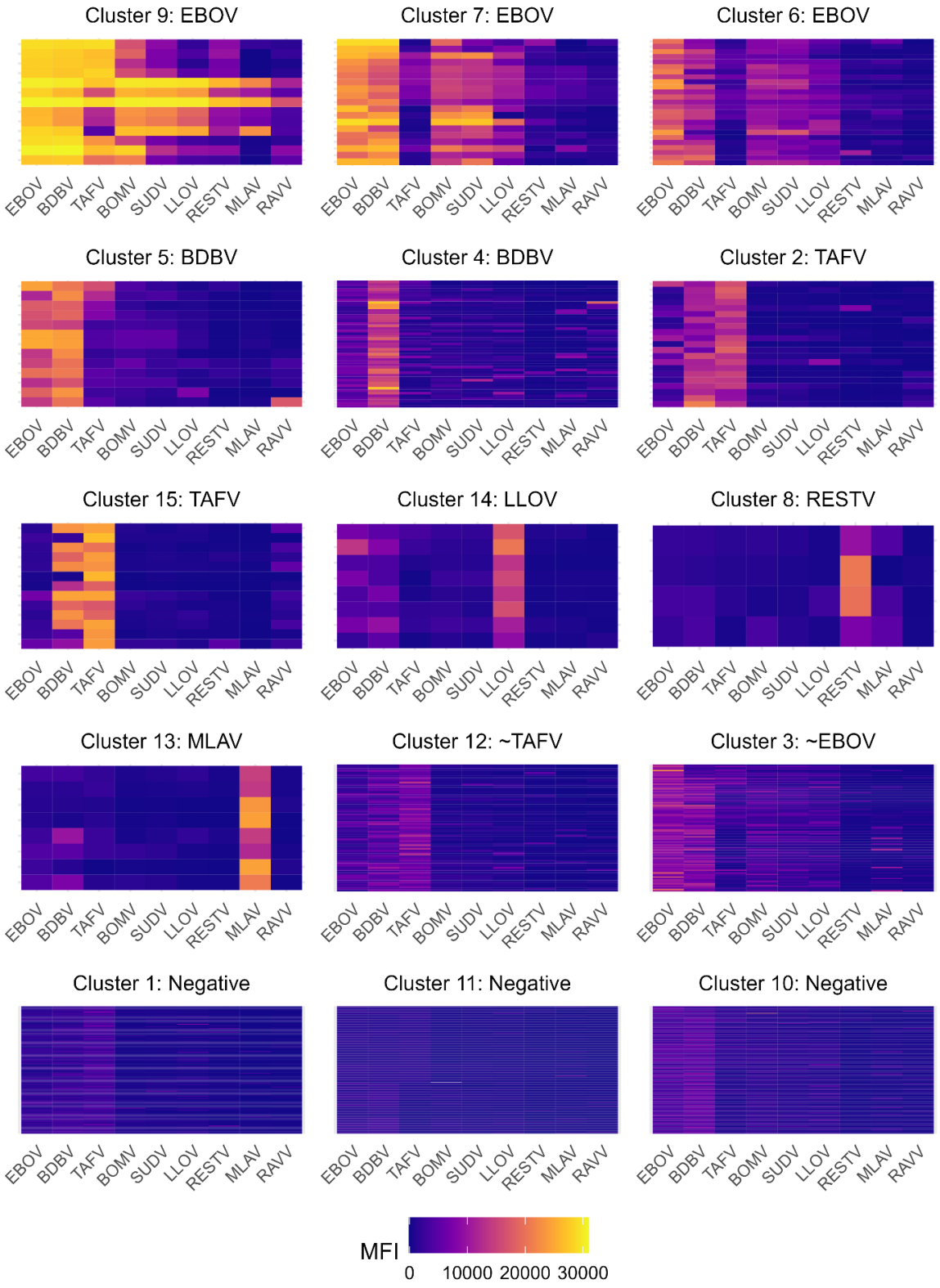


Figure 32 Individual anti-filovirus glycoprotein responses in wildlife hunting communities, Forested Guinea. Anti-filovirus GP antibody responses of individuals clustered by *K*-means clustering, Guinean wildlife hunters, 2017 and 2023 (n=1159) and classed as EBOV (a, b, c), BDBV (d, e), TAFV (f,g), LLOV (h), RESTV (i), MLAV (j), and low or negative (k, l, m, n o).

Table 16 Results from Guinean wildlife hunting cohort (2017 and 2023) *K*-means clustering algorithm analysis for *k*=15.

Combined (2017 and 2023) *K*-means cluster (*k*=15)	**Count**	**Percentage (%)**	**Biological annotation**
1	179	15.85	Negative
2	22	1.95	TAFV
3	93	8.24	EBOV
4	49	4.34	BDBV
5	13	1.15	BDBV
6	25	2.21	EBOV
7	19	1.68	EBOV
8	4	0.35	RESTV
9	13	1.15	EBOV
10	240	21.26	-
11	376	33.30	-
12	67	5.93	TAFV
13	8	0.71	MLAV
14	8	0.71	LLOV
15	13	1.15	TAFV
Total	**1129**		

Table 17 Categorization of immune responses from the Guinean wildlife hunting cohort (2017 and 2023) following *K*-means clustering algorithm analysis (*k*=15).

Category	Count	Percentage (%)
EBOV cluster	150	13.29
BDBV cluster	62	5.49
TAFV cluster	98	8.68
RESTV cluster	4	0.35
MLAV cluster	8	0.71
LLOV cluster	8	0.71

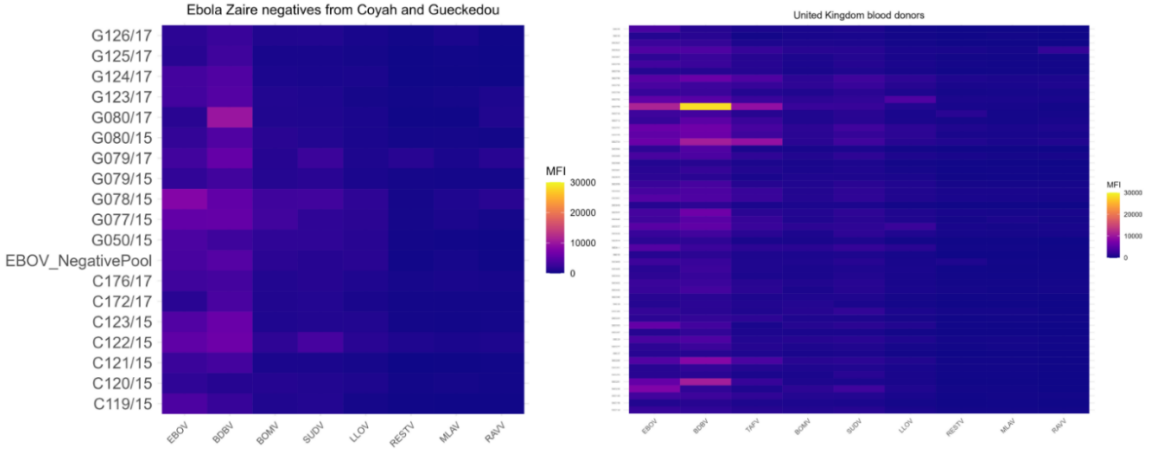


Figure 33 Individual anti-filovirus glycoprotein antibody responses in EBOV-negative, Coyah and Guéckédou, Republic of Guinea (n=15) and UK blood donors (n=63).

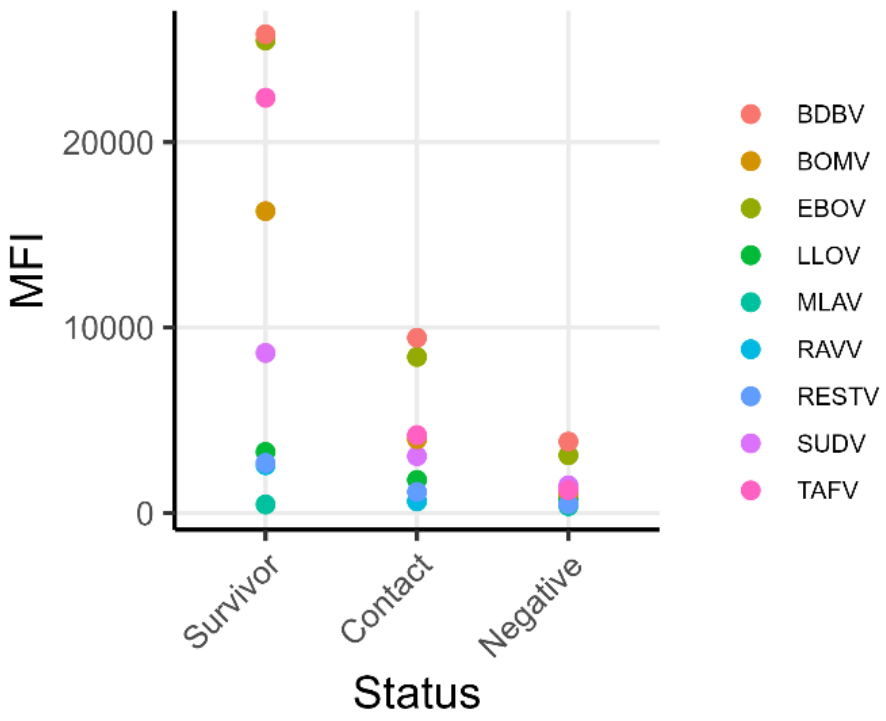


Figure 34 Average anti-filovirus glycoprotein antibody responses of EVD survivors

Anti-filovirus responses of PCR-confirmed EBOV survivors 12- to 24-months post infection (n=114), EBOV contacts (n=66), and negatives (n=15) from Coyah and Guéckédou, Republic of Guinea.

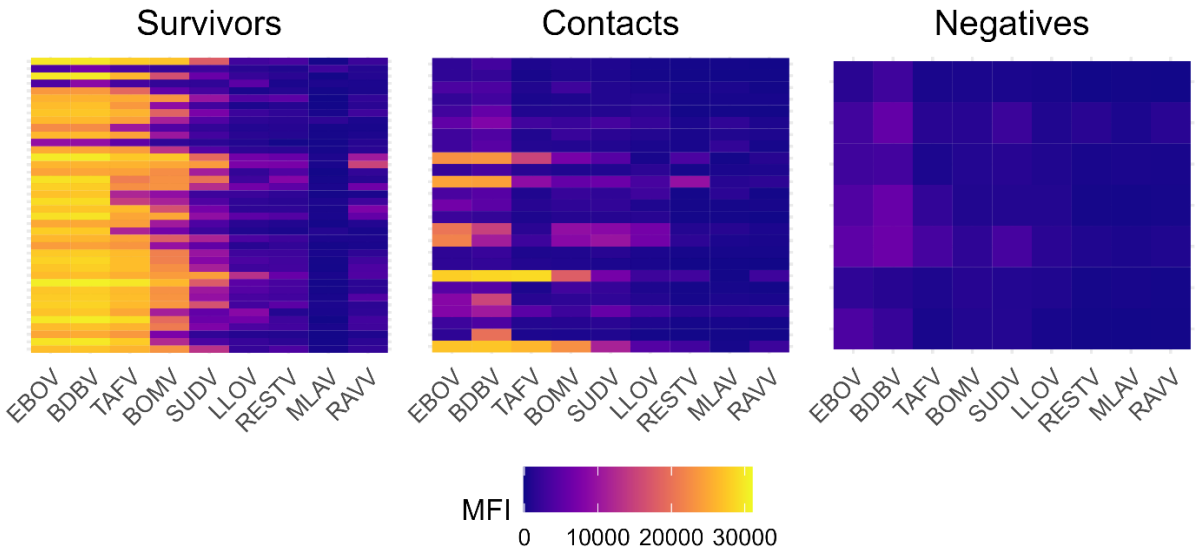


Figure 35 Individual anti-filovirus glycoprotein antibody responses of EVD survivors

Anti-filovirus responses of PCR-confirmed EBOV survivors 12- to 24-months post infection (n=114), EBOV contacts (n=66), and negatives (n=15) from Coyah and Guéckédou, Republic of Guinea.

Anti-filovirus reactivity in Ugandan farmers

While the Ugandan farmer cohort (n=79) also showed considerable anti-filovirus reactivity, when partitioned into *k*=6 clusters, the vast majority of these filovirus reactive antigenic exposure profiles (Clusters 3, 4 and 5) were considered to be most plausibly explained by broad cross-reactivity following EBOV exposure. Only one cluster (Cluster 5) showed MLAV-specific IgG antibody binding in the absence of EBOV, however, at this low seroprevalence cannot be interpreted as a reliable signal of spillover. Similar results can be seen for *k*=3 clusters (Figure 38).

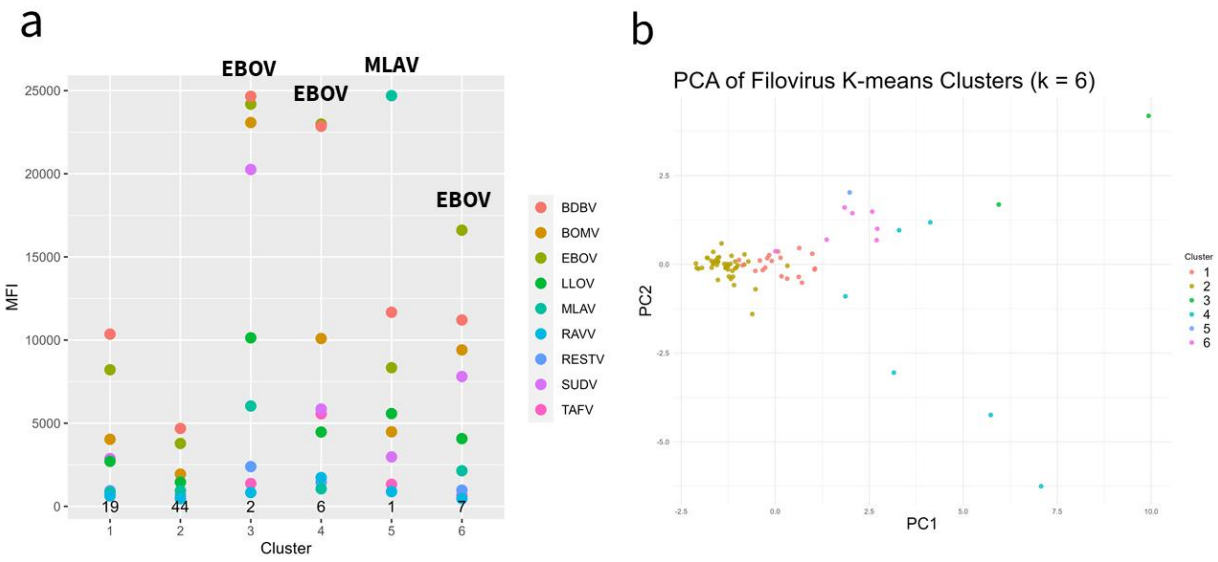


Figure 36 Anti-filovirus glycoprotein antibody responses of Ugandan farmers. Individuals clustered by *K*-means clustering (*k*=6) in Ugandan farmers (n=79) (b) Principal component analysis of *K*-means clustering results for *k*=6.

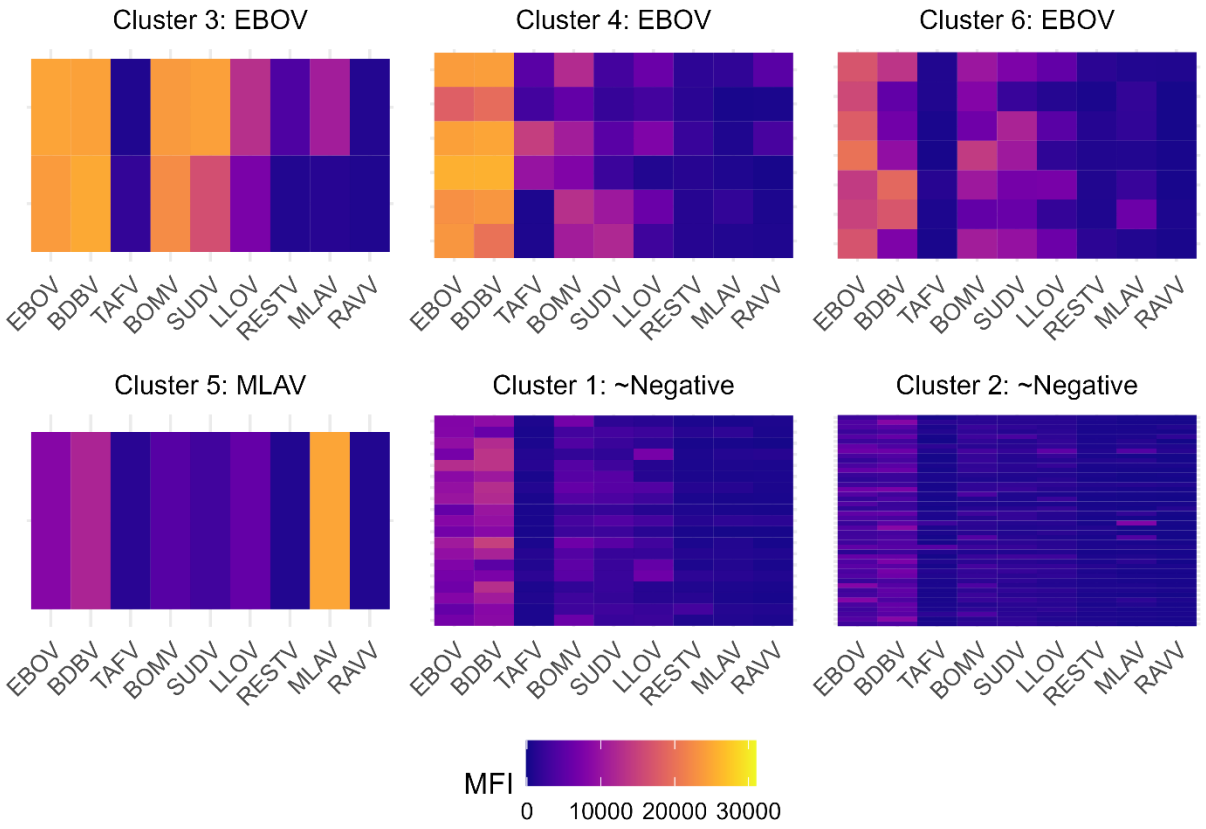


Figure 37 Individual anti-filovirus glycoprotein antibody responses in Uganda (*k*=6). Responses of individuals clustered by *K*-means clustering (*k*=6), Ugandan farmers (n=79) and classed as EBOV (a, b, c), MLAV (d), and negative (e, f).

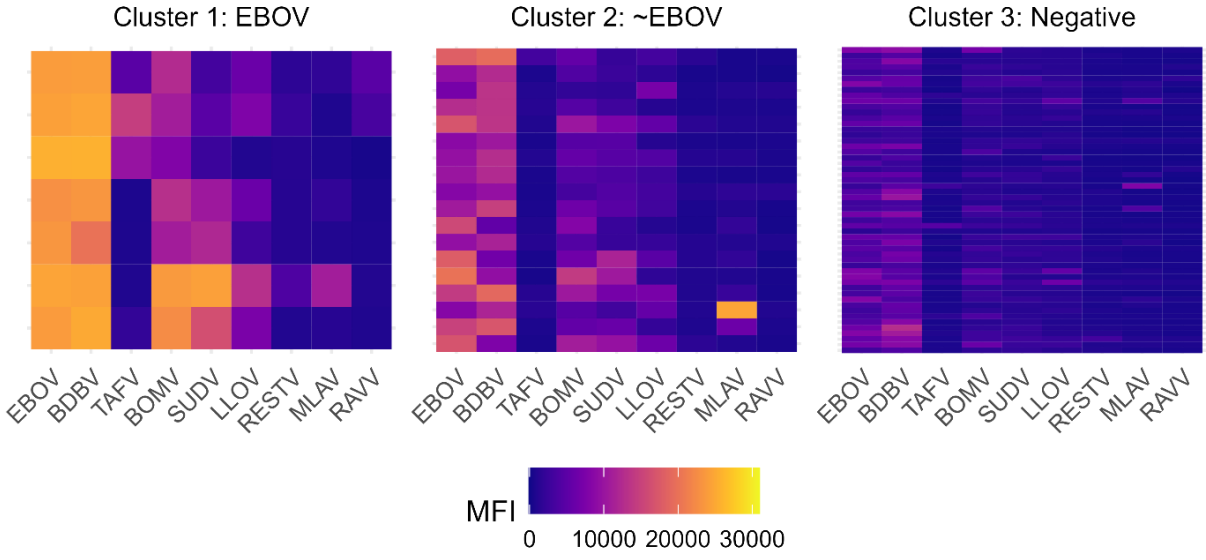


Figure 38 Individual anti-filovirus glycoprotein antibody responses in Uganda (*k*=3).

4.2.6. Filovirus neutralizing activity in Guinean WLHs

Filovirus neutralizing activity in Guinean WLHs

Guinean wildlife hunting community members with antibody profiles consistent with exposure to BDBV, TAFV, BOMV, RESTV, MLAV and LLOV were then assessed for their ability to neutralize the filovirus in parallel with Ebola virus-Makona PV. Neutralising ability was tested by a lentivirus-backbone filovirus GP PVNA or a VSV-backbone PVNA for MLAV. A pool of PCR-confirmed EBOV-Makona survivors from 2014 was included for comparison. Negative controls included an EBOV-negative Guinean pool from Coyah and Guéckédou (n=3) and a UKBD.

Of those tested from the BDBV cluster, 8 individuals neutralised BDBV more strongly than they neutralised EBOV, and neutralised BDBV more strongly than the EBOV survivor pool. Two of these individuals were household contacts (JAB135, JAB136), and came from villages which reported no cases of EBOV. Persistent responses were shown by those resampled in 2023 (JAB297, JAB376). The remaining samples (including the EBOV survivor pool) showed stronger neutralisation of EBOV, with some neutralisation of BDBV. Of the individuals tested from the TAFV cluster, 5 individuals from 2023 neutralised TAFV more strongly than they neutralised EBOV. Of the LLOV cluster, 1 individual had stronger neutralising ability against LLOV than EBOV without overlapping 95% confidence intervals (Figure 41). All samples from the BOMV and RESTV cluster neutralised EBOV more strongly than BOMV or RESTV, though all showed some neutralising activity against both. No samples from the MLAV cluster neutralized VSV-EBOV or VSV-MLAV. In all neutralisation assays, the PCR-confirmed EBOV survivor pool showed strong neutralisation responses against EBOV-Makona (NT50 90, 95% CI: 57 – 142), and also demonstrated a lower level of cross-neutralisation of BDBV, RESTV, TAFV and LLOV (but not MLAV).

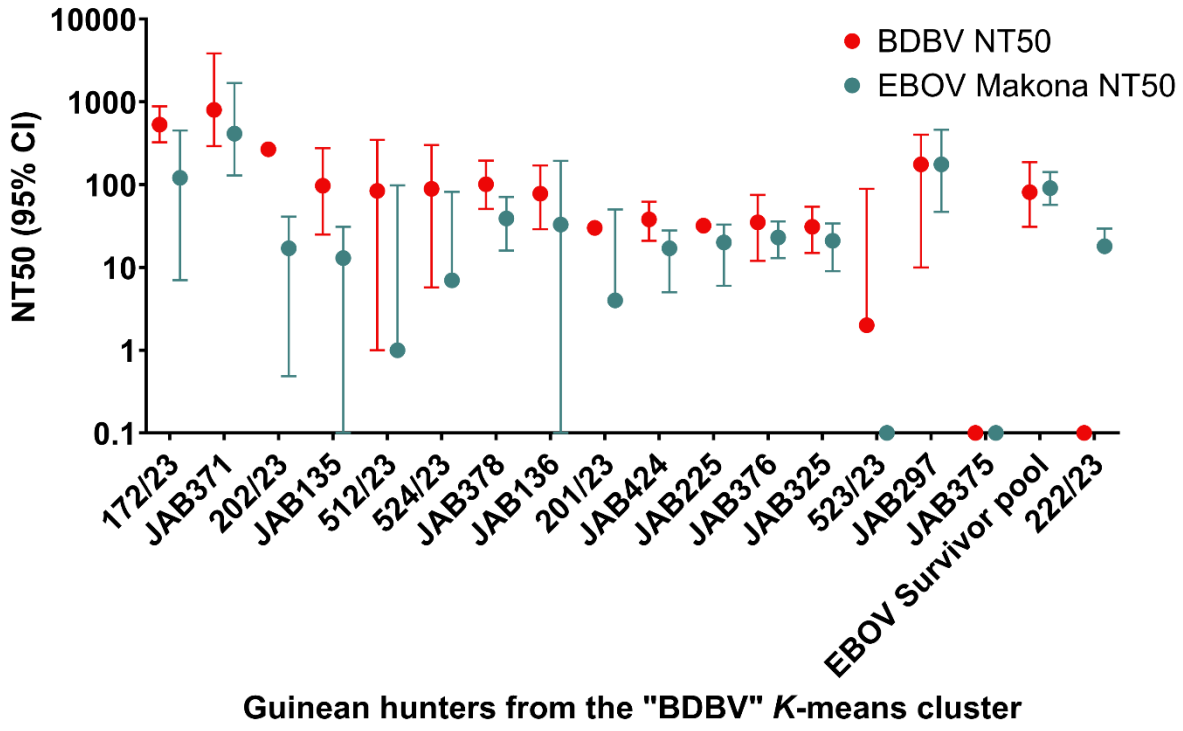


Figure 39 Neutralising ability of Guinean wildlife hunter sera against Bundibugyo (BDBV) and Ebola (EBOV) viruses by PVNA. Samples were tested in parallel BDBV and EBOV lentiviral backbone pseudotyped virus neutralisation assays. Samples tested are those which were identified following *K*-means clustering as showing specific binding antibody responses against BDBV. NT50 values and 95% confidence intervals were calculated using nonlinear regression in GraphPad Prism 10.0.3. All samples were tested in triplicate. The EBOV survivor pool consists of n=3 PCR-confirmed EBOV survivors 3 – 14 months post-infection. Negative controls included an EBOV-negative Guinean pool (n=3) and UK blood donor: neither showed any neutralizing activity.

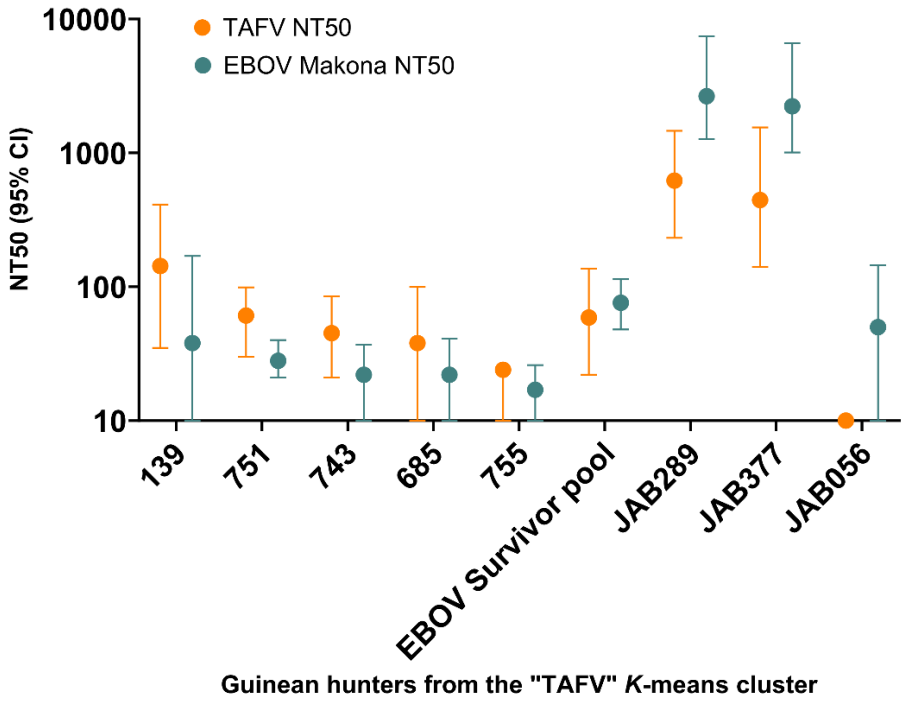


Figure 40 Neutralising ability of Guinean wildlife hunter sera against Taï Forest virus (TAFV) and Ebola (EBOV) viruses by pseudotyped virus neutralisation assay.

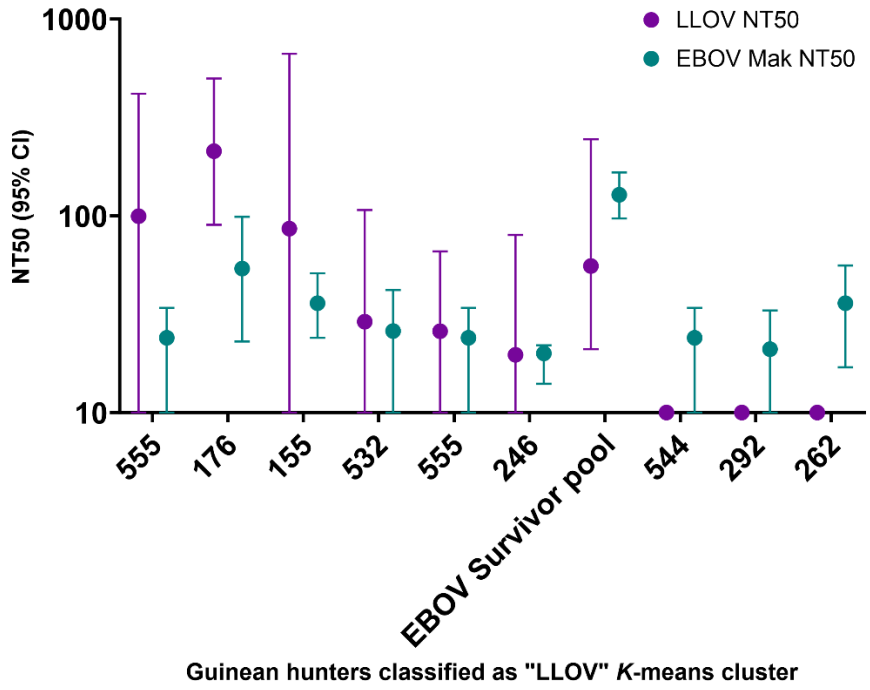


Figure 41 Neutralising ability of Guinean wildlife hunter sera against Lloviu (LLOV) and Ebola-Makona (EBOV) viruses by pseudotyped virus neutralisation assay.

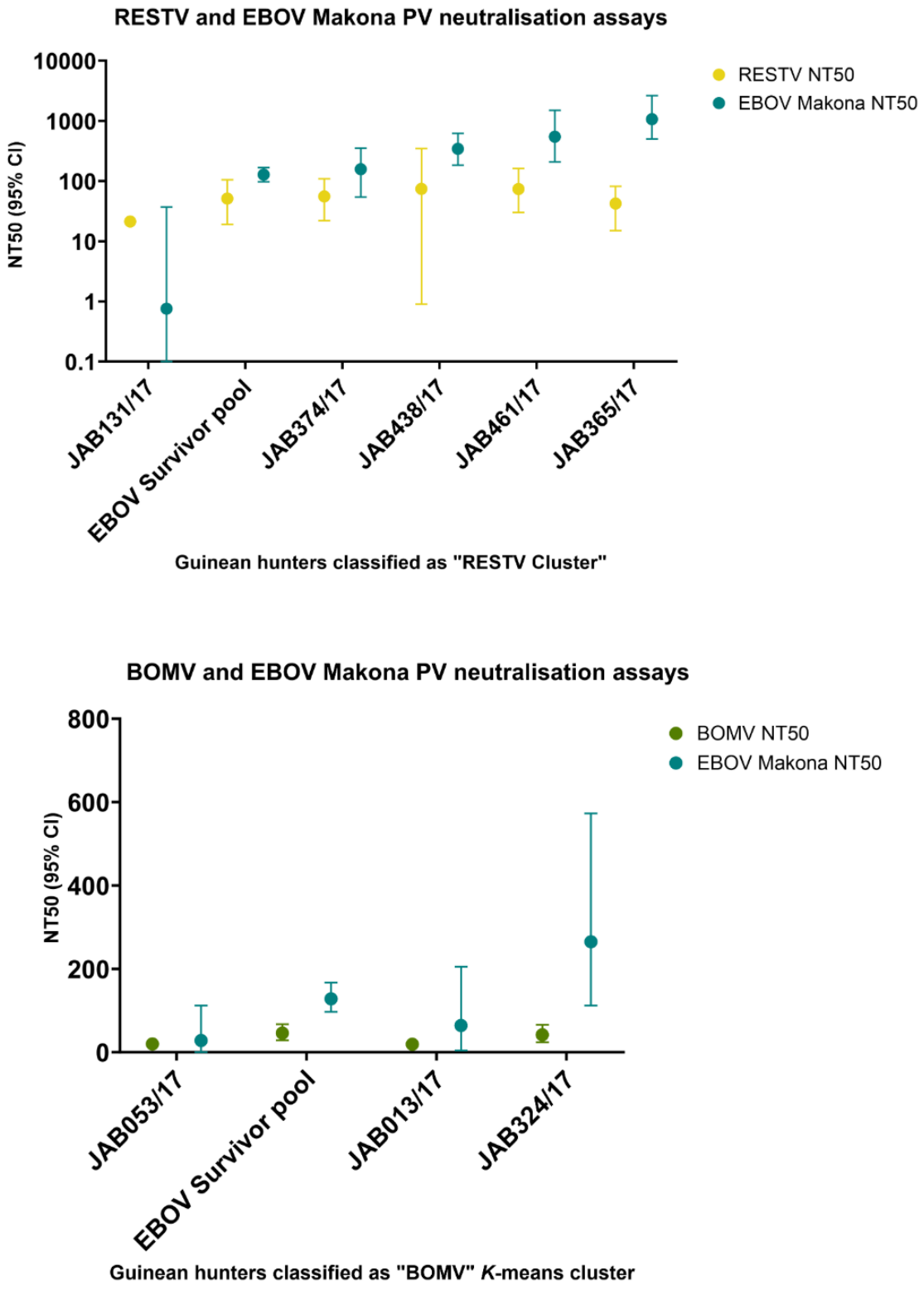


Figure 42 Neutralising ability of Guinean wildlife hunter sera against Reston (RESTV) and Ebola-Makona (EBOV) viruses and Bombali (BOMV) and Ebola (EBOV) Makona viruses by pseudotyped virus neutralisation assay.

4.2.7. Durable EBOV antibody responses, 6 years post 2013 – 2016 West African EVD epidemic and antibody decay rates

For individuals with detectable EBOV antibodies in 2017, a comparison of 2017 to 2023 demonstrated the durability of anti-EBOV antibodies (Figure 43). Antibody decay rates were modelled as an exponential decrease from time of infection, with a regression model fitted to IgG antibody data from each individual above a seropositivity threshold for EBOV in 2017 who was resampled in 2023. The seropositivity threshold was calculated as the mean antibody level (EBOV-GP MFI) of the presumed EBOV-seronegative population (UKBD cohort) plus 5 standard deviations. Based on the population average of these models, the EBOV IgG antibody half-life was estimated as 7.5 years (Figure 43).

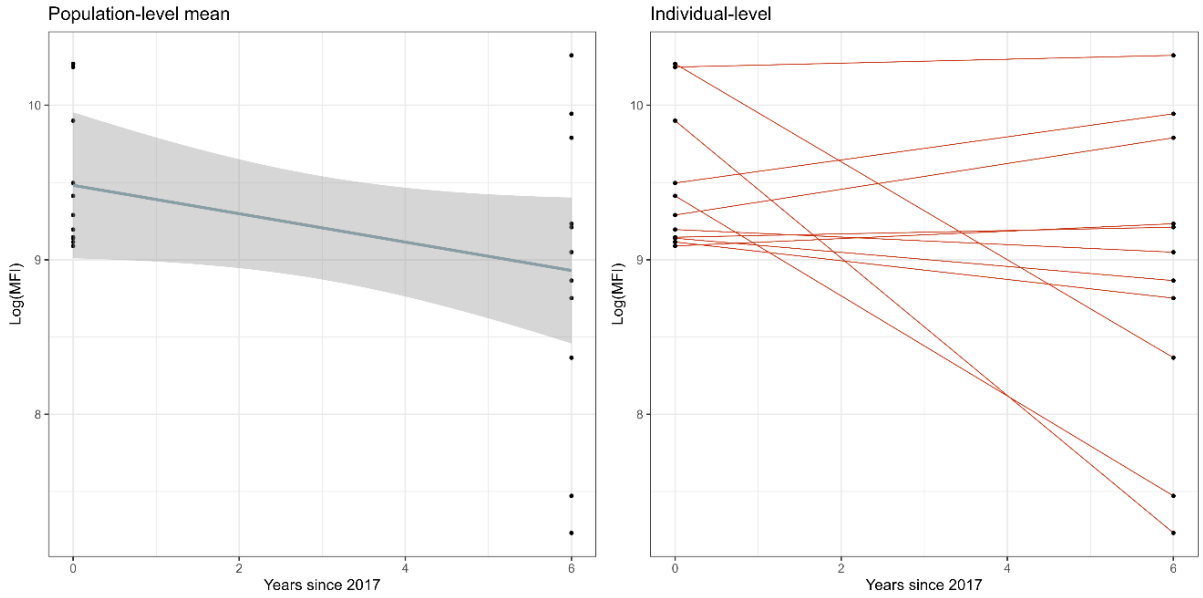


Figure 43 Population-level mean (with 95% confidence interval (shaded)) and individual-level antibody decay models for Ebola virus amongst those identified as seropositive in 2017. IgG responses were measured by multiplex microsphere-based immunoassay (MMIA) in background subtracted median fluorescence units. Antibody decay rates were modelled as an exponential decrease from time of infection, with a regression model fitted to IgG antibody data from each individual above a seropositivity threshold for EBOV in 2017 who was resampled in 2023.

Antibody decay rates were modelled for all other filoviruses as the population average of all individual linear regression models with a negative slope (fitted to IgG antibody data for each individual sampled in 2017 and 2023) (Appendix: Table 22). The overall population-level distribution of antibody responses for the majority of filoviruses increased from 2017 to 2023, with the exception of TAFV and RESTV (Appendix: Figure 60), driven by a positive slope in the majority of individuals (Appendix: Figure 61).

4.2.8. Seroconversion observed in Guinean WLHs between 2017 and 2023

Resampled individuals (2017 and 2023) who were classified in clusters of interest were plotted, with some demonstrating apparent antigen exposure (LLOV- and MLAV-like) during the 6 years (Figure 44).

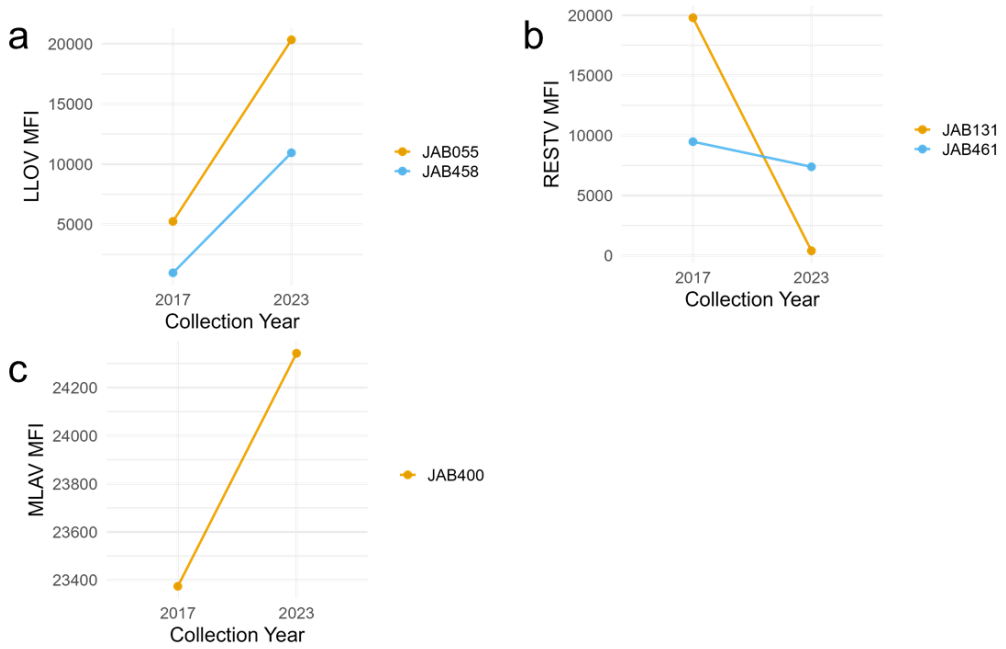


Figure 44 Individual anti-filovirus glycoprotein IgG responses of Guinean wildlife hunters in 2017 and 2023 against (a) LLOV (b) RESTV (c) MLAV. IgG responses measured by multiplex microsphere-based immunoassay (MMIA) in background subtracted median fluorescence units (MFI-bg) on the Luminex platform.

4.2.9. Antigen reactivity in Guinean WLHs by village

Population-level Ebola virus (EBOV) immunity, 6 years post- 2013-2016 West African EVD epidemic

As demonstrated in individual decay models, a village-level comparison of 2017 to 2023 found population-level EBOV-antibodies remained high 6 years post-epidemic, providing support to idea of a long-lived antibody response following EBOV infection. Interestingly, the breadth of the (presumed) cross-reactive antibody response against closely-related filoviruses (particularly TAFV) narrowed over the course of 6 years (Figure 45, Figure 46). This corroborates previous findings that the serological cross-reactivity seen between antigenically related viruses, which titres away with phylogenetic distance, also decreases with antibody concentration.

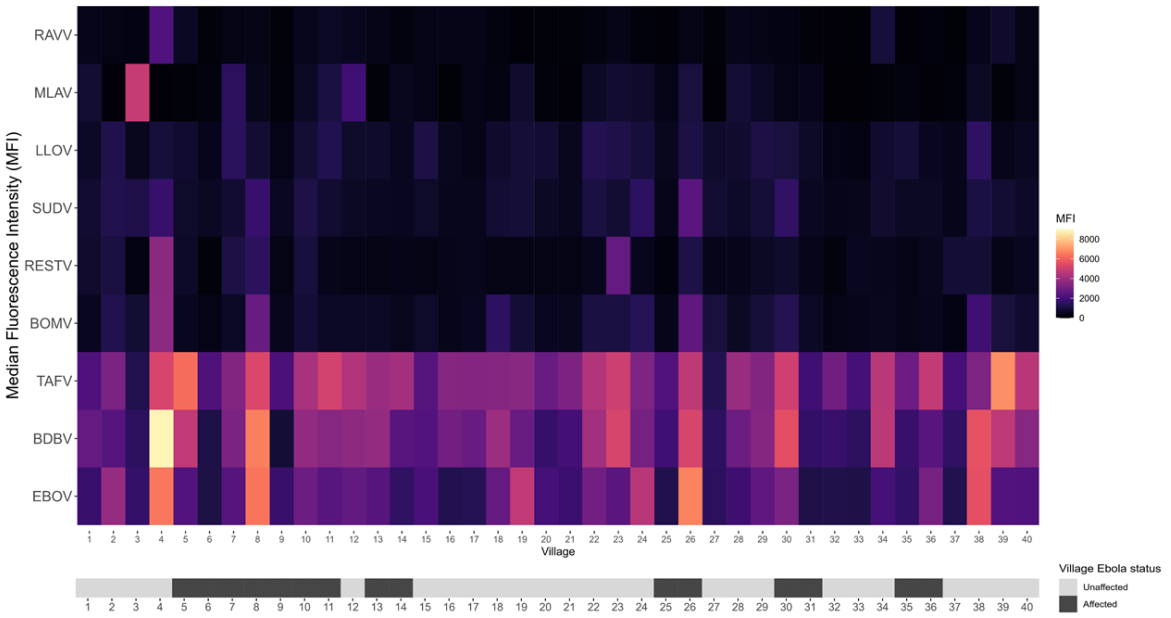


Figure 45 Geometric mean anti-filovirus IgG responses amongst Guinean wildlife hunters in 2017, stratified by village. IgG responses were measured by multiplex microsphere-based immunoassay (MMIA) in background subtracted median fluorescence units. Villages were determined to be affected or unaffected by the 2014-16 West African Ebola virus epidemic based on official Nzérékoré Ministry of Health designations followed by key informant interviews of healthcare workers and village leaders.

Village names					
1	Oulimè	15	Massadou	29	Singuèga
2	Kpaou	16	Zobroma	30	Wotoula
3	Koyamah	17	Waleno	31	Doizea
4	Maraou	18	Ballassou	32	Ozaolazou
5	Zinigrozou	19	Namouyapoulou	33	Kpovolaou
6	Koballaga	20	Orémai	34	Touweleou
7	Zenié	21	Kassanka	35	Banaou
8	Fassankony	22	Nyanguezazou	36	Vassaizeazou
9	Nobrotono	23	Sovaou	37	Wattanka
10	Iyézou	24	Bodolazou	38	Baizea
11	Kpoda	25	Bofossou	39	Deguedeou
12	Avilissou	26	Kpagouloumè	40	Sassaguizezou
13	Irié	27	Dohomai		
14	Malewoita	28	Sèlèga		

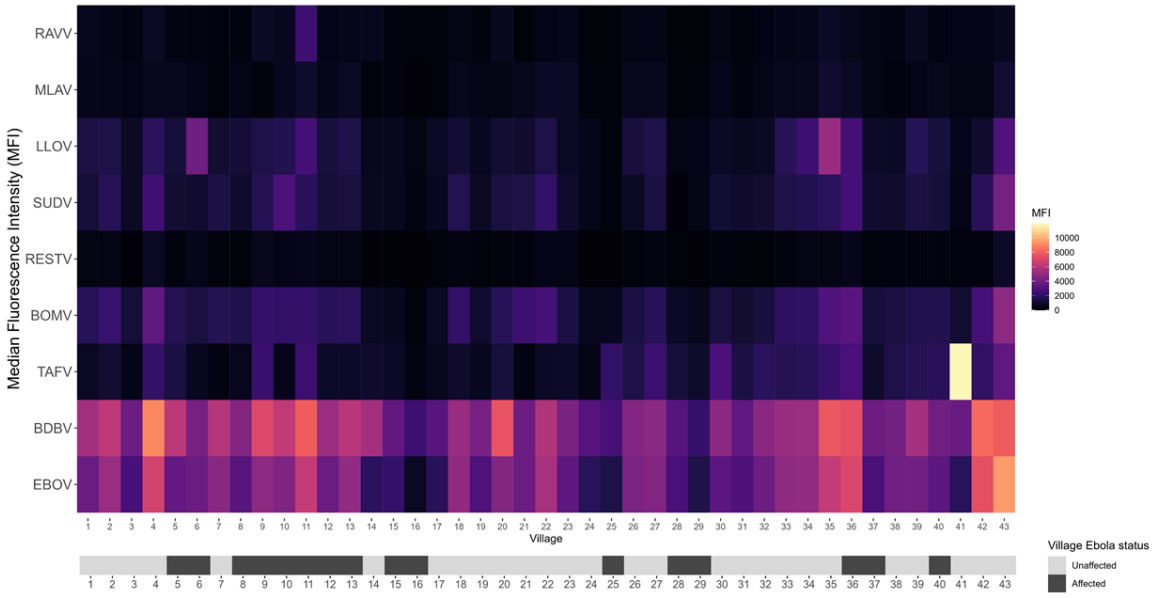


Figure 46 Geometric mean anti-filovirus IgG responses amongst Guinean wildlife hunters in 2023, stratified by village. IgG responses were measured by multiplex microsphere-based immunoassay (MMIA) in background subtracted median fluorescence units. Villages were determined to be affected or unaffected by the 2014-16 West African Ebola virus epidemic based on official Nzérékoré Ministry of Health designations followed by key informant interviews of healthcare workers and village leaders.

Village name					
1	Oulimè	16	Seredou	31	Bouolazou
2	Kpaou	17	Massadou	32	Bodolazou
3	Koyamah	18	Zobroma	33	Sèlèga
4	Maraou	19	Waleno	34	Singuèga
5	Malewoita	20	Balassou	35	Koudouma
6	Oliguizezou	21	Namouyapoulou	36	Wotoula
7	Brebezou	22	Lowouma	37	Doizea
8	Koballaga	23	Oremai	38	Ozaolazou
9	Zenié	24	Kassanka	39	Touweleou
10	Fassankony	25	Gueckedou	40	Banaou
11	Tribai	26	Nyakpezazou	41	Deguedeou
12	Iyezou	27	Sovaou	42	Baizea
13	Kpoda	28	Bofossou	43	Sassaguizezou
14	Avilissou	29	Kpagouloumè		
15	Irié	30	Dohomai		

Investigation of village-level hotspots for Taï Forest, Bundibugyo and Mĕnglà viruses in locations unaffected by the 2013 – 2016 West African EVD epidemic

Questionnaire data revealed low migration and movement of individuals between villages, allowing for village-level spatial analyses. Geometric mean antibody responses were calculated for each filovirus antigen by village, and revealed marked village-level heterogeneity (Figure 47 to Figure 49) but no spatial autocorrelation between the villages (Figure 50, Figure 51, Figure 52). Deguedeou (Village 39 in 2017 and Village 41 in 2023), a village unaffected by the 2013 – 2016 West African EVD epidemic, was identified for an increased mean Taï Forest virus (TAFV) reactivity, in the absence of anti-EBOV antibodies (p<0.0001) in both 2017 and 2023.

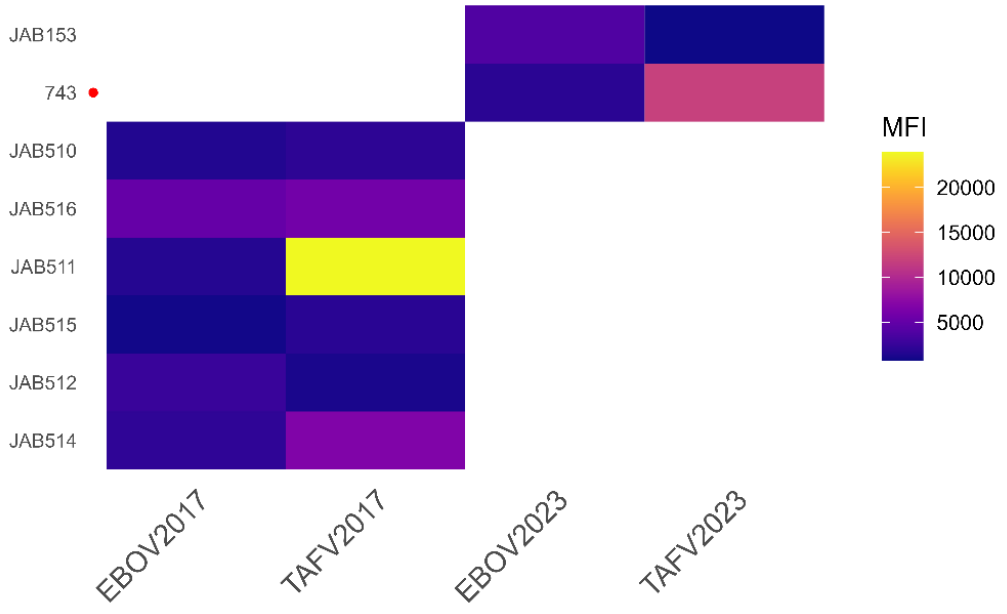


Figure 47 Individual IgG responses to Ebola virus (EBOV) and TAFV virus amongst Guinean wildlife hunters from Deguedeou in 2017 and 2023. IgG responses were measured by multiplex microsphere-based immunoassay (MMIA) in background subtracted median fluorescence units. Red dot denotes an individual with a higher NT50 for TAFV than EBOV in parallel lentiviral pseudotyped virus neutralisation tests.

Maraou (Village 4), similarly showed significantly increased BDBV responses (p<0.0001), which were higher than the mean EBOV responses in both 2017 and 2023. Some of the highest BDBV-neutralising individuals identified were from Maraou, and demonstrated superior neutralising activity against BDBV than EBOV in the PVNA. Maraou was confirmed by both official Macenta Ministry of Health designations and key informant interviews of healthcare workers and village leaders to be unaffected by the 2013 – 2016 West African EVD epidemic.

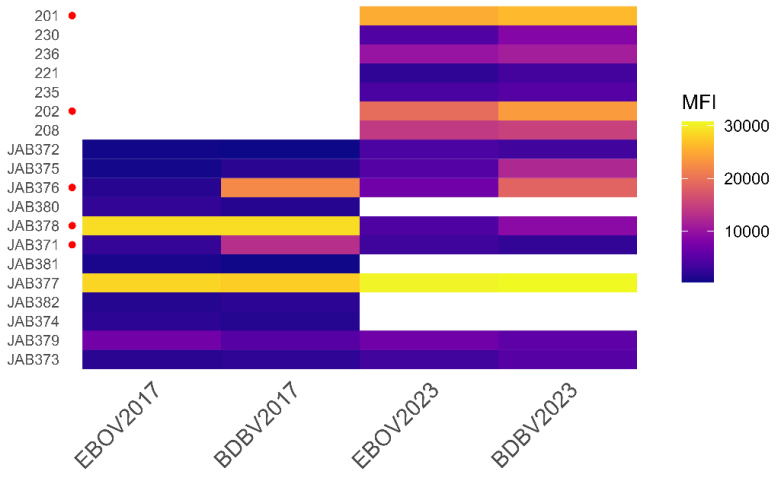


Figure 48 Individual IgG responses to Ebola (EBOV) and Bundibugyo (BDBV) viruses amongst Guinean wildlife hunters from Maraou in 2017 and 2023. IgG responses were measured by multiplex microsphere-based immunoassay (MMIA) in background subtracted median fluorescence units. Red dots denote individuals with a higher NT50 for BDBV than EBOV in parallel lentiviral pseudotyped virus neutralisation tests.

In 2017, one village (Coyamah) appeared to have a significantly higher mean antibody response binding to MLAV, a phylogenetically distinct bat filovirus first identified in China (p<0.0001) (Village 3). However, this signal can be entirely attributed to a single individual with persistent MLAV-specific antibodies in both 2017 and 2023 (Figure 49).

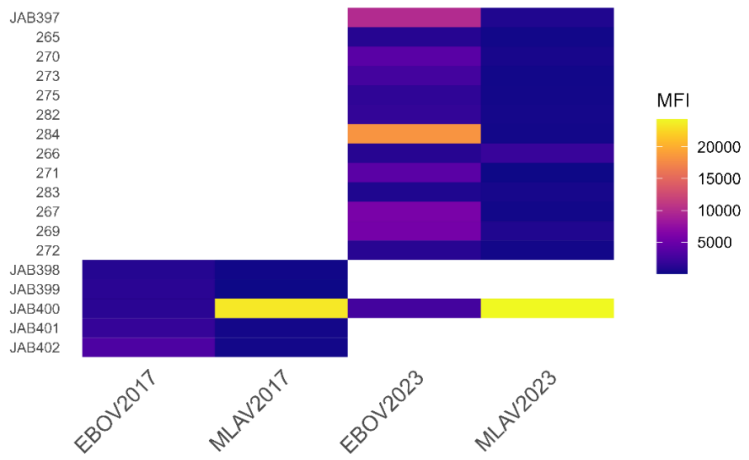


Figure 49 Individual IgG responses to Ebola (EBOV) and MLAV viruses amongst Guinean wildlife hunters from Coyamah in 2017 and 2023

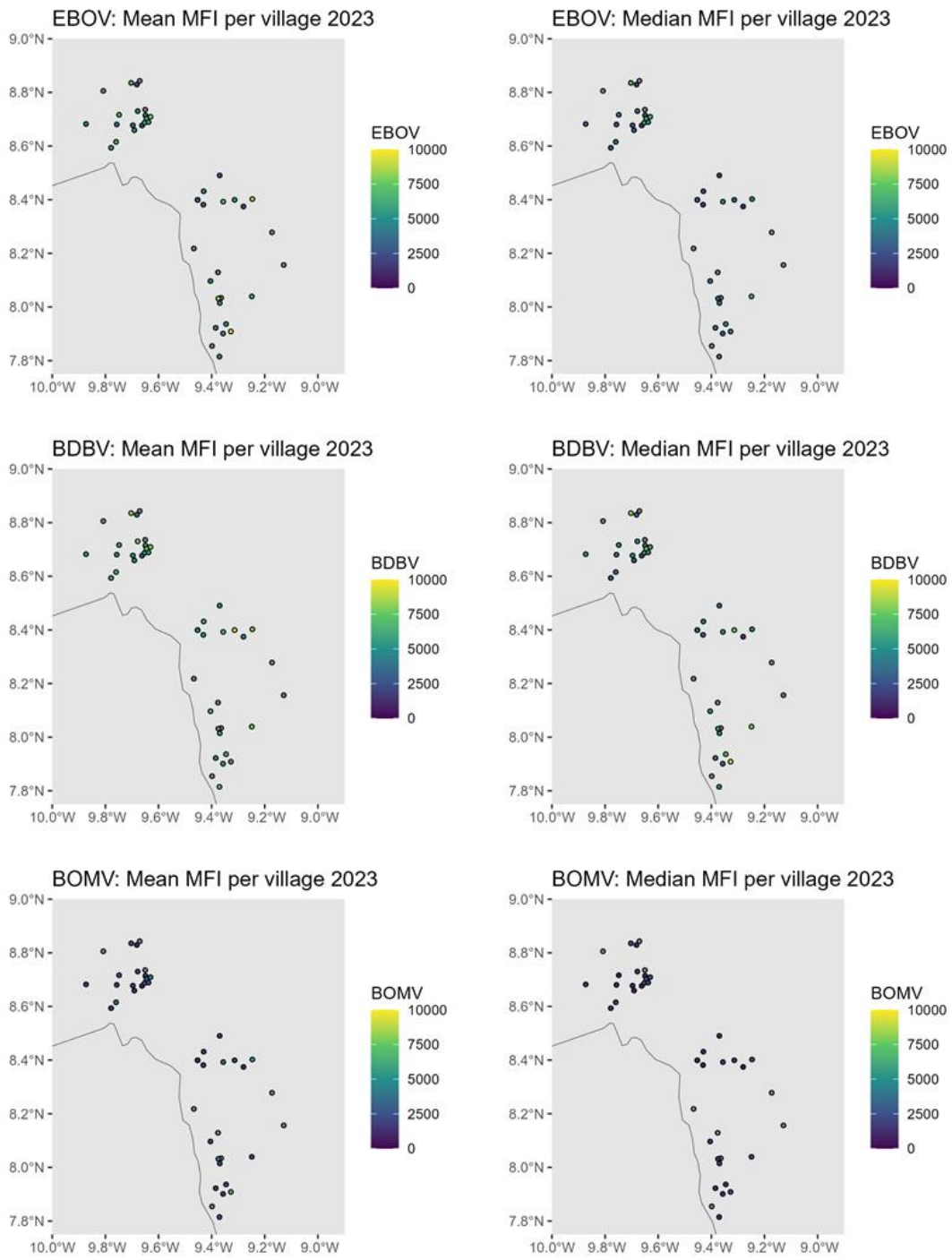


Figure 50 Village-level IgG responses (mean and median) to filovirus antigens (EBOV, BDBV, BOMV) amongst Guinean wildlife hunters in 2023

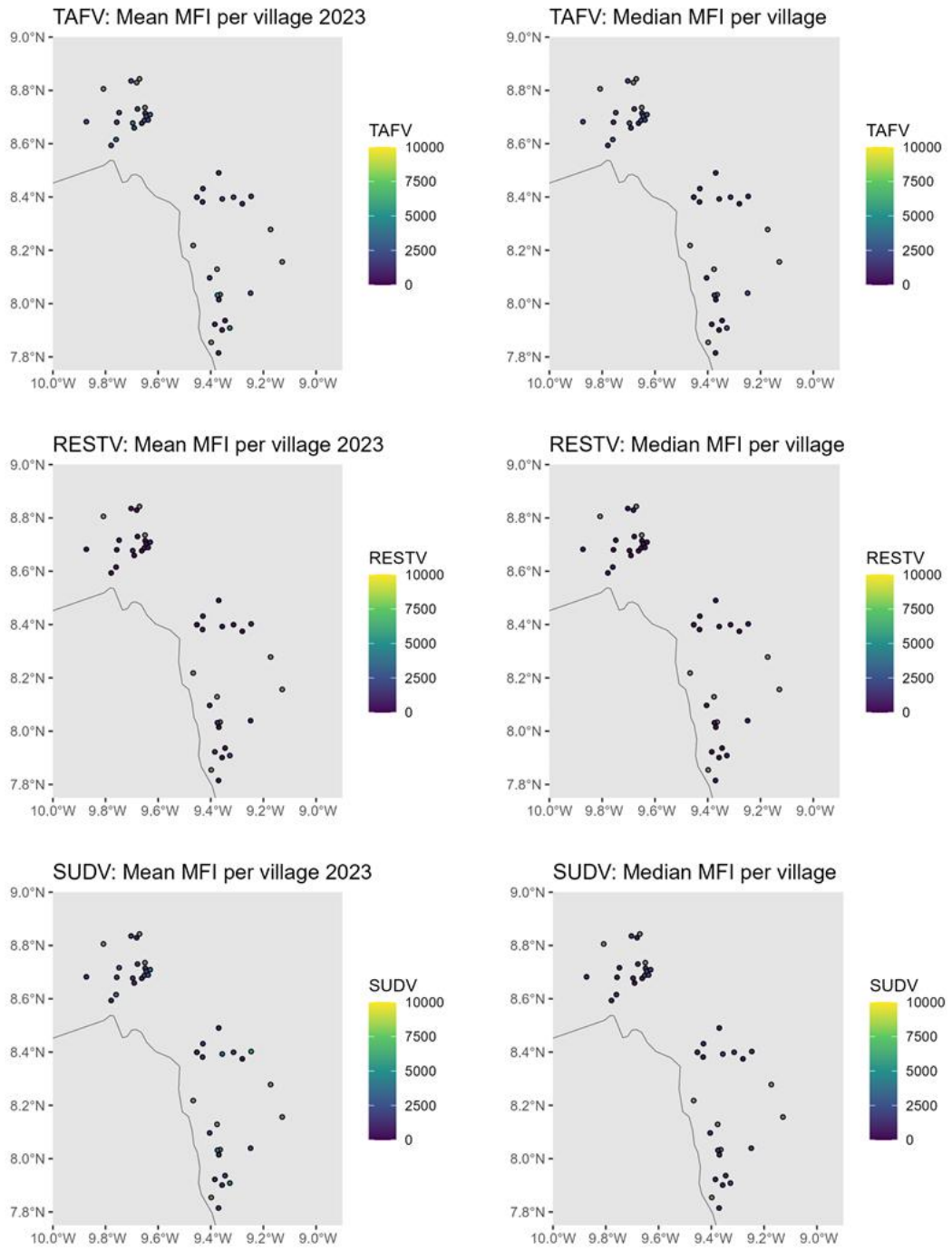


Figure 51 Village-level IgG responses (mean and median) to filovirus antigens (TAFV, RESTV, SUDV) amongst Guinean wildlife hunters in 2023

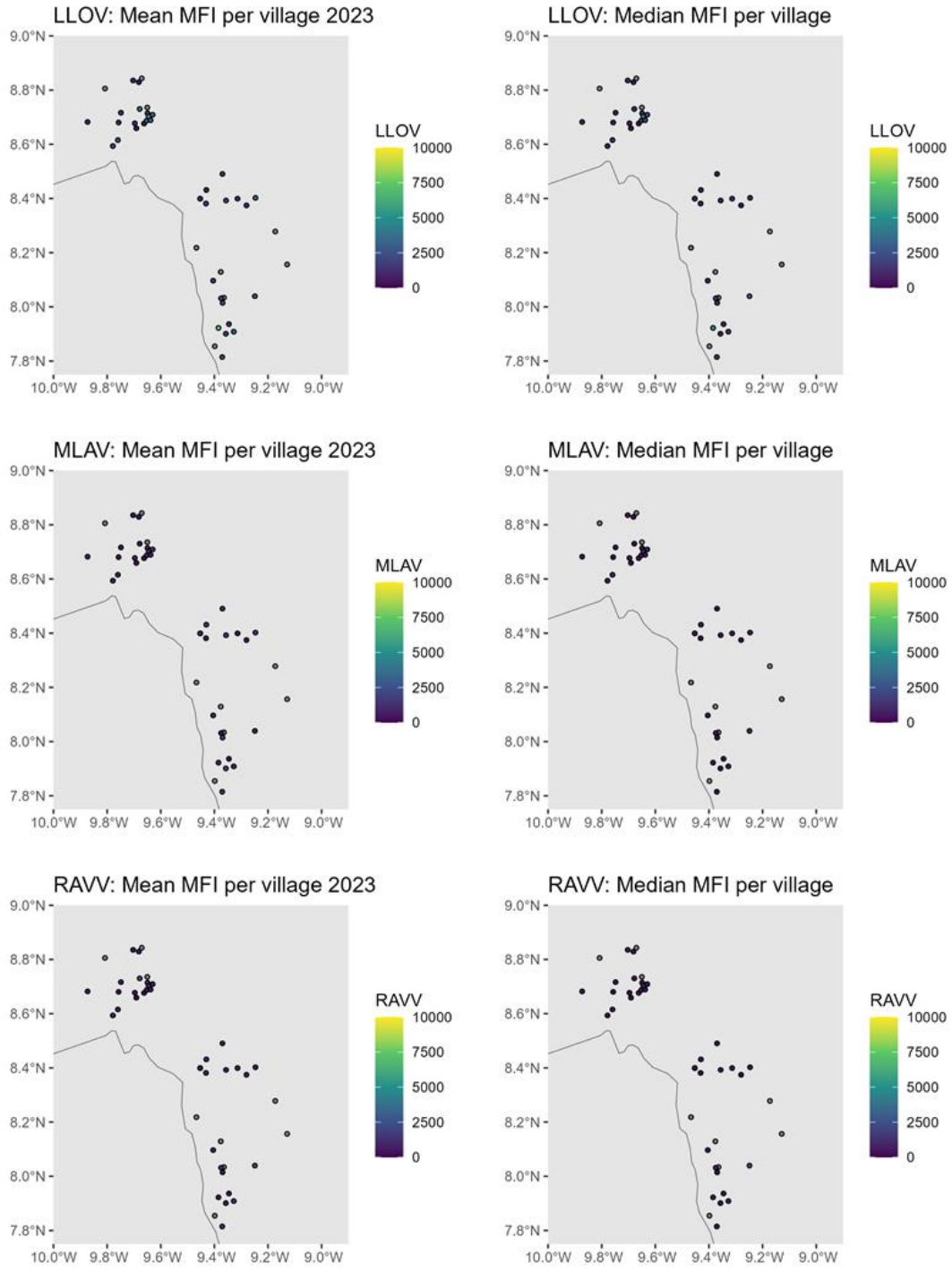


Figure 52 Village-level IgG responses (mean and median) to filovirus antigens (LLOV, MLAV, RAVV) amongst Guinean wildlife hunters in 2023. IgG responses were measured by multiplex microsphere-based immunoassay (MMIA) in background subtracted median fluorescence units.

4.2.10. Risk factors for filovirus seropositivity

Population-level distributions between WLHs and non-hunters

No significant population-level differences were identified between WLHs and close contacts (Appendix, Figure 62), or bat hunters and non-hunters (Appendix, Figure 63) in Forested Guinea.

Linear regression analysis of risk factors associated with individual antigens in Guinean WLH cohort 2023 and Ugandan farmers

Individual-level risk factors were investigated for the 2023 cohort in univariable and multivariable statistical models using the extended questionnaire data. Antigen response distributions were right-skewed (Appendix, Figure 64) therefore log-transformed MFI (Figure 53) was examined as a continuous outcome for each individual antigen using linear regression.

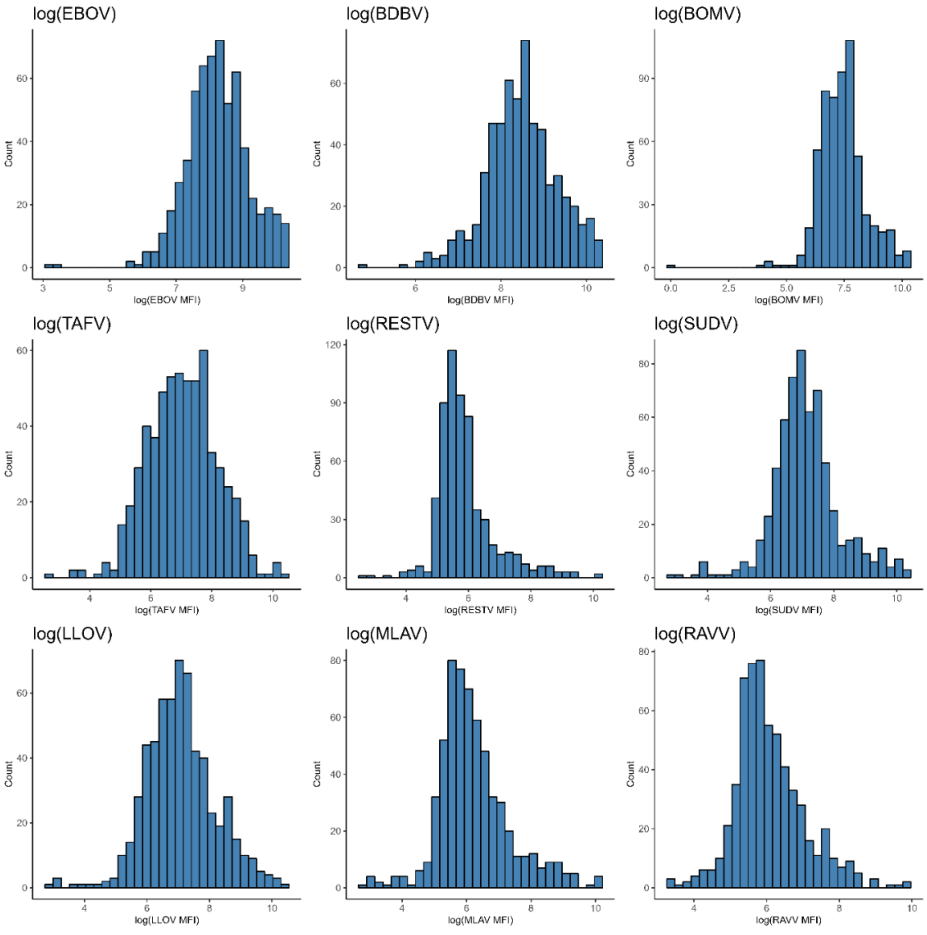


Figure 53 Anti-filovirus responses (log-transformed) amongst Guinean wildlife hunters 2023. IgG responses were measured by multiplex microsphere-based immunoassay (MMIA) in background subtracted median fluorescence units (MFI-bg) on the Luminex platform.

Univariate linear regression analysis of risk factors reported in the questionnaire found male sex to be significantly associated with increased anti-filovirus antibody responses (EBOV (β = 0.18, 95% CI:

0.02 to 0.33, $p = 0.025$), BDBV (β = 0.16, 95% CI: 0.02 to 0.30, $p = 0.021$), TAFV (β = 0.46, 95% CI: 0.27 to 0.64, $p < 0.001$), RESTV (β = 0.25, 95% CI: 0.09 to 0.40, $p = 0.002$) and RAVV (β = 0.27, 95% CI: 0.11 to 0.43, $p = 0.001$)) in the 2023 wildlife hunting cohort (Table 18). Surprisingly, healthcare work was not associated with increased EBOV reactivity, highlighting the dominance of community transmission (Appendix: Figure 65).

Both being a wildlife hunter (WLH) and exposure to wildlife hunting (WLH exposure: defined as being a WLH or household contact of a WLH) were significantly associated with increased TAFV (Figure 54) (WLH: β = 0.47, 95% CI: 0.29 to 0.65, $p < 0.001$, WLH exposure: β = 0.39, 95% CI: 0.20 to 0.59, $p < 0.001$) and RESTV seropositivity (WLH: β = 0.22, 95% CI: 0.07 to 0.37, $p = 0.004$, WLH exposure: β = 0.23, 95% CI: 0.07 to 0.39, $p = 0.006$)) (Figure 55). Consumption of bats was significantly associated with increased BOMV (β = 0.21, 95% CI: 0.02 to 0.40, $p = 0.029$), TAFV (β = 0.45, 95% CI: 0.23 to 0.66, $p < 0.001$), RESTV (β = 0.19, 95% CI: 0.02 to 0.37, $p = 0.032$), SUDV (β = 0.29, 95% CI: 0.09 to 0.49, $p = 0.005$), LLOV (β = 0.21, 95% CI: 0.00 to 0.42, $p = 0.045$) and RAVV (β = 0.26, 95% CI: 0.08 to 0.44, $p = 0.005$) seropositivity. Consumption of NHPs was significantly associated with increased BDBV seropositivity (β = 0.34, 95% CI: 0.06 to 0.63, $p = 0.019$) (Figure 56).

Table 18 Univariate linear regression analysis of risk factors for filovirus exposure in Guinean wildlife hunters, 2023

Predictor	Outcome (log (MFI))	β (Estimate)	95% CI	*p*-value
Sex (Male)	log (EBOV)	0.18	0.02 – 0.33	0.025
	log (BDBV)	0.16	0.02 – 0.30	0.021
	log (TAFV)	0.46	0.27 – 0.64	< 0.001
	log (RESTV)	0.25	0.09 – 0.40	0.002
	log (RAVV)	0.27	0.11 – 0.43	0.001
Wildlife hunting	log (TAFV)	0.47	0.29 – 0.65	< 0.001
	log (RESTV)	0.22	0.07 – 0.37	0.004
Wildlife hunting exposure	log (TAFV)	0.39	0.20 – 0.59	< 0.001
	log (RESTV)	0.23	0.07 – 0.39	0.006
Bat consumption	log (BOMV)	0.21	0.02 – 0.40	0.029
	log (TAFV)	0.45	0.23 – 0.66	< 0.001
	log (RESTV)	0.19	0.02 – 0.37	0.032
	log (SUDV)	0.29	0.09 – 0.49	0.005
	log (LLOV)	0.21	0.00 – 0.42	0.045
	log (RAVV)	0.26	0.08 – 0.44	0.005
Primate consumption	log (BDBV)	0.34	0.06 – 0.63	0.019

MFI = Median Fluorescence Intensity, CI = Confidence interval

By comparison, within the Ugandan farmer cohort, sex, exposure to wild animals or contact with bats were not associated with increased filovirus antigen reactivity when examined using univariate linear regression (Figure 57). Other predictor variables, including house wall, roof and floor material, exposure to rodents, exposure to sick contacts, caring for animals (sheep, cattle, goats, dogs, pigs, poultry, cats), slaughter of animals (sheep, cattle, forest hogs, wild rodents, primates) and being splashed with animal fluid during slaughtering were examined and found to be not significantly associated with filovirus reactivity in Ugandan farmers.

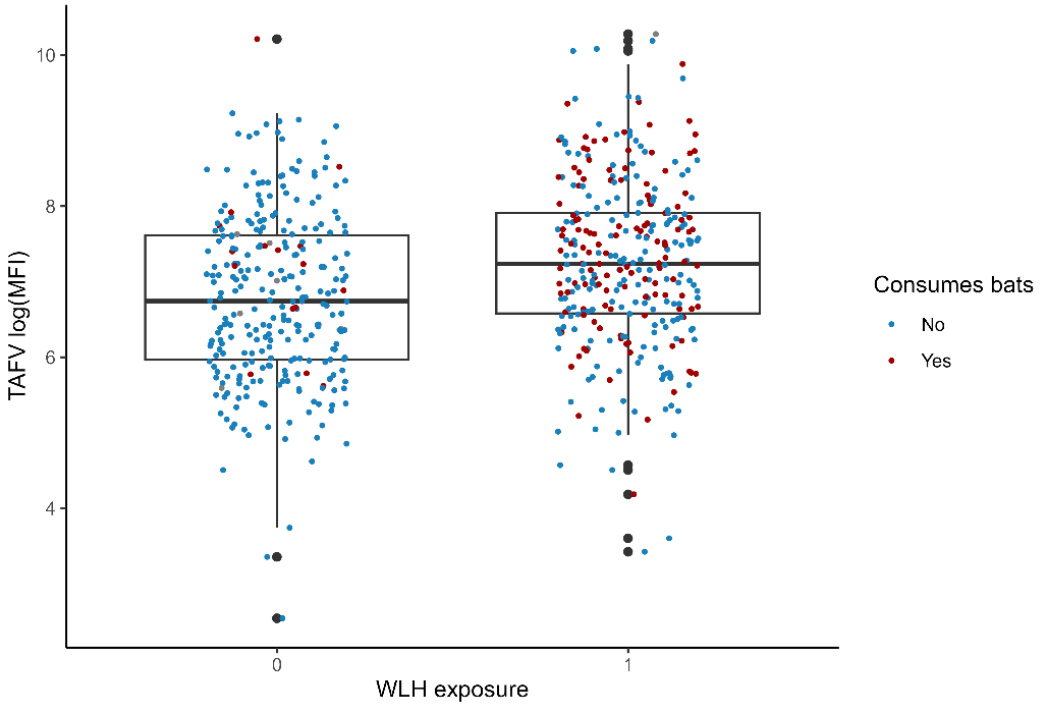


Figure 54 TAFV seropositivity by wildlife hunting exposure, 2023 among those who report bat consumption (1) and do not (0).

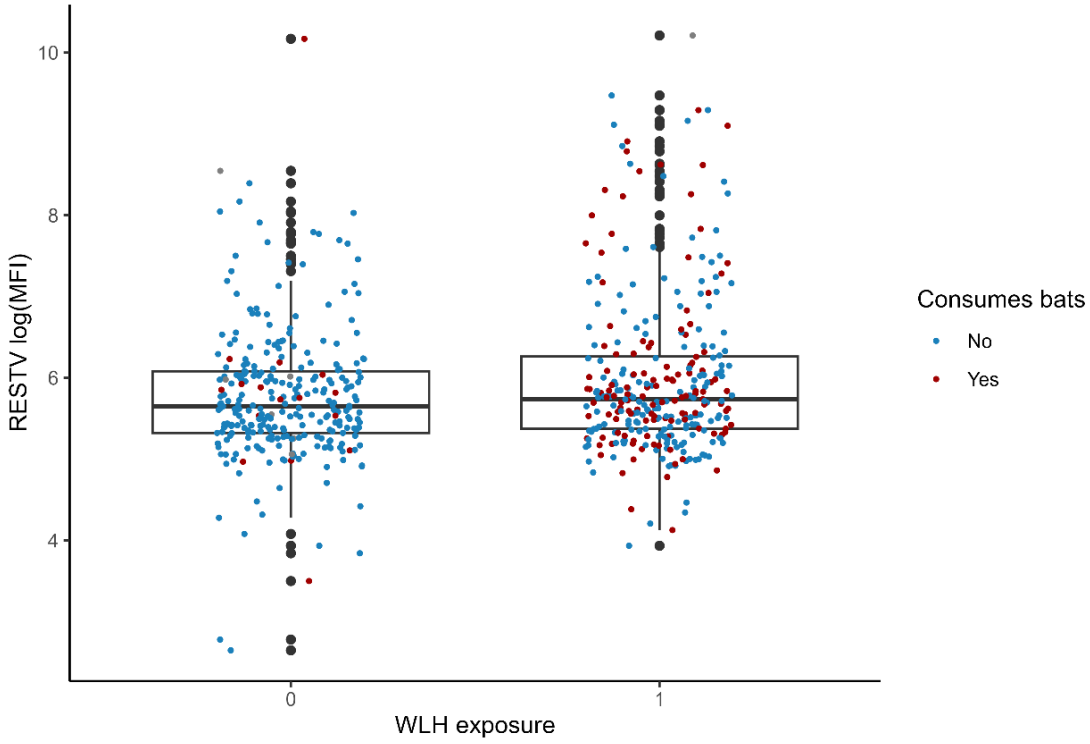


Figure 55 RESTV seropositivity by wildlife hunting exposure, 2023 among those who report bat consumption (1) and do not (0).

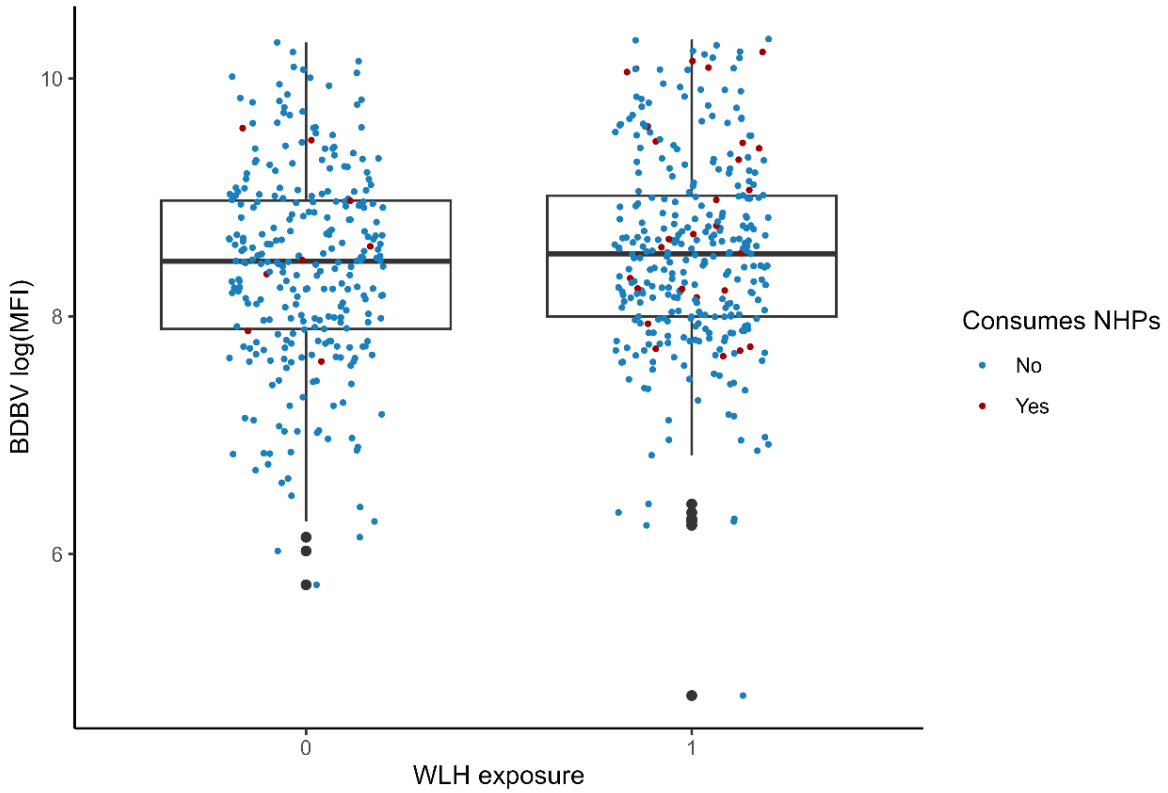


Figure 56 BDBV seropositivity by wildlife hunting exposure, 2023 among those who report nonhuman primate (NHP) consumption (1) and do not (0).

IgG responses were measured by multiplex microsphere-based immunoassay (MMIA) in background subtracted median fluorescence units (log (MFI)).

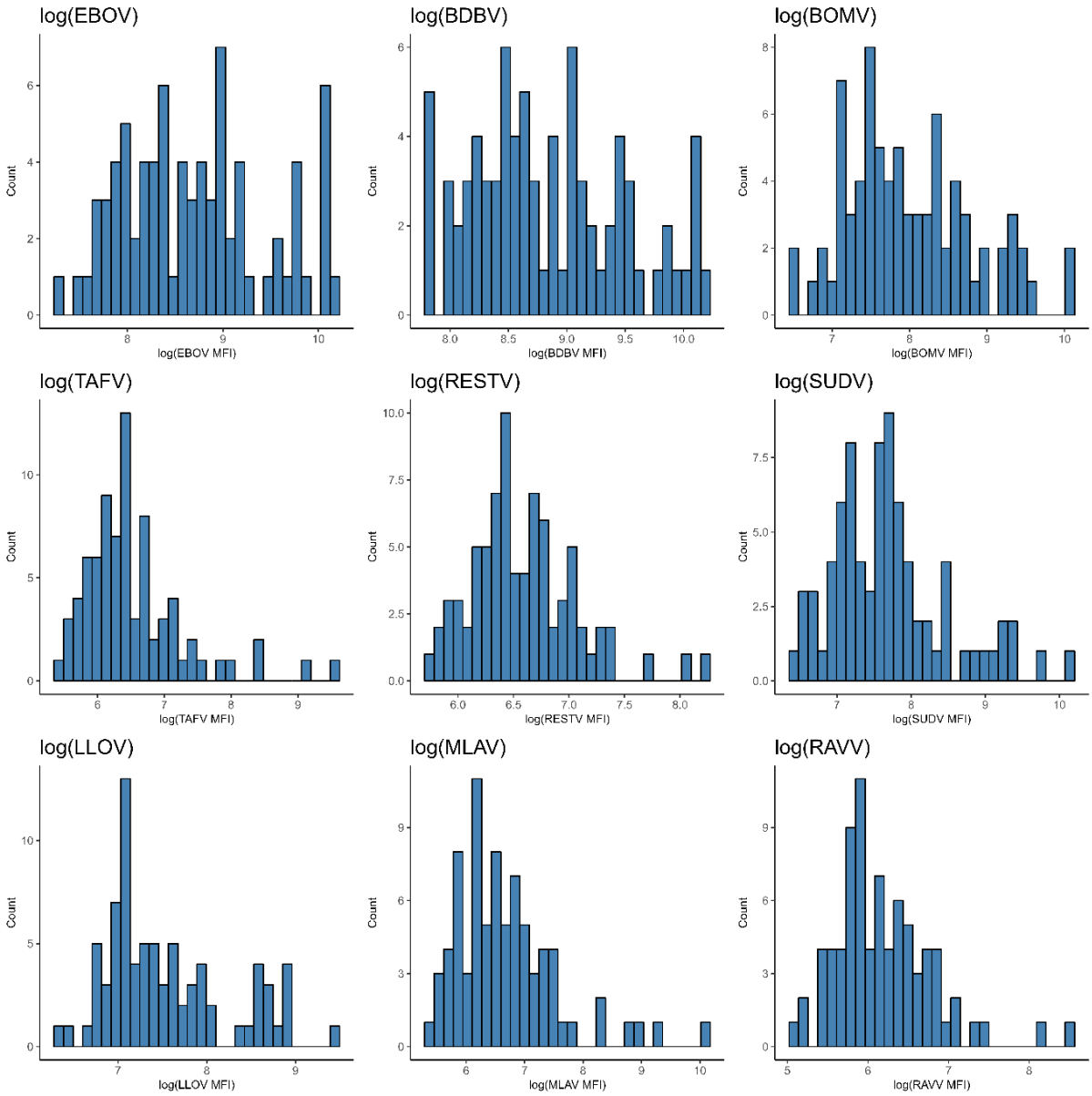


Figure 57 Anti-filovirus responses (log-transformed) amongst Ugandan farmers, 2017 to 2021.

IgG responses were measured by multiplex microsphere-based immunoassay (MMIA) in background subtracted median fluorescence units (MFI-bg) on the Luminex platform.

Logistic regression analysis of individual risk factors associated with filovirus clusters, Guinean WLHs 2017 and 2023

Logistic regression was utilised to examine the association between demographic and behavioural risk factors (from the extended 2023 questionnaire) and membership to filovirus clusters identified previously in *K*-means clustering (EBOV, BDBV, RESTV, MLAV, LLOV, TAFV) for WLHs in the 2023 cohort (Table 19).

Table 19 Outcome variables for logistic regression analysis, derived from *K*-means clustering analysis of Guinean wildlife hunter cohort 2023 (n=607).

Outcome*	Individuals within cluster n	Percentage of positive individuals % (n/N)
EBOV	86	14.2% (86/607)
BDBV	31	5.1% (31/607)
RESTV	0	0.0% (0/607)
MLAV	19	3.1% (19/607)
LLOV	8	1.3% (8/607)
TAFV	16	2.6% (16/607)

*SUDV and BOMV were excluded due to small sample sizes.

Sex was significantly associated with BDBV seropositivity, with the odds of being in the BDBV cluster 2.49 times higher amongst males (95% CI: 1.00–6.16, p = 0.049) compared to females. Nonhuman primate consumption was associated with higher odds of BDBV cluster seropositivity (OR = 3.49, 95% CI: 1.25–9.74, $p = 0.017$) (Table 21).

Occupation was significantly associated with MLAV cluster seropositivity (with increased odds amongst tradespersons compared to farmers (OR = 15.57, 95% CI: 2.76–87.80, $p = 0.002$)), however, interpretation was limited due to the small cell numbers.

Logistic regression was also performed to examine the association between demographic variables (from the abbreviated 2017 questionnaire) and *K*-means cluster membership from the combined 2017 and 2023 *K*-means clustering analysis, however, no significant associations were identified.

4.2.11. Influence of land cover patterns on exposure to zoonotic filoviruses in Guinean WLHs

Satellite-derived land-cover maps (Environmental Systems Research Institute, European Space Agency Sentinel-2) [324] of the study sites were used to extract measures of land cover and forest fragmentation (perimeter area ratio, shape-index and fractal dimension) from 2017 and 2023, which were examined for significance across varying spatial scales using a data-driven approach.

Forest loss and fragmentation was seen in satellite imagery over the study period. Multivariable logistic regression was then used to examine the association between environmental drivers and risk for each zoonotic virus (based on their *K*-means based antibody exposure profiles) and identified strong associations between landscape patterns and filovirus exposure. Models also examined individual risk-factors reported in the questionnaire, including age, sex, occupation and wildlife hunting, however these did not significantly improve the model.

Significant environmental variables were identified at various spatial scales for all antigens, with forest coverage and configuration (shape index, perimeter area ratios, fractal dimension index) found to be associated with EBOV, BDBV, TAFV, LLOV and MLAV reactivity. Differing landscape patterns were identified for each filovirus antigen, with EBOV exposure being negatively associated with tree coverage and forest fragmentation. Deforestation (within a 500 m radius of the village) and living in built areas were positively associated with BDBV seroreactivity. Reactivity to other filovirus antigens (TAFV, LLOV and MLAV) were associated with proximity to intact forest (5 – 10 km radius of the village) (Table 20).

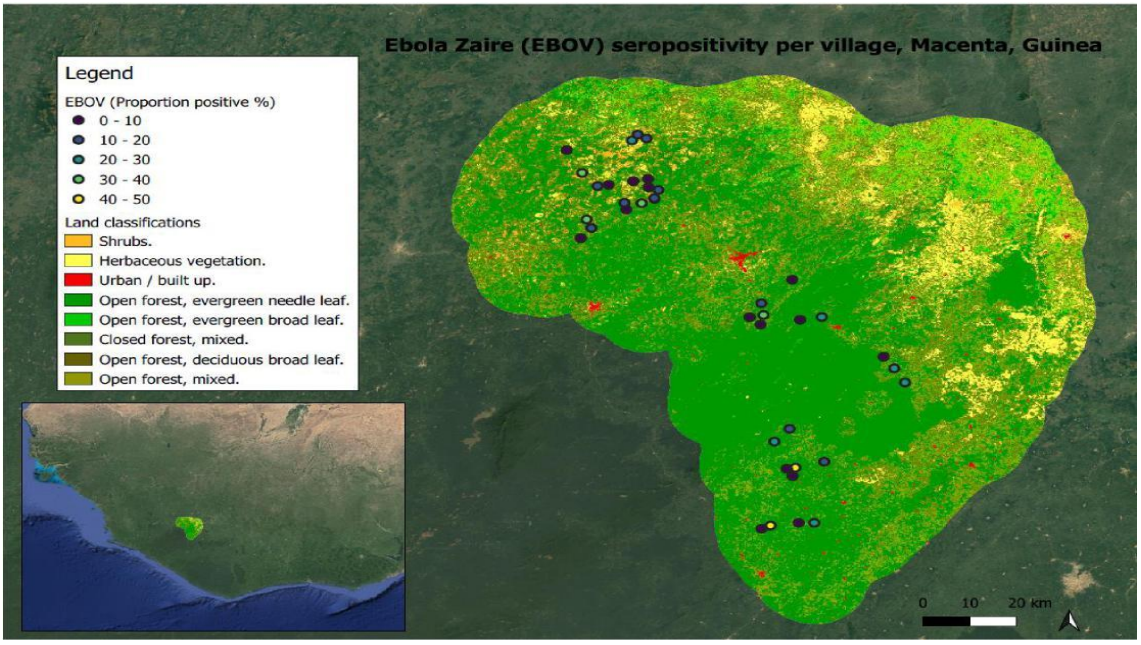


Figure 58 Landcover map of Forested Guinea, Republic of Guinea

Landcover classifications were derived from Environmental Systems Research Institute, European Space Agency Sentinel-2 satellite data, 2017. Villages with proportion of EBOV positivity (based on binary thresholds) are visualized. Figure created with QGIS 3.28.3.

Table 20 Significant associations between viral antigen exposure risk and environmental factors for wildlife hunters, 2017 and 2023 combined cohort

Viral antigen	Land cover type	Metric	Scale, m	Odds Ratio (95% CI)	p value
EBOV	Tree	Coverage (%)	2000	0.74 (0.59 – 0.93)	0.01
	Forest	Shape Index[1]	2000	0.82 (0.66 – 1.02)	0.07
	Forest	Perimeter Area Ratio[2]	10,000	0.86 (0.71 – 1.05)	0.13
BDBV	Built area	Coverage (%)	5000	3.29 (1.37 – 7.93)	0.01
	Forest	Shape Index[3]	500	1.37 (1.04 – 1.80)	0.02
TAFV	Forest	Fractal dimension	10,000	0.77 (0.62 – 0.96)	0.02
	Built area	Coverage (%)	5000	0.29 (0.09 – 0.91)	0.04
LLOV	Forest	Fractal dimension	5000	0.46 (0.22 – 0.95)	0.04
MLAV	Forest	Fractal dimension	10,000	0.55 (0.29 – 1.04)	0.07
	Trees	Coverage (%)	5000	4.31 (0.45 – 41.79)	0.21

1 Shape Index: Standardizes patch shape relative to a circle (most compact shape). A value of 1 represents a perfect circle; values >1 indicate elongated or irregular shapes. *Range: ≥1*-2. Perimeter-Area Ratio: Measure of the complexity of a forest patch's shape by comparing perimeter to area. Higher values indicate more irregular or fragmented shapes. *Range*: >0 (no fixed upper limit; increases with complexity). 3 Fractal dimension: Quantifies the complexity of a shape's boundary. Values closer to 1 indicate simple, smooth shapes; values approaching 2 reflect increasingly complex and irregular boundaries. Range: 1–2.

Logistic regression was then used to examine the association between environmental drivers and risk for each zoonotic virus (based on their *K*-means based antibody exposure profiles) amongst the 2023 WLH cohort only, which allowed for the examination of variables within the extended questionnaire, such as bat and NHP hunting. This identified significant associations between landscape patterns and filovirus exposure for BDBV, with NHP hunting found to be significantly positively associated with BDBV, retaining significance even in the multivariable model (Table 21).

Table 21 Univariable and multivariable logistic regression analysis of BDBV exposure in Guinean wildlife hunters (WLHs), 2023

Variable	Univariable regression Guinean WLHs 2023		Multivariable regression Guinean WLHs 2023	
	OR (95% CI)	*p*-value	aOR (95% CI)	*p*-value
Age	1.02 (0.99 – 1.05)	0.087	-	-
Sex	2.49 (1.00 – 6.16)	0.048	-	-
WLH	1.05 (0.91 – 1.10)	0.982	-	-
Perimeter area ratio (Forest) 2000 m	0.55 (0.35 – 0.86)	0.010	0.67 (0.41 – 1.09)	0.110
Built Area 10,000 m	3.14 (1.39 – 7.08)	0.010	2.34 (0.91 – 6.00)	0.080
Nonhuman primate hunting	3.50 (1.26 – 9.76)	0.017	5.03 (1.70 – 14.90)	0.004

OR = Odds Ratio, aOR = adjusted Odds ratio, CI = Confidence interval

4.3. Discussion

This chapter reports the detailed characterization of zoonotic filovirus spillover in a high-risk population of wildlife hunting communities residing within a rapidly deforesting area of Guinée forestière, Republic of Guinea in 2017 and 2023. The longitudinal nature of the surveillance, wherein 52.45% (268/511) of the 2017 cohort were resampled in 2023, allowed me to demonstrate the durability of the anti-EBOV antibody response in addition to ongoing seroconversion to other filoviruses within Forested Guinea. MMIA screening revealed increased seroreactivity to multiple filovirus species (EBOV, BDBV, TAFV, RESTV, MLAV, LLOV) within the WLH population when compared to multiple comparative cohorts, from urban settings within Guinea (Coyah, Guéckédou), Uganda, and the UK. While serosurveillance has historically been confounded by the cross-reactive antibody responses induced by EBOV infections [295], I utilized an unsupervised machine-learning clustering algorithm to identify groups of individuals with species-specific serological responses. Several of these individuals were shown to neutralize other filoviruses (BDBV, TAFV, LLOV) more strongly than EBOV in parallel pseudotyped virus neutralisation assays. Spatial and epidemiological investigations of these BDBV positive individuals identified village- and household-level clustering, furthering the case for true spillover. Further, an investigation of wildlife hunting practices identified a strong positive association between the consumption of NHPs and BDBV seropositivity. Finally, satellite-derived remote sensing data revealed unique environmental risk factors for the pathogens, illustrating differences in the potential pathways of exposure.

Serological screening of Guinean sera demonstrated a broad and durable B-cell mediated antibody response to EBOV, 10 years on from the 2013 – 2016 West African EVD epidemic, supporting previous observations of long-lived anti-EBOV IgG binding and neutralisation [220, 257] as well as orthoebolavirus species cross-reactivity [274] and cross-neutralisation [325]. The persistence of antibodies following infection is central to understanding long-term immunity and informing public health interventions, however, a clear consensus has yet to be reached. Previous studies on EVD survivors have hypothesised that the immune response generated during infection provides lifelong protection, with an early and robust antibody response strongly associated with EVD survival [220, 257, 326]. Less optimistically, a 2021 study of EVD survivors from Sierra Leone by Adaken *et al.* applied a pharmacodynamic model of antibody kinetics which, rather than following a simple exponential decay, followed a multistage trajectory characterized by an initial decay phase, restimulation, and subsequent secondary decay phase, with a 95% depletion of antibody levels within 0.5 – 2 years p.i. and an estimated half-life of 77-100 days [327]. A 2021 study of Guinean EVD survivors by Diallo *et al.* also observed an apparent antibody "wax-and-wane" (with overall decrease) in some individuals, but observed that the percentage probability of being seropositive for EBOV GP at 5 years p.i. was 76.17% (67.33 – 83.39) [292]. Based on the population average of my exponential decay models (which did not account for antigenic boosting), I estimated the EBOV-GP IgG antibody half-life to be 7.5 years, aligning more closely with studies reporting antibodies at 11 [328, 329] and even 40 years p.i. [257].

The high seroprevalence of anti-EBOV GP antibodies observed in the Guinean study population (6.9% (78/1129) based on a conservative (5 standard deviation) cut-off derived from the UKBD population) is comparable to estimates from nearby EVD-affected regions. For example, EBOV GP seropositivity was reported at 3.57% (95% CI: 1.55–6.92%, 8/224) in the general adult population of Meliandou village in Forested Guinea [277], 7.2% (63/878) in western Guinea [303], or 8.4% (95% CI: 7.0 – 10.0%, 107/1282) in neighbouring Sierra Leone [305]. The consistently high seroprevalence reported across these studies lends credence to the somewhat controversial notion of asymptomatic or paucisymptomatic EBOV infection. The increase in population-level seroreactivity across all antigens was potentially due to the increased number of freeze-thaw cycles in the 2017 WLH sera samples, compared to the 2023 samples.

In addition to EBOV, the MMIA detected significant immunoreactivity in Forested Guinea to multiple other zoonotic filoviruses of known and unknown human infectivity, including BDBV, TAFV, BOMV and LLOV. These findings are consistent with a 2022 multiplexed serosurvey conducted in non-epidemic western Guinea, which reported reactivity to SUDV-GP (16%), BDBV-GP (3.8%) and RESTV-GP (0.8%) and BOMV-GP (0.6%) [303]. This study identified higher reactivity to GP than to VP40 or NP, which some may interpret as evidence that seropositivity based on GP reactivity alone may overestimate seroprevalence and risk misattribution of species. However, given that GP—the sole

viral protein expressed on the virion surface—is the main target of the humoral response in EVD survivors [314, 325, 330], and that anti-GP antibodies decline less rapidly than anti-NP or anti-VP40 antibodies [292], it could equally be argued that using other target antigens may underestimate seroprevalence.

Ugandan immunoreactivity to multiple filoviruses was unsurprising given that Uganda has reported multiple outbreaks of viral haemorrhagic fevers, including the 2000 SUDV outbreak in Gulu district (14), the 2007 BDBV outbreak in Bundibugyo district [331], 2022 SUDV outbreak in Mubende district [332] and imported cases (n=3) during the 2019 EBOV outbreak in the DRC [333].

Similarly, while the single BDBV-seroreactive case detected in the UK blood donor cohort may appear unexpected, it is consistent with previous reports of low-level filovirus seroreactivity in non-endemic populations. For example, EBOV seropositivity of 2.1% (90% CI: 0.13 – 4.07%) was observed in blood donors from Lancaster, UK [334] and 0.85% (11/1288) seropositivity was reported in a heterogenous population sampled from Germany, 1972 – 1991 [335]. This sporadic apparent reactivity has been hypothesised to result from structural similarities between immunological epitopes, for example, a region of maximal structural superimposition identified between EBOV and measles morbillivirus NPs. While useful for comparing populations over time and space, these findings affirm the need for caution when interpreting the results of these serological assays at the individual level.

In terms of interpreting this reactivity, seropositivity was initially determined using thresholds calculated using two commonly employed approaches for multiplex bead-based immunoassays: (i) comparison with a presumed seronegative cohort (UKBDs) and (ii) finite mixture modelling [336]. Under this paradigm, higher MFI values reflect recent or repeated exposure to the relevant antigen. However, this interpretation is complicated by the heterotypic cross-reactivity of antibodies, and further hindered by the absence of PCR-confirmed international standards, absence of verified negative controls, and the lack of harmonized assay methodology.

Calculating a threshold based on population measures (mean and standard deviation) of the antibody distribution in the presumed seronegative cohort was unsuitable due to the differing immunological background between the Guinean and the UKBD populations. The use of a finite mixture model is theoretically able to produce assay-specific cut-off values based on a distribution of MFI values more closely resembling the true seronegative subpopulation. However, both methods utilize a binary classification system and thus are inherently susceptible to misclassification due to heterotypic cross-reactivity, as was demonstrated in the cohort of PCR-confirmed EBOV survivors in Chapter 3. Here, >40% of EBOV survivors were also co-positive for BDBV, BOMV, RESTV and SUDV. While we cannot categorically exclude the possibility that some EBOV survivors were also exposed to other filovirus antigens, this can be reasonably attributed to cross-reactivity over multiple infection.

For these reasons, an unsupervised machine-learning approach was utilized to partition the data into qualitatively different immunological or "exposure" profiles rather than using a binary endpoint to translate a continuous MFI. *K*-means clustering, a centroid-based algorithm developed for lower dimensional spaces, was selected based on the dimensionality and expected underlying structure of the data (regular, spherical clusters) [337]. Clustering methods, particularly those performed in high-dimensional space, may be susceptible to ultimately meaningless random chance interactions within complex biological systems. And in particular, the *K*-means algorithm depends heavily on the selection of the correct value for *k*. In order to mitigate this, we evaluated the results across a range of values for *k*, while cluster validation methods provided confidence in the biological relevance, stability and fitness of the cluster results. Indeed, the clustering results provided genuine biological insight, and in contrast to the initial examination of antibody distributions between the Guinean WLH and Ugandan cohort (which appeared similar), clustering analysis revealed multiple species-specific non-EBOV clusters unique to the WLH cohort. These results emphasize the value of serological testing against multiple antigens, particularly related pathogens that co-circulate in a population, in order to better characterize the true seroprevalence of each pathogen and their cross-reactive relationships.

Individuals highlighted by *K*-means clustering were down-selected for confirmatory and discriminatory testing by parallel PVNAs. While the virus neutralisation assay remains the gold standard for assessing the functionality of antibodies in blocking viral entry, it necessitates the use of live authentic virus and thus Biosafety Level-4 (BSL-4) containment. Pseudotyped viruses (PV)—chimeric particles consisting of a retroviral or vesicular stomatitis virus (VSV) nucleocapsid core within a lipid envelope bearing heterologous glycoproteins—offer an acceptable surrogate. In fact, PVNAs have been found to be more sensitive, with a lower limit of detection when it comes to discriminating samples with lower neutralising activity [338]. The appropriate selection of the core bears critical importance: while previous studies have reported better correlations between VSV backbones and authentic EBOV virus [224], the data presented in Chapter 3 informed the use of a lentiviral backbone for all filoviruses except MLAV.

Five individuals demonstrated higher neutralizing activity against BDBV than against EBOV-Makona virus. PVNAs were standardised to the extent possible (performed in parallel using identical protocols, controls, reagents, pseudoviral production methods and assay input titres), however, uncontrolled variables such as defective particle ratios, GP expression on plasma membranes etc. may have introduced variability between assays. There is also the remote possibility of cross-reactivity from a related pathogen inducing higher neutralizing titres against a non-infecting pathogen than the infecting one, possibly due to poor antigen quality or assay antigens being poorly matched to the circulating viruses. Even so, these findings provide serological evidence that these individuals were exposed to a virus more antigenically similar to BDBV than EBOV. Individual-level epidemiological data further support this hypothesis, as two of these individuals were marital partners residing in a village unaffected

by EBOV. Their spousal relationship increases the probability that both were infected with the same BDBV-like virus, rather each independently developing an atypical post-EBOV IgG response skewed towards cross-reactive epitopes. If the latter were true, and their polyclonal response primarily targeted highly-conserved structural features of the GP, it could be expected that these cross-reactive antibodies would recognise multiple members of the tested heterologous ebolavirus species, rather than being restricted to BDBV and EBOV. This hypothesis is further supported by spatial heterogeneity, with Maraou village, which was EBOV-unaffected, found to have significantly higher mean BDBV antibody response in 2017 and 2023. As a final thread of evidence, NHP hunting was found to be positively associated with anti-BDBV antibody responses in multivariable analysis, as was the case in the 2012 DRC BDBV outbreak, where many patients reported close contact with bushmeat [339].

Other putative zoonotic filovirus spillover events, such as TAFV virus, were also epidemiologically plausible, especially given the geographic proximity to the only known human case, which occurred following contact with a dead chimpanzee in neighbouring Côte d'Ivoire. While there was overlap of the NT50 95% confidence intervals, 5 individuals who showed specific IgG binding against TAFV and minimal binding against EBOV also neutralized TAFV more strongly. Similar to BDBV, TAFV was found in 2023 to be spatially clustered in a village which was not affected by EBOV in 2013 – 2016.

Other serological signatures of potential exposure were identified, including responses to viruses of unknown human infectivity and pathogenicity, namely BOMV, which was recovered from free-tailed bats in neighbouring Sierra Leone; LLOV and MLAV. Given our current understanding of these viruses and their geographic distribution, I hypothesise that the binding seen against the latter viral antigens in the Guinean wildlife hunting population is the result of cross-reactivity following infection with a related zoonotic filovirus (known or novel).

While BOMV is known to circulate in bat reservoirs in the area, its spillover potential remains unknown. While wild-type BOMV GP does not efficiently mediate viral entry into human cells under experimental conditions, minimal mutations in the receptor-binding domain were required to improve viral entry and enhance binding to human NPC1, suggesting some potential for host-switching [340]. Pseudotyped virus neutralisation assays showed similarly potent neutralisation of both BOMV GP and EBOV GP pseudotyped viruses, which was a surprising finding given the lack of anti-EBOV binding antibodies identified by the MMIA screen. This may be due to differences in the presentation, availability or glycosylation of conformational epitopes on the soluble trimeric recombinant glycoprotein ectodomains conjugated to beads as compared to GPs decorating the envelope of a lentiviral particles. Taken together, these results may suggest infection with a virus antigenically equidistant, but distinct, from both EBOV and BOMV.

This chapter presents evidence of possible seroconversion to LLOV or, more likely, a related virus occurring between 2017 and 2023, highlighting the value of longitudinal surveillance. Unlike other

filoviruses, LLOV is not known to be endemic to the region, and only 1/8 individuals were found to exhibit more potent neutralisation of LLOV (compared to EBOV). Taken together, this provides initial evidence of the circulation of an antigenically related cuevavirus in the region. The overall seroreactivity seen against multiple filovirus species in this population is consistent with other studies which identified evidence of EBOV circulation from Forested Guinea prior to the 2013 – 2016 West African EVD epidemic [301], implying ongoing spillover.

Binding antibodies against Měnglà virus were identified in 0.7% (8/1129) of the Guinean cohort, however, no samples in the MLAV cluster neutralized either VSV-MLAV or VSV-ZEBOV, which may indicate infection with a divergent virus which is antigenically related enough for binding but not cross-neutralisation.

Wildlife hunting practices were investigated through a 123-item questionnaire (administered by Dr. Joseph Akoi Bore and Zézé Onivogui in Toma and French) which represents the most detailed investigation of wildlife hunting activities in the region to date. While the self-reported nature of the questionnaire may lead to biases (such as social desirability bias in the normative direction), we attempted to mitigate this through the use of local researchers who provided an anonymous and value-neutral environment for interviewees. The survey clarified the ubiquity (90% of respondents), frequency (median of 7 days per month), seasonality and nature (spanning activities from hunting, to butchering and consumption) of wildlife exposure within our purposively sampled study population. While majority of wildlife hunting was reported as year-round, bat hunting and exposure were found to be highly seasonal, with 92% of respondents (122/133) reporting hunting at the start of the dry season only. Given the spatiotemporally variable nature of filovirus shedding (e.g., seasonal pulses of Marburg virus circulation during *Rousettus aegyptiacus* juvenile breeding seasons [18]), a high-resolution understanding of human interactions with wildlife reservoirs provides critical insight into windows of risk for zoonotic transmission. Future research directions could focus on fine-scale human movement and animal tracking to better quantify and characterize exposure at the human-animal interface.

Pathogen exposure occurs to varying extents across the spectrum of activities, from hunting to handling, butchering and consumption of prepared product (cooked, smoked, dried, cured). The relative risks of these activities are important to characterize, as some activities (such as carcass butchering) may constitute greater risk as they involve exposure to a comprehensive range of fresh tissue and bodily fluid types. Indeed, studies investigating simian foamy virus (SFV) infection in the Democratic Republic of Congo found increased risk of SDV infection in persons preparing NHPs for consumption or carrying NHP carcasses from the forest, though there was insufficient evidence for an elevated risk of SFV infection from NHP hunting after controlling for age and gender in multivariable models. Interestingly however, they also found that low exposure activities, such as daily entrance into the

forest, placed persons at elevated risk for SFV infection, which they speculated could be due to environmental exposure to urine and faeces [341].

Behavioural risk factors were investigated using univariable and multivariable statistical models, with different classifications of the serological data as outcome variables. When examining single antigen reactivity as a continuous variable (log (MFI)) in a linear regression model, male sex, wildlife hunting, exposure to wildlife hunting (i.e., including close contacts of WLHs), bat consumption and NHP consumption were all found to be significantly associated with various filoviruses. While this approach allowed us to examine all antigens, it did not adjust for cross-reactivity, and therefore may predominantly reflect the risk factors for EBOV infection. Further, while these models allow us to assess the direction and statistical significance of these predictor variables, it is difficult to interpret the clinical significance of the beta (which translates to a unit increase or decrease in log (MFI)). It is for this reason that we chose to assess the risk factor with logistic regression models. While male sex and wildlife hunting lost significance, importantly, NHP consumption was found to be strongly associated with increased BDBV reactivity in both univariable and multivariable models, revealing a potentially tractable exposure pathway. While it was initially hypothesized that male sex would be associated with increased filovirus reactivity, due to the predominance of men in wildlife hunting, our questionnaires revealed that men and women were ubiquitously exposed to wildlife carcasses during the butchering and cooking process.

Given the spatial heterogeneity of the data, I examined the role of local land-use change on zoonotic spillover. Varying associations within landscape factors are potentially indicative of differing transmission pathways. For example, EBOV exposure was negatively associated with tree coverage and forest fragmentation, potentially reflecting the predominance of human-to-human transmission over zoonotic spillover pathways. BDBV, pathogen also noted for ongoing nonzoonotic transmission, was associated with living in built areas with very proximal deforestation (within 500 m), potentially reflecting the risk of encroachment into forest. By contrast, other filovirus pathogens (TAFV, LLOV, MLAV) were associated with areas near larger patches of intact forest, potentially reflecting exposure which occurs during hunting (where WLHs may move deeper into the forest) as opposed to peridomestic transmission at forest-village edges. Analyses were limited by the spatial resolution of the data (collected at the village level), and further investigation of this hypothesized transmission pathway through extensive population-based surveys and individual GPS tracking would better characterise how the interaction of hunting behaviours and the local environment may drive risk. Together, this highlights the potential role of local movements and habitat fragmentation in driving these spillover risks. Conservation in this context may protect local communities by serving as an ecological countermeasure against pathogen spillover.

A major limitation in the study design was the targeted sampling of Guinean hunting populations. While this may increase probability of detecting zoonotic virus exposures, population-based surveys would be needed to assess seroprevalence and wider exposure risks. Exposure to wildlife meat was ubiquitous amongst the Guinean study population, which severely limited my ability to examine associations between wildlife meat and virus exposure, independent of confounders such as socioeconomic status and remoteness. Despite this, differences in the relative risk posed by the consumption of different animal species (e.g., NHPs, bats) were identified, likely reflecting the wildlife reservoirs or intermediate hosts of these pathogens. Further, overall population-level differences could still be seen between hunters and their close contacts, potentially highlighting the additional risks of increased time in the forest or exposure to fresh bodily fluids.

Unfortunately, due to our age-based exclusion criteria, early-life exposure could not be evaluated, despite documented wildlife hunting practices (rodents) amongst children [342]. The value of such data is highlighted by Hounmenou *et al.* who identified anti-EBOV antibodies in children from rural western Guinea born after the 2013 – 2016 West African EVD epidemic, which are unlikely to be maternally derived, given their age [303]. In future, higher resolution longitudinal measurements over a wider age range could allow for model-based estimates of seroconversion rates or a force of infection for endemic pathogens, and more accurate modelling of antibody decay.

As discussed above, attempts to classify villages as either affected or unaffected by the 2013 – 2016 West African EVD epidemic will be biased by both underreporting and misdiagnosis of historical EBOV cases, due to social stigma, lack of access to healthcare facilities, and the endemicity of malaria and typhoid fever. Further, participant medical history (i.e., prior EBOV infection) was not available.

4.4. Appendix

4.4.1. Methodology of literature rapid review: Summary of published orthoebolavirus seroprevalence studies conducted in West Africa, 1978 – 2025

Review design and protocol

I conducted a rapid literature review to synthesize evidence on orthoebolavirus seroprevalence in West Africa from 1 January 1978 to 13 August 2025.

Eligibility criteria

Population: Humans residing in West African countries (Benin, Burkina Faso, Cape Verde, Côte d'Ivoire, Gambia, Ghana, Guinea, Guinea-Bissau, Liberia, Mali, Mauritania, Niger, Nigeria, Senegal, Sierra Leone, Togo) and Cameroon sampled in any setting (community, healthcare, occupational risk groups, outbreak investigations).

Exposure/Context: Studies conducted in outbreak and non-outbreak contexts, including general population samples, asymptomatic contacts, individuals with fever of unknown origin (FUO), and healthcare or high-risk workers.

Outcomes: Primary outcome was seroprevalence of antibodies against any *Orthoebolavirus* species (Ebola virus (EBOV), Sudan virus (SUDV), Bundibugyo virus (BDBV), Taï Forest virus (TAFV), Reston virus (RESTV), Bombali virus (BOMV)) measured by any serological assay. Where reported, I extracted assay, antigen targets (e.g., GP, NP, VP40), assay cut-offs, and confirmatory/neutralisation results.

Study designs: Cross-sectional serosurveys and cohort studies reporting point or period seroprevalence. I excluded case reports/series without denominator data, studies exclusively in animals, assay development papers without population estimates, challenge studies, and vaccine immunogenicity trials.

Time and language: Publications from 1978–2025 in English or French. Conference abstracts were included if they reported sufficient methods and numerators/denominators.

Information sources

I searched MEDLINE (via PubMed), Embase, Web of Science Core Collection, and Scopus. Reference lists of included studies and relevant reviews were hand-searched. Grey literature was limited to WHO/Ministries of Health technical reports when methods and denominators were available.

Search strategy

The search combined controlled vocabulary and free-text terms for orthoebolaviruses and serology, filtered to West Africa. An example PubMed string was: (ebolavirus OR ebola OR "Zaire ebolavirus" OR EBOV OR SUDV OR BDBV OR "Bundibugyo" OR "Taï Forest" OR TAFV OR RESTV OR BOMV) AND (seroprevalen* OR serosurv* OR serolog* OR antibody OR IgG OR IgM).

No study-design filters were applied.

Study selection

Records were de-duplicated (EndNote) and screened for eligibility.

Data extraction

Extraction was performed by one reviewer. A standardized form captured: bibliographic details; country/setting; outbreak context; sampling year(s); assay platform (IF, ELISA, MMIA, Luminex, rapid tests, neutralization), antigen targets (GP, GP-m, NP, VP40, whole virions, whole-virus lysate); proportion seropositive (numerator/denominator), and 95% confidence intervals when provided or calculable.

Data synthesis

I summarised a narrative synthesis structured by country, period (pre-2013 vs. 2013–2016 outbreak vs. post-2016), population (general community vs. contacts vs. high-risk/occupational vs. symptomatic FUO), and assay type/antigen.

4.4.2. Anti-filovirus antibody response histograms fitted with a Gaussian mixture model

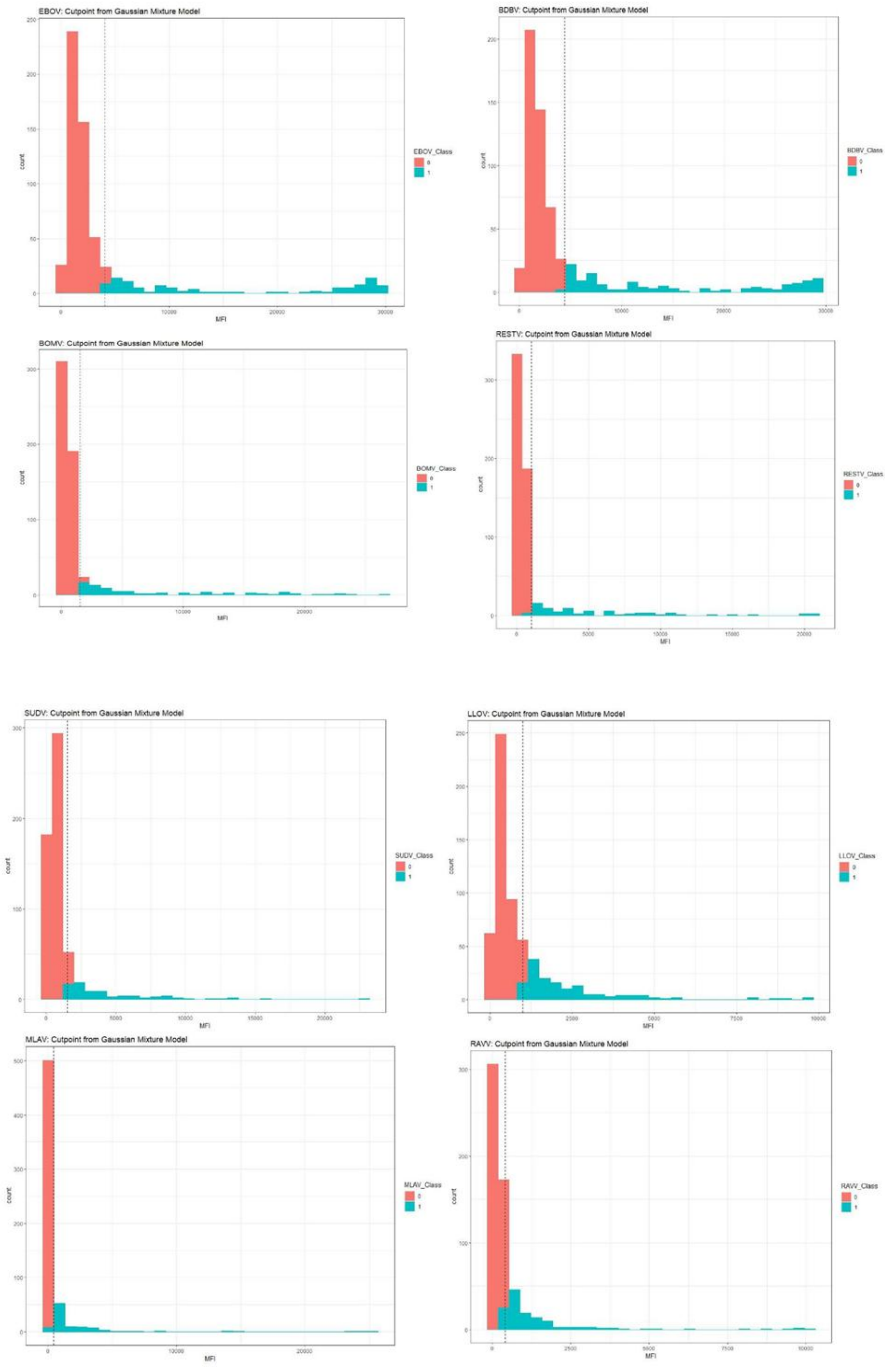


Figure 59 Anti-filovirus antibody response histograms fitted with a Gaussian mixture model

with 2 components reflecting the seropositive (class=1) and seronegative (class=0) subpopulations and probabilistic serological cut-point (indicated by the dotted line).

4.4.3. Antibody decay rates for non-EBOV filoviruses in WLHs, Forested Guinea

Table 22 Antibody decay rates and half-lives of filovirus responses observed in Guinean wildlife hunters (WLHs), 2017 to 2023

Antigen	Mean decay rate (per year)	Mean half-life (years)	Individuals with negative model slopes (n)	Percentage of individuals with negative model slopes % (n/N)
BDBV	0.12	5.67	39	16.0 (39/244)
BOMV	0.17	5.10	24	9.6 (24/250)
TAFV	0.20	3.46	166	66.7 (166/249)
RESTV	0.13	5.42	127	52.0 (127/244)
SUDV	0.14	5.01	49	19.3 (49/254)
LLOV	0.14	4.99	35	14.1 (35/249)
MLAV	0.16	4.40	32	12.9 (32/249)
RAVV	0.16	4.43	48	18.9 (48/254)

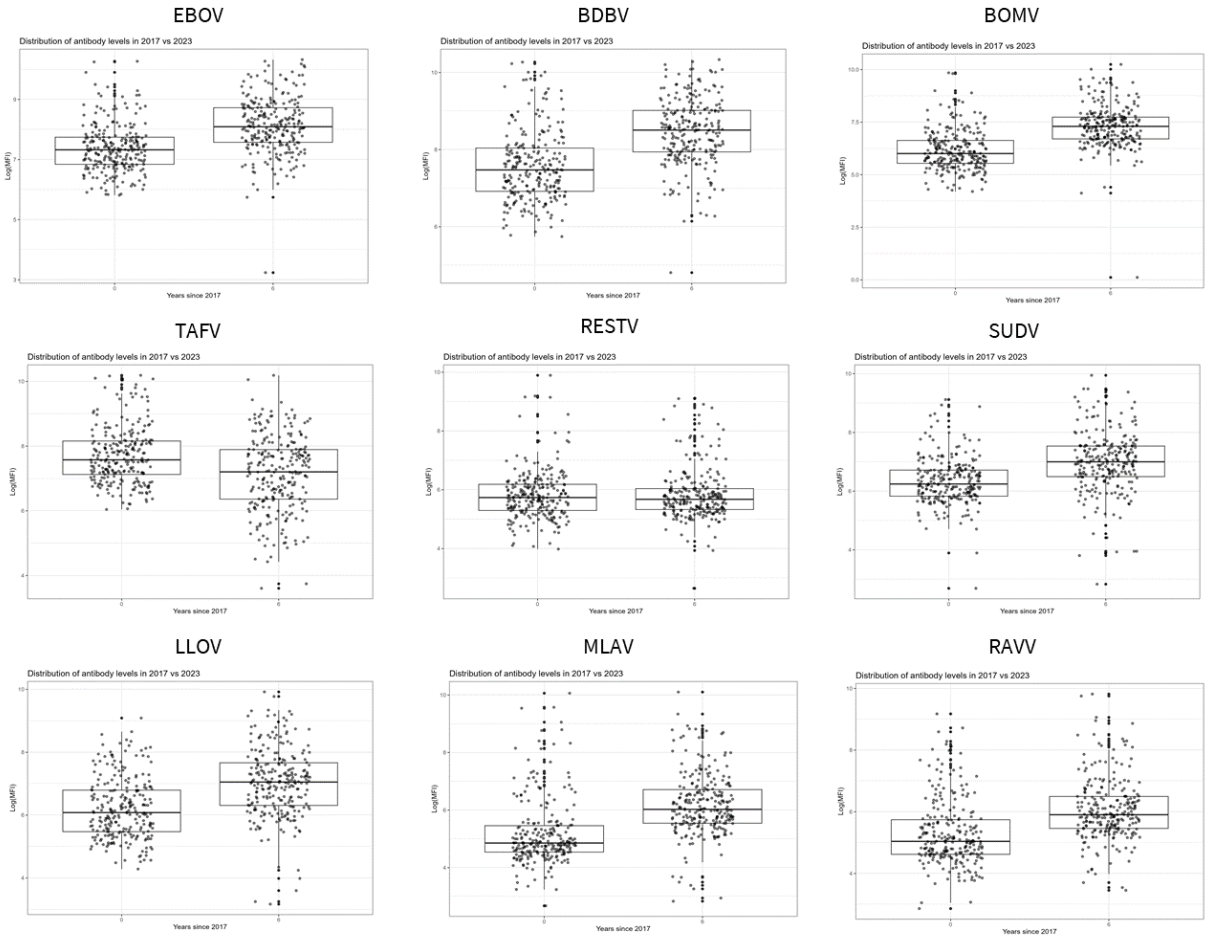


Figure 60 Anti-filovirus glycoprotein IgG distributions (log (MFI) among Guinean wildlife hunters in 2017 compared to 2023. IgG responses measured by multiplex microsphere-based immunoassay (MMIA) in background subtracted median fluorescence units (MFI-bg) on the Luminex platform.

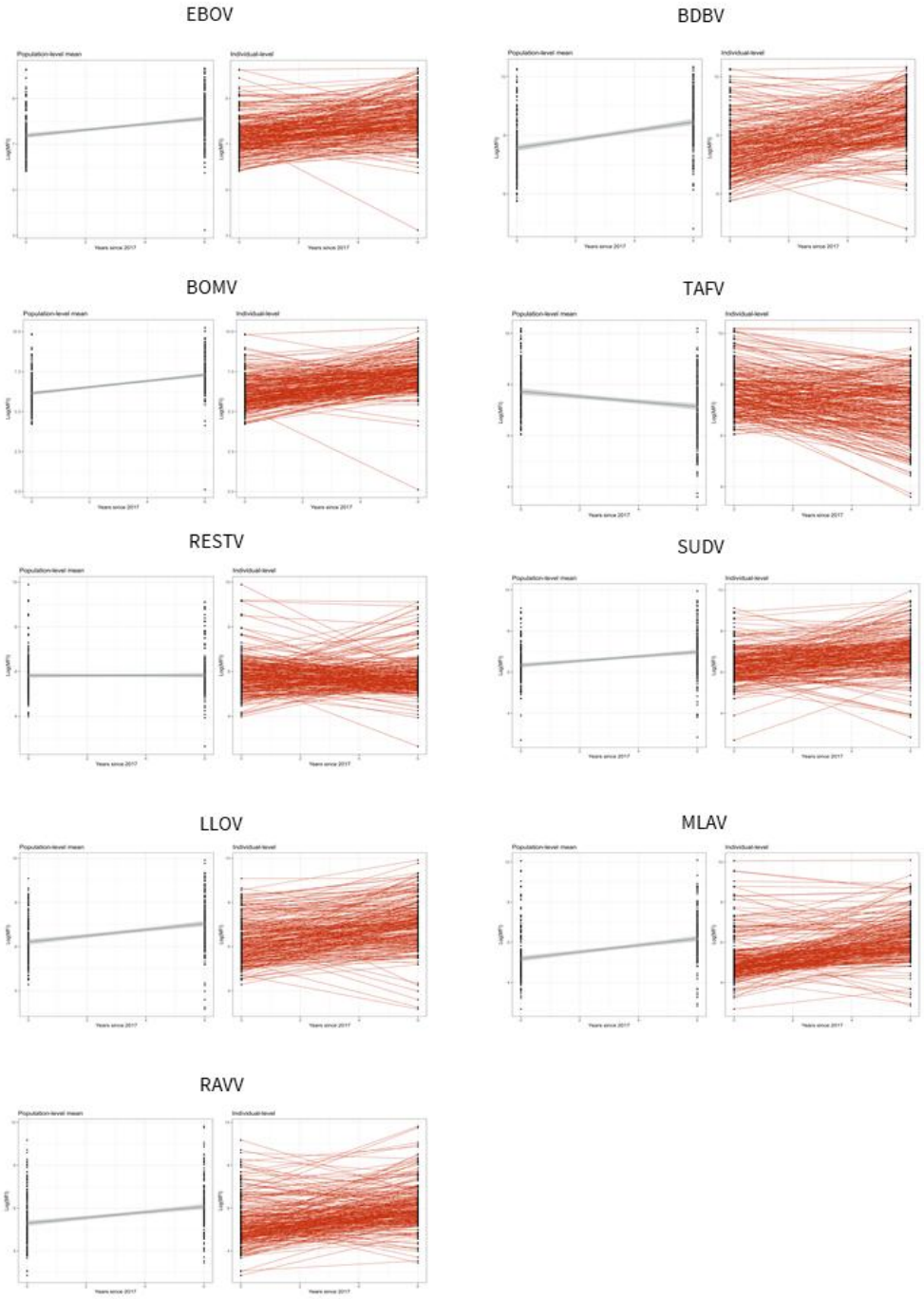


Figure 61 Individual anti-filovirus glycoprotein IgG responses of Guinean wildlife hunters in 2017 and 2023. IgG responses measured by multiplex microsphere-based immunoassay (MMIA) in background subtracted median fluorescence units (MFI-bg) on the Luminex platform.

4.4.4. Population-level reactivity to filovirus antigens amongst WLHs and close contacts in Forested Guinea

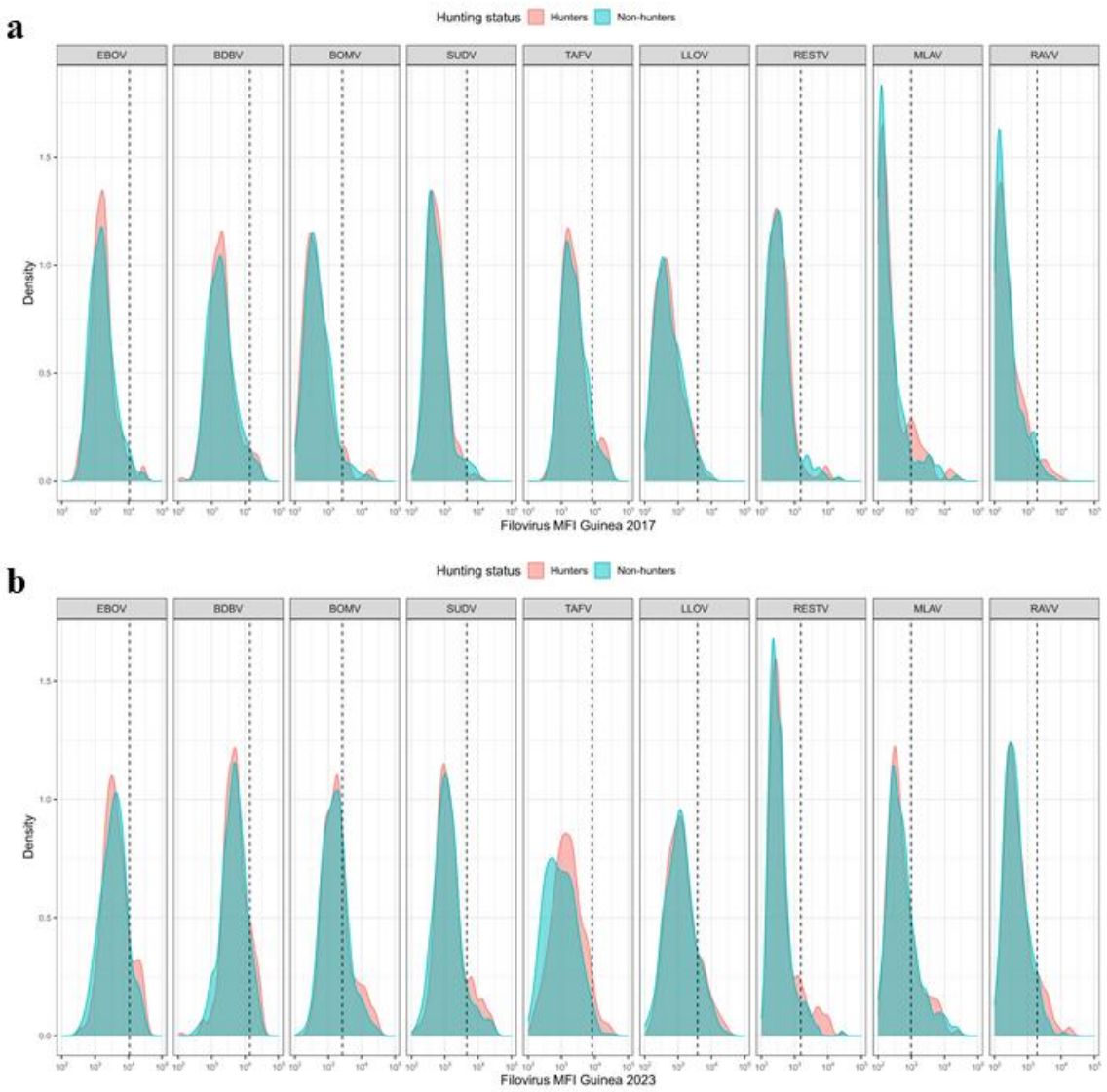


Figure 62 Anti-filovirus Glycoprotein IgG distributions among Guinean wildlife hunter (WLH) 2017 cohort (a) and 2023 cohort (b) in WLHs compared to non-hunters. IgG responses measured by multiplex microsphere-based immunoassay (MMIA) in background subtracted median fluorescence units (MFI-bg) on the Luminex platform. Dashed vertical lines mark seropositivity cut-offs based on the presumed unexposed non-endemic cohort (UK blood donor) by calculating five standard deviations above the background subtracted (MFI-bg) mean.

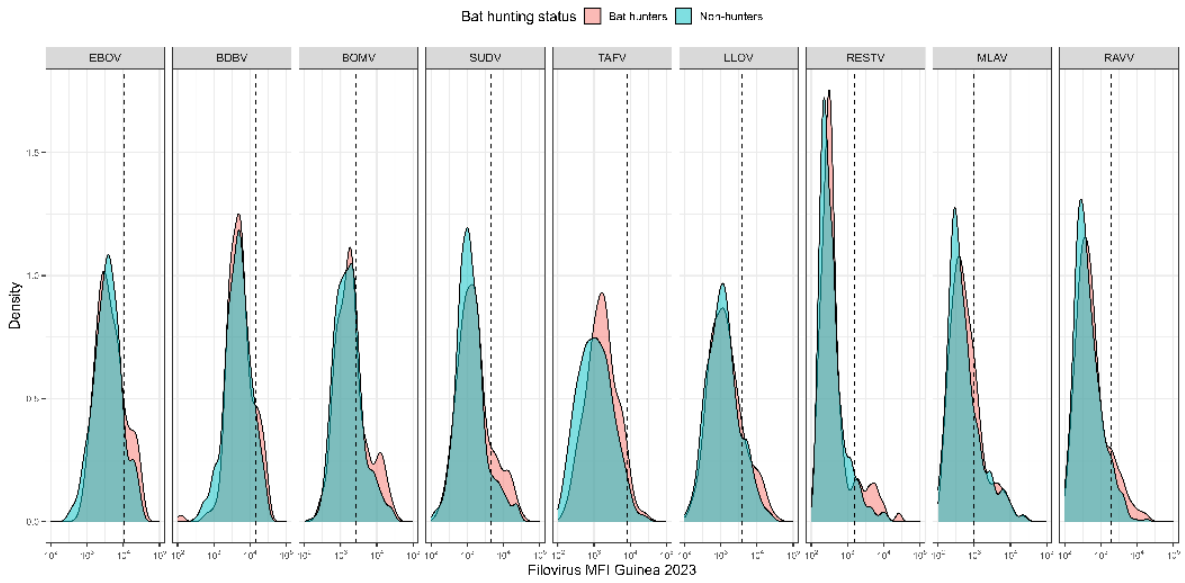


Figure 63 Anti-filovirus glycoprotein IgG distributions among Guinean wildlife hunter (WLH) 2023 cohort (n=648) bat hunters compared to non-hunters. IgG responses measured by multiplex microsphere-based immunoassay (MMIA) in background subtracted median fluorescence units (MFI-bg) on the Luminex platform. Dashed vertical lines mark seropositivity cut-offs based on the presumed unexposed non-endemic cohort (UK blood donor) by calculating five standard deviations above the background subtracted (MFI-bg) mean.

4.4.5. Linear regression analysis of risk factors associated with individual antigens, Guinean WLH cohort 2023

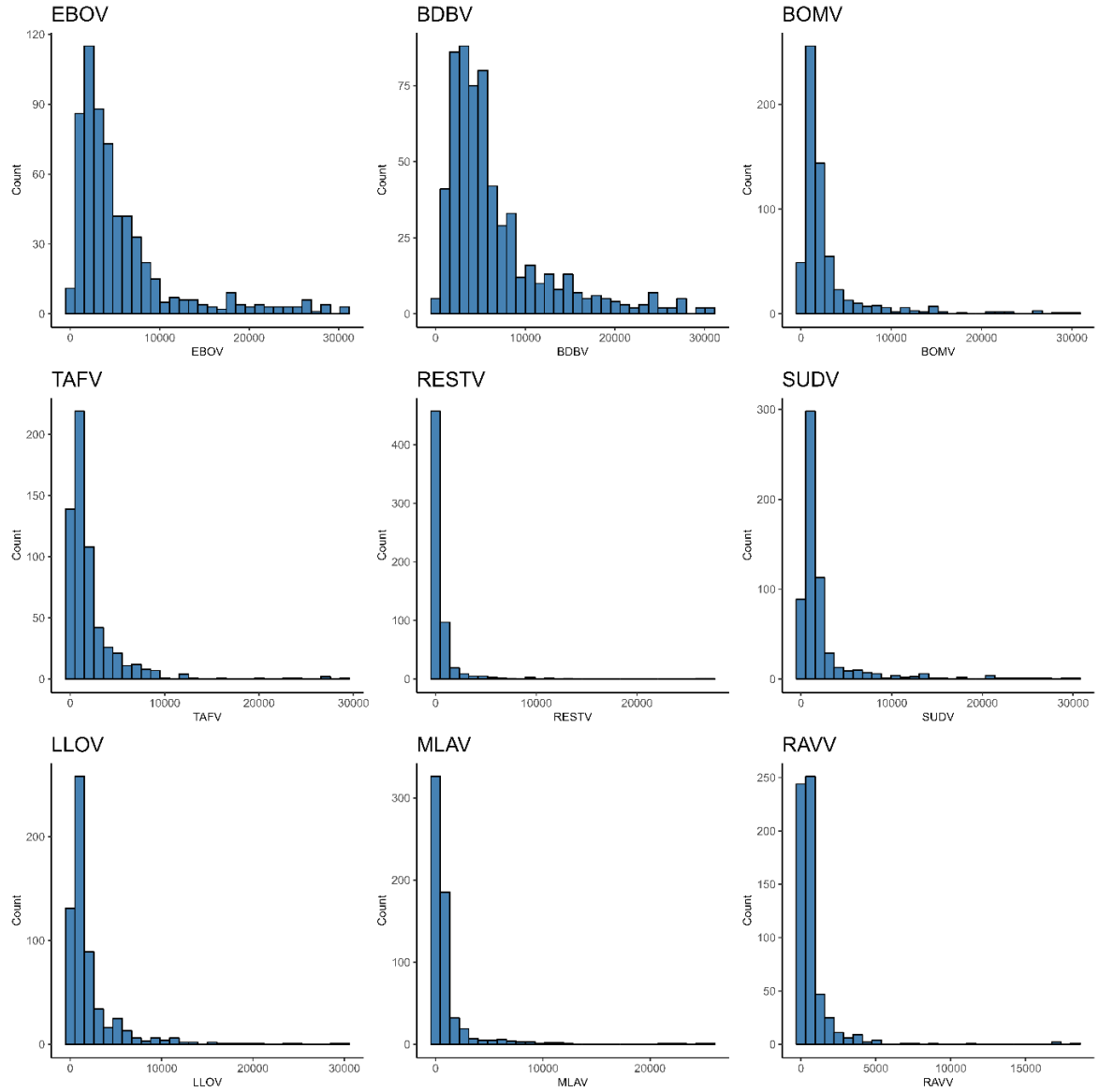


Figure 64 Anti-filovirus responses amongst Guinean WLHs 2023. IgG responses were measured by multiplex microsphere-based immunoassay (MMIA) in background subtracted median fluorescence units (MFI-bg) on the Luminex platform.

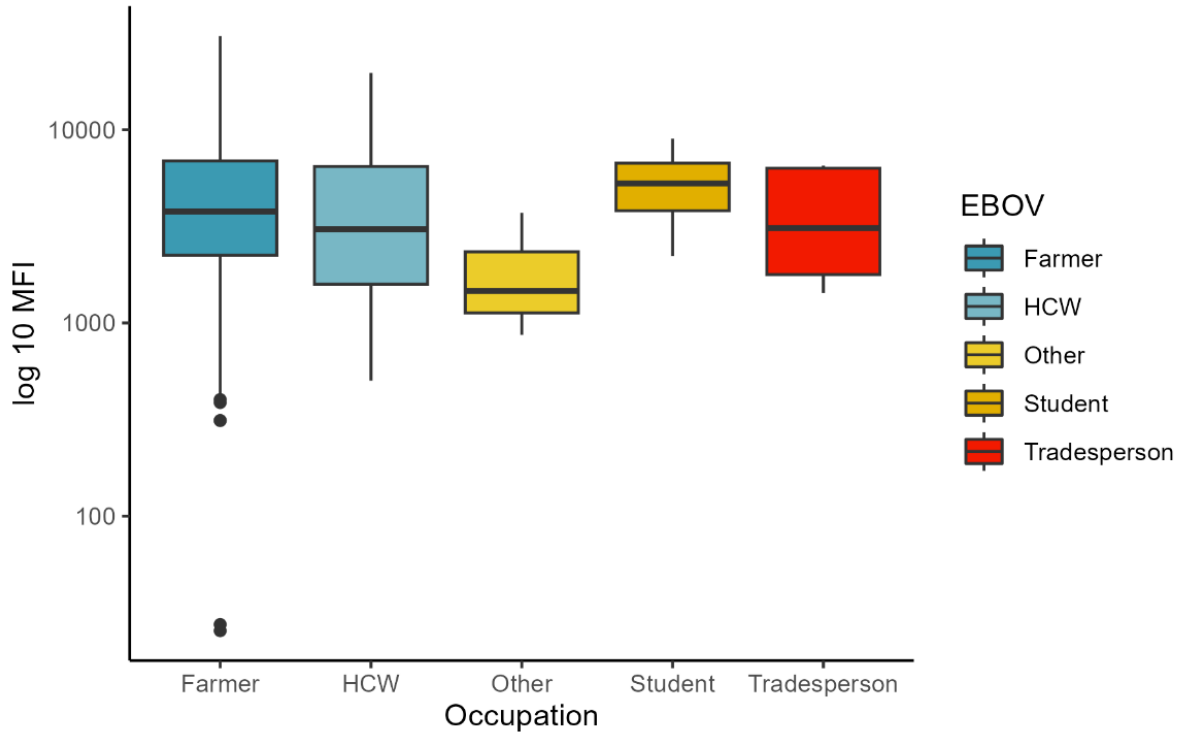


Figure 65 Anti-Ebola virus glycoprotein antibody responses by occupation, Guinean wildlife hunters (WLHs), 2023. IgG responses measured by multiplex microsphere-based immunoassay (MMIA) in median fluorescence units (MFI) on the Luminex platform.

Chapter 5

Emerging viral surveillance in wildlife workers, Eastern Australia

5.1. Introduction

5.1.1. Paramyxovirus spillover and detection in eastern Australia

5.1.1.1. Human emergence of three novel zoonotic viruses in Australia 1994-1997

The east coast of Australia has been the site of multiple zoonotic spillover events and novel virus isolations, consistently implicating its urban and periurban colonies of *Pteropus* species fruit bats (flying foxes). Between 1994 and 1997, the unprecedented emergence of 3 novel zoonotic viruses, all isolated from a single host genus, brought attention to the significance of paramyxoviruses and their reservoir hosts to the region.

5.1.1.1.1. Hendra virus (HeV) in 1994

Most notable of these is the highly pathogenic Hendra virus (HeV), which first emerged in 1994 in Brisbane, Queensland (QLD), following an outbreak of acute equine respiratory disease that resulted in the deaths of 14 horses and 1 human [343]. Since then, HeV has continued to cause outbreaks, with an overall human CFR of 57% across 55 reported events involving 108 equine cases, 7 human cases and 4 human deaths.

Early seroepidemiological investigations of wild and domestic animals (native terrestrial wildlife, rodents, cattle, dogs and cats) were initiated in search of the viral reservoir, concluding with the isolation of HeV and detection of antibodies in all 4 species of flying foxes found in mainland Australia [344-346]. Seroprevalences reported in pteropids have ranged from 25% to 64% [346-348] with differences

in seropositivity and virus excretion observed between different species (with *P. alecto* identified as being particularly epidemiologically important in infection dynamics).

With respect to spillover, interestingly, all human infections have resulted from contact with infected horses, and there is no evidence to date of direct flying fox to human transmission. In the only published serological survey of Australian bat carers, 128 carers were found to be HeV antibody-negative by ELISA, including a carer who received a deep puncture wound from a HeV antibody-positive bat [349].

The precise mechanism and route of transmission from natural hosts (flying foxes) to spillover hosts (horses) remains unknown, however, investigations of natural settings demonstrate HeV excretion in pteropid bat urine [350], and experimental infections indicate horses are susceptible to via oronasal exposure [351].

5.1.1.1.2. Australian bat lyssavirus (ABLV) in 1996

Australian bat lyssavirus (ABLV), a virus antigenically and genetically similar to classical rabies virus, was first isolated in 1996 from a Black flying fox (*P. alecto*) in northern New South Wales (NSW) during active surveillance catalysed by the discovery of HeV. Since then, ABLV has been detected in all 4 mainland species of flying fox and multiple species of microbat, including the yellow-bellied sheath-tailed bat (*Saccolaimus flaviventris*). Unlike the other described viruses, which are believed to circulate asymptomatically in bats, ABLV infection can cause a nonspecific, nonsuppurative meningoencephalitis, presenting clinically as depression and paralysis [352].

The prevalence of ABLV, as detected by fluorescent antibody test, in 366 sick, injured, or orphaned bats in southern QLD was 6% [353]. Importantly for wildlife carers, such bats have a significantly higher crude prevalence of ABLV infection (p <0.001) compared to healthy wild-caught or captive bats [353]. To date, retrospective case investigation studies have found no evidence of ABLV infection in domestic animal species [353].

Direct transmission from bats to humans has been recognised 4 times, each resulting in a fatal encephalitis resembling classical rabies. Of these infections, 2 occurred in bat carers, including a 39-year-old scratched by a yellow-bellied sheath tailed bat [11] and a 27-year-old woman bitten by a flying fox [12].

The discovery of ABLV triggered a large national public health campaign which sought to raise public awareness of the risks posed by bats, particularly in south-east QLD, where large colonies of bats inhabit suburban areas. Vaccine protection trials in mice conducted by the US Centers for Disease Control and Prevention (CDC) demonstrated that the classical rabies vaccine elicited protective immunity, supporting the policy decision to use the human diploid cell vaccine (HDCV) for human ABLV prophylaxis [354]. Pre-exposure vaccination against rabies and regular (biannual) antibody titre checks

are recommended for individuals with frequent bat contact, particularly in high-risk occupations such as wildlife carers and veterinarians. Further, postexposure treatment (PET), consisting of vaccination and potentially human rabies immunoglobulin (HRIG), is offered to individuals following potential exposure (defined as a bat bite, scratch, or percutaneous or permucosal exposure to bat saliva or neural tissue), unless ABLV infection can be ruled out in the animal. In a study of individuals reporting ABLV exposure to public health units in southern QLD between 1996-1999, voluntary animal handlers accounted for 39% of reports, their family members for 12%, professional animal handlers for 14%, and community members for 35%, highlighting the importance of the volunteer caring community as an interface [353].

In 1997, QLD introduced mandatory surrender of any bat involved in a potential human exposure for post-mortem ABLV testing. Notifications of ABLV exposure subsequently declined, and anecdotal evidence suggests that underreporting may occur due to reluctance among wildlife carers to surrender bats for culling [353].

5.1.1.1.3. Menangle virus (MenV) in 1997

Menangle virus (MenV) was first identified in 1997 as the causative pathogen of a severe reproductive disease outbreak in a commercial piggery in NSW [355]. Two piggery workers with high-level exposure developed acute influenza-like illness and rashes, and were later shown to have neutralising antibodies [355].

Post-outbreak investigations into the reservoir identified a large breeding colony of grey-headed and little red fruit bats 200 m from the affected piggery, prompting a serological survey which identified neutralising antibodies in 42/125 sera samples from nearby colonies (grey-headed, black and spectacled flying foxes), highlighting them as a likely reservoir [356]. In 2012, MenPV was isolated from black flying fox urine, and found to have a nucleotide sequence 94% identical to the pig isolate, providing further evidence of a bat origin [357]. As with HeV, the mechanism or route of transmission from bats to the spillover host (in this case, pigs) remains unknown.

5.1.1.2. Virological discovery of novel viruses in *Pteropus* species in Eastern Australia: Cedar virus (CedV), Yeppoon virus (YepV), Grove virus (GroV)

The discovery of HeV spurred ongoing investigations into viral ecology, genetic diversity and infection dynamics across multiple *Pteropus* bat colonies in eastern Australia. The virological investigations led

to the isolation of multiple novel paramyxoviruses from pteropid bat urine, including Cedar virus (CedV) [163], Yeppoon virus (YepV) [358] and Grove virus (GroV) [358].

CedV, despite genetic and structural similarities to HeV, is considered the only non-pathogenic henipavirus [359], having been shown to infect but not cause disease in several experimental animal models, including ferrets [163], guinea pigs, Syrian hamsters [168] and Type I IFN Receptor Knock-out (IFNAR-KO) mice [360]. As described in the introduction, this attenuation has been attributed to the lack of key virulence factors and thus its inability to counter the host type I IFN response. This property has been exploited for its use as a low-containment experimental surrogate for more virulent henipaviruses such as HeV and Nipah virus (NiV) [359].

Our current understanding is that CedV is localised to Australia, circulating in all 4 mainland species of the pteropid fruit bat at an estimated seroprevalence (obtained following virus neutralisation tests) of 26.6%, though temporal variation in antibody levels suggest this may wax and wane on a seasonal basis [361].

To date, there is no empirical evidence of CedV zoonosis, though it has been shown to infect human-derived (HeLa and HEK293-T) cell lines in vitro [163]. While CedV-reactive antibodies have recently been detected in human populations in Cambodia, these have been cross-reactive to multiple related henipaviruses, and thus are thought to more likely represent exposure to an antigenically related paramyxovirus [362]. These findings highlight how both the zoonotic potential and true geographic distribution of these viruses remain largely uncharacterized.

The zoonotic potential of the latter viruses (GroV, YepV) is also yet to be characterised, though data from a comparative growth study found YepV to grow well in human- (HeLa), monkey- (Vero) and pig- (PK15a) derived cell-lines, highlighting it as another potential target for ongoing surveillance and infection studies [358].

5.1.2. *Pteropus* species fruit bats or "flying foxes" and human conflict

Four species of *Pteropus* spp. flying foxes are distributed throughout mainland Australia, where they serve a critical role as long-distance seed dispersers and pollinators, feeding primarily on floral resources and fruits in a wide range of vegetation communities. Despite their critical ecological and economic importance, populations are threatened by human persecution and ongoing habitat loss, and 2 of the 4 species (spectacled flying-fox (*P. conspicillatus*) and grey-headed flying-fox (*P. poliocephaus*)) are listed as vulnerable under Australia's Environment Protection and Biodiversity Conservation Act (1999).

These colonial species form large aggregations known as "roost sites" or "camps" (hereafter known as roosts) in exposed tree branches, which size from hundreds to hundreds of thousands of individuals

[363]. Roosts serve several purposes: as daytime rest stops for foraging animals, stopover sites for migrating animals, and maternity colonies, and may be inhabited continuously, irregularly or seasonally [363].

Other life history traits relevant to viral ecology include their seasonal and synchronous reproduction, which is speculated to allow for pathogen persistence within reservoir populations, and potentially producing periods of increased human risk [18]. Of the Australian species, each has a single annual birth pulse, occurring October–November for grey-headed and black flying-foxes, and April–May for little red flying-foxes [363].

The geographical distribution and migration patterns of the pteropids are determined by the distribution and phenology of food sources, and they regularly cover long distances in search of ephemeral floral and fruit resources in native forests. Broadly, the spectacled flying fox (*P. conspicillatus*), occurs in northern and eastern parts of QLD; the black flying fox (*P. alecto*), has a broad geographic distribution across northern Australia, the little red flying fox (*P. scapulatus*), can be found across northern and eastern Australia, and the grey-headed flying fox (*P. poliocephalus*) occurs in eastern and south-eastern Australia (Figure 66).

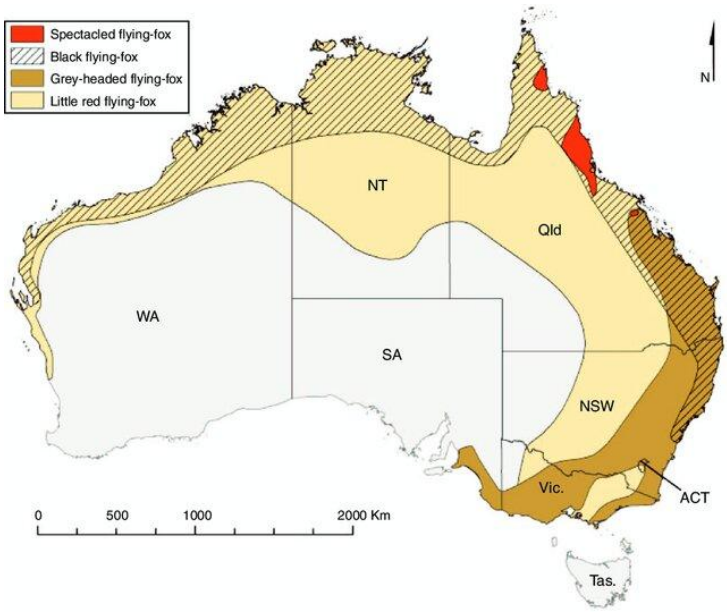


Figure 66 Distribution of the four Australian mainland *Pteropus* spp. by Timmiss et al., 2021 [364]

As anthropogenically-driven forest loss and fragmentation reduce the quantity and connectivity of native and seasonally critical food plants, flying foxes have been forced to seek alternative food sources. These colonially roosting bats readily adapt to urban landscapes, leading to range expansion and the establishment of roosts in Australian towns and cities, often in excess of 50,000 of individuals [365,

366], increasing proximity to human and domestic animal hosts. Alongside urbanisation and range expansion, longitudinal studies have identified the fragmentation or fissioning of roost populations which has been attributed to land clearing of native winter flowering trees in south-eastern Australia [367], alongside increases in exotic winter food sources in urban and agricultural areas [365].

The resultant roosting by flying foxes in urban and periurban areas, in addition to the encroachment of urban areas into existing camps, has resulted in increased human contact, and therefore conflict, with the noise, odour, faeces, and concerns regarding diseases transmission becoming highly contentious and politicised issues. Ecological pressures (such as food shortages) and the associated physiological stress simultaneously increase the shared environment with humans and the pathogen excreted into this environment, driving increased cumulative risk [368]. This phenomena has been convincingly presented in 25 years of land-use use and ecological data used to mechanistically model how El Niño events preceding the loss of winter foraging habitat triggered periods of nutritional and energetic stress in flying foxes [36]. These stressors drove ecological adaptations in flying foxes (population fissioning into agricultural areas) which resulted in spillover of HeV into horses [36].

5.1.3. Wildlife and flying fox rehabilitators and rescuers in Australia

The landscape of wildlife rescue and rehabilitation in Australia is dominated by an informal network of non-profit volunteer organisations such as Bat Rescue Inc., Wildcare Australia, and the RSPCA Wildlife Hospital, which serve a critical role in the conservation of native species. Flying foxes, and to a lesser extent, microbats, typically end up in care following man-made hazards (e.g., barbed wire, large-aperture fruit netting, power lines) and extreme weather events (e.g., heat waves). Volunteer wildlife rescuers and rehabilitators (known hereafter as carers), rescue and care for injured, ill, and orphaned flying foxes, either solo or more typically, as part of an organisation. The goal of rehabilitation is release to the wild, though in the case of permanent injury, animals will be either euthanised or (less commonly) kept in permanent care.

Rescue and care of these animals involves prolonged close contact, and typically includes daily interactions such as treating injuries and hand-feeding pups. Such interactions pose a significant hazard to carers, and surveys of QLD volunteers report significant exposure to all 4 species, through bites (74%), scratches (88%), and direct contact with bat blood (60%) [349].

Personal protective equipment (PPE) and rabies vaccination can be used to protect against ABLV and other zoonoses, however, little is known on the true uptake of these countermeasures in wildlife caring communities.

Further, with the exception of the 1996 HeV serosurvey, no comprehensive serosurveillance of this high-risk population has been reported [349], and any studies of human-bat interactions in Australia

incorporating carers have focused primarily on potential ABLV exposures. Given the known circulation of multiple paramyxoviruses of uncharacterised zoonotic potential, this highlights a critical gap in our understanding, and consequently, our preparedness.

5.1.4. Chapter aims

This chapter aims to:

(1) Investigate the seroepidemiology of select paramyxoviruses and filoviruses in human populations with significant exposure to wildlife (in particular flying foxes) in the eastern coast of Australia.

Here, I hypothesise that wildlife workers with prolonged close contact with flying foxes will have increased seroreactivity to multiple paramyxoviruses known to circulate in flying fox populations (CedV, YepV, GroV), but not HeV virus (known to be poorly transmissible directly from bats) or filoviruses (not believed to circulate in the region).

(2) Understand perceptions of zoonotic disease risk and explore safety practices through semi-structured interviews with volunteer rescuers, carers, veterinary and zoo professionals.

Here, I hypothesise that wildlife workers will demonstrate significant heterogeneity in their individualized safety practices, which will have been developed through experiential learning, and be informed by their personal perceptions of risk.

(3) Integrate patient and public involvement (PPI) activities throughout all phases of the research cycle of this study.

a. Rationale: Given that volunteer wildlife carers represent a hard-to-reach population with documented historical distrust of researchers and government health services, these engagement activities are essential for ensuring research relevance, establishing trust, and maximizing the impact and uptake of study findings within this community.
b. The PPI strategy was developed with four primary objectives that addressed both methodological and ethical considerations specific to this population.
    i. First, early engagement aimed to improve participant recruitment by establishing relationships and credibility within wildlife care networks prior to formal data collection.
    ii. Second, activities were designed to address existing concerns about scientific research that had previously limited this community's participation in studies.

iii. Third, the co-production of research instruments, particularly the semi-structured interview guide, drew upon carers' subject matter expertise to ensure questions captured relevant aspects of their work.
iv. Finally, development of an effective dissemination strategy with direct public input to ensure that findings reach and benefit the wildlife caring community in accessible and meaningful ways.

(4) Perform a metagenomic analysis of bat faecal, urine and spat (indigestible fruit pulp, skin and seeds spat out by flying foxes after extracting the juice) samples collected from the homes of wildlife carers, using sequence-independent amplification and short-read and long-read sequencing of RNA viruses.
    a. Here, I hypothesise that sequencing will identify a rich and diverse virome reflecting both active host infections, in addition to diet-derived sequences from plant and insect viruses. I hypothesise that CedV virus and other regionally circulating paramyxoviruses will be present, which will be reflected in the paired serological samples of the exposed wildlife workers.

5.2. Results

5.2.1. Patient and public involvement (PPI) activities

Patient and public involvement (PPI) activities engaging Australian wildlife workers were conducted throughout the study design, implementation and results dissemination phases. Key activities, outcomes and impacts were as described in Table 23.

Table 23 Patient and public involvement (PPI) activities

Study phase	Activity	Outcomes	Impacts
Design	During the design phase, an advisory panel (n=3) was established comprising experienced wildlife carers who consulted on study design, outreach and development of the interview guide.	The panel provided critical insights that directly shaped recruitment strategies, including recommendations for trusted communication channels, appropriate terminology, and timing considerations that aligned with seasonal wildlife care demands. The advisory panel's contributions resulted in substantial modifications to the original research approach. Their insights led to the development of recruitment materials that emphasised the practical benefits of participation for wildlife carers and the broader conservation community, rather than focusing solely on academic outcomes. Panel members identified key gatekeepers within wildlife organisations who could facilitate introductions to potential participants, enhancing the credibility of recruitment efforts. Additionally, their feedback on the interview guide ensured that questions addressed the unique challenges and contexts of wildlife rehabilitation work, including aspects that researchers had not initially considered.	Enhanced study relevance and acceptability within the wildlife care community. More effective recruitment strategies and interview questions tailored to this community.
Recruitment phase	A public forum was conducted during the recruitment phase. Attendance included wildlife carers (n=11) representing	The forum format facilitated bidirectional communication, allowing researchers to clarify the study's purpose and methods while carers shared their perspectives on critical issues requiring investigation. Participants expressed appreciation for being consulted early in the research process, with many noting that previous studies had failed to seek their input until after data collection was complete. This early consultation demonstrably increased trust, as	Increased trust between carers and researchers, addressing concerns of scientific interference.

	various experience levels and specializations.	evidenced by several attendees who had initially expressed scepticism subsequently volunteering to participate and encouraging their networks to do the same. Feedback from the forum led to important adjustments in the research approach. Carers emphasized the need for flexible interview scheduling that accommodated the unpredictable nature of wildlife emergencies, resulting in the adoption of extended recruitment windows and multiple rescheduling options. They also highlighted the importance of acknowledging the voluntary nature of their work and the financial constraints many carers face, leading to the provision of participation incentives.	
Dissemination phase (ongoing)	The dissemination phase, currently ongoing, has maintained the collaborative approach established during earlier phases. Advisory panel members have been instrumental in reviewing preliminary findings and ensuring interpretations accurately reflect the realities of wildlife care work. Their input has been particularly valuable in contextualising results within the broader challenges facing the wildlife care sector, including resource limitations, and climate change impacts. Panel members collaborated in developing a Plain English summary that translates key findings into accessible language while maintaining scientific accuracy. This summary will be distributed to all study participants and circulated through wildlife organisation newsletters, social media platforms, and carer networks. The panel's recommendations for dissemination channels extended beyond traditional academic outlets to include wildlife care conferences, training workshops, and online forums where carers regularly exchange information. A second public forum is scheduled to present final results directly to the wildlife care community, with online sessions planned to ensure geographic accessibility. These forums will feature interactive components allowing carers to discuss implications of findings for their practice and contribute to recommendations for policy and support services. The advisory panel has been instrumental in structuring these sessions to maximise engagement and ensure that diverse voices within the wildlife care community are heard.		

5.2.2. Study sites

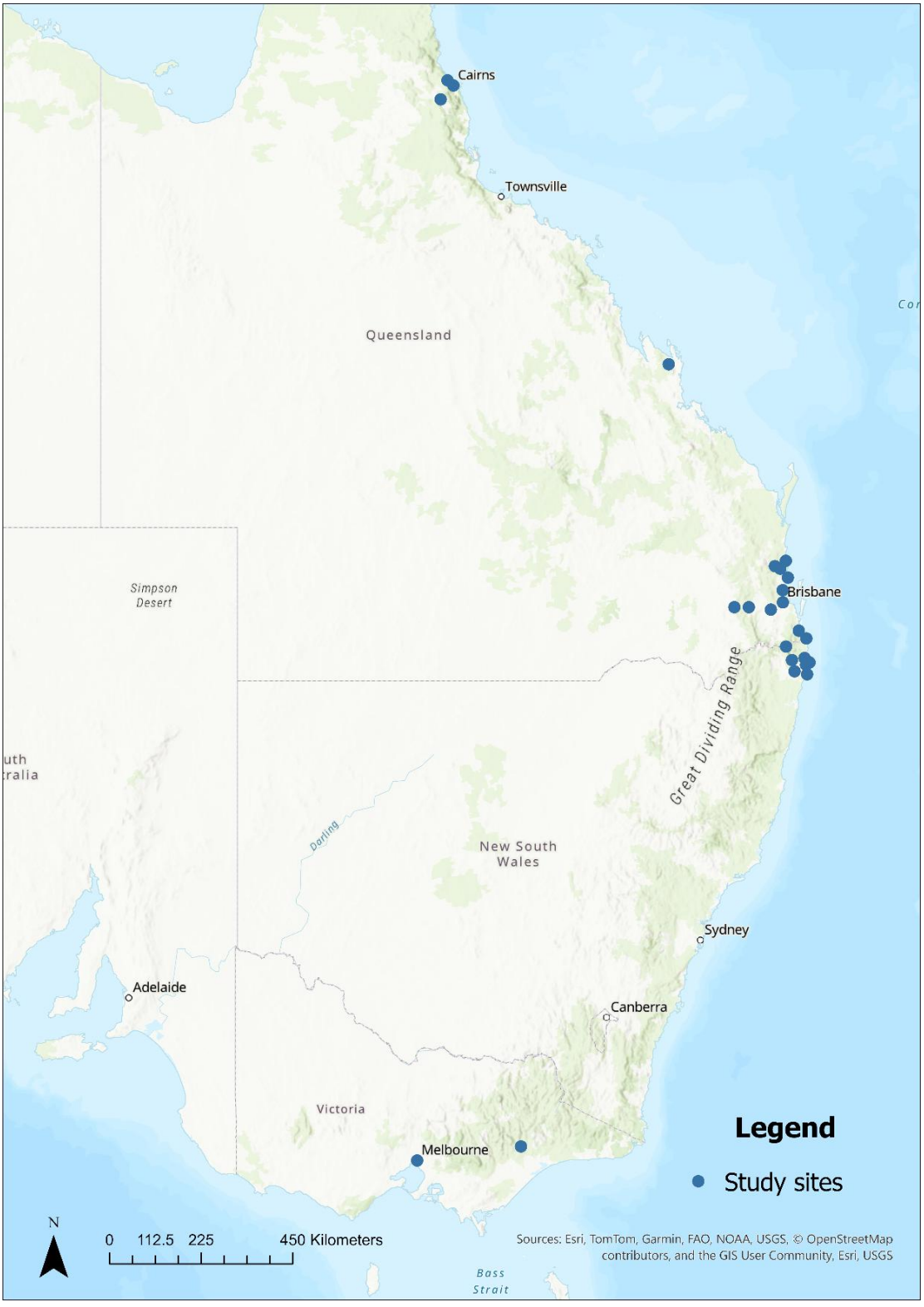


Figure 67 Study sites for surveillance of Australian wildlife workers

5.2.3. Characteristics of study participants

A total of 108 wildlife workers were recruited to the study from across Eastern Australia (Figure 67), of which 104 (95.4%) completed the semi-structured interviewing. As intended by the purposive sampling method, majority of participants were volunteer (unpaid) wildlife workers. Of these, the majority (88.2%, 67/76) considered themselves to be wildlife carers, though all performed rescues as necessary. Wildlife caring in these contexts involves hand-reading of orphaned pups, wound management, administration of medication and fluids, housing (typically within human residences) and flight rehabilitation (typically within wildlife-specific facilities), all with the ultimate goal of release back into the wild.

A subpopulation of volunteers was identified who performed rescues only (e.g., collection of injured animals and transport to veterinary clinics, hospitals or rehabilitators for ongoing care). Such scenarios typically involve public reporting to wildlife hotlines, operated by volunteers who then dispatch rescuers based on availability and proximity. Participants reported that this most commonly involved the rescue of orphaned, injured or ill animals often following entanglement in barbed wire fencing or large-aperture fruit netting, electrocution from power lines, heat stress following adverse weather events, starvation and pup abandonment following starvation events. Participants with professional or occupational exposure (e.g., veterinarians, veterinary technicians and nurses, zoo workers, ecologists) were also identified, and comprised 26.9% (28/104) of the study population (Table 24).

Table 24 Different roles (volunteer and professional) amongst study participants

Category	Primary role	n	%
Volunteer	Carer	67	64.4
	Rescuer only	9	8.7
Professional	Wildlife vet	9	8.7
	Wildlife nurse	12	11.5
	Vet	3	2.9
	Vet nurse	1	1.0
	Zoo worker	3	2.9

The demographic characteristics of the study population are presented in Table 25. Both volunteer and professional wildlife workers were predominantly female (84.2% and 85.7% respectively), though age demographics differed significantly. Among volunteers, the largest proportion (25.0%) comprised individuals aged over 70 years, while the professional workforce was primarily (60.7%) 30 – 40 years of age.

Table 25 Demographic characteristics of Australian wildlife worker study population (n=108), 2023

Characteristic	Volunteer wildlife roles (rescuers & carers)[1] n (%)	Professional wildlife roles[2] n (%)	Controls n (%)
Total no. of participants	76 (70.4)	28 (25.9)	4 (3.7)
Sex			
Male	12 (15.8)	4 (14.3)	1 (25)
Female	64 (84.2)	24 (85.7)	3 (75)
Age, group by years			
<30	8 (10.5)	8 (28.57)	0 (0)
30- 40	13 (17.11)	17 (60.71)	1 (25.0)
40- 50	13 (17.11)	3 (10.71)	2 (50.0)
50- 60	8 (10.53)	0 (0)	1 (25.0)
60-70	15 (19.74)	0 (0)	0
>70	19 (25)	0 (0)	0
Age, years			
Mean [Range]	53 [19 – 81]	34 [24 – 57]	51.8 [33 – 60]
Region			
FN QLD	12 (15.8)	0 (0)	0 (0)
SE QLD	50 (65.8)	22 (78.6)	4 (100)
NSW	5 (6.6)	6 (21.4)	0 (0)
VIC	9 (11.8)	0 (0)	0 (0)

1 Volunteer roles defined as unpaid wildlife rehabilitation, caring and rescuing. 2 Professional roles defined as paid wildlife roles e.g., veterinarian, veterinary technician or nurse, zoo workers, field ecologists. 3 Controls defined as residents of SE QLD without any reported wildlife contact.

Abbreviations: FN QLD: Far North Queensland; SE QLD: South east Queensland, NSW: New South Wales, VIC: Victoria.

5.2.4. Exposure in wildlife workers in Eastern Australia

5.2.4.1. Quantification of wildlife exposure

Study participants reported between 1 and 50 years of total experience working with Australian wildlife, with a median of 7 years (Figure 68).

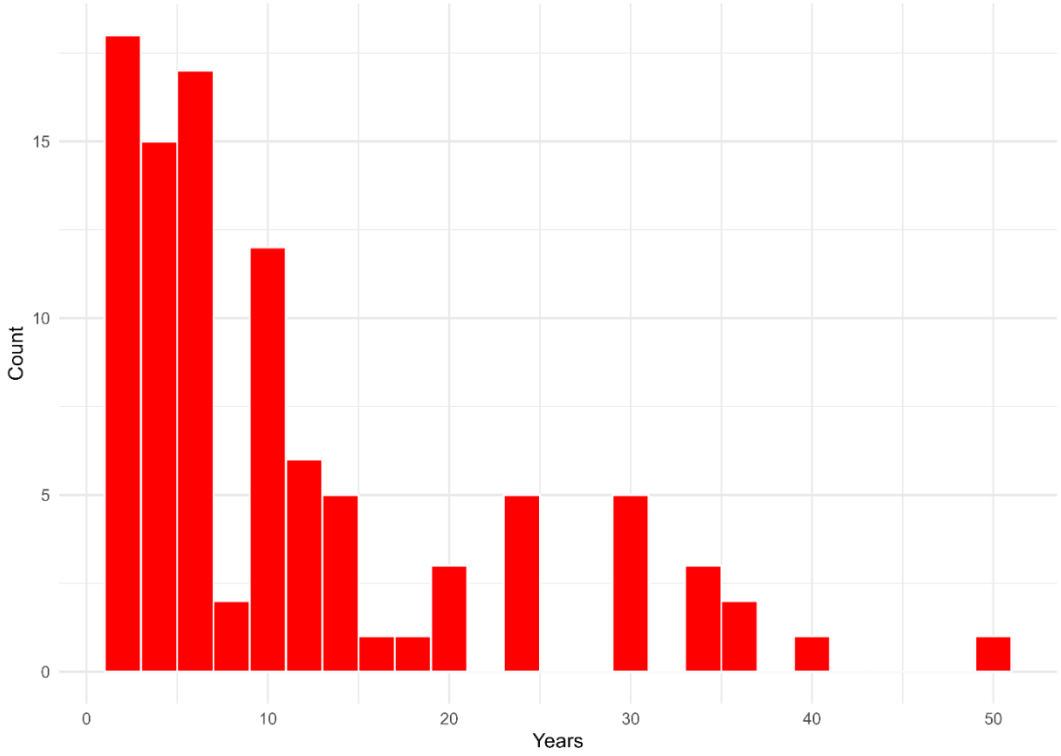


Figure 68 Years of experience with Australian wildlife

5.2.4.2. Flying fox and microbat exposure

Of the respondents, 88/92 individuals reported exposure to flying foxes, with the majority (39/92, 42.4%) reporting handling 5 – 50 individual flying foxes in an average year. Notably, 8.7% (8/92) reported exposure to significant numbers of animals, handling >500 flying foxes per year, all of whom were volunteer carers or rescuers. Of the respondents, 79/88 (89.8%) individuals reported exposure to microbats, with the majority (46/88, 52.3%) handling 5 – 50 microbats per year. Unlike flying foxes, no individuals reported handling >500 individual animals per year, reflecting differences in their rehabilitation (no creche or aviary).

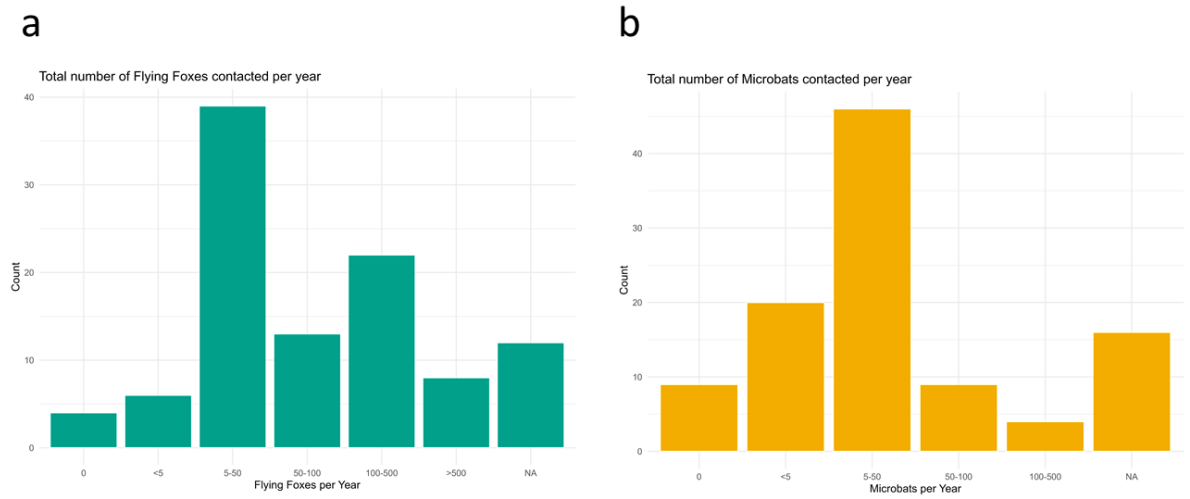


Figure 69 Contact with (a) Flying foxes (b) Microbats in Australian wildlife workers, 2023

5.2.4.3. Exposure to flying fox species

Wildlife workers typically reported exposure to multiple of the 4 Australian mainland species of flying fox. Responses differed by region, reflecting the known host range of these pteropid species (Figure 70).

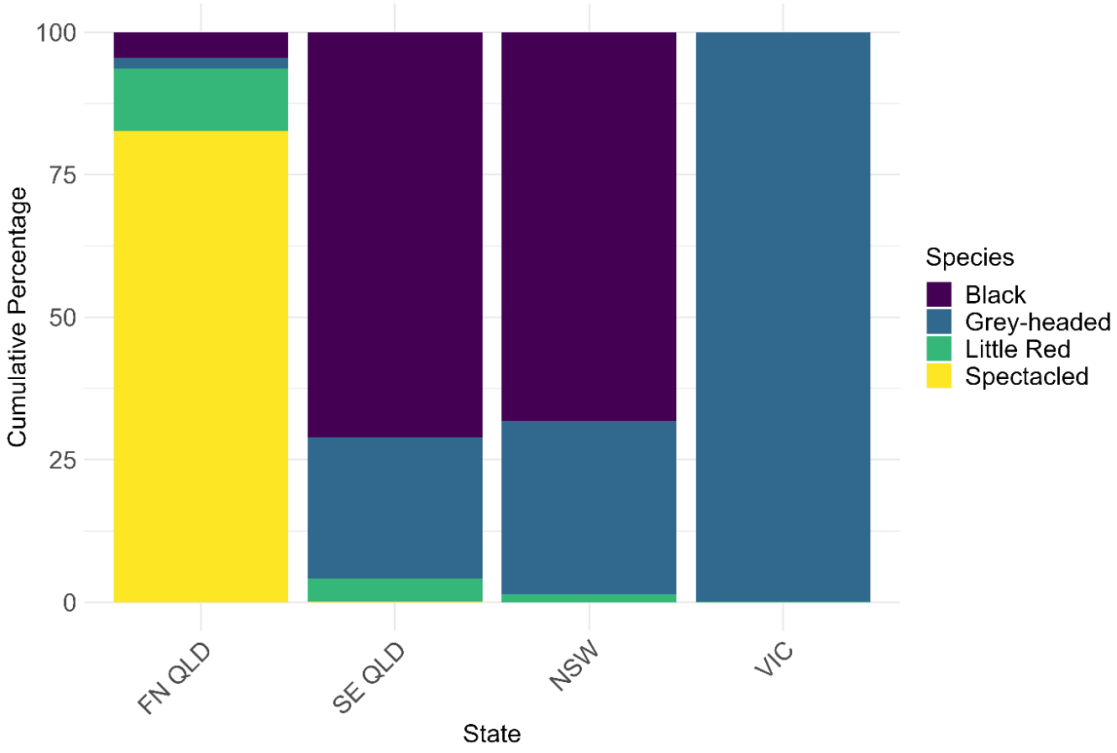


Figure 70 Exposure to flying fox species in Australian wildlife workers, 2023

5.2.5. Safety practices amongst wildlife workers

5.2.5.1. Usage of personal protective equipment (PPE)

The use of PPE was assessed through open-ended discussions following the prompt "please describe what you would typically wear when handling flying foxes and/or microbats". Several categories of PPE were mentioned, and thematically categorised as shown in

Table 26. A notable subset of participants (27 mentions, 30.7% of question respondents) reported minimal or no PPE use, particularly once the animal is "in care" and during routine care activities. Thick gloves were the most frequently described PPE (29 mentions, 33.0% of respondents), used typically during rescue and handling of wild adult flying foxes (Figure 71). Towels were the second most frequently used tool (27 mentions, 30.7% of respondents), serving as protection against bites and scratches during both rescues and rehabilitation.

Table 26 Categories of personal protective equipment (PPE) used by Australian wildlife workers when handling flying foxes

PPE category	Subcategory	Example quotes	Frequency (Percentage of respondents)
None		"Usually nothing", "No PPE", "No gloves", "None"	27 (30.7%)
Towel		"Towel", "Thick towel"	27 (30.7%)
Hand protection	Gloves (thick)	"Thick gloves", "Leather", "Suede", "Gardening gloves", "Paramedic gloves", "Needle proof gloves"	29 (33.0%)
	Gloves (thin)	"Thin gloves", "Cotton gloves"	8 (9.1%)
	Gloves (medical)	"Nitrile gloves", "Latex gloves", "Surgical gloves"	5 (5.7%)
Arm protection	Gauntlets	"Gauntlets", "Welding gauntlets", "Armlets", "Arm guards"	26 (29.5%)
	Neoprene sleeves	"Neoprene sleeves"	9 (10.2%)
Clothing		"Long sleeves", "Workwear", "Trousers", "Apron", "Bat jumper"	19 (21.6%)
Eye protection		"Eye protection", "Glasses", "Sun glasses"	5 (5.7%)

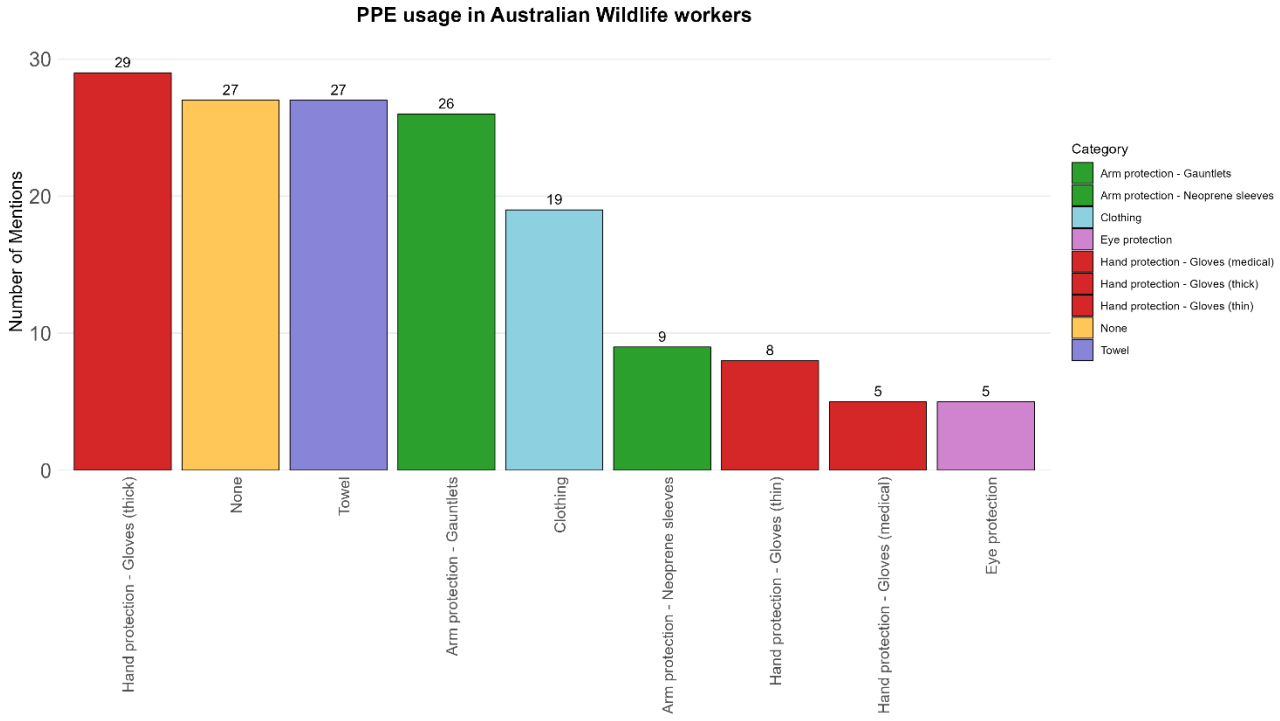


Figure 71 Personal protective equipment (PPE) usage in Australian wildlife workers when handling flying foxes, 2023

5.2.5.1.1. Drivers of PPE usage

Usage of PPE varied significantly between roles. Based on interview responses, 100% of rescuers (6/6), 100% of veterinarians (8/8) and 94.4% of veterinary nurses (17/18) used at least some PPE while handling flying foxes and microbats, compared to 57.4% (25/61) of carers (Figure 72). Amongst carers, PPE usage was not significantly associated with either age (Figure 73) or degree of flying fox contact (Figure 74).

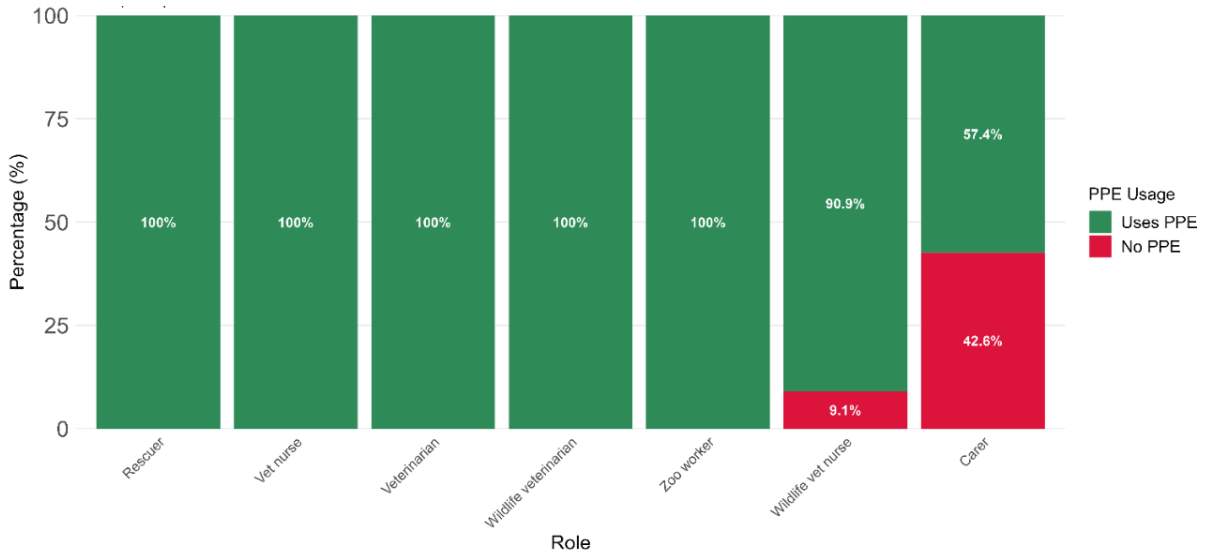


Figure 72 Personal protective equipment (PPE) usage for handling flying foxes and microbats, by wildlife workers by role, 2023

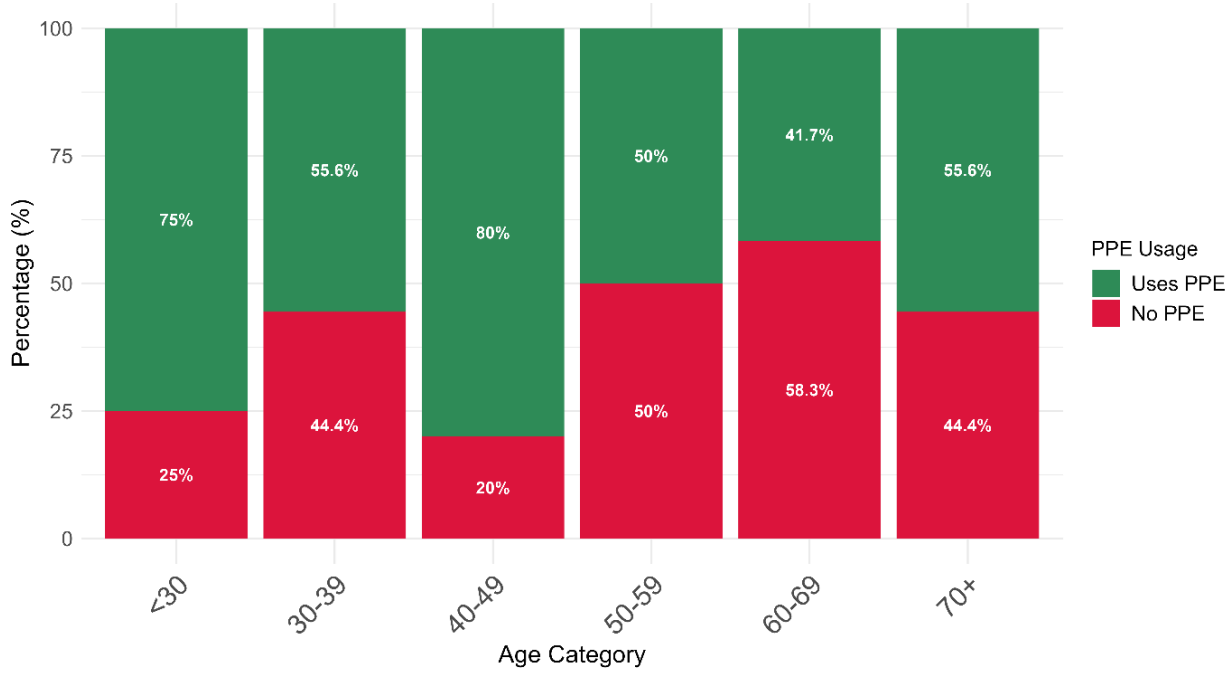


Figure 73 Personal protective equipment (PPE) usage for handling flying foxes and microbats, by wildlife workers, by age

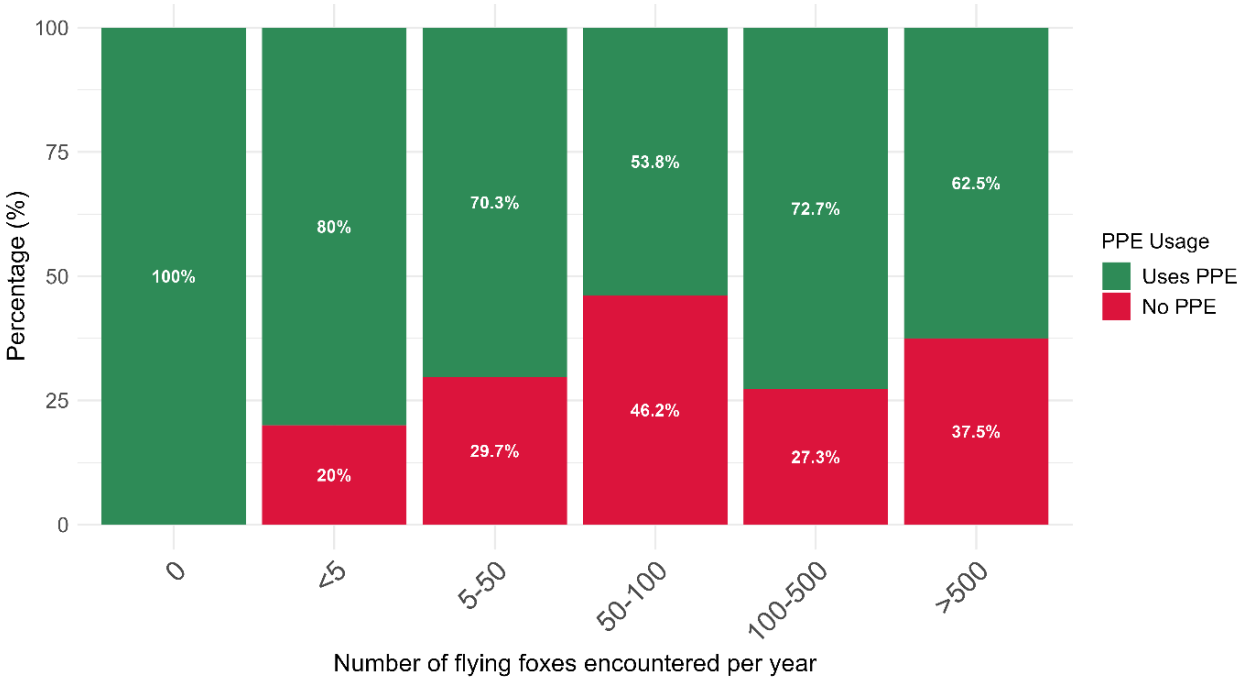


Figure 74 Personal protective equipment (PPE) usage for handling flying foxes and microbats, by wildlife workers, by frequency of flying fox contact per year

5.2.5.1.2. Thematic analysis of PPE usage

Several key themes (Table 27) emerged from the inductive analysis of PPE utilisation patterns, which overall demonstrated carers seeking to balance practicality and perceived risk, and reflected situational decision-making based on accumulated experience and practical constraints.

Table 27 Thematic analysis of personal protective equipment (PPE) usage amongst Australian wildlife workers, 2023

Theme	Description	Representative quotes
Context-dependent PPE usage	PPE usage varied significantly based on the specific wildlife handling context, as informed by their experiential knowledge. Cited considerations include: • Species (microbats vs. flying foxes) • Age of the animal (orphans vs. adults) • Clinical presentation of the animals (healthy vs. neurological)	“What I do for an adult trapped in a barbed wire fence is very different to an orphaned baby” "I’ll use thick gloves if [they’re] looking neurological, and a towel for rescue. Usually nothing otherwise."

	• Status of the animal (wild vs. in-care)
	• Type of activity
	  ○ No PPE or clothing for routine activities
	  ○ Thin gloves for medical procedures
	  ○ Thick gloves, gauntlets and towels for rescues, except barbed wire (bare hands)
	• Audience: comprehensive PPE for public-facing activities
		"Thick gloves for rescue with finger tips cut off. And gloves up to the elbow for bush rescues. At home, I'll use cotton arthritis gloves from chemist for orphans."
		
		"I'll use only armlets for babies, but also gloves for adults. I'll have bare hands with barbed wire."
		
		"…usually nothing for PPE…however, I will use thin surgical gloves for microbats."

Motivations for usage of different PPE categories	Majority of the PPE categories (towels, thick gloves, thin gloves, gauntlets, neoprene sleeves, clothing, eye protection) were used primarily for the prevention of physical injuries (scratches and bites), with only certain categories (medical gloves) being motivated by zoonotic risk reduction.	"I'll use fingerless gloves to protect [my] fragile skin from scratches."
Minimal PPE approach	A notable subset of participants reported minimal or no PPE use, particularly during routine care activities, citing habituation, inconvenience of using PPE for frequent activities, prioritization of animal comfort, dexterity and safety. A subtheme which emerged was that carers felt that they were more likely to get bitten while using cumbersome PPE (e.g., gloves) due to reduced dexterity and sensitivity during handling. A second subtheme was the difficulty of wearing gloves while disentangling animals from barbed wire.	"If I use gloves then I'm more likely to get bitten…"

Institutional vs. individual practice	Veterinary professionals demonstrated more standardized protocols in clinical settings with access to medical-grade PPE (e.g., nitrile, latex gloves). Volunteer carers showed greater variation in practices, often developing personalized systems based on available resources, experience, and their affiliated organisations. This included home-based adaptations (e.g., cutting gloves to make them fingerless for improved dexterity), resource-conscious choices (e.g., reusing gloves).	

5.2.5.2. Response to injuries or zoonotic exposures from flying foxes or bats amongst Australian wildlife workers

5.2.5.2.1. Types of responses and their frequency

Individual responses to injuries were assessed in the open-ended responses to the prompt "please describe what you would do following a bite/scratch/exposure to bodily fluids from a flying fox or bat". Several categories of responses were mentioned, and thematically categorised as shown in

Table 28. Of individuals who had experienced a bite, scratch or exposure to bodily fluids from a flying fox or microbat, the majority of responses demonstrated consistent use of cleaning (with soap and water) as a baseline method, in combination with antiseptic agents. Here, iodine-based disinfectants emerged as the primary choice (mentioned in 53.4% of responses) with alcohol-based disinfectants as a secondary option (Figure 75). A proportion of participants (6.9%) reported minimal to no intervention, with their responses reflecting a normalised exposure to minor injuries and confidence in their immunization status (Figure 75). All rehabilitators were vaccinated against rabies, and described a reliance on vaccination status as primary protection against ABLV (which was the major perceived risk).

A typical response for serious injury followed the following steps: (Appendix: Figure 85).

Step 1: Initial Response (No action, Clean with soap)

Step 2: Disinfection (Iodine-based, Alcohol-based, other antiseptic)

Step 3: Medical Response (ABLV vaccination, ABLV titre testing)

Step 4: Follow-up (Reporting, Monitoring of animal for signs of illness)

Table 28 Responses to injuries or zoonotic exposures from flying foxes or bats

Response	Subcategory	Counted words	Frequency (% of respondents)
No action		"Usually nothing"	4 (6.9%)
Cleaning and washing with soap and water		"Wash with soap and water" "Clean wound"	38 (65.5%)
Disinfectant or antiseptic	Alcohol-based disinfectant	"Alcohol" "60% alcohol spray" "Hand sanitiser"	4 (6.9)
	Iodine-based disinfectant	"Betadine" "Iodine"	31 (53.4%)
	Peroxide	"Peroxide"	2 (3.4)
	Chlorhexidine	"Chlorhexidine"	3 (5.2)
	F10	"F10"	2 (3.4)
ABLV post-exposure response	ABLV PEP	"ABLV vaccination" "ABLV booster" "Rabies booster"	20 (34.5%)
	ABLV titre test	"Titre test"	1 (1.7)
Reporting	Report to affiliated wildlife care organisation (e.g., president)	"Call president" "Report to president" "Report to [redacted] phoneline"	6 (10.3)
	Report to government or public health department	"Call QLD Health" "Contact health authorities"	2 (3.4)
Monitoring of animal		"If showing signs, escalate" "If animal is showing signs afterwards – ABLV testing"	3 (5.2)

Note: Percentages may add to >100% as respondents provide multiple responses.

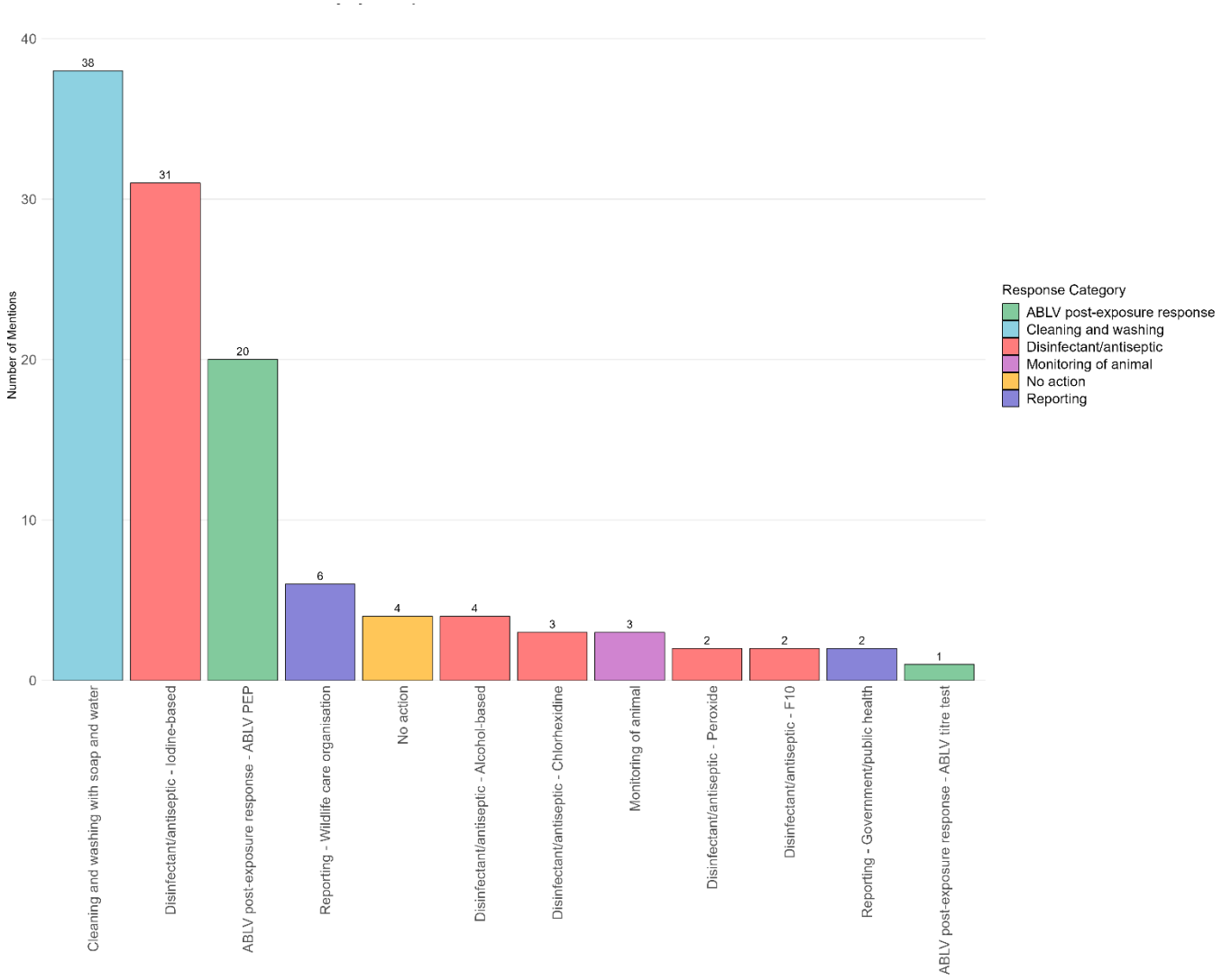


Figure 75 Frequency analysis of responses to the question: "please describe what you would do following a bite/scratch/exposure to bodily fluids from a flying fox or bat".

5.2.5.2.2. Drivers of responses to injury and exposure

The responses to flying fox injury or exposure varied across participant groups, with professional staff (veterinarians, veterinary nurses) showing greater adherence to medicalised protocols (disinfectant use, ABLV post-exposure protocols, public health reporting) as compared to volunteers. Heterogeneity was also seen between the responses of experienced (>10 years) compared to new (<2 years) carers, with experienced handlers demonstrating greater reliance on basic cleaning of wounds and lower reporting rates (Appendix: Figure 86).

5.2.5.2.3. Thematic analysis of response to injuries or zoonotic exposures

Several key themes (Table 29) emerged from the inductive analysis of responses to injuries or exposures from flying foxes. Similar to responses regarding PPE usage, these data demonstrated carers developing individualised response protocols based on their experiences, available resources, and organisational safety culture. It corroborated anecdotal evidence of mistrust in public health systems.

Table 29 Thematic analysis of response to injuries or zoonotic exposures in Australian wildlife workers, 2023

Theme	Description	Representative quotes
Stratified response systems based on risk assessments	Several participants described protocols that varied based on injury severity and animal presentation. Key patterns: • Differentiation between minor scratches and serious bites • Enhanced protocols for neurologically symptomatic animals • Escalation pathways to medical assessment and ABLV testing based on ongoing monitoring of the animal • Documentation and reporting systems within wildlife caring organisations	"If it's minor - nothing. If it's serious - betadine and a bandaid. If [the animal is] showing signs afterwards – then ABLV testing and vaccination as required."
Perceived risk of zoonoses	The perceived risk of zoonoses varied between participants. One subtheme which emerged was the acknowledgement of the idea that wildlife workers could be "patient zero" or "canaries in the coal mine" for spillover, while another was the belief that "the risk of infection from flying foxes is overstated".	"I just hope there's no hideous infection which I might not know about until it's too late" "When I got bitten…I panicked" "If there's an outbreak, I might be patient zero, or I

		might be the one who has immunity and survives” “We're not dropping like flies. I can only think of one person got sick and they don't know what is was” “We are the canaries in the coal mine”
Government and public health system mistrust	Several volunteer participants expressed mistrust in government and public health systems. Their concerns included: • Discrepancies between state public health departments regarding their post-exposure protocols • Over-vaccinating of ABLV and associated health risks • Ulterior motives of governments and scientists which do not prioritise animal welfare or conservation	“No one knows if we can trust the government…” “Why do the Queensland and New South Wales health departments do different things?” “I am very concerned about ABLV over-boosting”
Institutional vs. individual practice - Formalized Medical Protocols	Veterinary professionals and some organizations demonstrated more standardized, medically-oriented approaches. Key patterns included: • Access to medical-grade disinfectants (chlorhexidine, F10) • Systematic ABLV vaccination and testing protocols • Documentation and reporting requirements	

	Meanwhile, carers showed greater variation in practices, often developing personalized systems based on available resources and experience. Here, key patterns were: • Prioritisation of animal welfare • Post-exposure monitoring approaches in more experienced carers	

5.2.6. Perceived risk amongst wildlife workers in Eastern Australia

Perceptions of risk regarding zoonotic infections were assessed in the question: "I am concerned about contracting an infection from wildlife". Here, differences were apparent between veterinary professionals, who were more likely to agree or strongly agree, compared to volunteers, who were more likely to disagree or strongly disagree. Low concern about infection was correlated with no PPE usage (p = 0.02) (Figure 77).

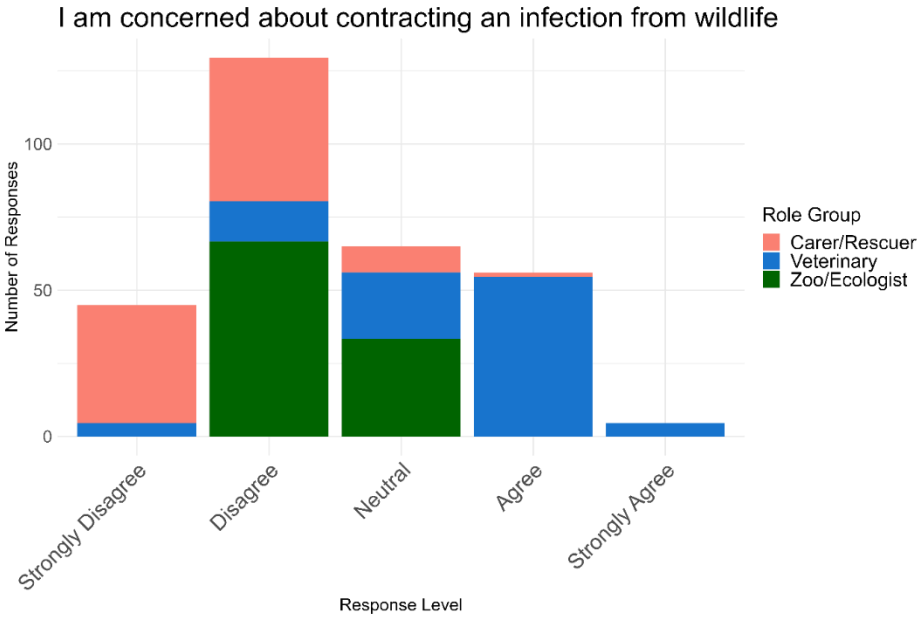


Figure 76 Responses amongst Australian wildlife workers to the statement: I am concerned about contracting an infection from wildlife

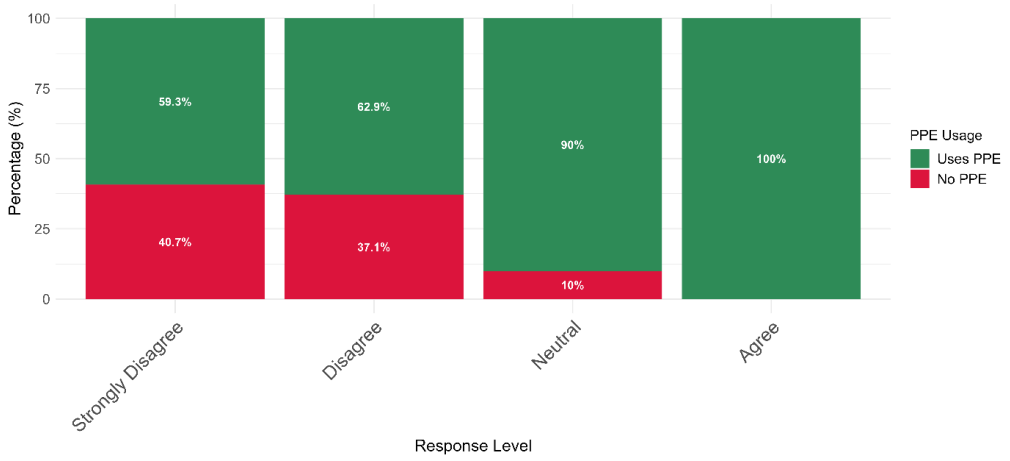


Figure 77 Personal protective equipment (PPE) usage by response to Q1: I am concerned about contracting an infection from wildlife

The majority of respondents (90.9%) agreed with the statement "I take sufficient precautions to protect myself" (Figure 78). Reported PPE usage did not differ significantly between individuals who believed they took sufficient precautions and those who did not ($p = 0.79$) (Figure 79). Notably, 26.6% of individuals who strongly agreed with the statement reported using no PPE. Most respondents also believed they had sufficient training and resources to protect themselves. Disagreement with this statement was observed exclusively among veterinary professionals (Figure 80), who highlighted particular concerns regarding the performance of bat caesareans or necropsies in closed rooms without range-hoods.

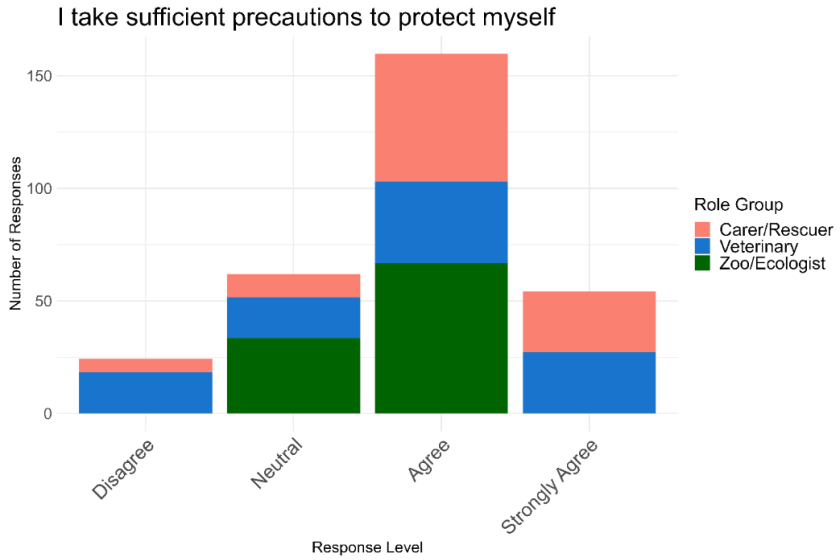


Figure 78 Responses amongst Australian wildlife workers to the statement: I take sufficient precautions to protect myself.

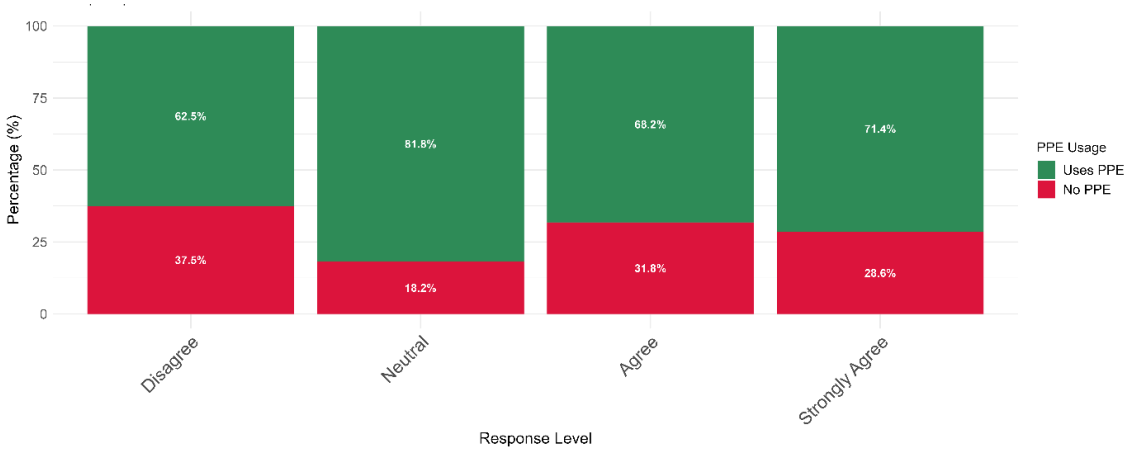


Figure 79 Personal protective equipment (PPE) usage by response to the question: I take sufficient precautions to protect myself.

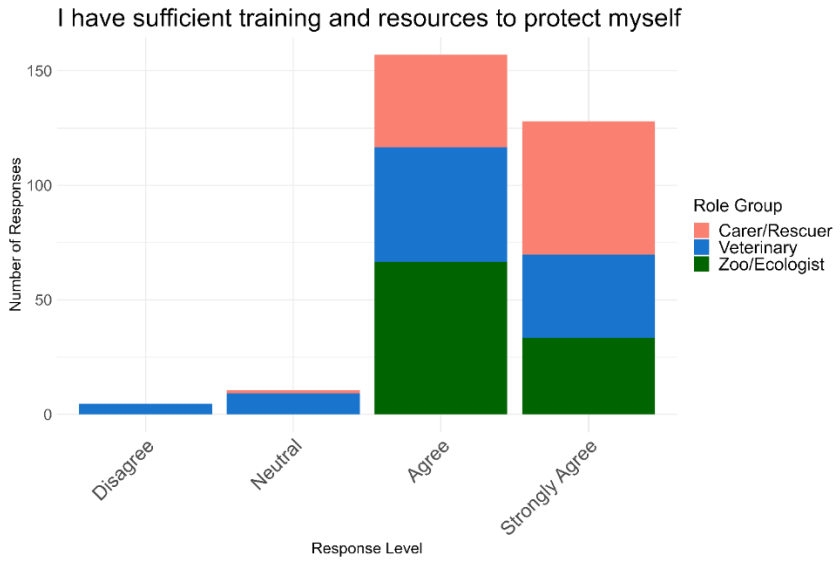


Figure 80 Responses amongst Australian wildlife workers to the statement: I have sufficient training and resources to protect myself.

5.2.7. Serological exposure to viral antigens amongst flying fox carers in Australia

Australian wildlife worker sera were screened using a MMIA for binding IgG antibodies against a panel of filovirus and paramyxovirus attachment proteins. No significant differences were seen between the population-level distributions of IgG antibodies against filoviruses (Figure 81) or paramyxoviruses (Figure 82) when compared to the non-wildlife exposed control cohort of UKBDs. Within the individual-level responses, one sera sample demonstrated seroreactivity greater than 5 standard deviations above the mean of the UKBD population for MLAV (Figure 83).

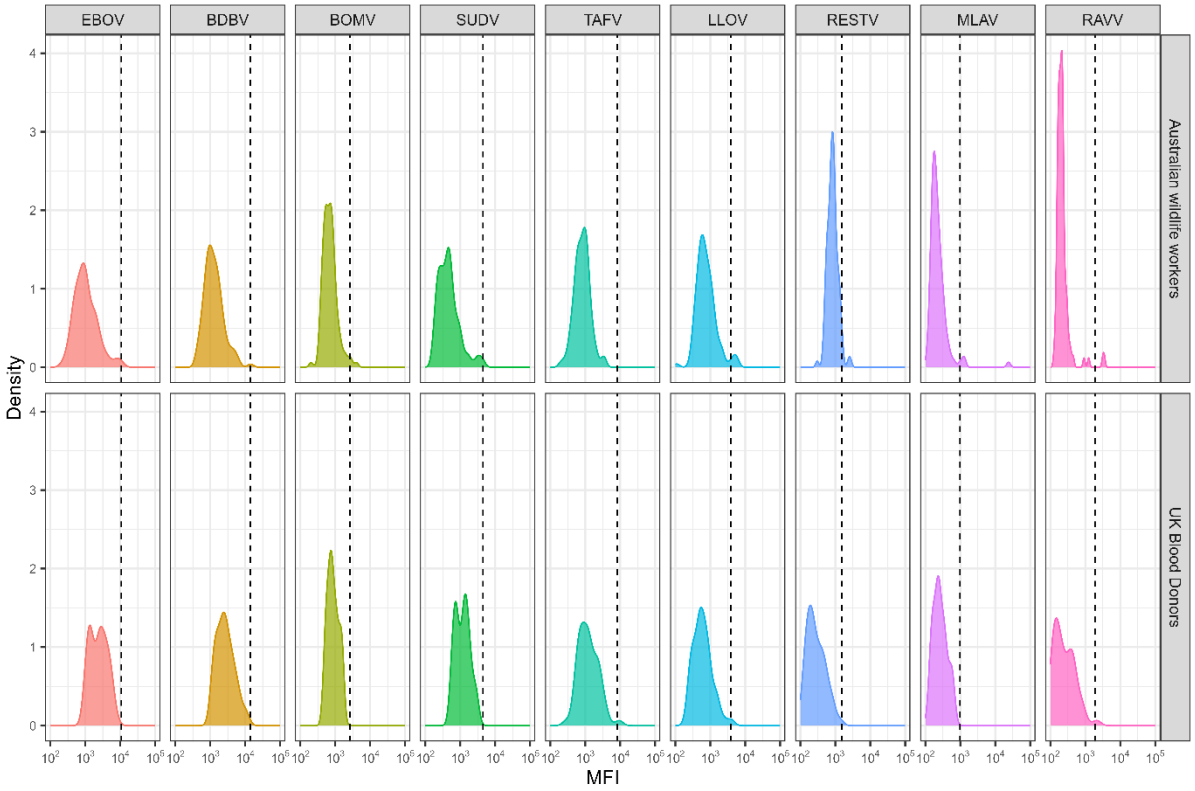


Figure 81 Anti-filovirus glycoprotein IgG distributions among Australian wildlife workers (n=104) and the United Kingdom blood donor cohort (n=63). IgG responses were measured by multiplex microsphere-based immunoassay (MMIA) in background subtracted median fluorescence units (MFI-bg) on the Luminex platform. Dashed vertical lines mark seropositivity cut-offs based on the presumed unexposed non-endemic cohort (UK blood donor) by calculating five standard deviations above the background subtracted (MFI-bg) mean.

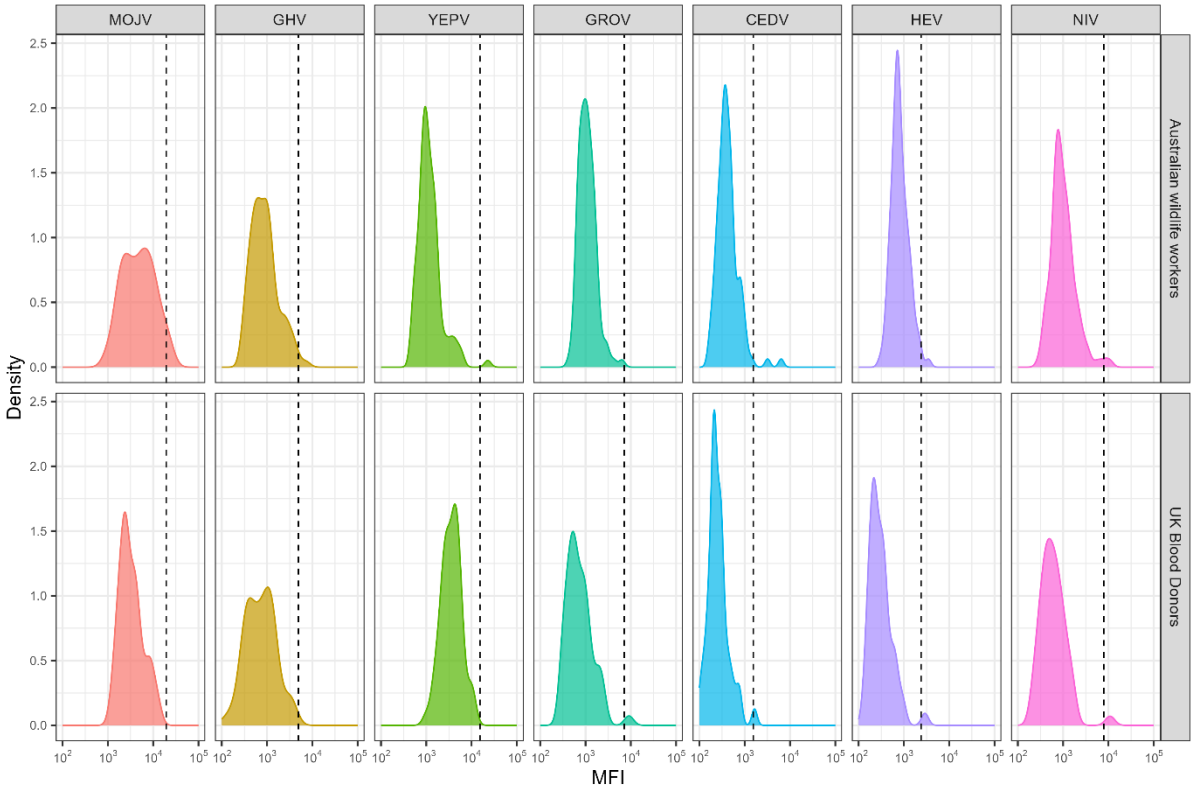


Figure 82 Anti-paramyxovirus glycoprotein IgG distributions among Australian wildlife workers (n=104) and the United Kingdom blood donor cohort (n=63). IgG responses were measured by multiplex microsphere-based immunoassay (MMIA) in background subtracted median fluorescence units (MFI-bg) on the Luminex platform. Dashed vertical lines mark seropositivity cut-offs based on the presumed unexposed non-endemic cohort (UK blood donor) by calculating five standard deviations above the background subtracted (MFI-bg) mean.

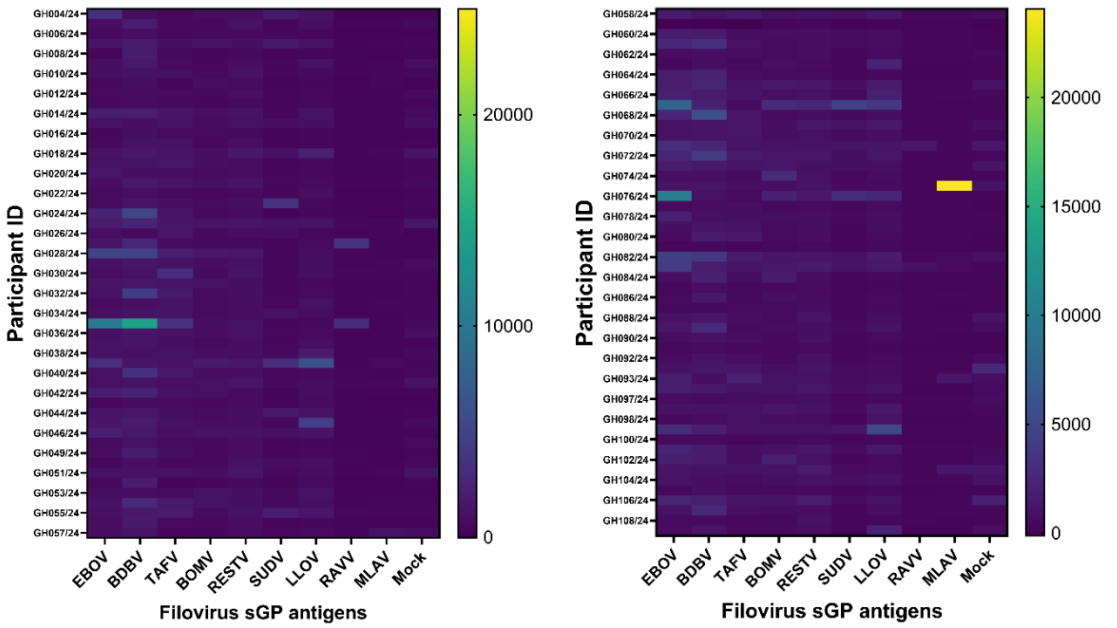


Figure 83 Anti-filovirus glycoprotein IgG responses of Australian wildlife workers (n=104).

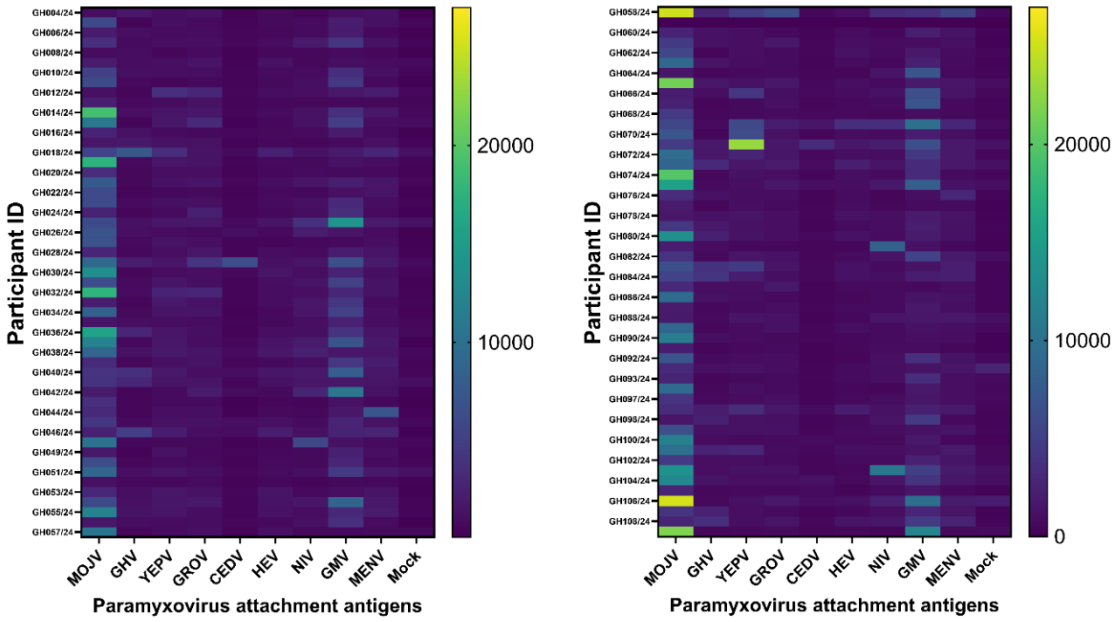


Figure 84 Anti-paramyxovirus glycoprotein IgG responses of Australian wildlife workers (n=104).IgG responses were measured by multiplex microsphere-based immunoassay (MMIA) in background subtracted median fluorescence units (MFI-bg) on the Luminex platform.

5.2.7.1. Cedar virus (CedV) neutralisation of high binding samples

The 5 individuals with the highest seroreactivity to CedV on MMIA were tested by Dr. Emily Clayton, University of Oxford, for neutralising activity in a recombinant luciferase CedV microneutralisation assay. No samples showed any evidence of neutralising antibodies.

5.2.8. Metagenomic sequencing of samples from flying foxes and bats in wildlife rehabilitation across East Coast Australia

Pooled environmental samples (n=32) were collected between March and April 2023 from all flying foxes or microbats found in-care within the homes of study participants. Samples included fresh faeces, urine or spats from various flying fox and microbat species. Samples were pooled by collection site (n=8) and viral particles were enriched through homogenization, filtration, and DNase treatment prior to RNA extraction.

Total RNA-sequencing of 8 pools by Oxford Nanopore Technology MinION resulted in a total of 3,942,124 classified reads with a total length of 1,785,185,788 bp. Between 80.0 – 95.4% of reads after filtering were unclassified. Of the classified reads, 75,280 reads (1.91%), with a total length of 41,762,238 bp (2.34%), were viral. Among them, 41,490,494 bp (99.35%) had similarity to eukaryotic viruses, covering viruses from plants, invertebrates and vertebrates. The majority of viral sequences detected in faecal samples were diet-derived and classified to pathogenic plant viruses: Papaya ringspot and Watermelon crinkle leaf-associated virus 1 and 2 or insect viruses.

Sequences classified to 10 viruses of vertebrate species were identified (Table 30). Bat coronavirus sequences were identified in 4/8 pools (50%) and showed high sequence similarity to previously reported reference genomes from Australia. In barcode 07, a read exhibited 93% nucleotide identity over bases 7870 to 8408 when aligned to the complete RNA genome of a bat coronavirus (GenBank accession: ON872523.1), originally isolated from *Pteropus poliocephalus* faecal pellets in Australia (unpublished; direct submission to GenBank). The alignment region had a coverage depth ranging from 0.72 x to 1 x, with a highly significant E-value of 10^{-292}. In barcode 05, a more extensive alignment was observed, with 91% average nucleotide identity across approximately 10,900 aligned bases derived from 15 distinct read alignments spanning multiple regions of the same reference genome (ON872523.1). The associated E-value was 10^{-268}, indicating a statistically robust match. None of the paramyxoviruses or filoviruses included in the serological screening panel, including HeV, CedV, GroV, YepV, were found in any of the specimens.

Table 30 Vertebrate viruses

Virus	Barcode (pool)	Total bases*	Identity (%) **	E-value	Best hit
Bat faecal associated dicistrovirus 3	01	10,549	91.6	10^{-274}	ON872536.1 Partial RNA genome from Australia, 2019
Bat faecal associated retrovirus 2	03	212	90.4	10^{-85}	ON872532.1 Partial RNA genome from *Pteropus poliocephalus*, Australia 2019
	04	213	91.6	10^{-88}	
	05	374	88.0	10^{-168}	
	08	6386	93.5	10^{-190}	
Bat faecal coronavirus	01	2340	85.9	10^{-182}	ON872523.1 Complete RNA genome from *Pteropus poliocephalus*, Australia 2019
	05	10,900	91.7	10^{-268}	
	07	549	93.0	10^{-292}	
	08	23,741	92.1	10^{-250}	
Flying-fox retrovirus	04	4,403	92.0	10^{-232}	MK040728.1 Complete RNA genome from *Pteropus Alecto*, Australia, 2018
Human blood-associated dicistrovirus	05	4,441	92.8	10^{-226}	OQ835731.1 Complete RNA genome from blood in Cameroon, Nigeria, Peru[369]
Parus major densovirus	01	161	96.9	10^{-49}	NC_031450.1 Complete DNA virus identified from Great tit (*Parus major*), China, 2016[370]
Posa-like virus	01	1,617	94.3	10^{-19}	MG553250.1 Partial RNA sequence identified from faeces, multiple regions (Ethiopia, Venezuela)
	03	543	94.0	10^{-18}	
	08	751	94.0	10^{-18}	
	09	1,098	93.6	10^{-18}	
Protoparvovirus chiropteran 1	02	625	88.0	10^{-294}	NC_029797.1 Complete DNA sequence from faeces of *Pteropus vampyrus*, Indonesia
	04	2,685	87.6	10^{-242}	
Pteropox virus	08	159	93.6	10^{-71}	NC_030656.1 Complete DNA sequence from skin of *Pteropus scapulatus*, Australia, 2015[371]

Respirovirus laryngotracheitidis	03	103	92.5	10^{-34}	NC_003461.1 Known human pathogen. Complete RNA sequence from clinical isolate from human, USA, 2002.
	08	894	91.3	10^{-31}	
Rolda virus	01	1,247	91.1	10^{-25}	Complete RNA sequence from *Myotis californicus*, USA, 2021

* Number of bases within all the reads aligning to a given taxon. ** Average percent-identity of alignments to NCBI NT/NR.*** Average expectation value (E-value) of alignments to NCBI NT/NR. The Expectation value (E-value) is a parameter that describes the number of matches one can "expect" to see by chance when searching a database of a particular size. The closer to 0 the more significant the alignment. For example, a raw E-value of 1 would indicate that in a database of the current size one might expect to see 1 match with a similar score simply by chance. Notably, short alignments will have relatively high E-values because the calculation of the E-value takes into account the length of the query sequence and shorter sequences have a higher probability of occurring in the database purely by chance. E-value < 10^{-10} point to significant taxon matches whereas E-values >0 represent non-significant or spurious taxon matches.

5.3. Discussion

The study design relies on the targeted sampling of volunteer wildlife carers who are a decentralised and hard-to-reach population with historical mistrust in government agencies and scientists. Here, patient and public involvement (PPI) activities yielded measurable improvements in both research quality and community engagement. Recruitment targets were exceeded and the geographic and demographic diversity of participants surpassed initial projections, attributed largely to the trust established through PPI activities and peer endorsement within carer networks.

Interview data demonstrated greater depth and candour than was expected from a marginalized and sceptical population. Participants frequently referenced the public forum or advisory panel involvement as factors that convinced them to share sensitive information about their experiences, including mental health challenges, conflicts with authorities, and financial hardships associated with wildlife care. This openness enriched the dataset and enabled more nuanced analysis of the complex factors affecting risk perception and decision-making.

The involvement of wildlife carers (from the advisory panel) in interpreting results enhanced the validity and applicability of findings. Panel members drew on their contextual knowledge to explain apparent contradictions in the data and highlight practical implications for wildlife care practice and policy.

The study provided updated demographics of volunteer wildlife rescuers and carers in Australia. As expected from anecdotal reports, majority (64/76, 84.2%) were female. The data supported concerns expressed in carer interviews, showing the population to be heavily skewed towards an older demographic, with 25% (19/76) volunteers over 70 years of age. This age structure should inform relevant public health decisions, as it may affect susceptibility to disease, response to vaccinations, and optimal communication strategies.

Wildlife workers in this study demonstrated substantial experience (median 7 years) and extensive exposure to all species of flying foxes and microbats. Notably, 8.7% (8/92) of participants handled over 500 individual flying foxes annually, with these high-volume carers typically exposed to large numbers of adults through crèche facilities and flight schools. Exposure patterns aligned predictably with geographic distributions: carers in northern coastal Australia were predominantly exposed to spectacled flying foxes, while those in south-eastern QLD and northern NSW reported similar proportions of black and grey-headed flying foxes, and Victorian carers encountered almost exclusively grey-headed flying foxes. Given that paramyxovirus dynamics are believed to vary between species, these geographic exposure patterns provide crucial information for risk assessment.

PPE and Safety

While many rehabilitators demonstrated safety practices informed by years of lived experience, the analysis revealed significant heterogeneity and a lack of standardization that could inform targeted interventions to improve wildlife carer safety. The qualitative data provided valuable insights into decision-making processes, barriers to accessing PPE resources, practical constraints, and the critical role of organizational culture and individual risk perception in shaping safety practices.

Participants described highly variable PPE practices, ranging from comprehensive layered protection protocols (e.g., nitrile gloves under thick protective gloves) to minimal or no PPE usage among a substantial proportion (30.7%) of respondents. PPE usage differed significantly by professional role, with veterinarians and nurses more likely to utilize multiple forms of protection compared to volunteers. This disparity may reflect differential workplace PPE availability, enhanced zoonotic risk awareness through veterinary training, or greater likelihood of encountering sick rather than healthy animals. Exposure responses were similarly influenced by role, which may be due to clinical settings providing access to specialized disinfectants such as chlorhexidine and F10. Experienced carers (as compared to newer carers) favoured basic wound cleaning and animal monitoring approaches over formal reporting protocols. This pattern may reflect the development of specialized techniques (such as animal monitoring) that only experienced carers feel confident applying, habituation to perceived risk over time, or responses to recent changes in official guidance and training protocols. While awareness of ABLV risk was high, as evidenced by 100% rabies vaccination rates, concern regarding other zoonotic

infections was less prominent. This led to over-reliance on vaccination status rather than comprehensive PPE-based protection strategies.

Qualitative data revealed that home-adaptations (e.g., cutting fingertips off gloves) and seemingly paradoxical choices (e.g., avoiding thick gloves) were driven by carers' experience that reduced dexterity and tactile sensitivity increased bite risk. This highlights the need for PPE designs that balance safety with functionality, particularly for specialized tasks such as disentangling animals from barbed wire or other rescue scenarios.

Despite significant variation in PPE usage and injury response protocols, almost all participants (90.9%) agreed that they take "sufficient precautions to protect" themselves. However, this self-assessment revealed a notable disconnect: while 90.9% reported taking sufficient precautions, 26.6% used minimal or no PPE. This discrepancy may reflect several factors, including imperfect recall or social desirability bias during interviews. Alternatively, this dissonance may highlight fundamentally different conceptualizations of "sufficient protection." Carers may believe zoonotic risk to be minimal and therefore consider PPE unnecessary, or they may rely primarily on non-PPE protective measures such as careful handling techniques and ABLV vaccination status rather than barrier protection.

Seroreactivity, as measured by the MMIA, was minimal in the wildlife caring population. While a single individual demonstrated reactivity to MLAV, based on evidence from the literature discussed in previous chapters, it is consistent with previous reports of low-level filovirus seroreactivity in non-endemic populations, and likely does not represent true exposure. As no differences in the IgG distribution of wildlife carer and control populations were identified, relationships between seroreactivity and personal safety practices (such as PPE use) and geographic variation were not examined.

These seronegative results, combined with the extensive close contact described by participants (including bites, scratches, daily feeding and wound management, often without PPE), provide compelling evidence that the examined viruses, despite circulating at high seroprevalences in flying foxes, are not readily transmissible from bats to humans through direct contact. However, these findings emphatically do not address the zoonotic or pandemic potential of other bat-borne viruses that may remain unrecognized.

The semi-structured qualitative design enabled rich, detailed responses that provided insight into actual practices, with natural language responses revealing the reasoning underlying participant behaviours. The inductive thematic analysis approach identified patterns across responses while attending to both explicit content and implicit assumptions, and recognized divergent cases and minority practices within this diverse population. As with all interview-based research designs, limitations include potential discrepancies between self-reported and actual practices, as well as possible response bias toward socially desirable answers.

Metagenomic sequencing

This chapter included an additional component involving the metagenomic sequencing of environmental samples from bats residing within carers' homes. This section was designed to identify scenarios where CedV (or YepV, GroV, HeV etc.) was actively being shed by bats whose carers lacked CedV antibodies, thereby strengthening evidence that direct transmission remains unlikely even in high-exposure settings. However, no CedV or other paramyxoviruses were detected in any bat faecal samples.

A metagenomic approach was selected to comprehensively characterize viral diversity while bypassing the limitations of targeted assays and enabling detection of both known and novel viruses. Consistent with other bat virome studies, a substantial proportion of sequences showed low nucleotide similarity to known viral sequences and remained unclassified following BLAST-based taxonomic analysis. Some of these sequences may represent previously unknown or genetically divergent viruses. The majority of identified contigs and reads mapped to an extensive array of viral families, predominantly vertebrate viruses (mostly mammalian), invertebrate (insect) and plant viruses, and bacteriophages.

Reads mapping to bat coronavirus sequences were detected in 50% of pools (4/8), showing high sequence similarity to previously reported Australian reference genomes. This finding was consistent with other bat metagenomic studies identifying sequences belonging to the alphacoronaviruses and betacoronaviruses in bat faecal samples. Several large-scale bat virome studies conducted in Southeast Asia and southern China have identified multiple coronavirus sub-lineages [372, 373]. In studies conducted in South Africa and Argentina, alphacoronavirus sequences detected in bat guano formed distinct clades separate from human pathogenic strains, whereas others report betacoronaviruses related to Middle East Respiratory syndrome (MERS)-CoV [374-376].

Several viruses of veterinary importance were identified. Unlike previous studies which examined Australian flying foxes in Christmas Island [377], I detected viruses associated with pathogenic outcomes in bats, including flying fox retrovirus, pteropox virus and protoparvoviruses. This may reflect the study population of rehabilitated rather than healthy bats. Retrovirus detection was consistent with other studies where these sequences were abundant in fresh faecal samples, possibly resulting from endogenous retroviral integration or exogenous pathogenic viruses [372, 378].

Interestingly, some DNA viruses (e.g., Protoparvovirus chiropteran 1, Pteropox virus) were identified, possibly due to the presence of viral messenger RNA transcribed from the DNA genomes of these viruses, or even the presence of some traces of viral DNA after the extraction step. Parvovirus sequences, representing small single-stranded DNA viruses capable of causing severe disease, were also detected. These sequences often cluster within the Dependoparvovirus genus, and several studies have identified novel bat parvovirus variants. For example, investigations in Southeast China and Europe have recovered parvovirus sequences with significant divergence from known species,

suggesting that bats harbour unique parvoviral lineages [373, 375]. These viruses exhibit high genome variation and have demonstrated species-jumping capability, with protoparvovirus host-switching events documented among cats, dogs, and raccoons, highlighting potential zoonotic concerns [379, 380].

Abundant sequences from diet-derived insect and plant viruses provided insights into bat foraging behaviour and ecological interactions. Notably, the majority of plant virus sequences were related to biosecurity-relevant pathogens: Papaya ringspot virus and Watermelon crinkle leaf-associated viruses 1 and 2. While these detections do not indicate bat infection, they demonstrate the potential utility of bat surveillance for agricultural biosecurity monitoring.

Detected insect-derived viruses were primarily classified within the Densovirinae subfamily (Parvoviridae family), which typically infect arthropods but have been detected in mammalian faecal viromes (rodents) and human blood samples [369]. Of interest was the detection of parus major densovirus, previously identified in Swiss bat tissue samples with electron microscopy confirmation of densovirus-like particles [381]. Dicistroviruses – a sister family to the picornaviruses – also normally infect invertebrates as the natural hosts, however, have been described in human febrile illnesses and human metagenomic studies. The human blood-associated dicistrovirus identified in barcode 05 had 92.8% similarity (4441 bases) to a dicistrovirus genome assembled with 11.8 x average coverage depth from a human blood sample from Cameroon [369].

Of the viral reads, 0.65% had high similarity to known phages, reflecting the bat bacterial microbiome. Some of these phages, or bacteriophages, may be of clinical and public health interest, due to their highly-selective lytic action against pathogenic and antibiotic resistant strains of bacteria and their biofilms (Appendix, Table 33).

This pilot study was constrained by small and uneven sample sizes due to opportunistic collection, limiting statistical power and generalisability. Metagenomic analysis of environmental samples presents additional challenges including sample degradation and higher ratios of plant and insect viruses relative to host-associated viruses. Interpretation and comparison to studies within the literature is challenged by differences in the sensitivity of detection, which is known to vary by sample type, preparation (e.g., virus enrichment, such as nuclease treatment, centrifugation, filtration), amplification methods, sequencing depth, and bioinformatic pipelines.

Future investigations could incorporate longitudinal sampling of all bats in care to assess temporal viral shedding patterns, larger sample sizes, and paired virological sampling to evaluate the currently unknown risk of reverse zoonotic transmission (anthropozoonosis).

Critical gaps identified and recommendations

Volunteer wildlife rehabilitators represent a critical yet underappreciated component of native species conservation and public health protection. These dedicated individuals commit substantial personal time and financial resources while facing significant mental and physical health challenges, including burnout and injury risk. Their work serves dual conservation and public safety functions: preserving culturally and ecologically important native species while safely removing potentially dangerous animals from public contact.

Based on this chapter, several key recommendations emerge to support carer safety and effectiveness. Firstly, the establishment of standardised, Australia-specific safety guidelines for wildlife rehabilitation is urgently needed. Priority should be given to Australia-wide standardization of health department guidelines for bite response protocols, ensuring consistent, evidence-based emergency management across jurisdictions.

Secondly, while the majority of carers reported feeling adequately trained and resourced for self-protection, the development of evidence-based, context-specific safety protocols for different wildlife care scenarios would help standardise responses, particularly benefiting carers not affiliated with established organizations. These protocols should address the heterogeneity in current practices while incorporating the practical knowledge of experienced carers.

Thirdly, government initiatives should ensure affordable, appropriate PPE availability for volunteer carers. Importantly, support for evidence-based equipment modifications is needed—acknowledging and guiding practical PPE adaptations that balance safety with functionality.

Finally, it is essential to support wildlife carers in safely fulfilling their vital role by providing them with comprehensive, accessible information to inform their risk assessment and safety decisions. This includes transparent communication about zoonotic risks, practical guidance on risk mitigation, and acknowledgment of the valuable service they provide to both conservation and public health objectives.

These recommendations recognise that effective wildlife rehabilitation requires balancing conservation goals, public health protection, and carer safety, a complex challenge that requires coordinated, evidence-based policy responses and adequate resource allocation to support this critical volunteer workforce.

5.4. Appendix

5.4.1. Injury response patterns in wildlife workers, 2023

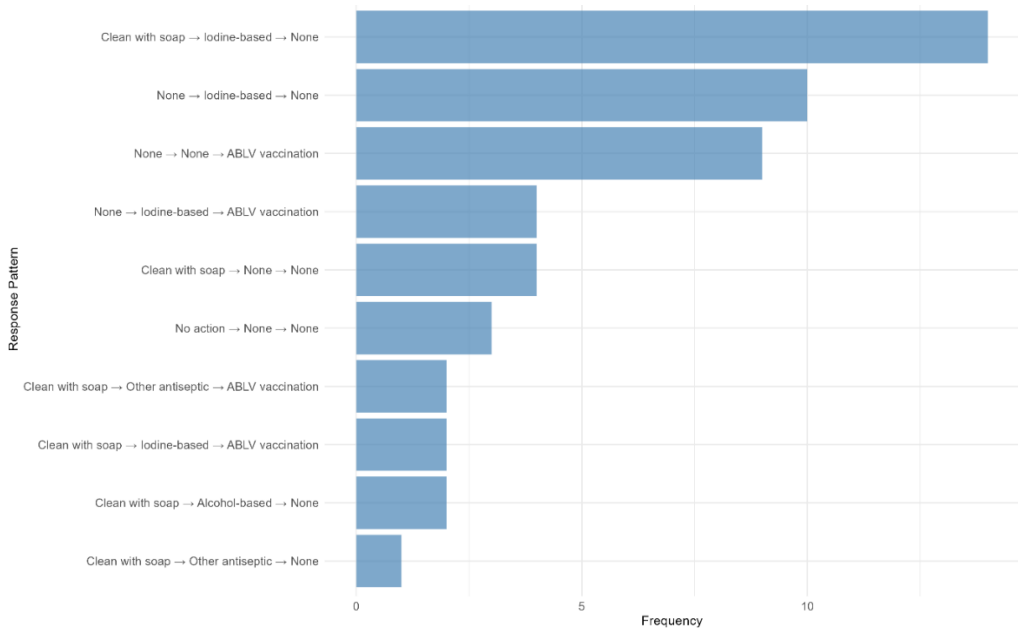


Figure 85 Most common injury response patterns in Australia wildlife workers, 2023

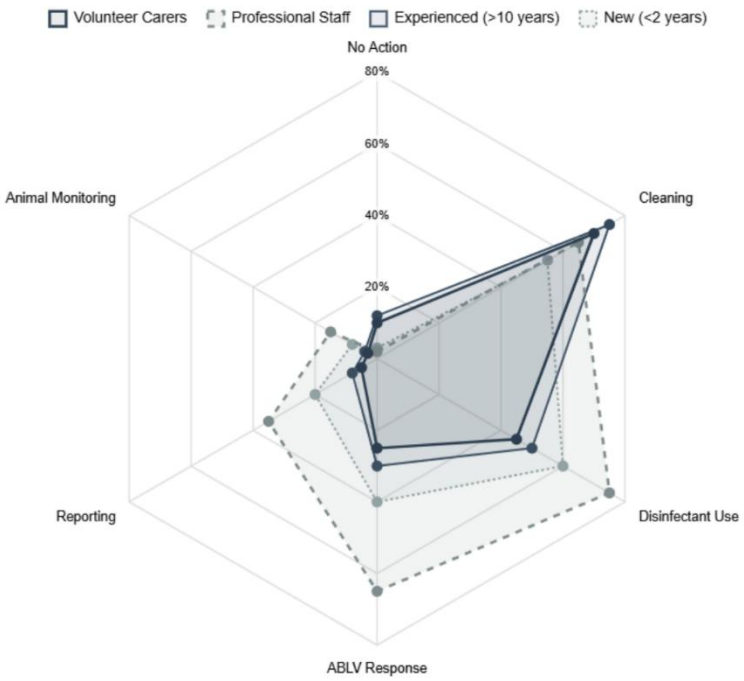


Figure 86 Thematic emphasis in flying fox injury and exposure responses across participant groups

5.4.2. Metagenomic sequencing of environmental bat samples

Screening of 8 pools sequenced by Illumina identified a total of 120397482 total reads, of which 86448235 (71.8%) were classified. Of the classified reads, a total of 103684 (0.12%) were viral with the percentage of viral reads ranging from 0.001% to 0.81% between the pools (Table 31).

Table 31 Kraken2 classification of Illumina reads

Pool	Total reads	No of reads classified	No of viral reads	% viral reads	Viruses
121	29,186,457	20,949,652	2,148	0.01	Parsus major densovirus, King virus
122	11,601,217	8,735,927	70,538	0.807	Parus major densovirus, Apple hammerhead viroid-like circular RNA
123	11,731,172	8,960,943	85	0.001	Papaya ringspot virus
124	10,488,790	5,854,969	81	0.001	
125	13,875,449	11,524,529	6,392	0.055	Papaya ringspot virus
126	23,424,518	16,826,424	24,249	0.144	Papaya ringspot virus, Watermelon crinkle leaf-associated virus 1 (Bunyavirales)
127	10,089,609	4,935,365	107	0.002	Papaya ringspot virus
128	10,000,270	8,660,426	84	0.001	Papaya ringspot virus

5.4.2.1. Plant viruses

The majority of viral sequences detected in faecal samples were classified to pathogenic plant viruses: Papaya ringspot and Watermelon crinkle leaf-associated virus 1 and 2. Across all samples, 19428387 bases from barcode 01, 02, 03, 04, 05, 06, 07, 08, 09 were classified to the Potyvirus family Papaya ringspot virus ranging from 91.1% (Barcode 01) to 93.9 % identity (Barcode 05). Across all samples, 272572 bases and 224485 bases were classified to the Coguvirus family Watermelon crinkle leaf-

associated virus 1 and 2 respectively, from barcodes 02, 05, 07 and 08 with identities ranging from 93.4% (Barcode 2) to 93.8% (Barcode 12).

5.4.2.2. Insect viruses

Many bases were classified to insect viruses, particularly members of the subfamily *Densovirinae*, family *Parvoviridae*. In Barcode 01, Nanopore mNGS pipeline v0.7 identified a total of 48 reads with a total of 19,751 bases had similarity to the family *Parvoviridae*, classified to 7 viral species including *Densovirinae* spp. (15,449 bases, 37 reads with 94.4% identity, E-value 10^{-203}), Pangolin densovirus A1 (1,572 bases, 4 reads with 93.0, E=10^{-200}), Pangolin densovirus T2 (2 reads, 945 bases, 91.8%, E=10^{-234}), Pangolin densovirus A3 (937 bases, 2 reads, 94.8%, E=10^{-253}). Reads assembled to parus major densovirus was detected in Barcode 01.

A human blood-associated dicistrovirus identified in barcode 05 had 92.8% similarity (4441 bases) to a dicistrovirus genome assembled with 11.8 x average coverage depth from a human blood sample from Cameroon [369]. Dicistroviruses – a sister family to the picornaviruses – normally infect invertebrates as the natural hosts, however, have been described in human febrile illnesses and human metagenomic studies.

5.4.2.3. Vertebrate viruses

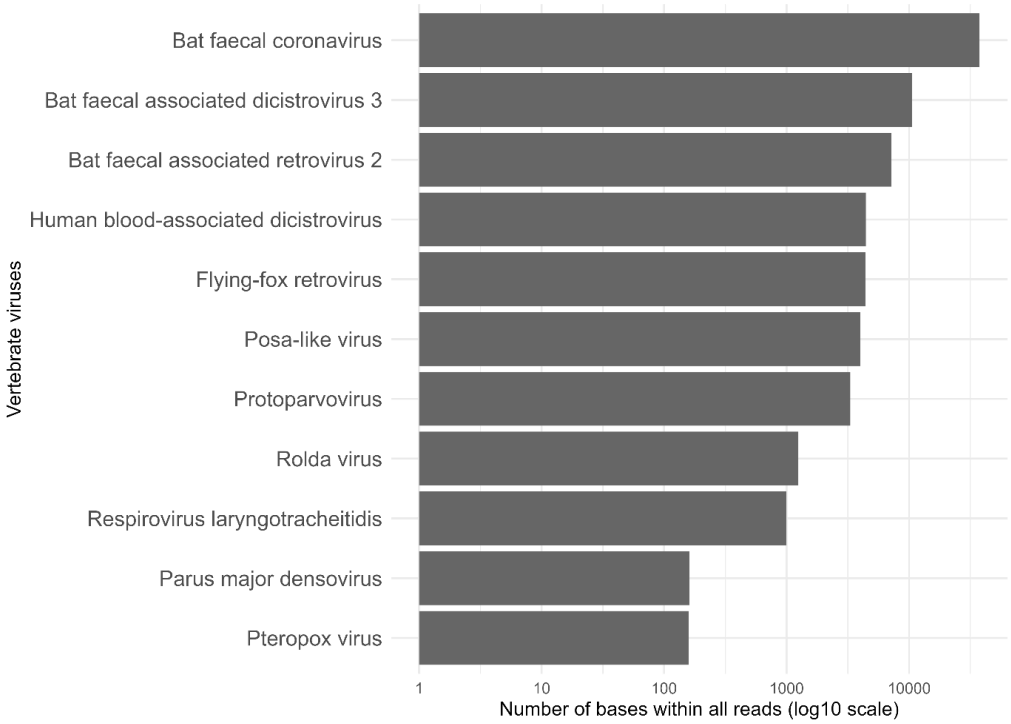


Table 32 Summary of reads classified to vertebrate viruses in Australian bat samples

5.4.2.4. Bacteriophages

Of the remaining viral reads, 271,744 bp (0.65%) had high similarity (>90%) to sequences of known phages, including Escherichia phage UPEC01 (94.5% identity), Klebsiella phage Kpn13 (98.4 % identity), Klebsiella phage Kpn12 (95.3% identity), Klebsiella phage Kpn74 (99.5% identity), Pseudomonas phage phiPA1-3 (98.3% identity), Salmonella phage Shemara (93.1% identity) and Yersinia phage YerA41 (93.0% identity).

Table 33 Select phages and uses, identified in Australian bat samples

Phage	Identity (%)	Target Bacterium	Type	Uses
Escherichia phage UPEC01	94.5	*Escherichia coli* (UPEC strains)	Gram-negative rod	Escherichia phage UPEC01 is a bacteriophage that specifically targets uropathogenic *Escherichia coli* (UPEC) which is the primary cause of urinary tract infections (UTIs) [382].
Klebsiella phage Kpn74	99.5	*Klebsiella pneumoniae*	Gram-negative rod	Therapeutic potential against multidrug-resistant *Klebsiella pneumoniae* [383]. *Klebsiella* spp. can cause a wide array of infections in humans including UTIs, pneumonia and respiratory tract infections, septicaemia, soft tissue and wound infections etc.
Klebsiella phage Kpn13	98.4	*Klebsiella pneumoniae*	Gram-negative rod	Therapeutic potential against multidrug-resistant *Klebsiella pneumoniae* [383]. Phages Kpn13 and Kpn12 have been specifically studied for their efficacy in treating *K. pneumoniae*-induced burn wound infections. In a mouse model, these phages significantly decreased mortality rates and bacterial counts in various organs when administered intraperitoneally [384].
Klebsiella phage Kpn12	95.3	*Klebsiella pneumoniae*	Gram-negative rod	Therapeutic potential against multidrug-resistant *Klebsiella pneumoniae* [383]. Phages Kpn13 and Kpn12 have been specifically studied for their efficacy in treating *K. pneumoniae*-

				induced burn wound infections. In a mouse model, these phages significantly decreased mortality rates and bacterial counts in various organs when administered intraperitoneally [384].
Pseudomonas phage phiPA1-3	98.3	*Pseudomonas aeruginosa*	Gram-negative rod	Therapeutic effect and anti-biofilm ability being assessed against multiple drug-resistant and carbapenem-resistant *P. aeruginosa* [385] which causes opportunistic infections in wounds, burns, lungs (e.g., cystic fibrosis).
Salmonella phage Shemara	93.1	*Salmonella enterica*	Gram-negative rod	Therapeutic, food safety or biocontrol potential against Salmonella infections, especially against antibiotic-resistant strains which causes foodborne illness (gastroenteritis, diarrhoea, typhoid fever depending on serovar) [386].
Yersinia phage YerA41	93.0	*Yersinia spp.*	Gram-negative rod	Yersinia phages could help control food contamination or serve as specific, sensitive tools for rapid bacterial detection in food products [387]. YerA41 is a Myoviridae bacteriophage originally isolated for its ability to infect *Yersinia ruckeri*, the causative agent of enteric redmouth disease in salmonid fish [388].

Chapter 6

Discussion

This thesis investigates the viral spillover of priority pathogens using a One Health, multi-pathogen serosurveillance model for characterising high-risk interfaces between humans, wildlife and the environment. In this final chapter, I summarise and discuss the main findings and conclusions from each chapter, and outline future directions for this work.

Performance of serological assays for filovirus antibody detection

The inherent biological, technical, and logistical complexities associated with Ebola serology must be carefully addressed to ensure accurate and reliable surveillance data. High assay sensitivity and specificity are critical, yet difficult to achieve due to inherent cross-reactivity among filovirus antigens and the dynamic, often waning nature of the humoral immune response. Filovirus serosurveillance is further challenged by the lack of established international standards, variability in assay performance, differences in antigen selection, and the complexities of standardizing protocols across laboratory settings.

In an attempt to address some of these challenges, I describe the use of an envelope glycoprotein (GP)-based MMIA, consisting of nine filovirus GP antigens, for the detection of anti-EBOV antibodies in a well-characterized cohort of Guinean Ebola virus disease (EVD) survivors and contacts from the 2013 – 2016 West African EVD outbreak. I demonstrate a 95.96% sensitivity and 98.61% specificity for the detection of anti-EBOV antibodies by GP expressed as recombinant trimeric ectodomains. Furthermore, I demonstrate strong agreement between the MMIA and a whole virus EBOV ELISA and authentic virus neutralization assay. Finally, I present the optimisation of a filovirus GP pseudotyped virus neutralisation assay for use as a surrogate for authentic virus neutralisation in assessing functional antibody responses. While both the MMIA and PVNA identified significant serological cross-reactivity induced by EBOV-infection against antigenically related filovirus species, a multiple antigen approach allowed for a side-by-side comparison of immunoreactivity, allowing for a degree of species differentiation.

Having demonstrated the suitability of these serological methods for the high-throughput surveillance of multiple pathogens in a filovirus endemic population, in Chapter 4, I apply them to the surveillance of a population of WLHs in Forested Guinea, Republic of Guinea.

Zoonotic filovirus exposure in WLHs in Forested Guinea (Guinée forestière), Republic of Guinea 2017 – 2023

In this chapter I characterise zoonotic filovirus spillover events in wildlife hunting communities in Forested Guinea and draw comparison to geographically distinct non-wildlife hunting cohorts in the United Kingdom, Uganda and urban Guinea.

A cohort of WLHs and close contacts were longitudinally sampled from 40 villages in 2017 (n=511) and 44 villages in 2023 (n=648) in Forested Guinea. Sera were screened with an MMIA panel of 9 filoviruses, demonstrating IgG binding against Ebola (EBOV) and filovirus species including Bundibugyo (BDBV), Taï Forest (TAFV), Bombali (BOMV), Lloviu (LLOV), Reston (RESTV) and Měnglà (MLAV) viruses. I applied a unique approach utilizing unsupervised machine learning clustering followed by parallel pseudotyped neutralisation assays in order to disentangle the cross-reactive antibody responses which often confound serosurveillance. This approach identified species-specific neutralisation of EBOV, BDBV and TAFV, as well as likely cross-neutralisation of BOMV, LLOV and MLAV, suggesting multiple zoonotic virus spillover events. Village- and household-level clustering of BDBV cases, as well as significant positive associations with the consumption of nonhuman primates in multivariable modelling, provide multiple lines of evidence for true spillover of multiple filovirus species. By comparison, non-wildlife hunting cohorts in urban Guinea and Uganda showed filovirus reactivity which was most plausibly explained by EBOV-only exposure.

The longitudinal nature of the Guinean WLH data demonstrates seroconversion to LLOV and MLAV over the 6 years, highlighting ongoing circulation in the region. Additionally, it allowed me to demonstrate the durability of the anti-EBOV antibody response 10 years post-outbreak, with antibody decay modelling estimating an IgG half-life of 7.5 years.

Statistical investigations of high-resolution satellite-derived land-cover data identified unique environmental risk factors for various filovirus species, including forest fragmentation, highlighting the importance of landscape configuration in driving pathogen spillover and providing insight into potentially differing transmission pathways.

In Chapter 5, I sought to apply similar methodologies to another high-risk human-wildlife interface, where reservoir hosts face environmental pressure.

Emerging viral infection surveillance in wildlife workers, Eastern Australia

Eastern Australia has been the site of multiple zoonotic spillover events (Hendra and Menangle virus) and novel virus isolations (Cedar, Yeppoon and Grove virus), all of which have implicated its urban and periurban colonies of *Pteropus* species fruit bats. Wildlife carers and rescuers report extensive exposure to flying foxes, however, with the exception of a 1995 serosurvey into HeV, no serological surveillance of this high-risk population has been reported.

I recruited and screened a cohort of wildlife rehabilitators, rescuers, veterinary and zoo professionals (n=109) from Far North Queensland, South-east Queensland, New South Wales and Victoria using an MMIA panel of 9 filovirus GP and 9 paramyxovirus attachment antigens, and found no difference in reactivity as compared to a UK-based control cohort (n=63). A metagenomic analysis of faecal, urine and saliva samples from in-care bats reflected a diverse virome (majority plant- and insect-derived), including partial bat faecal coronavirus sequences, but did not identify shedding of any of the paramyxoviruses of interest.

Participants had a median of 7 years of wildlife exposure, with 42.4% handling 5 – 50 individual flying foxes in an average year while others (8.7%) handling in excess of 500 flying foxes per year. All 4 mainland species of flying fox (black, grey-headed, little red and spectacled) were represented, with exposure reflecting their known geographic ranges.

Semi-structured interviews with participants (n=104) revealed significant heterogeneity in safety practices, with 30.7% using no personal protective equipment (PPE). Thematic responses reflected carers' situational decision-making, typically based on considerations such as the species, age, clinical presentation of the animal (neurological vs. healthy) and type of activity (caring vs. rescuing). Both PPE usage, post-exposure (bite, scratch etc.) responses, and perceptions of zoonotic risk varied by role, with veterinarians being significantly more likely to use PPE, adhere to medicalised post-exposure protocols and agree with the statement, "I am concerned about contracting an infection from wildlife". In an interesting dissonance between perception of risk and behaviour, of the 90.9% of respondents agreed they took "sufficient precautions", 26.6% did not use PPE.

In conclusion, despite prolonged close contact with high volumes of flying foxes over many years, often without PPE, participants were not seroreactive to HeV, MenV, CedV, YepV or GroV viruses, which are known to circulate in these species, providing the first observational evidence for the limited direct transmissibility of these paramyxoviruses in natural settings. However, these findings are not generalisable to all viruses of spillover potential, and standardized safety guidelines, improved PPE accessibility, and evidence-based training protocols are needed to support the critical conservation and public health work performed by volunteer wildlife rehabilitators.

Concluding remarks and future directions

Zoonotic spillover presents a global public health threat, but is a poorly understood phenomenon. High-risk interfaces often suffer from limited surveillance capacity, and the co-circulation of multiple antigenically related pathogens coupled with asymptomatic or paucisymptomatic infections obscures true disease burden. This thesis sought to address some of these knowledge gaps by investigating high-risk interfaces in areas with documented fatal spillover events (EBOV, MARV in Forested Guinea and HeV in Eastern Australia) which remain otherwise uncharacterised.

A commonly cited challenge of gaining a functional understanding of spillover is the complex ecology of host-host and virus-host interactions which must align for successful viral host-range shifts. These chapters demonstrate the value of integrated One Health surveillance that investigates the interlocking hierarchical levels of ecological, epidemiological and behavioural determinants of pathogen exposure. Future work investigating the distribution and intensity of infection in the reservoir hosts (through longitudinal viral detection and/or serology), quantifying pathogen pressure and human exposure (through environmental and bushmeat carcass sampling), and experimental investigations of host susceptibility would allow a more complete characterisation of these interfaces, enabling their use as model systems of spillover.

Serological surveillance represents an important opportunity to overcome the limitations of classical event-based disease surveillance, which relies on single-pathogen testing of infections when symptomatic individuals present for care. Such traditional approaches fail to detect infrequent spillover events, and are limited by asymptomatic infections, non-specific symptomology, heterogenous health-seeking behaviour and barriers to healthcare access. By contrast, high-throughput multi-pathogen platform technologies proved valuable in gaining a deeper understanding of the antigenic landscape in contexts like Forested Guinea with co-circulation of antigenically-related and novel pathogens. A natural extension of this work would employ pathogen-agnostic platforms, such as Phage ImmunoPrecipitation Sequencing (PhIP-Seq), which probes serum antibody-repertoire binding specificities using synthetic oligonucleotide libraries encoding peptide tiles spanning the entire human viral proteome. While a useful development, such phage-displayed peptidomes face the limitations of oligo synthesis (only up to 90 amino acids), and lack discontinuous epitopes, disulphide linkages, and post-translational modifications, therefore may perform optimally in combination with methodologies interrogating full-length, native proteins.

Advances in these platform technologies will require improved analytical methodologies to optimise the epidemiological inferences to be gained from multi-pathogen serological data. An extension of current work could involve refining the use of machine learning algorithms for the unsupervised clustering of high-dimensional data, and the inclusion of phylogenetic relationships as a model input.

Taken together, the findings of this thesis highlight the critical importance of improving the health and economic security of communities living in hotspots while safeguarding ecosystems from further deforestation, degradation and fragmentation. Expanding surveillance in high-risk populations not only enables early detection of emerging pathogens, but provides a foundation for developing targeted interventions which are acceptable to the at-risk communities. Strengthening local diagnostic capabilities through sustained capacity-building programs, collaborative partnerships, and the establishment of decentralised laboratory networks will be essential components of ongoing efforts to ensure global health and security.

References

1. Bernstein, A.S., et al., *The costs and benefits of primary prevention of zoonotic pandemics.* Science advances, 2022. **8**(5): p. eabl4183.
2. Greenwood, E.J., F. Schmidt, and J.L. Heeney, *The Evolution of SIV in Primates and the Emergence of the Pathogen of AIDS*, in *Primates, Pathogens, and Evolution*. 2013, Springer. p. 291–327.
3. Heeney, J.L., A.G. Dalgleish, and R.A. Weiss, *Origins of HIV and the evolution of resistance to AIDS.* Science, 2006. **313**(5786): p. 462–6.
4. Marani, M., et al., *Intensity and frequency of extreme novel epidemics.* Proceedings of the National Academy of Sciences, 2021. **118**(35): p. e2105482118.
5. Parrish, C.R., et al., *Cross-species virus transmission and the emergence of new epidemic diseases.* Microbiology and Molecular Biology Reviews, 2008. **72**(3): p. 457–470.
6. Smith, G.J.D., et al., *Origins and evolutionary genomics of the 2009 swine-origin H1N1 influenza A epidemic.* Nature, 2009. **459**(7250): p. 1122–1125.
7. Garten, R.J., et al., *Antigenic and Genetic Characteristics of Swine-Origin 2009 A(H1N1) Influenza Viruses Circulating in Humans.* Science, 2009. **325**(5937): p. 197–201.
8. Parrish, C.R., P.R. Murcia, and E.C. Holmes, *Influenza virus reservoirs and intermediate hosts: Dogs, horses, and new possibilities for influenza virus exposure of humans.* J Virol, 2015. **89**(6): p. 2990–2994.
9. Hood, G. and M. Carroll, *Host–pathogen interactions of emerging zoonotic viruses: bats, humans and filoviruses.* Current Opinion in Virology, 2024: p. 101436.
10. Wolfe, N.D., C.P. Dunavan, and J. Diamond, *Origins of major human infectious diseases.* Nature, 2007. **447**(7142): p. 279–283.
11. Morse, S.S., et al., *Prediction and prevention of the next pandemic zoonosis.* The Lancet, 2012. **380**(9857): p. 1956–1965.
12. Lloyd-Smith, J.O., et al., *Epidemic dynamics at the human-animal interface.* science, 2009. **326**(5958): p. 1362–1367.
13. Woolhouse, M.E. and S. Gowtage-Sequeria, *Host range and emerging and reemerging pathogens.* Emerging infectious diseases, 2005. **11**(12): p. 1842.
14. Alexander, K.A., et al., *The Ecology of Pathogen Spillover and Disease Emergence at the Human-Wildlife-Environment Interface*, in *The Connections Between Ecology and Infectious Disease*, C.J. Hurst, Editor. 2018, Springer International Publishing: Cham. p. 267–298.
15. Plowright, R.K., et al., *Pathways to zoonotic spillover.* Nature Reviews Microbiology, 2017. **15**(8): p. 502–510.
16. Belanov, E.F., et al., *[Survival of Marburg virus infectivity on contaminated surfaces and in aerosols].* Vopr Virusol, 1996. **41**(1): p. 32–4.
17. Pawęska, J.T., et al., *Shedding of Marburg Virus in Naturally Infected Egyptian Rousette Bats, South Africa, 2017.* Emerg Infect Dis, 2020. **26**(12): p. 3051–3055.
18. Amman, B.R., et al., *Seasonal pulses of Marburg virus circulation in juvenile Rousettus aegyptiacus bats coincide with periods of increased risk of human infection.* PLoS Pathog, 2012. **8**(10): p. e1002877.
19. Prescott, J., et al., *Postmortem stability of Ebola virus.* Emerging infectious diseases, 2015. **21**(5): p. 856.
20. Huijbregts, B., et al., *Ebola and the decline of gorilla Gorilla gorilla and chimpanzee Pan troglodytes populations in Minkebe Forest, north-eastern Gabon.* Oryx, 2003. **37**(4): p. 437–443.
21. Walsh, P.D., et al., *Catastrophic ape decline in western equatorial Africa.* Nature, 2003. **422**(6932): p. 611–4.
22. Rouquet, P., et al., *Wild animal mortality monitoring and human Ebola outbreaks, Gabon and Republic of Congo, 2001–2003.* Emerging infectious diseases, 2005. **11**(2): p. 283.
23. Bermejo, M., et al., *Ebola outbreak killed 5000 gorillas.* Science, 2006. **314**(5805): p. 1564.

24. Leroy, E.M., et al., *Multiple Ebola virus transmission events and rapid decline of central African wildlife.* Science, 2004. **303**(5656): p. 387–390.
25. Pourrut, X., et al., *Spatial and temporal patterns of Zaire ebolavirus antibody prevalence in the possible reservoir bat species.* The Journal of infectious diseases, 2007. **196**(Supplement_2): p. S176–S183.
26. Carette, J.E., et al., *Ebola virus entry requires the cholesterol transporter Niemann–Pick C1.* Nature, 2011. **477**(7364): p. 340–343.
27. Côté, M., et al., *Small molecule inhibitors reveal Niemann–Pick C1 is essential for Ebola virus infection.* Nature, 2011. **477**(7364): p. 344–348.
28. Batra, J., et al., *Protein interaction mapping identifies RBBP6 as a negative regulator of Ebola virus replication.* Cell, 2018. **175**(7): p. 1917–1930. e13.
29. Streicker, D.G., et al., *Host phylogeny constrains cross-species emergence and establishment of rabies virus in bats.* Science, 2010. **329**(5992): p. 676–679.
30. Kuiken, T., et al., *Host species barriers to influenza virus infections.* Science, 2006. **312**(5772): p. 394–397.
31. Longdon, B., et al., *The evolution and genetics of virus host shifts.* PLoS pathogens, 2014. **10**(11): p. e1004395.
32. Pulliam, J.R. and J. Dushoff, *Ability to replicate in the cytoplasm predicts zoonotic transmission of livestock viruses.* The Journal of infectious diseases, 2009. **199**(4): p. 565–568.
33. Jones, K.E., et al., *Global trends in emerging infectious diseases.* Nature, 2008. **451**(7181): p. 990–993.
34. Plowright, R.K., et al., *Land use-induced spillover: a call to action to safeguard environmental, animal, and human health.* Lancet Planet Health, 2021. **5**(4): p. e237–e245.
35. Kessler, M.K., et al., *Changing resource landscapes and spillover of henipaviruses.* Ann N Y Acad Sci, 2018. **1429**(1): p. 78–99.
36. Eby, P., et al., *Pathogen spillover driven by rapid changes in bat ecology.* Nature, 2022.
37. Olivero, J., et al., *Recent loss of closed forests is associated with Ebola virus disease outbreaks.* Sci Rep, 2017. **7**(1): p. 14291.
38. Rulli, M.C., et al., *The nexus between forest fragmentation in Africa and Ebola virus disease outbreaks.* Scientific reports, 2017. **7**(1): p. 41613.
39. Gibb, R., et al., *Zoonotic host diversity increases in human-dominated ecosystems.* Nature, 2020. **584**(7821): p. 398–402.
40. Mills, J.N., K.L. Gage, and A.S. Khan, *Potential influence of climate change on vector-borne and zoonotic diseases: a review and proposed research plan.* Environ Health Perspect, 2010. **118**(11): p. 1507–14.
41. Carlson, C.J., et al., *Climate change increases cross-species viral transmission risk.* Nature, 2022: p. 1–1.
42. Stephens, P.R., et al., *Characteristics of the 100 largest modern zoonotic disease outbreaks.* Philosophical Transactions of the Royal Society B, 2021. **376**(1837): p. 20200535.
43. Brierley, L., et al., *Quantifying global drivers of zoonotic bat viruses: a process-based perspective.* The American Naturalist, 2016. **187**(2): p. E53–E64.
44. Lee-Cruz, L., et al., *Mapping of Ebola virus spillover: Suitability and seasonal variability at the landscape scale.* PLoS Negl Trop Dis, 2021. **15**(8): p. e0009683.
45. Milbank, C. and B. Vira, *Wildmeat consumption and zoonotic spillover: contextualising disease emergence and policy responses.* Lancet Planet Health, 2022. **6**(5): p. e439–e448.
46. Stephens, P.R., et al., *Drivers of African Filovirus (Ebola and Marburg) Outbreaks.* Vector-Borne and Zoonotic Diseases, 2022. **22**(9): p. 478–490.
47. Fallah, M.P., et al., *Quantifying poverty as a driver of Ebola transmission.* PLoS neglected tropical diseases, 2015. **9**(12): p. e0004260.
48. Leroy, E.M., et al., *Human Ebola outbreak resulting from direct exposure to fruit bats in Luebo, Democratic Republic of Congo, 2007.* Vector-borne and zoonotic diseases, 2009. **9**(6): p. 723–728.
49. Kamins, A.O., et al., *Characteristics and risk perceptions of Ghanaians potentially exposed to bat-borne zoonoses through bushmeat.* EcoHealth, 2015. **12**(1): p. 104–120.

50. Languon, S. and O. Quaye, *Filovirus Disease Outbreaks: A Chronological Overview.* Virology (Auckl), 2019. **10**: p. 1178122x19849927.
51. Coltart, C.E., et al., *The Ebola outbreak, 2013-2016: old lessons for new epidemics.* Philos Trans R Soc Lond B Biol Sci, 2017. **372**(1721).
52. Georges, A.-J., et al., *Ebola hemorrhagic fever outbreaks in Gabon, 1994–1997: epidemiologic and health control issues.* The Journal of infectious diseases, 1999. **179**(Supplement_1): p. S65–S75.
53. Akoi Boré, J., et al., *Serological evidence of zoonotic filovirus exposure among bushmeat hunters in Guinea.* Nature Communications, 2024. **15**(1): p. 4171.
54. Richardson, E.T., et al., *Biosocial Approaches to the 2013-2016 Ebola Pandemic*. Health Hum Rights, 2016. **18**(1): p. 115–128.
55. Organization, W.H., *Pathogens Prioritization: A scientific framework for epidemic and pandemic research preparedness*. 2024, World Health Organization: Geneva. p. 38.
56. Olival, K.J. and D.T. Hayman, *Filoviruses in bats: current knowledge and future directions.* Viruses, 2014. **6**(4): p. 1759–88.
57. Velásquez, G.E., et al., *Time from infection to disease and infectiousness for Ebola virus disease, a systematic review.* Clinical Infectious Diseases, 2015. **61**(7): p. 1135–1140.
58. Baize, S., et al., *Defective humoral responses and extensive intravascular apoptosis are associated with fatal outcome in Ebola virus-infected patients.* Nature medicine, 1999. **5**(4): p. 423–426.
59. Sanchez, A., et al., *Analysis of human peripheral blood samples from fatal and nonfatal cases of Ebola (Sudan) hemorrhagic fever: cellular responses, virus load, and nitric oxide levels.* Journal of virology, 2004. **78**(19): p. 10370–10377.
60. Eisfeld, A.J., et al., *Multi-platform 'Omics Analysis of Human Ebola Virus Disease Pathogenesis.* Cell Host & Microbe, 2017. **22**(6): p. 817–829.e8.
61. Ruibal, P., et al., *Unique human immune signature of Ebola virus disease in Guinea.* Nature, 2016. **533**(7601): p. 100–104.
62. Nei, M. and S. Kumar, *Molecular Evolution and Phylogenetics*. 2000: Oxford University Press.
63. Saitou, N. and M. Nei, *The neighbor-joining method: a new method for reconstructing phylogenetic trees.* Molecular biology and evolution, 1987. **4**(4): p. 406–425.
64. Gascuel, O., *BIONJ: an improved version of the NJ algorithm based on a simple model of sequence data.* Molecular biology and evolution, 1997. **14**(7): p. 685–695.
65. Tamura, K., G. Stecher, and S. Kumar, *MEGA11: Molecular Evolutionary Genetics Analysis Version 11*. Molecular Biology and Evolution, 2021. **38**(7): p. 3022–3027.
66. Wan, W., et al., *Structure and assembly of the Ebola virus nucleocapsid.* Nature, 2017. **551**(7680): p. 394–397.
67. Leung, D.W., et al., *Ebolavirus VP35 is a multifunctional virulence factor.* Virulence, 2010. **1**(6): p. 526–31.
68. Johnson, K.A., et al., *The Ebola Virus matrix protein, VP40, requires phosphatidylinositol 4,5-bisphosphate (PI(4,5)P2) for extensive oligomerization at the plasma membrane and viral egress.* Scientific Reports, 2016. **6**(1): p. 19125.
69. Lee, J.E., et al., *Structure of the Ebola virus glycoprotein bound to an antibody from a human survivor.* Nature, 2008. **454**(7201): p. 177–182.
70. Volchkov, V.E., et al., *Processing of the Ebola virus glycoprotein by the proprotein convertase furin.* Proceedings of the National Academy of Sciences, 1998. **95**(10): p. 5762–5767.
71. Takada, A., et al., *A system for functional analysis of Ebola virus glycoprotein.* Proceedings of the National Academy of Sciences, 1997. **94**(26): p. 14764–14769.
72. Wool-Lewis, R.J. and P. Bates, *Characterization of Ebola virus entry by using pseudotyped viruses: identification of receptor-deficient cell lines.* Journal of virology, 1998. **72**(4): p. 3155–3160.
73. Martin, B., et al., *Filovirus proteins for antiviral drug discovery: A structure/function analysis of surface glycoproteins and virus entry.* Antiviral Research, 2016. **135**: p. 1–14.

74. Sanchez, A., et al., *The virion glycoproteins of Ebola viruses are encoded in two reading frames and are expressed through transcriptional editing.* Proceedings of the National Academy of Sciences, 1996. **93**(8): p. 3602–3607.
75. Sanchez, A., et al., *Biochemical analysis of the secreted and virion glycoproteins of Ebola virus.* Journal of virology, 1998. **72**(8): p. 6442–6447.
76. Mohan, G.S., et al., *Antigenic Subversion: A Novel Mechanism of Host Immune Evasion by Ebola Virus.* PLOS Pathogens, 2012. **8**(12): p. e1003065.
77. Geisbert, T.W., et al., *Pathogenesis of Ebola hemorrhagic fever in cynomolgus macaques: evidence that dendritic cells are early and sustained targets of infection.* The American journal of pathology, 2003. **163**(6): p. 2347–2370.
78. Bray, M. and T.W. Geisbert, *Ebola virus: the role of macrophages and dendritic cells in the pathogenesis of Ebola hemorrhagic fever.* The international journal of biochemistry & cell biology, 2005. **37**(8): p. 1560–1566.
79. Saeed, M.F., et al., *Cellular entry of ebola virus involves uptake by a macropinocytosis-like mechanism and subsequent trafficking through early and late endosomes.* PLoS pathogens, 2010. **6**(9): p. e1001110.
80. Mühlberger, E., et al., *Comparison of the transcription and replication strategies of Marburg virus and Ebola virus by using artificial replication systems.* Journal of virology, 1999. **73**(3): p. 2333–2342.
81. Bharat, T.A., et al., *Structural dissection of Ebola virus and its assembly determinants using cryo-electron tomography.* Proceedings of the National Academy of Sciences, 2012. **109**(11): p. 4275–4280.
82. Bausch, D.G. and L. Schwarz, *Outbreak of Ebola virus disease in Guinea: where ecology meets economy.* PLoS neglected tropical diseases, 2014. **8**(7): p. e3056.
83. Towner, J.S., et al., *Marburgvirus genomics and association with a large hemorrhagic fever outbreak in Angola.* Journal of virology, 2006. **80**(13): p. 6497–6516.
84. Carroll, S.A., et al., *Molecular evolution of viruses of the family Filoviridae based on 97 whole-genome sequences.* Journal of virology, 2013. **87**(5): p. 2608–2616.
85. Carroll, M.W., et al., *Temporal and spatial analysis of the 2014-2015 Ebola virus outbreak in West Africa.* Nature, 2015. **524**(7563): p. 97–101.
86. Kawuki, J., T.H. Musa, and X. Yu, *Impact of recurrent outbreaks of Ebola virus disease in Africa: a meta-analysis of case fatality rates.* Public Health, 2021. **195**: p. 89–97.
87. Heymann, D.L., et al., *Ebola hemorrhagic fever: lessons from Kikwit, Democratic Republic of the Congo.* The Journal of infectious diseases, 1999. **179**(Supplement_1): p. S283–S286.
88. World Health Organization, *Ebola haemorrhagic fever in Zaire, 1976.* Bull World Health Organ, 1978. **56**(2): p. 271–93.
89. World Health Organization, *Ebola haemorrhagic fever in Sudan, 1976.* Bull. World Health Organ, 1976. **56**: p. 247–270.
90. Judson, S.D., et al., *Ecological contexts of index cases and spillover events of different ebolaviruses.* PLoS pathogens, 2016. **12**(8): p. e1005780.
91. Marí Saéz, A., et al., *Investigating the zoonotic origin of the West African Ebola epidemic.* EMBO molecular medicine, 2015. **7**(1): p. 17–23.
92. Fairhead, J., M. Leach, and D. Millimouno, *Spillover or endemic? Reconsidering the origins of Ebola virus disease outbreaks by revisiting local accounts in light of new evidence from Guinea.* BMJ Global Health, 2021. **6**(4): p. e005783.
93. Grard, G., et al., *Emergence of divergent Zaire ebola virus strains in Democratic Republic of the Congo in 2007 and 2008.* The Journal of infectious diseases, 2011. **204**(suppl_3): p. S776–S784.
94. Keita, A.K., et al., *Resurgence of Ebola virus in 2021 in Guinea suggests a new paradigm for outbreaks.* Nature, 2021. **597**(7877): p. 539–543.
95. Kinganda-Lusamaki, E., et al., *Integration of genomic sequencing into the response to the Ebola virus outbreak in Nord Kivu, Democratic Republic of the Congo.* Nature medicine, 2021. **27**(4): p. 710–716.

96. Diallo, B., et al., *Resurgence of Ebola Virus Disease in Guinea Linked to a Survivor With Virus Persistence in Seminal Fluid for More Than 500 Days.* Clinical Infectious Diseases, 2016. **63**(10): p. 1353–1356.
97. Perry, D.L., et al., *Ebola virus localization in the macaque reproductive tract during acute Ebola virus disease.* The American Journal of Pathology, 2018. **188**(3): p. 550–558.
98. Zeng, X., et al., *Identification and pathological characterization of persistent asymptomatic Ebola virus infection in rhesus monkeys.* Nature microbiology, 2017. **2**(9): p. 1–11.
99. Sissoko, D., et al., *Ebola virus persistence in breast milk after no reported illness: a likely source of virus transmission from mother to child.* Clinical Infectious Diseases, 2017. **64**(4): p. 513–516.
100. Yeh, S., J.B. Varkey, and I. Crozier, *Persistent Ebola Virus in the Eye.* The New England journal of medicine, 2015. **373**(20): p. 1982–1983.
101. Meek, O., K. Fornace, and M.W. Carroll, *Ebola virus persistence: implications for human-to-human transmission and new outbreaks.* Exploration of Medicine, 2025. **6**: p. 1001333.
102. Liu, J., et al., *Ebola virus persistence and disease recrudescence in the brains of antibody-treated nonhuman primate survivors.* Science Translational Medicine, 2022. **14**(631): p. eabi5229.
103. Jacobs, M., et al., *Late Ebola virus relapse causing meningoencephalitis: a case report.* The Lancet, 2016. **388**(10043): p. 498–503.
104. Deen, G.F., et al., *Ebola RNA Persistence in Semen of Ebola Virus Disease Survivors - Final Report.* N Engl J Med, 2017. **377**(15): p. 1428–1437.
105. Thorson, A., et al., *Systematic review of the literature on viral persistence and sexual transmission from recovered Ebola survivors: evidence and recommendations.* BMJ open, 2016. **6**(1): p. e008859.
106. Blackley, D.J., et al., *Reduced evolutionary rate in reemerged Ebola virus transmission chains.* Science advances, 2016. **2**(4): p. e1600378.
107. Rodriguez, L., et al., *Persistence and genetic stability of Ebola virus during the outbreak in Kikwit, Democratic Republic of the Congo, 1995.* The Journal of infectious diseases, 1999. **179**(Supplement_1): p. S170–S176.
108. Varkey, J.B., et al., *Persistence of Ebola Virus in Ocular Fluid during Convalescence.* N Engl J Med, 2015. **372**(25): p. 2423–7.
109. Bower, H., et al., *Delivery of an Ebola virus-positive stillborn infant in a rural community health center, Sierra Leone, 2015.* The American journal of tropical medicine and hygiene, 2016. **94**(2): p. 417.
110. Thorson, A.E., et al., *Persistence of Ebola virus in semen among Ebola virus disease survivors in Sierra Leone: A cohort study of frequency, duration, and risk factors.* PLOS Medicine, 2021. **18**(2): p. e1003273.
111. Soka, M.J., et al., *Prevention of sexual transmission of Ebola in Liberia through a national semen testing and counselling programme for survivors: an analysis of Ebola virus RNA results and behavioural data.* The Lancet Global Health, 2016. **4**(10): p. e736–e743.
112. Sissoko, D., et al., *Persistence and clearance of Ebola virus RNA from seminal fluid of Ebola virus disease survivors: a longitudinal analysis and modelling study.* The Lancet Global Health, 2017. **5**(1): p. e80–e88.
113. Purpura, L.J., et al., *Ebola Virus RNA in Semen from an HIV-Positive Survivor of Ebola.* Emerg Infect Dis, 2017. **23**(4): p. 714–715.
114. Calain, P., L. Roux, and D. Kolakofsky, *Defective interfering genomes and Ebola virus persistence.* The Lancet, 2016. **388**(10045): p. 659–660.
115. Bosworth, A., et al., *Analysis of an Ebola virus disease survivor whose host and viral markers were predictive of death indicates the effectiveness of medical countermeasures and supportive care.* Genome medicine, 2021. **13**(1): p. 1–18.
116. Mate, S.E., et al., *Molecular evidence of sexual transmission of Ebola virus.* New England Journal of Medicine, 2015. **373**(25): p. 2448–2454.
117. Arias, A., et al., *Rapid outbreak sequencing of Ebola virus in Sierra Leone identifies transmission chains linked to sporadic cases.* Virus Evol, 2016. **2**(1): p. vew016.

118. Young, D.F., et al., *The switch between acute and persistent paramyxovirus infection caused by single amino acid substitutions in the RNA polymerase P subunit.* PLoS pathogens, 2019. **15**(2): p. e1007561.
119. Banadyga, L., et al., *Atypical Ebola virus disease in a nonhuman primate following monoclonal antibody treatment is associated with glycoprotein mutations within the fusion loop.* MBio, 2021. **12**(1): p. 10.1128/mbio. 01438–20.
120. Breman, J.G., et al., *A search for Ebola virus in animals in the Democratic Republic of the Congo and Cameroon: ecologic, virologic, and serologic surveys, 1979–1980.* The Journal of infectious diseases, 1999. **179**(Supplement_1): p. S139–S147.
121. Leirs, H., et al., *Search for the Ebola virus reservoir in Kikwit, Democratic Republic of the Congo: reflections on a vertebrate collection.* The Journal of infectious diseases, 1999. **179**(Supplement_1): p. S155–S163.
122. Reiter, P., et al., *Field investigations of an outbreak of Ebola hemorrhagic fever, Kikwit, Democratic Republic of the Congo, 1995: arthropod studies.* The Journal of infectious diseases, 1999. **179**(Supplement_1): p. S148–S154.
123. Pattyn, S.R. *Ebola virus haemorrhagic fever. Proceedings of an International Colloquium on Ebola Virus Infection and Other Haemorrhagic Fevers held in Antwerp, Belgium, 6-8 December, 1977*. in *Ebola virus haemorrhagic fever. Proceedings of an International Colloquium on Ebola Virus Infection and Other Haemorrhagic Fevers held in Antwerp, Belgium, 6-8 December, 1977.* 1978. Elsevier/North-Holland Biomedical Press, 335 Jan van Galenstraat, PO Box 211 ….
124. World Health Organization, *WHO-led collaborative study in Cote D'Ivoire to identify the natural host reservoir of the Ebola virus.* . 1995, Press Release WHO/93 Geneva.
125. Morvan, J.M., et al., *Identification of Ebola virus sequences present as RNA or DNA in organs of terrestrial small mammals of the Central African Republic.* Microbes and infection, 1999. **1**(14): p. 1193–1201.
126. Swanepoel, R., et al., *Experimental inoculation of plants and animals with Ebola virus.* Emerg Infect Dis, 1996. **2**(4): p. 321–5.
127. Turell, M.J., D.S. Bressler, and C.A. Rossi, *Short report: lack of virus replication in arthropods after intrathoracic inoculation of Ebola Reston virus.* Am J Trop Med Hyg, 1996. **55**(1): p. 89–90.
128. Leroy, E.M., et al., *Fruit bats as reservoirs of Ebola virus.* Nature, 2005. **438**(7068): p. 575–576.
129. Towner, J.S., et al., *Marburg virus infection detected in a common African bat.* PloS One, 2007. **2**(8): p. e764.
130. Schuh, A.J., et al., *Modelling filovirus maintenance in nature by experimental transmission of Marburg virus between Egyptian rousette bats.* Nat Commun, 2017. **8**: p. 14446.
131. Amman, B.R., et al., *Oral shedding of Marburg virus in experimentally infected Egyptian fruit bats (Rousettus aegyptiacus).* Journal of wildlife diseases, 2015. **51**(1): p. 113–124.
132. Jones, M.E., et al., *Experimental Inoculation of Egyptian Rousette Bats (Rousettus aegyptiacus) with Viruses of the Ebolavirus and Marburgvirus Genera.* Viruses, 2015. **7**(7): p. 3420–42.
133. Paweska, J.T., et al., *Experimental Inoculation of Egyptian Fruit Bats (Rousettus aegyptiacus) with Ebola Virus.* Viruses, 2016. **8**(2).
134. Swanepoel, R., et al., *Studies of reservoir hosts for Marburg virus.* Emerg Infect Dis, 2007. **13**(12): p. 1847–51.
135. Towner, J.S., et al., *Isolation of genetically diverse Marburg viruses from Egyptian fruit bats.* PLoS Pathog, 2009. **5**(7): p. e1000536.
136. Guito, J.C., et al., *Asymptomatic Infection of Marburg Virus Reservoir Bats Is Explained by a Strategy of Immunoprotective Disease Tolerance.* Curr Biol, 2021. **31**(2): p. 257–270.e5.
137. Caron, A., et al., *Ebola Virus Maintenance: If Not (Only) Bats, What Else?* Viruses, 2018. **10**(10).
138. Gryseels, S., et al., *Role of wildlife in emergence of Ebola virus in Kaigbono (Likati), Democratic Republic of the Congo, 2017.* Emerging infectious diseases, 2020. **26**(9): p. 2205.

139. Leendertz, S.A.J., et al., *Assessing the evidence supporting fruit bats as the primary reservoirs for Ebola viruses.* EcoHealth, 2016. **13**(1): p. 18–25.
140. Szentiványi, T., P. Christe, and O. Glaizot, *Bat flies and their microparasites: current knowledge and distribution.* Frontiers in Veterinary Science, 2019. **6**: p. 115.
141. Kemenesi, G., et al., *Isolation of infectious Lloviu virus from Schreiber's bats in Hungary.* Nature Communications, 2022. **13**(1): p. 1706.
142. Pourrut, X., et al., *Large serological survey showing cocirculation of Ebola and Marburg viruses in Gabonese bat populations, and a high seroprevalence of both viruses in Rousettus aegyptiacus.* BMC infectious diseases, 2009. **9**(1): p. 1–10.
143. Changula, K., et al., *Seroprevalence of filovirus infection of Rousettus aegyptiacus bats in Zambia.* The Journal of Infectious Diseases, 2018. **218**(suppl_5): p. S312–S317.
144. Kuzmin, I.V., et al., *Marburg virus in fruit bat, Kenya.* Emerging infectious diseases, 2010. **16**(2): p. 352.
145. Hayman, D.T., et al., *Ebola virus antibodies in fruit bats, Ghana, West Africa.* Emerg Infect Dis, 2012. **18**(7): p. 1207–9.
146. De Nys, H.M., et al., *Survey of Ebola viruses in frugivorous and insectivorous bats in Guinea, Cameroon, and the Democratic Republic of the Congo, 2015–2017.* Emerging infectious diseases, 2018. **24**(12): p. 2228.
147. Hayman, D.T., et al., *Long-term survival of an urban fruit bat seropositive for Ebola and Lagos bat viruses.* PloS one, 2010. **5**(8): p. e11978.
148. Ogawa, H., et al., *Seroepidemiological prevalence of multiple species of filoviruses in fruit bats (Eidolon helvum) migrating in Africa.* The Journal of infectious diseases, 2015. **212**(suppl_2): p. S101–S108.
149. Baker, M.L., M. Tachedjian, and L.-F. Wang, *Immunoglobulin heavy chain diversity in Pteropid bats: evidence for a diverse and highly specific antigen binding repertoire.* Immunogenetics, 2010. **62**(3): p. 173–184.
150. Yang, X.-L., et al., *Genetically diverse filoviruses in Rousettus and Eonycteris spp. bats, China, 2009 and 2015.* Emerging infectious diseases, 2017. **23**(3): p. 482.
151. Yuan, J., et al., *Serological evidence of ebolavirus infection in bats, China.* Virol J, 2012. **9**: p. 236.
152. Lebarbenchon, C., et al., *Bombali ebolavirus in Mops condylurus bats (Molossidae), Mozambique.* Emerging infectious diseases, 2022. **28**(12): p. 2583.
153. Forbes, K.M., et al., *Bombali virus in Mops condylurus bat, Kenya.* Emerging Infectious Diseases, 2019. **25**(5): p. 955.
154. Goldstein, T., et al., *The discovery of Bombali virus adds further support for bats as hosts of ebolaviruses.* Nature microbiology, 2018. **3**(10): p. 1084–1089.
155. Kareinen, L., et al., *Range expansion of Bombali virus in Mops condylurus bats, Kenya, 2019.* Emerging infectious diseases, 2020. **26**(12): p. 3007.
156. Ramírez de Arellano, E., et al., *First Evidence of Antibodies Against Lloviu Virus in Schreiber's Bent-Winged Insectivorous Bats Demonstrate a Wide Circulation of the Virus in Spain.* Viruses, 2019. **11**(4): p. 360.
157. Negredo, A., et al., *Discovery of an ebolavirus-like filovirus in Europe.* PLoS Pathog, 2011. **7**(10): p. e1002304.
158. Kemenesi, G., et al., *Re-emergence of Lloviu virus in Miniopterus schreibersii bats, Hungary, 2016.* Emerging microbes & infections, 2018. **7**(1): p. 1–4.
159. Murray, K., et al., *A Morbillivirus that Caused Fatal Fisease in Horses and Humans.* Science, 1995. **268**(5207): p. 94–97.
160. Chua, K.B., et al., *Fatal encephalitis due to Nipah virus among pig-farmers in Malaysia.* The Lancet, 1999. **354**(9186): p. 1257–1259.
161. Ching, P.K.G., et al., *Outbreak of henipavirus infection, Philippines, 2014.* Emerging infectious diseases, 2015. **21**(2): p. 328.
162. Pernet, O., et al., *Evidence for henipavirus spillover into human populations in Africa.* Nature Communications, 2014. **5**(1): p. 5342.
163. Marsh, G.A., et al., *Cedar virus: a novel Henipavirus isolated from Australian bats.* 2012.

164. Wu, Z., et al., *Novel Henipa-like virus, Mojiang Paramyxovirus, in rats, China, 2012.* Emerg Infect Dis, 2014. **20**(6): p. 1064–6.
165. Vanmechelen, B., et al., *The characterization of multiple novel paramyxoviruses highlights the diverse nature of the subfamily Orthoparamyxovirinae.* Virus Evolution, 2022. **8**(2).
166. Madera, S., et al., *Discovery and Genomic Characterization of a Novel Henipavirus, Angavokely Virus, from Fruit Bats in Madagascar.* J Virol, 2022. **96**(18): p. e0092122.
167. Rodriguez, J.J., C.D. Cruz, and C.M. Horvath, *Identification of the nuclear export signal and STAT-binding domains of the Nipah virus V protein reveals mechanisms underlying interferon evasion.* Journal of virology, 2004. **78**(10): p. 5358–5367.
168. Schountz, T., et al., *Differential innate immune responses elicited by Nipah virus and Cedar virus correlate with disparate in vivo pathogenesis in hamsters.* Viruses, 2019. **11**(3): p. 291.
169. Kolakofsky, D., et al., *Paramyxovirus mRNA editing, the 'rule of six'and error catastrophe: a hypothesis.* Journal of general virology, 2005. **86**(7): p. 1869–1877.
170. Xu, K., et al., *Host cell recognition by the henipaviruses: Crystal structures of the Nipah G attachment glycoprotein and its complex with ephrin-B3.* Proceedings of the National Academy of Sciences, 2008. **105**(29): p. 9953–9958.
171. Dhondt, K.P., et al., *Type I interferon signaling protects mice from lethal henipavirus infection.* J Infect Dis, 2013. **207**(1): p. 142–51.
172. Oguntuyo Kasopefoluwa, Y., et al., *Structure-guided mutagenesis of Henipavirus receptor-binding proteins reveals molecular determinants of receptor usage and antibody-binding epitopes.* Journal of Virology, 2024. **98**(3): p. e01838–23.
173. Gamble, A., et al. *Drivers and Distribution of Henipavirus-Induced Syncytia: What Do We Know?* Viruses, 2021. **13**, DOI: 10.3390/v13091755.
174. Juman, M.M., O. Restif, and D.J. Becker, *Paramyxoviruses in Old World fruit bats (Pteropodidae): an open database and synthesis of sampling effort, viral positivity, and coevolution.* bioRxiv, 2025: p. 2025.03.10.642350.
175. Geldenhuys, M., et al., *Overview of Bat and Wildlife Coronavirus Surveillance in Africa: A Framework for Global Investigations.* Viruses, 2021. **13**(5).
176. Becker, D.J., et al., *Temporal and spatial limitations in global surveillance for bat filoviruses and henipaviruses.* Biol Lett, 2019. **15**(12): p. 20190423.
177. Venette, R.C., R.D. Moon, and W.D. Hutchison, *Strategies and statistics of sampling for rare individuals.* Annual review of entomology, 2002. **47**: p. 143.
178. He, B., et al., *Filovirus RNA in fruit bats, China.* Emerging infectious diseases, 2015. **21**(9): p. 1675.
179. Yang, X.L., et al., *Characterization of a filovirus (Měnglà virus) from Rousettus bats in China.* Nat Microbiol, 2019. **4**(3): p. 390–395.
180. Shi, M., et al., *The evolutionary history of vertebrate RNA viruses.* Nature, 2018. **556**(7700): p. 197–202.
181. Karan, L.S., et al., *Bombali virus in Mops condylurus bats, Guinea.* Emerging infectious diseases, 2019. **25**(9): p. 1774.
182. Phelps, K.L., et al., *Bat Research Networks and Viral Surveillance: Gaps and Opportunities in Western Asia.* Viruses, 2019. **11**(3).
183. Crowley, D., et al., *Identifying Suspect Bat Reservoirs of Emerging Infections.* Vaccines (Basel), 2020. **8**(2).
184. Plowright, R.K., et al., *Ecological dynamics of emerging bat virus spillover.* Proceedings of the royal society B: biological sciences, 2015. **282**(1798): p. 20142124.
185. Anderson, R.M. and R.M. May, *Population biology of infectious diseases: Part I.* Nature, 1979. **280**(5721): p. 361–367.
186. Paweska, J.T., et al., *Virological and serological findings in Rousettus aegyptiacus experimentally inoculated with vero cells-adapted hogan strain of Marburg virus.* PloS One, 2012. **7**(9): p. e45479.
187. Calisher, C.H., et al., *Bats: important reservoir hosts of emerging viruses.* Clinical microbiology reviews, 2006. **19**(3): p. 531–545.

188. Wang, L.-F., P.J. Walker, and L.L.M. Poon, *Mass extinctions, biodiversity and mitochondrial function: are bats 'special' as reservoirs for emerging viruses?* Current Opinion in Virology, 2011. **1**(6): p. 649–657.
189. Baker, M., T. Schountz, and L.F. Wang, *Antiviral immune responses of bats: a review.* Zoonoses and public health, 2013. **60**(1): p. 104–116.
190. Görföl, T., et al., *Lloviu Virus in Europe is an Emerging Disease of Concern.* EcoHealth, 2022. **19**(1): p. 5–7.
191. Brook, C.E. and A.P. Dobson, *Bats as 'special' reservoirs for emerging zoonotic pathogens.* Trends Microbiol, 2015. **23**(3): p. 172–80.
192. Luis, A.D., et al., *A comparison of bats and rodents as reservoirs of zoonotic viruses: are bats special?* Proc Biol Sci, 2013. **280**(1756): p. 20122753.
193. Olival, K.J., et al., *Host and viral traits predict zoonotic spillover from mammals.* Nature, 2017. **546**(7660): p. 646–650.
194. Mollentze, N. and D.G. Streicker, *Viral zoonotic risk is homogenous among taxonomic orders of mammalian and avian reservoir hosts.* Proceedings of the National Academy of Sciences, 2020. **117**(17): p. 9423–9430.
195. Cui, J., et al., *Evolutionary relationships between bat coronaviruses and their hosts.* Emerging infectious diseases, 2007. **13**(10): p. 1526.
196. Xie, J., et al., *Dampened STING-Dependent Interferon Activation in Bats.* Cell Host Microbe, 2018. **23**(3): p. 297–301.e4.
197. Ahn, M., et al., *Dampened NLRP3-mediated inflammation in bats and implications for a special viral reservoir host.* Nature microbiology, 2019. **4**(5): p. 789–799.
198. Ahn, M., et al., *Unique loss of the PYHIN gene family in bats amongst mammals: implications for inflammasome sensing.* Scientific reports, 2016. **6**(1): p. 1–7.
199. Kuzmin, I.V., et al., *Innate immune responses of bat and human cells to filoviruses: commonalities and distinctions.* Journal of virology, 2017. **91**(8): p. e02471–16.
200. Wynne, J.W., et al., *Comparative transcriptomics highlights the role of the activator protein 1 transcription factor in the host response to ebolavirus.* Journal of virology, 2017. **91**(23): p. e01174–17.
201. Holzer, M., et al., *Differential transcriptional responses to Ebola and Marburg virus infection in bat and human cells. Sci Rep 6: 34589*. 2016.
202. Goh, G., et al., *Complementary regulation of caspase-1 and IL-1β reveals additional mechanisms of dampened inflammation in bats.* Proceedings of the National Academy of Sciences, 2020. **117**(46): p. 28939–28949.
203. Zhang, D. and A.T. Irving, *Antiviral effects of interferon-stimulated genes in bats.* Front Cell Infect Microbiol, 2023. **13**: p. 1224532.
204. Bondet, V., et al., *Constitutive IFNα protein production in bats.* Frontiers in Immunology, 2021. **12**: p. 735866.
205. Zhou, P., et al., *Contraction of the type I IFN locus and unusual constitutive expression of IFN-α in bats.* Proceedings of the National Academy of Sciences, 2016. **113**(10): p. 2696–2701.
206. Chionh, Y.T., et al., *High basal heat-shock protein expression in bats confers resistance to cellular heat/oxidative stress.* Cell Stress Chaperones, 2019. **24**(4): p. 835–849.
207. Koh, J., et al., *ABCB1 protects bat cells from DNA damage induced by genotoxic compounds.* Nature communications, 2019. **10**(1): p. 1–14.
208. Laing, E.D., et al., *Enhanced Autophagy Contributes to Reduced Viral Infection in Black Flying Fox Cells.* Viruses, 2019. **11**(3): p. 260.
209. Irving, A.T., et al., *Lessons from the host defences of bats, a unique viral reservoir.* Nature, 2021. **589**(7842): p. 363–370.
210. Pavlovich, S.S., et al., *The Egyptian rousette genome reveals unexpected features of bat antiviral immunity.* Cell, 2018. **173**(5): p. 1098–1110. e18.
211. Arnold, C.E., et al., *Transcriptomics reveal antiviral gene induction in the Egyptian rousette bat is antagonized in vitro by Marburg virus infection.* Viruses, 2018. **10**(11): p. 607.
212. Lee, A.K., et al., *De novo transcriptome reconstruction and annotation of the Egyptian rousette bat.* BMC genomics, 2015. **16**(1): p. 1–11.

213. Prendergast, B.J., et al., *Periodic arousal from hibernation is necessary for initiation of immune responses in ground squirrels.* American Journal of Physiology-Regulatory, Integrative and Comparative Physiology, 2002. **282**(4): p. R1054–R1062.
214. Bouma, H.R., H.V. Carey, and F.G. Kroese, *Hibernation: the immune system at rest?* Journal of leukocyte biology, 2010. **88**(4): p. 619–624.
215. George, D.B., et al., *Host and viral ecology determine bat rabies seasonality and maintenance.* Proceedings of the National Academy of Sciences, 2011. **108**(25): p. 10208–10213.
216. O'Shea, T.J., et al., *Bat flight and zoonotic viruses.* Emerging infectious diseases, 2014. **20**(5): p. 741.
217. Levesque, D., et al., *High Body Temperature is an Unlikely Cause of High Viral Tolerance in Bats.* Journal of Wildlife Diseases, 2021. **57**(1): p. 238–241.
218. Miller, M.R., et al., *Broad and temperature independent replication potential of filoviruses on cells derived from old and new world bat species.* The Journal of Infectious Diseases, 2016. **214**(suppl_3): p. S297–S302.
219. Arnold, B.F., et al., *Integrated Serologic Surveillance of Population Immunity and Disease Transmission.* Emerg Infect Dis, 2018. **24**(7): p. 1188–1194.
220. Thom, R., et al., *Longitudinal antibody and T cell responses in Ebola virus disease survivors and contacts: an observational cohort study.* The Lancet Infectious Diseases, 2021. **21**(4): p. 507–516.
221. Bore, J.A., *Seroprevalence of Ebola and Lassa virus in the Republic of Guinea, Macenta prefecture*, in *School of Biosciences*. 2020, University of Kent: Kent. p. 150.
222. Thompson, C.P., et al., *Detection of neutralising antibodies to SARS-CoV-2 to determine population exposure in Scottish blood donors between March and May 2020.* Euro Surveill, 2020. **25**(42).
223. Roe, M.D., et al., *Performance of an envelope glycoprotein-based multiplex immunoassay for Ebola virus antibody detection in a cohort of Ebola virus disease survivors.* Journal of Virological Methods, 2024: p. 115057.
224. Steeds, K., et al., *Pseudotyping of VSV with Ebola virus glycoprotein is superior to HIV-1 for the assessment of neutralising antibodies.* Scientific Reports, 2020. **10**(1): p. 14289.
225. Zufferey, R., et al., *Multiply attenuated lentiviral vector achieves efficient gene delivery in vivo.* Nature biotechnology, 1997. **15**(9): p. 871–875.
226. Jacks, T., et al., *Characterization of ribosomal frameshifting in HIV-1 gag-pol expression.* Nature, 1988. **331**(6153): p. 280–283.
227. Engelman, A. and P. Cherepanov, *The structural biology of HIV-1: mechanistic and therapeutic insights.* Nature Reviews Microbiology, 2012. **10**(4): p. 279–290.
228. Niwa, H., K. Yamamura, and J. Miyazaki, *Efficient selection for high-expression transfectants with a novel eukaryotic vector.* Gene, 1991. **108**(2): p. 193–9.
229. Edgar, R.C., *MUSCLE: multiple sequence alignment with high accuracy and high throughput.* Nucleic Acids Res, 2004. **32**(5): p. 1792–7.
230. Kangro, H.O. and B.W. Mahy, *Virology methods manual*. 1996: Elsevier.
231. Crawford, K.H., et al., *Protocol and reagents for pseudotyping lentiviral particles with SARS-CoV-2 spike protein for neutralization assays.* Viruses, 2020. **12**(5): p. 513.
232. Amaya, M., et al., *A recombinant Cedar virus based high-throughput screening assay for henipavirus antiviral discovery.* Antiviral Res, 2021. **193**: p. 105084.
233. Laing, E.D., et al., *Rescue and characterization of recombinant cedar virus, a non-pathogenic Henipavirus species.* Virology journal, 2018. **15**: p. 1–12.
234. Reyes, G.R. and J.P. Kim, *Sequence-independent, single-primer amplification (SISPA) of complex DNA populations.* Mol Cell Probes, 1991. **5**(6): p. 473–81.
235. Wood, D.E. and S.L. Salzberg, *Kraken: ultrafast metagenomic sequence classification using exact alignments.* Genome Biology, 2014. **15**(3): p. R46.
236. Bankevich, A., et al., *SPAdes: a new genome assembly algorithm and its applications to single-cell sequencing.* Journal of computational biology, 2012. **19**(5): p. 455–477.
237. Altschul, S.F., et al., *Basic local alignment search tool.* Journal of molecular biology, 1990. **215**(3): p. 403–410.

238. Li, H., *Aligning sequence reads, clone sequences and assembly contigs with BWA-MEM.* arXiv preprint arXiv:1303.3997, 2013.
239. Li, H., *Minimap2: pairwise alignment for nucleotide sequences.* Bioinformatics, 2018. **34**(18): p. 3094–3100.
240. Li, H., et al., *The sequence alignment/map format and SAMtools.* bioinformatics, 2009. **25**(16): p. 2078–2079.
241. Fujii, Y., et al., *Serological Surveillance Development for Tropical Infectious Diseases Using Simultaneous Microsphere-Based Multiplex Assays and Finite Mixture Models.* PLOS Neglected Tropical Diseases, 2014. **8**(7): p. e3040.
242. Vyse, A.J., et al., *Interpreting serological surveys using mixture models: the seroepidemiology of measles, mumps and rubella in England and Wales at the beginning of the 21st century.* Epidemiology & Infection, 2006. **134**(6): p. 1303–1312.
243. Maechler, M., *Cluster: cluster analysis basics and extensions.* R package version 2.0. 7–1, 2018.
244. Kassambara, A. and F. Mundt, *Extract and visualize the results of multivariate data analyses [R package factoextra version 1.0. 7].* Comprehensive R Archive Network (CRAN), 2020.
245. Rousseeuw, P.J., *Silhouettes: a graphical aid to the interpretation and validation of cluster analysis.* Journal of computational and applied mathematics, 1987. **20**: p. 53–65.
246. Tibshirani, R., G. Walther, and T. Hastie, *Estimating the number of clusters in a data set via the gap statistic.* Journal of the royal statistical society: series b (statistical methodology), 2001. **63**(2): p. 411–423.
247. Flowers, B., K.-T. Huang, and G.O. Aldana, *Analysis of the habitat fragmentation of ecosystems in Belize using landscape metrics.* Sustainability, 2020. **12**(7): p. 3024.
248. Liu, Z., C. He, and J. Wu, *The relationship between habitat loss and fragmentation during urbanization: an empirical evaluation from 16 world cities.* PLoS One, 2016. **11**(4): p. e0154613.
249. Longet, S., et al., *Influence of Landscape Patterns on Exposure to Lassa Fever Virus, Guinea.* Emerg Infect Dis, 2023. **29**(2): p. 304–313.
250. Brock, P.M., et al., *Predictive analysis across spatial scales links zoonotic malaria to deforestation.* Proceedings of the Royal Society B, 2019. **286**(1894): p. 20182351.
251. Hesselbarth, M.H., et al., *landscapemetrics: an open-source R tool to calculate landscape metrics.* Ecography, 2019. **42**(10): p. 1648–1657.
252. Fornace, K.M., et al., *Environmental risk factors and exposure to the zoonotic malaria parasite Plasmodium knowlesi across northern Sabah, Malaysia: a population-based cross-sectional survey.* The Lancet Planetary Health, 2019. **3**(4): p. e179–e186.
253. Bates, D., et al., *Fitting linear mixed-effects models using lme4.* Journal of statistical software, 2015. **67**: p. 1–48.
254. Pattyn, S., et al., *Isolation of Marburg-like virus from a case of haemorrhagic fever in Zaire.* Lancet, 1977: p. 573–574.
255. Wulff, H. and J.V. Lange, *Indirect immunofluorescence for the diagnosis of Lassa fever infection.* Bulletin of the World Health Organization, 1975. **52**(4-6): p. 429.
256. Broadhurst, M.J., J.G. Brooks Tim, and R. Pollock Nira, *Diagnosis of Ebola Virus Disease: Past, Present, and Future.* Clinical Microbiology Reviews, 2016. **29**(4): p. 773–793.
257. Rimoin, A.W., et al., *Ebola virus neutralizing antibodies detectable in survivors of the Yambuku, Zaire outbreak 40 years after infection.* The Journal of infectious diseases, 2018. **217**(2): p. 223–231.
258. Ksiazek, T.G., et al., *ELISA for the Detection of Antibodies to Ebola Viruses.* The Journal of Infectious Diseases, 1999. **179**(Supplement_1): p. S192–S198.
259. Saijo, M., et al., *Laboratory diagnostic systems for Ebola and Marburg hemorrhagic fevers developed with recombinant proteins.* Clinical and Vaccine Immunology, 2006. **13**(4): p. 444–451.
260. Logue, J., et al., *Use of the Filovirus Animal Non-Clinical Group (FANG) Ebola virus immuno-assay requires fewer study participants to power a study than the Alpha Diagnostic International assay.* J Virol Methods, 2018. **255**: p. 84–90.

261. Ayouba, A., et al., *Development of a Sensitive and Specific Serological Assay Based on Luminex Technology for Detection of Antibodies to Zaire Ebola Virus.* J Clin Microbiol, 2017. **55**(1): p. 165–176.
262. O'Hearn, A.E., et al., *Serosurveillance of viral pathogens circulating in West Africa.* Virology journal, 2016. **13**(1): p. 163.
263. Graham, H., D.J. Chandler, and S.A. Dunbar, *The genesis and evolution of bead-based multiplexing.* Methods, 2019. **158**: p. 2–11.
264. Satterly Neal, G., et al., *Comparison of MagPix Assays and Enzyme-Linked Immunosorbent Assay for Detection of Hemorrhagic Fever Viruses.* Journal of Clinical Microbiology, 2016. **55**(1): p. 68–78.
265. Cao, Z., et al., *The Application of a Safe Neutralization Assay for Ebola Virus Using Lentivirus-Based Pseudotyped Virus.* Virol Sin, 2021. **36**(6): p. 1648–1651.
266. Kainulainen, M.H., et al., *A public, cross-reactive glycoprotein epitope confounds Ebola virus serology.* Journal of Medical Virology, 2024. **96**(10): p. e29946.
267. Krähling, V., et al., *Development of an antibody capture ELISA using inactivated Ebola Zaire Makona virus.* Med Microbiol Immunol, 2016. **205**(2): p. 173–83.
268. Jayanthi, W., et al., *Development of Pandemic Vaccines: ERVEBO Case Study.* Vaccines, 2021.
269. Wilkinson, D.E., et al., *Comparison of platform technologies for assaying antibody to Ebola virus.* Vaccine, 2017. **35**(9): p. 1347–1352.
270. Bentley, E.M., et al., *Cross-Neutralisation of Novel Bombali Virus by Ebola Virus Antibodies and Convalescent Plasma Using an Optimised Pseudotype-Based Neutralisation Assay.* Trop Med Infect Dis, 2021. **6**(3).
271. Flyak, A.I., et al., *Cross-Reactive and Potent Neutralizing Antibody Responses in Human Survivors of Natural Ebolavirus Infection.* Cell, 2016. **164**(3): p. 392–405.
272. Misasi, J., et al., *Structural and molecular basis for Ebola virus neutralization by protective human antibodies.* Science, 2016. **351**(6279): p. 1343–6.
273. Wilson, J.A., et al., *Epitopes involved in antibody-mediated protection from Ebola virus.* Science, 2000. **287**(5458): p. 1664–6.
274. MacNeil, A., Z. Reed, and P.E. Rollin, *Serologic cross-reactivity of human IgM and IgG antibodies to five species of Ebola virus.* PLoS Negl Trop Dis, 2011. **5**(6): p. e1175–e1175.
275. Gayedyu-Dennis, D., et al., *Identifying Paucisymptomatic or Asymptomatic and Unrecognized Ebola Virus Disease Among Close Contacts Based on Exposure Risk Assessments and Screening Algorithms.* J Infect Dis, 2023. **227**(7): p. 878–887.
276. Fuentes, S., et al., *Human Antibody Repertoire following Ebola Virus Infection and Vaccination.* iScience, 2020. **23**(3): p. 100920.
277. Timothy, J.W., et al., *Early transmission and case fatality of Ebola virus at the index site of the 2013–16 west African Ebola outbreak: a cross-sectional seroprevalence survey.* The Lancet Infectious Diseases, 2019. **19**(4): p. 429–438.
278. Koundouno, F.R., et al., *Detection of Marburg Virus Disease in Guinea.* N Engl J Med, 2022. **386**(26): p. 2528–2530.
279. Eby, P., et al., *Pathogen spillover driven by rapid changes in bat ecology.* Nature, 2022: p. 1–3.
280. Rulli, M.C., et al., *The nexus between forest fragmentation in Africa and Ebola virus disease outbreaks.* Scientific reports, 2017. **7**(1): p. 1–8.
281. Pourrut, X., et al., *The natural history of Ebola virus in Africa.* Microbes Infect, 2005. **7**(7-8): p. 1005–14.
282. Makenov, M.T., et al., *Marburg virus in Egyptian Rousettus bats in Guinea: investigation of Marburg virus outbreak origin in 2021.* PLoS Neglected Tropical Diseases, 2023. **17**(4): p. e0011279.
283. Seifert, S.N., et al., *Zaire ebolavirus surveillance near the Bikoro region of the Democratic Republic of the Congo during the 2018 outbreak reveals presence of seropositive bats.* PLOS Neglected Tropical Diseases, 2022. **16**(6): p. e0010504.
284. Lauri, K., et al., *Range Expansion of Bombali Virus in Mops condylurus Bats, Kenya, 2019.* Emerging infectious diseases, 2020.

285. Camille, L., et al., *Bombali Ebolavirus in Mops condylurus Bats (Molossidae), Mozambique.* Emerging infectious diseases, 2022.
286. Tóth, G.E., et al., *Isolation and genome characterization of Lloviu virus from Italian Schreibers's bats.* Scientific Reports, 2023. **13**(1): p. 11310.
287. Jahrling, P., et al., *Preliminary report: isolation of Ebola virus from monkeys imported to USA.* The lancet, 1990. **335**(8688): p. 502–505.
288. Formenty, P., et al., *Ebola virus outbreak among wild chimpanzees living in a rain forest of Cote d'Ivoire.* The Journal of infectious diseases, 1999. **179**(Supplement_1): p. S120–S126.
289. Le Guenno, B., et al., *Isolation and partial characterisation of a new strain of Ebola virus.* The lancet, 1995. **345**(8960): p. 1271–1274.
290. Formenty, P., et al., *Human infection due to Ebola virus, subtype Côte d'Ivoire: clinical and biologic presentation.* J Infect Dis, 1999. **179 Suppl 1**: p. S48–53.
291. Dobbs, K.R., A. Lobb, and A.E. Dent, *Ebola virus disease in children: epidemiology, pathogenesis, management, and prevention.* Pediatric Research, 2024. **95**(2): p. 488–495.
292. Diallo, M.S.K., et al., *Temporal evolution of the humoral antibody response after Ebola virus disease in Guinea: a 60-month observational prospective cohort study.* The Lancet Microbe, 2021. **2**(12): p. e676–e684.
293. Bower, H. and J.R. Glynn, *A systematic review and meta-analysis of seroprevalence surveys of ebolavirus infection.* Scientific data, 2017. **4**(1): p. 1–9.
294. Ramassamy, J.-L., et al., *High Seroreactivities to Orthoebolaviruses in Rural Cameroon: A Case-Control Study on Nonhuman Primate Bites and a Cross-sectional Survey in Rural Populations.* The Journal of Infectious Diseases, 2024. **230**(5): p. e1067–e1076.
295. Semancik, C.S., et al., *Prevalence of human filovirus infections in sub-Saharan Africa: A systematic review and meta-analysis protocol.* Systematic reviews, 2024. **13**(1): p. 218.
296. Surtees, R., et al., *Development of a multiplex microsphere immunoassay for the detection of antibodies against highly pathogenic viruses in human and animal serum samples.* PLoS Neglected Tropical Diseases, 2020. **14**(10): p. e0008699.
297. Steffen, I., et al., *Serologic prevalence of Ebola virus in equatorial Africa.* Emerging infectious diseases, 2019. **25**(5): p. 911.
298. Knobloch, J., E.J. Albiez, and H. Schmitz, *A serological survey on viral haemorrhagic fevers in liberia.* Annales de l'Institut Pasteur / Virologie, 1982. **133**(2): p. 125–128.
299. Van der Waals, F.W., et al., *Hemorrhagic fever virus infections in an isolated rainforest area of central Liberia. Limitations of the indirect immunofluorescence slide test for antibody screening in Africa.* Tropical and geographical medicine, 1986. **38**(3): p. 209–214.
300. Tomori, O., et al., *Viral hemorrhagic fever antibodies in Nigerian populations.* The American journal of tropical medicine and hygiene, 1988. **38**(2): p. 407–410.
301. Keita, A.K., et al., *Serological Evidence of Ebola Virus Infection in Rural Guinea before the 2014 West African Epidemic Outbreak.* Am J Trop Med Hyg, 2018. **99**(2): p. 425–427.
302. Bane, S., et al., *Ebola Virus IgG Seroprevalence in Southern Mali.* Emerging Infectious Diseases, 2021. **27**(6): p. 1681.
303. Hounmenou, C.G., et al., *Ebola virus circulation in a non-epidemic Guinean rural area: A mixed-method approach to assessing endemicity.* Int J Infect Dis, 2024. **146**: p. 107129.
304. Richardson, E.T., et al., *Minimally symptomatic infection in an Ebola 'hotspot': a cross-sectional serosurvey.* PLoS neglected tropical diseases, 2016. **10**(11): p. e0005087.
305. Manno, D., et al., *Ebola Virus Glycoprotein IgG Seroprevalence in Community Previously Affected by Ebola, Sierra Leone.* Emerg Infect Dis, 2022. **28**(3): p. 734–738.
306. Schoepp, R.J., et al., *Undiagnosed acute viral febrile illnesses, Sierra Leone.* Emerging infectious diseases, 2014. **20**(7): p. 1176.
307. Safronetz, D., et al., *Vectorborne infections, Mali.* Emerging Infectious Diseases, 2016. **22**(2): p. 340.
308. Boisen, M.L., et al., *Multiple circulating infections can mimic the early stages of viral hemorrhagic fevers and possible human exposure to filoviruses in Sierra Leone prior to the 2014 outbreak.* Viral immunology, 2015. **28**(1): p. 19–31.

309. Dedkov, V.G., et al., *Differential laboratory diagnosis of acute fever in guinea: preparedness for the threat of hemorrhagic fevers.* International Journal of Environmental Research and Public Health, 2021. **18**(11): p. 6022.
310. Glynn, J.R., et al., *Asymptomatic infection and unrecognised Ebola virus disease in Ebola-affected households in Sierra Leone: a cross-sectional study using a new non-invasive assay for antibodies to Ebola virus.* The Lancet infectious diseases, 2017. **17**(6): p. 645–653.
311. Kelly, J.D., et al., *Anatomy of a hotspot: chain and seroepidemiology of Ebola virus transmission, Sukudu, Sierra Leone, 2015–16.* The Journal of infectious diseases, 2018. **217**(8): p. 1214–1221.
312. Houlihan, C.F., et al., *Ebola exposure, illness experience, and Ebola antibody prevalence in international responders to the West African Ebola epidemic 2014–2016: A cross-sectional study.* PLoS medicine, 2017. **14**(5): p. e1002300.
313. Kelly, J.D., et al., *Clinical sequelae among individuals with pauci-symptomatic or asymptomatic Ebola virus infection and unrecognised Ebola virus disease in Liberia: a longitudinal cohort study.* The Lancet Infectious Diseases, 2022. **22**(8): p. 1163–1171.
314. Diallo, M.S.K., et al., *Prevalence of infection among asymptomatic and paucisymptomatic contact persons exposed to Ebola virus in Guinea: a retrospective, cross-sectional observational study.* The Lancet Infectious Diseases, 2019. **19**(3): p. 308–316.
315. Kelly, J.D., et al. *Association of lower exposure risk with paucisymptomatic/asymptomatic infection, less severe disease, and unrecognized Ebola virus disease: a seroepidemiological study*. in *Open forum infectious diseases*. 2022. Oxford University Press US.
316. Halfmann, P.J., et al., *Serological analysis of Ebola virus survivors and close contacts in Sierra Leone: A cross-sectional study.* PLoS Neglected Tropical Diseases, 2019. **13**(8): p. e0007654.
317. Clark, D.V., et al., *Long-term sequelae after Ebola virus disease in Bundibugyo, Uganda: a retrospective cohort study.* Lancet Infect Dis, 2015. **15**(8): p. 905–12.
318. Rowe, A.K., et al., *Clinical, virologic, and immunologic follow-up of convalescent Ebola hemorrhagic fever patients and their household contacts, Kikwit, Democratic Republic of the Congo.* The Journal of infectious diseases, 1999. **179**(Supplement_1): p. S28–S35.
319. Bertherat, E., et al., *Leptospirosis and Ebola virus infection in five gold-panning villages in northeastern Gabon.* Am J Trop Med Hyg, 1999. **60**(4): p. 610–5.
320. Leroy, E.M., et al., *Human asymptomatic Ebola infection and strong inflammatory response.* Lancet, 2000. **355**(9222): p. 2210–5.
321. Heffernan, R.T., et al., *Low seroprevalence of IgG antibodies to Ebola virus in an epidemic zone: Ogooue-Ivindo region, Northeastern Gabon, 1997.* The Journal of infectious diseases, 2005. **191**(6): p. 964–968.
322. Dean, N.E., et al., *Transmissibility and pathogenicity of Ebola virus: a systematic review and meta-analysis of household secondary attack rate and asymptomatic infection.* Clinical Infectious Diseases, 2016. **62**(10): p. 1277–1286.
323. Crozier, I., *Mapping a Filoviral Serologic Footprint in the Democratic Republic of the Congo: Who Goes There?* The Journal of Infectious Diseases, 2018. **217**(4): p. 513–515.
324. Karra, K., et al. *Global land use/land cover with Sentinel 2 and deep learning*. in *2021 IEEE international geoscience and remote sensing symposium IGARSS*. 2021. IEEE.
325. Flyak, A.I., et al., *Cross-reactive and potent neutralizing antibody responses in human survivors of natural ebolavirus infection.* Cell, 2016. **164**(3): p. 392–405.
326. Ksiazek, T., et al., *Clinical virology of Ebola hemorrhagic fever (EHF): virus, virus antigen, and IgG and IgM antibody findings among EHF patients in Kikwit, Democratic Republic of the Congo, 1995.* The Journal of infectious diseases, 1999. **179**(Supplement_1): p. S177–S187.
327. Adaken, C., et al., *Ebola virus antibody decay–stimulation in a high proportion of survivors.* Nature, 2021. **590**(7846): p. 468–472.
328. Corti, D., et al., *Protective monotherapy against lethal Ebola virus infection by a potently neutralizing antibody.* Science, 2016. **351**(6279): p. 1339–1342.

329. Natesan, M., et al., *Human survivors of disease outbreaks caused by Ebola or Marburg virus exhibit cross-reactive and long-lived antibody responses.* Clinical and Vaccine Immunology, 2016. **23**(8): p. 717–724.
330. Becquart, P., et al., *Identification of Continuous Human B-Cell Epitopes in the VP35, VP40, Nucleoprotein and Glycoprotein of Ebola Virus.* PLOS ONE, 2014. **9**(6): p. e96360.
331. Wamala, J.F., et al., *Ebola hemorrhagic fever associated with novel virus strain, Uganda, 2007-2008.* Emerg Infect Dis, 2010. **16**(7): p. 1087–92.
332. Bwire, G., et al., *Sudan Ebola virus (SUDV) outbreak in Uganda, 2022: lessons learnt and future priorities for sub-Saharan Africa.* BMC Med, 2023. **21**(1): p. 144.
333. Ilunga Kalenga, O., et al., *The Ongoing Ebola Epidemic in the Democratic Republic of Congo, 2018-2019.* N Engl J Med, 2019. **381**(4): p. 373–383.
334. Bishop, L.A., et al., *Immunological cross-reactions with paramyxovirus nucleoproteins may explain sporadic apparent ebolavirus seropositivity in European populations.* bioRxiv, 2020: p. 2020.03. 27.007195.
335. Becker, S., et al., *Evidence for occurrence of filovirus antibodies in humans and imported monkeys: do subclinical filovirus infections occur worldwide?* Medical microbiology and immunology, 1992. **181**(1): p. 43–55.
336. Chan, Y., et al., *Determining seropositivity—A review of approaches to define population seroprevalence when using multiplex bead assays to assess burden of tropical diseases.* PLOS Neglected Tropical Diseases, 2021. **15**(6): p. e0009457.
337. Ronan, T., Z. Qi, and K.M. Naegle, *Avoiding common pitfalls when clustering biological data.* Sci Signal, 2016. **9**(432): p. re6.
338. Cantoni, D., et al., *Correlation between pseudotyped virus and authentic virus neutralisation assays, a systematic review and meta-analysis of the literature.* Frontiers in immunology, 2023. **14**: p. 1184362.
339. Hulseberg, C.E., et al., *Molecular analysis of the 2012 Bundibugyo virus disease outbreak.* Cell Reports Medicine, 2021. **2**(8).
340. Li, L., et al., *Assessing risk of Bombali virus spillover to humans by mutagenesis analysis of viral glycoprotein.* hLife, 2024. **2**(1): p. 32–42.
341. Switzer, W.M., et al., *Novel simian foamy virus infections from multiple monkey species in women from the Democratic Republic of Congo.* Retrovirology, 2012. **9**(1): p. 100.
342. Douno, M., et al., *Hunting and consumption of rodents by children in the Lassa fever endemic area of Faranah, Guinea.* PLoS Neglected Tropical Diseases, 2021. **15**(3): p. e0009212.
343. Allworth, T., et al., *Equine morbillivirus in Queensland.* 1995.
344. Rogers, R., et al., *Investigation of a second focus of equine morbillivirus infection in coastal Queensland.* 1996.
345. Ward, M., et al., *Negative findings from serological studies of equine morbillivirus in the Queensland horse population.* 1996.
346. Young, P.L., et al., *Serologic evidence for the presence in Pteropus bats of a paramyxovirus related to equine morbillivirus.* Emerging infectious diseases, 1996. **2**(3): p. 239.
347. Halpin, K., et al., *Isolation of Hendra virus from pteropid bats: a natural reservoir of Hendra virus.* Journal of General Virology, 2000. **81**(8): p. 1927–1932.
348. Kohl, C., et al., *Hervey virus: Study on co-circulation with Henipaviruses in Pteropid bats within their distribution range from Australia to Africa.* PLOS ONE, 2018. **13**(2): p. e0191933.
349. Arklay, A., et al., *Screening of bat carers for antibodies to equine morbillivirus.* Communicable Diseases Intelligence, 1996. **20**(22).
350. Edson, D., et al., *Routes of Hendra Virus Excretion in Naturally-Infected Flying-Foxes: Implications for Viral Transmission and Spillover Risk.* PLOS ONE, 2015. **10**(10): p. e0140670.
351. Williamson, M., et al., *Transmission studies of Hendra virus (equine morbilli-virus) in fruit bats, horses and cats.* Australian veterinary journal, 1998. **76**(12): p. 813–818.
352. Hooper, P., et al., *Histopathology and immunohistochemistry of bats infected by Australian bat lyssavirus.* Australian Veterinary Journal, 1999. **77**(9): p. 595–599.

353. McCall, B.J., et al., *Potential exposure to Australian bat lyssavirus, Queensland, 1996-1999.* Emerging Infectious Diseases, 2000. **6**(3): p. 259.
354. Group, L.E., *Update on bat lyssavirus.* Commun Dis Intell, 1996. **20**: p. 535.
355. Chant, K., et al., *Probable human infection with a newly described virus in the family Paramyxoviridae. The NSW Expert Group.* Emerg Infect Dis, 1998. **4**(2): p. 273–5.
356. Philbey, A.W., et al., *An apparently new virus (family Paramyxoviridae) infectious for pigs, humans, and fruit bats.* Emerg Infect Dis, 1998. **4**(2): p. 269–71.
357. Barr, J.A., et al., *Evidence of bat origin for Menangle virus, a zoonotic paramyxovirus first isolated from diseased pigs.* Journal of General Virology, 2012. **93**(12): p. 2590–2594.
358. Barr, J., et al., *Isolation of multiple novel paramyxoviruses from pteropid bat urine.* Journal of General Virology, 2015. **96**(1): p. 24–29.
359. Sabir, A.J., et al., *Cedar virus biology and its applications as a surrogate for highly pathogenic henipaviruses.* Cell Insight, 2024. **3**(4): p. 100181.
360. Huaman, C., et al., *An in vivo BSL-2 model for henipavirus infection based on bioluminescence imaging of recombinant Cedar virus replication in mice.* Frontiers in chemical biology, 2024. **3**: p. 1363498.
361. Boardman, W.S.J., et al., *Seroprevalence of three paramyxoviruses; Hendra virus, Tioman virus, Cedar virus and a rhabdovirus, Australian bat lyssavirus, in a range expanding fruit bat, the Grey-headed flying fox (Pteropus poliocephalus).* PLOS ONE, 2020. **15**(5): p. e0232339.
362. Mittal, N., et al., *Serologic Evidence of Human Exposure to Bat-Borne Zoonotic Paramyxoviruses, Cambodia.* Viruses, 2025. **17**(8).
363. Lunn, T.J., et al., *Conventional wisdom on roosting behavior of Australian flying-foxes-A critical review, and evaluation using new data.* Ecol Evol, 2021. **11**(19): p. 13532–13558.
364. Timmiss, L.A., et al., *Threatened but not conserved: flying-fox roosting and foraging habitat in Australia.* Australian Journal of Zoology, 2021.
365. Williams, N.S., et al., *Range expansion due to urbanization: Increased food resources attract Grey-headed Flying-foxes (Pteropus poliocephalus) to Melbourne.* Austral Ecology, 2006. **31**(2): p. 190–198.
366. Tait, J., et al., *Are flying-foxes coming to town? Urbanisation of the spectacled flying-fox (Pteropus conspicillatus) in Australia.* PLoS one, 2014. **9**(10): p. e109810.
367. Eby, P., et al., *The distribution, abundance and vulnerability to population reduction of a nomadic nectarivore, the Grey-headed Flying-fox Pteropus poliocephalus in New South Wales, during a period of resource concentration.* Australian Zoologist, 2014. **31**(1): p. 240–253.
368. Becker, D.J., et al., *Ecological conditions predict the intensity of Hendra virus excretion over space and time from bat reservoir hosts.* Ecology Letters, 2023. **26**(1): p. 23–36.
369. Orf, G.S., et al., *Metagenomic Detection of Divergent Insect- and Bat-Associated Viruses in Plasma from Two African Individuals Enrolled in Blood-Borne Surveillance.* Viruses, 2023. **15**(4).
370. Yang, W.T., et al., *Genetic characterization of a densovirus isolated from great tit (Parus major) in China.* Infect Genet Evol, 2016. **41**: p. 107–112.
371. O'Dea, M.A., et al., *Genomic characterization of a novel poxvirus from a flying fox: evidence for a new genus?* J Gen Virol, 2016. **97**(9): p. 2363–2375.
372. Zheng, X.-y., et al., *Viral metagenomics of six bat species in close contact with humans in southern China.* Archives of Virology, 2018. **163**(1): p. 73–88.
373. Hu, D., et al., *Virome analysis for identification of novel mammalian viruses in bats from Southeast China.* Scientific Reports, 2017. **7**(1): p. 10917.
374. Geldenhuys, M., et al., *A metagenomic viral discovery approach identifies potential zoonotic and novel mammalian viruses in Neoromicia bats within South Africa.* PLOS ONE, 2018. **13**(3): p. e0194527.
375. Bolatti, E.M., et al., *Viral Metagenomic Data Analyses of Five New World Bat Species from Argentina: Identification of 35 Novel DNA Viruses.* Microorganisms, 2022. **10**(2): p. 266.
376. Shapiro, J.T., et al., *Metagenomic Analysis Reveals Previously Undescribed Bat Coronavirus Strains in Eswatini.* EcoHealth, 2021. **18**(4): p. 421–428.

377. Ortiz-Baez, A.S., et al., *Limited diversity of bat-associated RNA viruses in endangered and geographically isolated Christmas Island flying foxes.* One Health, 2025. **20**: p. 101060.
378. Yuan, L., et al., *Evidence for retrovirus and paramyxovirus infection of multiple bat species in China.* Viruses, 2014. **6**(5): p. 2138–2154.
379. Flanagan, M., et al., *Anticipating the species jump: surveillance for emerging viral threats.* Zoonoses and public health, 2012. **59**(3): p. 155–163.
380. Carrino, M., et al., *Molecular investigation of recent canine parvovirus-2 (CPV-2) in Italy revealed distinct clustering.* Viruses, 2022. **14**(5): p. 917.
381. Hardmeier, I., et al., *Metagenomic analysis of fecal and tissue samples from 18 endemic bat species in Switzerland revealed a diverse virus composition including potentially zoonotic viruses.* PLOS ONE, 2021. **16**(6): p. e0252534.
382. Matthieu, G., et al., *Bacteriophages to reduce gut carriage of antibiotic resistant uropathogens with low impact on microbiota composition.* Environmental microbiology, 2016.
383. Kumari, S., K. Harjai, and S. Chhibber, *Isolation and characterization of Klebsiella pneumoniae specific bacteriophages from sewage samples.* Folia microbiologica, 2010.
384. Seema, K., H. Kusum, and C. Sanjay, *Efficacy of bacteriophage treatment in murine burn wound infection induced by klebsiella pneumoniae.* Journal of microbiology and biotechnology, 2009.
385. Tsai, Y.C., et al., *Therapeutic effect and anti-biofilm ability assessment of a novel phage, phiPA1-3, against carbapenem-resistant Pseudomonas aeruginosa.* Virus Res, 2023. **335**: p. 199178.
386. Mengzhe, L., et al., *Broad-host-range Salmonella bacteriophage STP4-a and its potential application evaluation in poultry industry.* Poultry science, 2020.
387. Leon-Velarde, C.G., J.W. Jun, and M. Skurnik, *Yersinia Phages and Food Safety.* Viruses, 2019. **11**(12).
388. Leskinen, K., et al., *YerA41, a Yersinia ruckeri Bacteriophage: Determination of a Non-Sequencable DNA Bacteriophage Genome via RNA-Sequencing.* Viruses, 2020. **12**(6).